REMOVAL OF SOMAN FROM INJURED SKIN BY HAEMOSTATIC MATERIALS

by

CHRISTOPHER HUGH DALTON

A thesis submitted to the University of Birmingham for the degree of DOCTOR OF PHILOSOPHY

School of Biosciences

University of Birmingham

October 2013

The content and opinions stated in this thesis by the author do not necessarily represent the views or policy of her Britannic Majesty's Government.

ABSTRACT

The use of haemostatic materials that could be used to mitigate against the effects of the chemical warfare agent soman (GD) on contaminated personnel that may also present with wounds were investigated. To support the *in vitro* diffusion cell component of this work, the penetration rate of ^{14}C-GD into different receptor fluids was evaluated to enable determination of the most appropriate receptor fluid to use as a sink for GD. Of the receptor media evaluated only 50% aqueous ethanol was able to maintain sink conditions. A number of haemostatic materials were shown to retain haemostatic efficacy in the presence of blood contaminated with GD, and were also shown to irreversibly sequester GD. The lead candidate, WoundStat™, was shown to be as effective a decontaminant as the current in service countermeasure fullers' earth. Complementary *in vivo* studies using damaged ear skin in a terminally anaesthetised large white pig model showed that whilst use of WoundStat™ was not 100% effective in the prevention of mortality after GD poisoning, it did increase the therapeutic window where further nerve agent-specific medical countermeasures could be employed. Perhaps most importantly, application of Woundstat^{TM} onto GD contaminated damaged skin did not increase the toxicity of GD.

ACKNOWLEDGEMENTS

I would like to thank my supervisors Dr John Jenner and Prof Kevin Chipman for their guidance in the production of this thesis. I am also grateful for assistance from Stephen Rutter and Oliver Payne. Special thanks go to Dr Stuart Graham for proof reading this thesis. I would also like to thank the Health Protection Agency (HPA) and in particular Prof. Rob Chilcott for securing the funding that made this PhD possible, and, to the Defence Science Technology Laboratory (Dstl) for allowing me to complete this work. Thanks also go to Dr John Graham and Dr Ed Clarkson for hosting a visit to the United States Army Medical Research Institute of Chemical Defense (USAMRICD) where the final *in vivo* portion of this programme was carried out. Finally, special thanks go to my family for giving me the support necessary to undertake this work.

This work was funded by the Health Protection Agency (HPA) and conducted in support of the “Haemostatic Decontaminants for Penetrating Injuries Contaminated with CW Agents” project (DTRA Project ID Number 2.F0026_08_RC_C) and carried out at the Defence Science and Technology Laboratory (Dstl).

This thesis has resulted in a number of publications which were written in collaboration with other authors.

CONTENTS

FOREWORD

The improvised explosive device (IED) is a major threat that may be deployed by terrorists or insurgents on civilian or military populations. IED use has been cited as being the leading cause of explosively injured casualties during Operation Herrick in Afghanistan (Stalker, et al., 2011). The IED can be defined as being a “make shift” or homemade bomb which has often used by insurgents to attack military personnel and equipment. The loss of life and dehabilitating injury caused by these weapons is only too real, yet what if the explosive charge was not the primary hazard? What if an IED was merely a dissemination device for something more insidious, possibly a toxic chemical such as a chemical warfare (CW) agent? This threat has been previously alluded to (Weinbroum, et al., 2000). An IED is only one of a variety of ways that traumatically wounded casualties may be produced on the battlefield, ballistic injury from conventional weapons and even slips, trips and falls could cause wounds that may, in the event of a chemically contaminated battlefield, require decontamination.

The work presented in thesis investigates the use of materials that could be used to mitigate the effects of CW agents on contaminated personnel who also present with superficial and / or haemorrhaging wounds. Contaminated wounds of this type, would, left untreated, potentially lead to loss of life.

CHAPTER 1: INTRODUCTION

1.1. Dissemination of CW agents following explosion and incident resolution

The detonation of an explosive chemical weapon dissemination device would initiate a chain of events that could produce casualties with injuries of varying severity and levels of contamination. The response to, and resolution of, such an incident depends on whether the incident is primarily civilian or military in nature, although as a top level overview, the incident response for both scenarios may be considered similar. If one considers the incident and the implications it generates in chronological order it can be broken down into:

i. Detonation, the primary cause of traumatically injured casualties.

ii. Dissemination of liquid or particulate material within the device, possibly radiological, biological or chemical in nature (although for the purpose of this thesis, discussion will remain exclusively in the domain of the chemical). The dissemination would produce chemically contaminated casualties, some of whom will also exhibit traumatic injuries.

iii. Vapour dissemination in accordance with prevailing wind conditions at the incident site. The resultant vapour plume may cause additional, none traumatically injured casualties, downwind of the detonation site.

iv. Personnel located in neither the primary liquid contamination radius or in the downwind vapour plume who are likely to be uncontaminated, although this may not initially be known.

The standard response would be to cordon off the incident site (to prevent bystanders inadvertently encroaching into the area becoming further casualties) and to set up a casualty decontamination area upwind of the contamination. An orderly evacuation of casualties would then proceed from the incident site to the cordon and into the decontamination area (Figure 1.1) where medical triage would be carried out. After first aid and decontamination procedures had been completed, transport to a suitable hospital facility would be feasible.

The scenario outlined allows for medical aid to be given at the incident site itself, before, during or after decontamination, or at permanent medical facilities away from the incident site. In the case of haemorrhaging traumatic injury, treatment by necessity, must be immediate. Any chemical contamination will likely be seen as of secondary importance until haemostatic treatments have been successfully employed.

One of the key questions is as to whether the use of haemostatic treatments complicates the process of decontamination. The answer is almost certainly, as the two processes have to occur consecutively, the cessation of haemorrhage followed by decontamination of the wound site. The advantage of having a method of simultaneously preventing haemorrhage and decontaminating a wound site cannot therefore be overstated. This is where the primary focus of this thesis resides, the development of haemostatic materials that could be used as a dual treatment for both haemostasis and decontamination. However, it is likely that the surrounding

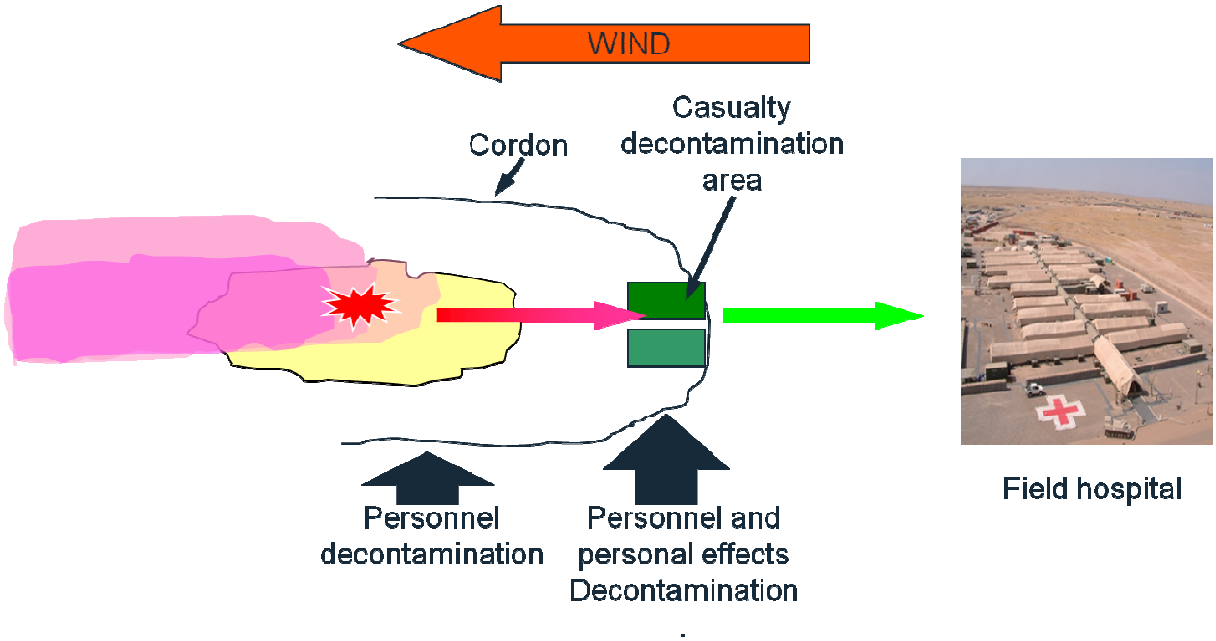

Figure 1.1: Schematic depicting the site of an agent release and where decontamination would take place. Wind direction will determine the direction of any vapour release from the incident, with decontamination facilities setup upwind.

undamaged skin of a traumatically injured casualty will also be contaminated. Rather than necessitating an increase in logistical burden by having a standard decontaminant and a haemostatic decontaminant deployed side by side, confirming that a haemostatic decontaminant could be used as a general decontaminant would be advantageous.

As outlined, further chemical agent deposition on personnel may occur from vapour dissemination. Chemical vapour poses not only a dermal hazard, but, also a respiratory hazard. A number of chemicals (including the chemical warfare agents investigated for this work programme) possess sufficient volatility to be considered a vapour hazard, and, although outside the scope of this thesis, provision of adequate respiratory protection should be an important consideration.

Upon reaching the decontamination area, immediately life threatening traumatic injuries would have been stabilised. The outstanding challenge remains one of chemical decontamination. Casualties can be split into two groups, contaminated and uncontaminated, although unless specific signs and symptoms have been exhibited, knowing the difference may be difficult to ascertain. The aim is now to progress though the decontamination area at a rate that will ensure any and all chemical deposits are removed, ideally with confirmation of zero remaining contamination upon egress from the decontamination unit.

The scope and complexity of managing an incident of this type cannot be understated. The project, of which the subject matter of this thesis forms a part, had the overall aim of refining and developing medical countermeasures and techniques which could be used in the management of incidents involving a chemically contaminated explosive device.

1.2. Rationale for selection of chemical contaminant

Although the scenario described would be valid for a wide range of toxic chemical disseminations, the most hazardous chemicals likely to be faced on the battlefield are the chemical warfare agents. Due to their acute toxicity the chemical warfare agents are of major concern and are the greatest challenge for a chemical decontaminant. Chemical warfare agents as a group possess a number of disparate mechanisms of action and physico-chemical properties, as such, an individual representative from three classes of chemical warfare agents was chosen as the starting point to commence this investigation, with this project primarily investigating first aid measures against a ‘G’ series nerve agent, soman (GD), although for completeness discussion of parallel projects involving the ‘V’ series nerve agent VX and the vesicant sulphur mustard, HD will be developed as necessary.

1.3. Medical countermeasures for haemostasis and decontamination

Logically, consideration first needs to be given to currently available medical countermeasures used in treating traumatic haemorrhaging injury and, separately, those used for skin decontamination of chemical warfare agents. A comparison of

any similarities between mechanisms of action for each type of countermeasure may offer opportunities for dual use countermeasure development. Haemostatic agents are defined as drugs or other agents that retard or stop bleeding. Mechanisms of action may be used to group similar haemostatic products, which briefly include electrostatic interactions with erythrocytes, activation of clotting factors or platelets, plasma absorption to concentrate clotting factors and use of tamponade effects.

Chemical warfare agent skin decontaminants are typically either powders or liquids that passively decontaminate or actively decontaminate the skin. Passive decontaminants such as Fullers' earth and M291 powder physically absorb chemical agents from the skin surface, but, do not actively decontaminate what they have absorbed. Active decontaminants, such as Reactive Skin Decontaminant Lotion (RSDL), incorporate active moieties that break down any chemical warfare agent it comes into contact with. Unfortunately, due to incompatibilities between these skin decontaminants and living systems, they are not amenable for use as candidate dual use haemostatic decontaminants. However, their mechanisms of action share similarities with the mechanisms of action of a number of haemostats and these similarities offer a potential route for exploration.

With the scope of the project outlined, the following sections detail the nature of traumatic injury, the action of chemical warfare agents on living systems and the experimental techniques that can be used and developed to determine the efficacy of candidate treatments.

1.4. Traumatic injury and medical management

Traumatic injury, whether blunt or penetrating in nature, is not the only complication of a blast injury (Plurad, 2011). The physical trauma resulting from exposure to the detonation of an explosive device may be described in terms of primary through to quaternary blast injury (Sakorafas and Peros, 2008). Primary injuries are typically realised close to the detonation and consist of the deleterious effects caused by blast overpressure. Most affected are the ears, lungs and gastrointestinal tract, and, although outward signs may on the whole be negligible, the internal injuries caused can be severe. Secondary injuries are those caused by objects thrown out of the explosion, such as shrapnel, and are one cause of blunt or penetrating injury. Tertiary injury occurs from air displacement within the explosion zone, with the wind generated capable of propelling casualties against solid objects resulting in a secondary source of blunt or penetrating injury. Quaternary injuries include neurological disorders, whether physical or psychosomatic, and flash burns. It is the resulting secondary and tertiary blast injuries that are primarily of interest for this research project.

After a traumatic injury event, uncontrolled bleeding is one of the leading causes of morbidity and death (Clifford, 2004;Alam, et al., 2005). The type of injury and how the injury is treated will vary between military combat casualties and civilian trauma patients (Carr, 2004) due to different demands on the medical services. One of the main differences is the transport time to a fixed hospital environment where emergency support and treatment can be given. For seriously injured civilians the

expectation will be for the casualty to reach hospital within an hour of injury in an urban area. In a combat zone, time to transport off the battlefield may be measured in hours. This problem may be exacerbated with the difficulties faced by emergency medical personnel in reaching a casualty quickly (Sakorafas and Peros, 2008). The type of traumatic injury between the civilian and military case may also be substantially different. Civilian traumatic injury is typified by blunt trauma, for which the “golden hour” therapeutic window for likely successful clinical outcome has been coined (Carr, 2004;Murdock, 2008). The time taken for a traumatically injured soldier to be evacuated to where medical support is available may increase the severity of the injury. The term the “platinum ten minutes” has been used to indicate the time by which successful intervention should be employed to the combat casualty (National Health Service, 2011).

The trauma generated by penetrating ballistic injury with consequent uncontrolled haemorrhage is responsible for approximately fifty percent of combat deaths (Alam, et al., 2005) and these deaths will likely occur before definitive medical care can be provided. The options for treating a combat casualty within the “platinum ten minutes” will likely be limited to the equipment immediately available and will be administered on a buddy aid basis. A number of commercial off the shelf (COTS) haemostats are amenable to battlefield use (Neuffer, et al., 2004) and are deployable within this time frame and hence will be the primary focus as potential decontamination candidates. An initial survey of the literature for haemostats with potential battlefield application, are shown in Table 1.1. The haemostats include Celox® (Clay, et al., 2010), FastAct™ (Alam, et al., 2005), Hemcon® (Robinson, 2004), QuikClot ACS+®

(Robinson, 2004), SuperQR (Kheirabadi, et al., 2009), Vitagel™ (Marchan and Andrews, 2009) and WoundStat™ (Kheirabadi, et al., 2009;Clay, et al., 2010). Recombinant Factor VIIa, although extensively used in both forward surgical teams and combat support hospitals, it is not currently deployable on the battlefield (Kembro, et al., 2008) and hence was not included.

Name	Physical Form	Composition	Mechanism of Action
Celox®	Solid	Granular chitosan polymer	Electrostatic interactions with erythrocytes to form a cross-linked clot
FastAct™	Liquid	Bovine proteins and antiseptic	Activation of clotting factor IX
Hemcon®	Dressing	Chitosan polymer based dressing	Platelet activation
QuikClot ACS+®	Solid	Synthetic zeolite.	Plasma absorption to concentrate clotting factors, tamponade (blockage or closure) effect and activation of coagulation pathways.
SuperQR	Solid	Potassium iron oxyacid salt mixed with a hydrophilic powder	Plasma absorption to concentrate clotting factors, tamponade (blockage or closure) effect and activation of coagulation pathways
Vitagel™	Liquid	Bovine microfibrillar collagen, thrombin and $CaCl_2$ combined with autologous plasma.	Mimics the final stage in the coagulation cascade.
WoundStat™	Solid	Mineral smectite.	Plasma absorption to concentrate clotting factors, tamponade (blockage or closure) effect and activation of coagulation pathways.

Table 1.1: Commercial off the shelf (COTS) haemostats which are amenable to battlefield first aid use.

1.5. Chemical warfare agents

1.5.1. Historical aspects

The use of Chemical Warfare agents as a means of waging war has evolved throughout human history (Chauhan, et al., 2008). During the 6th century BC, Helleborous roots were used to contaminate water supplies (Szinicz, 2005). The use of ignited pitch and sulphur during these early times has also been noted (Szinicz, 2005). During the middle ages, the use of arsenical smokes by the China Sung Dynasty was reported (Szinicz, 2005). The development of chemistry as a science saw increasing military sophistication with the development arsenic and sulphur explosive devices by Leonardo da Vinci in the 15th Century. The rise of the discipline of organic chemistry in the late 19th century, gave the ability to synthesise a multitude of novel organic compounds. Among these compounds were chemical weapons, such as sulphur mustard (SM) (Malhotra, et al., 1999;Balali-Mood and Hefazi, 2005), which saw extensive use during the First World War (WWI) and may still be used by aggressors on the battlefield of today.

The First World War saw use of chemical weapons on a previously unimaginable scale (Fries and West, 1921). Of the 150,000 tons of battle gases manufactured, 125,000 tons were used causing an estimated 1,296,853 casualties (Prentiss, 1937) which caused 1.32 % of the battlefield deaths from all weapons systems used (Riley, 2003). The classes of CW agent used can be divided into lacrimatory agents (e.g. ethylbromacetate), lung injurants (e.g. chlorine), systemic toxic agents (e.g.

hydrocyanic acid), vesicant agents (e.g. sulphur mustard) and respiratory irritants (e.g. diphenylchlorarsine) (Prentiss, 1937). Perhaps, the most notorious initial use of lethal chemicals was at Ypres, Belgium on the 22nd April 1915 (Vedder, 1925). German forces released a chlorine gas cloud that inflicted grave casualties on British, Canadian and French soldiers, estimated at 5,000 deaths and 15,000 wounded. The use of phosgene followed later that year, with sulphur mustard being introduced to the battlefield in July 1917. During the interwar years, and despite negative public opinion, chemical warfare agent use continued unabated, with large scale use of sulphur mustard by the Italians in Ethiopia in 1935 and 1936 (SIPRI, 1971). Perhaps, surprisingly, chemical weapons were not used on the European battlefield during the Second World War (WWII), although reported use was made by the Japanese military during incursions into China (Brown, 1968). Development of chemical warfare agents continued, with German development of the "G series" of nerve agents, initially tabun followed rapidly by sarin and soman between 1936 and 1944 (Szinicz, 2005). The "V series" of nerve agents originated from research at Imperial Chemical Industries (ICI) in the mid 1950's ((SIPRI, 1971)). From the close of the WWII to modern times, infrequent use of chemical warfare agents by various militaries to further their aims have been made. Putting to one side the use of non lethal (to humans) agents such as herbicides (e.g. Agent Orange as used during the Vietnam War (Tuyet and Johansson, 2001)), the Iran Iraq conflict probably serves as the most recent reminder of military chemical use (Bijani and Moghadamnia, 2002;Ghanei and Vosoghi, 2002). The attack at Halabja, 16th March 1988, produced large numbers of casualties (up to 5,000 deaths and 10,000 injured) on a predominantly Kurdish civilian population by the Iraqi military. More recent times have seen the domain of

the chemical warfare agent no longer being confined solely to military use (Brennan, et al., 1999;Vale, et al., 2007). Extremist organisations and cults have manufactured chemical weapons of various types for use on civilian targets. March 20th, 1995, saw use of sarin in the Tokyo metro system by members of the Aum Shinrikyo cult against Japanese civilians (Tokuda, et al., 2006). Although, only thirteen fatalities resulted, the potential for which nerve agents could be used to cause disruption and mass hysteria reverberated around the world. 2001 saw disruption to mail delivery systems with anthrax spores being mailed a number of recipients including two US senators (Schwartz, 2009). Most recently in the UK was the discovery of ricin at a property in Durham during 2009, purportedly for use in a terror attack (Engelbrecht, 2010).

1.5.2. Organisation for the Prohibition of Chemical Weapons

In an attempt to halt nations using chemical warfare agents in their perceived national interests, the Chemical Weapons Convention (CWC) was opened for signatory on 13th January 1993. The CWC came into force on 29th April 1997, with 87 state parties becoming bound by its terms and conditions under international law. The Organisation for the Prohibition of Chemical Weapons (OPCW) was formed and tasked with overseeing the implementation of the CWC with the 188 states that currently have membership. States being bound to the Convention have agreed to chemical disarmament. Essentially, this entails that currently held stockpiles of chemical weapons be destroyed along with any facilities capable of producing them. A verification regime was also put in place to limit transport and use of chemical warfare agents and a number of their precursors (full details are to be found on the

schedule 1, 2 and 3 lists within the annexes to the CWC). Although signatory states may no longer develop or use chemical warfare agents for aggressive purposes, it was seen as necessary for CW agents to continue to be used for the development of defensive research against future CW attack by non signatory states.

1.5.3. Chemical warfare agent definition, toxicity and properties

In today's context, the term Chemical Warfare Agent refers to a broad spectrum of very toxic chemicals (Evison, et al., 2002;Ramirez and Bacon, 2003). The Chemical Weapons Convention (CWC) defines a chemical weapon as: "Toxic chemicals and their precursors, except where intended for purposes not prohibited under this Convention, as long as the types and quantities are consistent with such purposes". Under this definition toxic chemical is given the meaning: "Any chemical which through its chemical action on life processes can cause death, temporary incapacitation or permanent harm to humans or animals. This includes all such chemicals, regardless of their origin or of their method of production, and regardless of whether they are produced in facilities, in munitions or elsewhere". It is important to note that subsets of chemical weapons (e.g. nerve and vesicating agents) vary widely in their acute toxicity and mechanisms of action. The potency spectrum (Figure 1.2) defines the approximate toxicity of chemical warfare agents within the boundaries of other toxic entities such as toxic industrial chemicals (TICs), toxins and biological agents. To generalise, a chemical warfare agent is not defined by any unique property. Dependent on environmental temperature, they can exist in a solid, liquid or gaseous state and dependant on the manufacturing process used may be

neat (of varying purity) or within a matrix, potentially solvated or in combination with another toxic entity. Confining the term chemical warfare agent to the “potency spectrum” definition we are considering a range of volatile liquids. Actual volatility is environment and specific agent dependent, and to a large degree accounts for how an individual agent is likely to be encountered and through which route(s) of entry it will be absorbed. Once absorption of a chemical warfare agent has occurred, lethal mammalian toxicity is typically of overriding concern. Traditionally, the LD_{50} value gives a good baseline comparison between the toxicities of different compounds. Estimated LD_{50}, LCt_{50} and AEGL values, for human exposure, to either a liquid or vapour exposure for a range of volatile liquid chemical warfare agents is given in Table 1.2. This can, however, be misleading, especially from a military point of view, where any form of incapacitation that can cause casualties will increase the logistic burden.

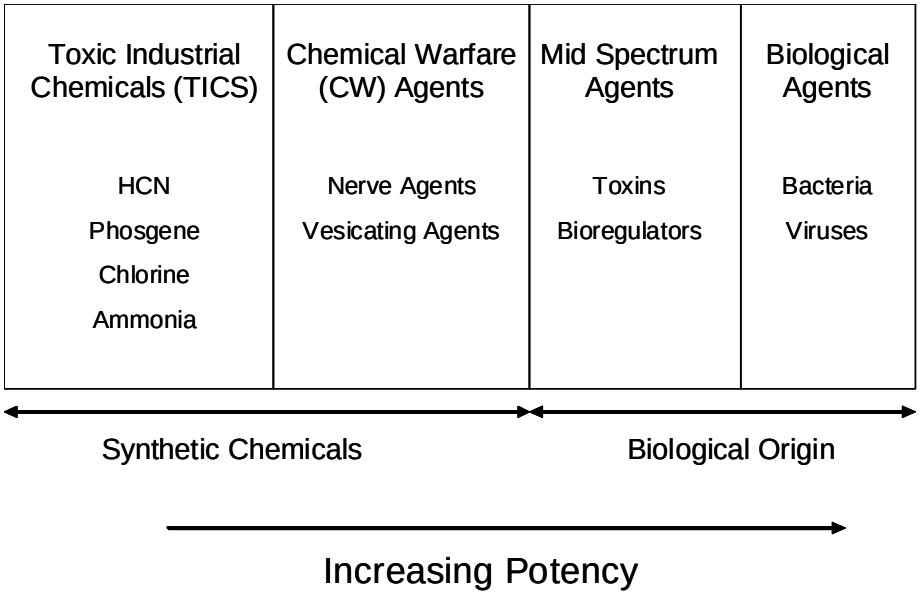

Figure 1.2: "Potency spectrum" of chemical and biological agents. Of the chemicals, although chlorine and phosgene were extensively used during WWI, they are regarded primarily as toxic industrial chemicals (TICS) rather than chemical warfare (CW) agents due to their industrial uses.

Potency Spectrum Area:	Chemical Warfare Agent				
Type:	Nerve Agent				Vesicant
Agent Name	Tabun (GA)	Sarin (GB)	Soman (GD)	VX	Sulphur Mustard (HD)
LD_{50}	21.4	24.3	5	0.07	20
LCt_{50}	70	35	35	15	900
AEGL-1 (Nondisabling)	0.069	0.069	0.035	0.0057	4.0
AEGL-2 (Disabling)	0.87	0.87	0.057	0.0065	6.0
AEGL-3 (Lethal)	7.6	3.8	3.8	0.29	39.0

Table 1.2: Estimated human LD_{50}, LCt_{50} and Acute Exposure Guideline Levels (AEGL) values for agents within the potency spectrum area of chemical warfare agents. Values given are in $mg.kg^{-1}$ (LD_{50}) for a percutaneous liquid exposure or $mg.min.m^{-3}$ (LCt_{50} and AEGL) for an inhaled vapour exposure. Given LCt_{50} values are for a 2 - 10 minute exposure, whereas, AEGL values are for a 10 minute exposure. The AEGL value considers the general population including susceptible individuals. NB. Due to assumed equipotent toxicity, values for GF (not shown) are the same as for GD. LD_{50} and LCt_{50} values are taken from an independent review of the U.S. Army's Chemical Defense Equipment Process Action Team (CDEPAT) review of the scientific basis for toxicity estimates in use by the Army (National Research Council (U.S.) and Committee on Toxicology, 1997). AEGL values are taken from work undertaken by the US National Research Council (Subcommittee on Acute Exposure Guideline Levels, et al., 2003).

1.5.4. Nerve agents

Organophosphate nerve agents and organophosphate pesticides may be classified as organophosphate anticholinesterases due to their similar mechanisms of action (Vale, et al., 2003). Whereas organophosphate pesticides have a number of applications in both agricultural use and in human and veterinary medicines, nerve agents do not. This lack of useful application is due to their inherent acute mammalian toxicity. Although the mechanism of action between the two groups of compounds is similar, and indeed organophosphate pesticides are often used as less toxic simulants of nerve agents, structurally there are differences which account for their varying toxicities. Organophosphates that are classified as nerve agents fall under schedule 1 of the CWC (Section 1.5.2).

Nerve agents are typically designated as either ‘G’ or ‘V’ agents, dependent on the country of discovery or magnitude of their toxicity (Cannard, 2006). Members of the ‘G’ series of nerve agents include tabun (GA, ethyl dimethylamidocyanophosphate), sarin (GB, isopropyl metylfluorophosphonate), soman (GD, pinacolyl methylfluorophosphonate) and cyclosarin (GF, methyl cyclohexylfluorophosphonate). The ‘V’ series of nerve agents are typified by the phosphonothioate VX. In their pure state, nerve agents are colourless liquids of varying physico-chemical properties (Table 1.3). As a general rule, the ‘G’ series of nerve agents are more volatile than the ‘V’ series of nerve agents. Of the ‘G’ series, GA, GD and GF are expected to present relevant contact hazards. Nerve agents are esters of phosphoric or phosphonic acids, as such; they have the generalised structure shown in Figure 1.3.

Designator	GA	GB	GD	GF	VX
Formula	$C_5H_{11}N_2O_2P$	$C_4H_{10}FO_2P$	$C_7H_{16}FO_2P$	$C_7H_{14}FO_2P$	$C_{11}H_{25}NO_2PS$
CAS No.	77-81-6	107-44-8	96-64-0	329-99-7	50782-69-9
Mol. Wt.	162.13	140.10	182.178	180.2	267.38
Physical state	Colourless to brown liquid	Colourless liquid	Colourless liquid	Liquid	Oily, amber coloured liquid
Odour	Faintly fruity	N/A	N/A	Peaches	Odourless
Solubility in water ($g.L^{-1}$ at 20℃)	72	Miscible	21	Almost insoluble	30 (at 25℃)
Vapour Pressure (mm Hg at 20℃)	0.037	2.10	0.40	0.044	0.0007
Vapour density (air=1)	5.63	4.86	6.33	6.2	9.2
Liquid density ($g.ml^{-1}$ at 25℃	1.073	1.102	1.0222	1.1327	1.006 (at 20℃)
Melting Point (℃)	-50	-56	-42	-30	-39
Boiling Point (℃)	78	158	198	239	298
Log K_{OW}	1.18	0.15	1.8	N/A	N/A

Table 1.3: Chemical and physical data for VX and the G series nerve agents. Data amalgamated from work carried out during the AEGL reviews (Subcommittee on Acute Exposure Guideline Levels, et al., 2003).

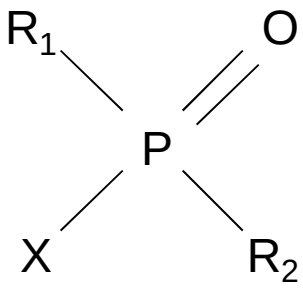

	R_1	R_2	X
Tabun, GA	CH_3CH_2O	$(CH_3)_2N$	CN
Sarin, GB	$(CH_3)_2CHO$	CH_3	F
Soman, GD	$(CH_3)_3C(CH_3)HO$	CH_3	F
VX	CH_3CH_2O	CH_3	$SCH_2CH_2N(CH(CH_3)_2)_2$

Figure 1.3: General nerve agent formula, where R = alkyl groups and X = an electronegative leaving group (e.g. Fluorine in the case of most of the ‘G’ series of agents). A nerve agent’s degree of toxicity depends upon the substituent groups attached to the phosphorus atom.

1.5.4.1. Absorption and toxicity

Nerve agents are generally encountered in either the liquid or vapour phase. In liquid form, skin penetration can be rapid and produces no overt damage to the skin itself, although local effects in the form of fasciculation and sweating may occur. As vapour, absorption across both the respiratory epithelium and cornea is rapid (Marrs, et al., 1996). Further routes of absorption include the oral route should contaminated food or water be encountered (Vale, et al., 2007). Toxicity may be as a result of binding to acetylcholinesterase (with consequent toxic effects manifested from acetylcholine accumulation) or as a direct toxic effect from binding at non-acetylcholinesterase targets (including other enzymes and direct interaction with cholinergic receptors) (Pope, et al., 2005). Toxicity may be either delayed or prolonged due to storage within “reservoirs” such as the lung or skin before gradual release of the nerve agent (Clement, 1982;Kadar, et al., 1985).

1.5.4.2. Mechanism of action

The mechanism of action of all the organophosphorous nerve agents is similar; in that they have a high, broad spectrum affinity for serine based esterases. The acute deleterious effects produced by nerve agents revolve around the inhibition of the acetylcholinesterase (AChE) enzyme (Maxwell, et al., 2006). However, there are three known types of cholinesterase, namely, AChE, butrylcholinesterase (BuChE) and erythrocyte cholinesterase which are all inhibited by nerve agents (Naguib, 2003). Acetylcholinesterase (EC 3.1.1.7) (Figure 1.4) is located primarily in the central nervous system (CNS) both at cholinergic synapses and neuromuscular

junctions (Arrowsmith, 2007). The role of AChE in the nervous system is to terminate cholinergic neuro-transmission of the neurotransmitter acetylcholine (ACh) (Pope, et al., 2005;RamaRao and Bhattacharya, 2012). Under normal physiological conditions, the substrate of acetylcholinesterase is acetylcholine. Reaction of acetylcholine at the active site of acetylcholinesterase gives rise to acetylation of the serine residue, with choline (Ch) being cleaved. Acetylcholinesterase is then regenerated by loss of the acetate group. The entire process occurs in a few milliseconds (Silman and Sussman, 2005) as shown in reaction scheme (RS) 1:

$$ACh + AChE \rightarrow ACh.AChE\ complex \rightarrow Acetylated\ AChE + Ch$$
$$\rightarrow AChE + Acetate \ldots RS\ 1$$

When a mammalian system is compromised by the ingress of nerve agent (NA) by any absorption route, the reaction scheme depicted in Figure 1.5 occurs. The first step gives rise to an acetylcholinesterase - nerve agent complex occurring at a rate dependent on the nerve agent and defined by the acetylcholinesterase inhibition rate constant (K_i). Acetylcholinesterase bound within the complex may spontaneously reactive at a rate dependent on the nerve agent and defined by the reactivation rate constant (K_r). These two steps are defined by the reaction scheme:

$$NA + AChE \overset{K_i}{\rightarrow} Phosphylated\ AChE + X^- \overset{K_r}{\rightarrow} AChE + Alkoxy\ alkylphosphonate \ldots RS\ 2$$

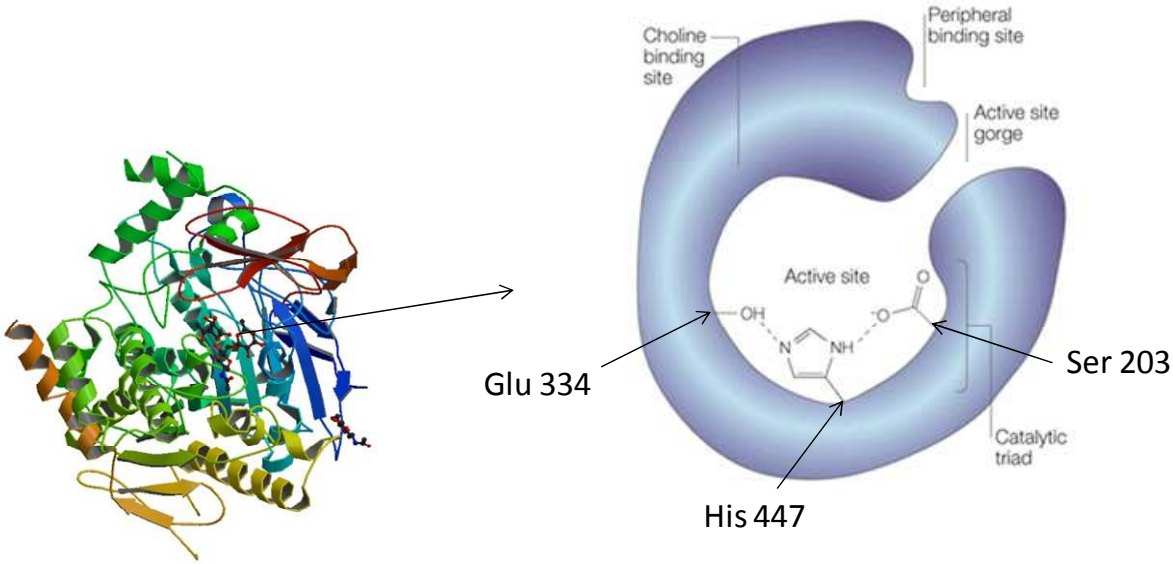

Figure 1.4: Left: Acetylcholinesterase (AChE) structure (ProteinBoxBot, 2007). Right: The active site of AChE contains residues of histidine, glutamic acid and serine, is located within a gorge where catalytic reactions may occur. Adapted from (Soreq and Seidman, 2001)

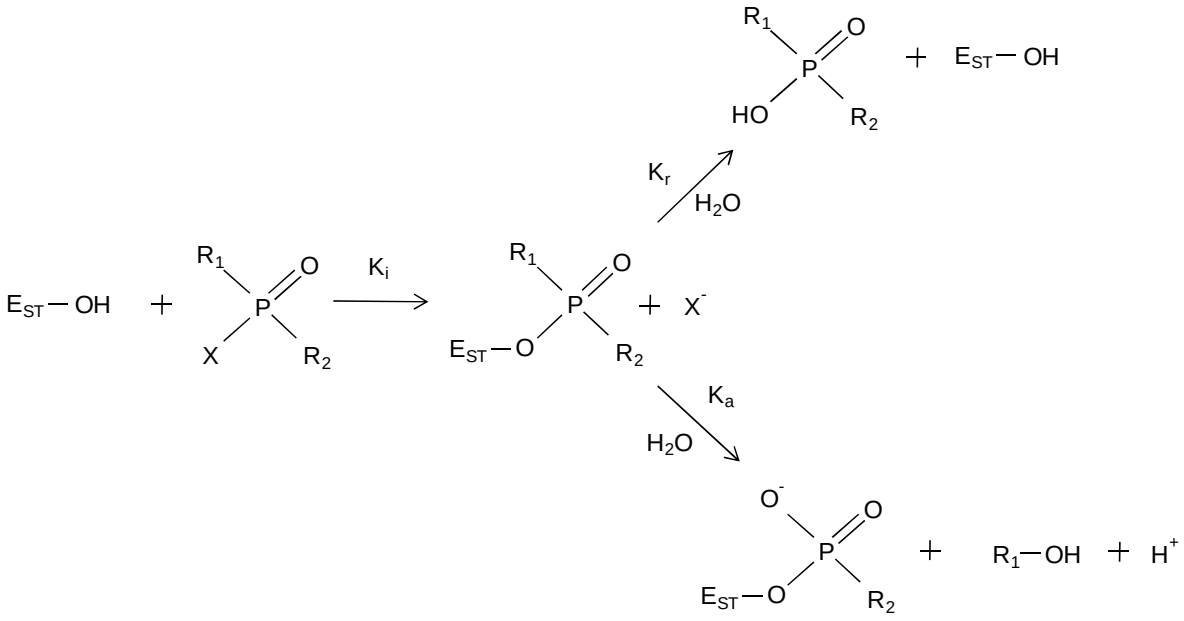

	K_i ($M^{-1}.min^{-1}$)	K_r (h^{-1})	K_a (h^{-1})
GA	$7.4 \pm 0.2 \times 10^6$	0	0.036 ± 0.001
GB	$2.7 \pm 0.1 \times 10^7$	0	0.228
GD	$9.2 \pm 0.4 \times 10^7$	0	6.6
GF	$4.9 \pm 0.006 \times 10^8$	0	0.099 ± 0.003
VX	$1.2 \pm 0.0002 \times 10^8$	0.021 ± 0.001	0.019 ± 0.001

Figure 1.5: Reactions of nerve agents with cholinesterase, where, E_{ST}-OH is endogenous cholinesterase. The groups R_1, R_2 and X attached to the nerve agent phosphorous atom are defined in Figure 1.3. The rate constants K_i (inhibition rate constant), K_r (spontaneous reactivation rate constant) and K_a (aging rate constant) are defined for GA, GB, GD, GF and VX (Worek, et al., 2004).

The most important reaction rate, as far as nerve agent toxicology is concerned, is the reactivation rate of AChE after its reaction with nerve agent. The dephosphylation reaction responsible for this proceeds at different rates for different nerve agents, and may be complicated by a further reaction, commonly described as “aging” (Figure 1.5). “Aging” involves the monodealkylation of the dialkyl-phosphonyl enzyme nerve agent complex which then becomes resistant to spontaneous reactivation and is an issue predominantly associated with Soman (GD). Soman has an "aging" half life of around 2 minutes after inhibition of human AChE (compared to Sarin (3 hours) and tabun (9 hours) (Worek, et al., 2005). The "aging" rate constants for individual nerve agents are defined in Figure 1.5.

For mammals suffering from nerve agent intoxication, reaction schemes one and two occur simultaneously as competitive reactions. The spontaneous reactivation rate of AChE after reaction with nerve agent is slow (in the order of hours to days). This can be compared to the reactivation rate of AChE after reaction with ACh which is rapid (in the order of milliseconds) (Silman and Sussman, 2005). Due to this, after reaction with nerve agent, the AChE is said to be inhibited. Reaction scheme 2 may be rewritten as reaction scheme 3, with a simplification to allow for the negligible reactivation of AChE after nerve agent complexation:

$$NA + AChE \xrightarrow{K_i} Phosphylated\ AChE + X^- \quad \dots RS\ 3$$

Inevitably this leads to a depletion of active AChE, and over time, depending on the amount of nerve agent present, the reaction schemes 1 and 3 may be combined and rewritten to account for AChE depletion (reaction scheme 4):

$$ACh + NA + Phosphylated\ AChE \rightarrow ACh + NA + Phosphylated\ AChE \ \ldots RS\ 4$$

The toxicological consequence of the AChE inhibition is that at the synaptic cleft (or neuromuscular junction) there is a rapid and unchecked accumulation of ACh.

If we consider the situation in the absence of nerve agent, reaction scheme 1 occurs without competition. Under these circumstances, the normal physiological role of acetylcholine hydrolysis by acetylcholinesterase occurs rapidly. In this situation, nerve impulses are transmitted from one synapse across the synaptic cleft by acetylcholine to the second synapse. After cholinergic transmission has been completed, the acetylcholine is released from the receptors to be hydrolysed by acetylcholinesterase. This break down terminates the effects of the nerve impulse. In the presence of nerve agent, reaction scheme 3 predominates. The phosphylated AChE is rendered unable to hydrolyse ACh (a situation termed as nerve conduction block). The accumulation of ACh in the synaptic cleft leads to a prolongation and intensification of the cholinergic effects, giving rise to the observed clinical manifestations of nerve agent poisoning, which include miosis, fasciculation, seizures, paralysis, apnoea and death (Marrs, et al., 1996;Friedewald, 2008).

1.5.4.3. Clinical manifestations

The classical clinical manifestations of nerve agent poisoning are related to the effects of acetylcholine accumulation at the cholinergic receptors (Masson, 2011). The cholinergic receptors are subdivided into muscarinic and nicotinic receptors (based on their sensitivity to muscarine and nicotine respectively) (Rang, et al., 1999). It is clear that nerve agent poisoning, via disruption of cholinergic transmission has consequences throughout the nervous system of a mammalian organism and not just at the central nervous system. These consequences may be grouped by receptor type and specific organ system effects. Muscarinic receptors are located in parasympathetic effector organs and may be divided into a number of subtypes which have different actions and are found in different locations. Briefly, M_1 receptors are found in neuronal tissue, M_2 receptors in the heart, M_3 receptors in glandular tissue, M_4 receptors in the striatum and M_5 in the brainstem and hippocampus (Marrs, et al., 1996). Muscarinic effects mediated by nerve agents can be split between glandular specific effects e.g. salivation, lacrimation, sweating, rhinorrhea and smooth muscle specific effects e.g. miosis, diarrhoea and bradycardia. Nicotinic receptors are ligand gated ion channels located in autonomic ganglia and skeletal muscle. Nicotinic effects mediated by nerve agents can be split between autonomic ganglia effects e.g. pallor, tachycardia, hypertension and skeletal muscle effects e.g. fasciculation. Mention must also be made of nerve agent effects which are not mediated via AChE. As previously raised, nerve agents have broad spectrum affinity for esterases and may even have a direct effect on muscarinic and nicotinic receptors. Other signal transduction pathways that are also susceptible to nerve agent effects include calcium signalling, protein kinase C, MAP kinase, transcription

factors, cytoskeletal proteins, oxidative stress and the immune system (RamaRao and Bhattacharya, 2012) .

1.5.4.4. Specific organ system effects

Nerve agent exposure via the respiratory route affects both mucous glands and smooth muscle (Marrs, et al., 1996). Glandular response gives rise to increased secretion manifesting in the forms of salivation (secretion from the mouth) and rhinorrhea (secretion from the nose). Smooth muscle effects are exhibited in the form of bronchospasm (coughing) and bronchoconstriction (wheezing, tightness in chest, dyspnoea). Muscular effects such as fasciculation, sweating and tremor are typical signs of nerve agent toxicity that may be located at the site of absorption (in the case of percutaneous poisoning) or as a result of more generalised systemic poisoning. The response of the eye to nerve agent challenge is that of miosis (constriction of the pupil). Low vapour concentrations may elicit this response (Genovese, et al., 2008), for which onset is rapid (in the order of minutes) and can take days to resolve (dependent upon dose) (Vale, et al., 2003;Yanagisawa, et al., 2006). Miosis is traditionally seen as an indicator to nerve agent vapour exposure, although, interestingly, miosis may still occur even if the eye is not directly exposed and is exhibited via systemic toxicity (Chilcott, et al., 2003). Further eye effects may be exhibited through the lachrymal gland (lacrimation) and the ciliary muscle (spasm). Eye effects are mediated via the muscarinic receptor. Due to potential muscarinic and nicotinic effects overlapping, cardiovascular effects may include either tachycardia or bradycardia (Friedewald, 2008).

1.5.4.5. Progression of injury

Progression of nerve agent intoxication will primarily depend on the route of absorption and the dose received, however, progression from mild to severe intoxication generally proceeds as: local effects such as ocular, respiratory and musculature effects which progresses onto cardiovascular and CNS effects including respiratory depression, apnoea and death.

1.5.4.6. Diagnosis and treatment

Survival of the acute cholinergic crisis caused by nerve agent ingress into the body will depend on a multitude of factors, including whether the correct diagnosis has been obtained and whether appropriate treatment has been given. Other than the signs and symptoms described, one of the routine methods available for diagnosis of nerve agent poisoning is whole blood cholinesterase determination (Zilker, 2005). Whole blood contains both erythrocyte cholinesterase (acetylcholinesterase within red blood cells) and butrylcholinesterase (within the plasma). As acetylcholinesterase is the enzyme affected by nerve agents at the neuromuscular junction and synapse, estimation of its depression using whole blood cholinesterase measurements is of great utility. Links have previously been made between percentage ChE inhibition and signs and symptoms of nerve agent poisoning (Chilcott, et al., 2003;Maxwell, et al., 2006;Murnford and Troyer, 2011;Hamilton, et al., 2004;Joosen, et al., 2008).

Research into medical countermeasures to treat nerve agent poisoning has been ongoing for at least sixty years, during that time significant advances have been made which support the currently practiced treatment regimes (Hamilton and Lundy, 2007). Treatment of nerve agent poisoning consists of two phases, immediate (first aid) treatment and decontamination which may be given close to the site of the exposure, followed by further pharmacological intervention and patient management in a hospital environment until the signs and symptoms of nerve agent toxicity have abated. Immediate decontamination may take place using an absorbent powder such as fullers' earth and / or using a decontaminant showering system depending on whether the incident takes place in a military or civilian scenario (Riley, 2003). Immediate pharmacological intervention (for military scenarios) is administered in the form of the combopen which contains a number of drugs which can alleviate nerve agent toxicity. The UK military issue combopen (Vale, et al., 2003) contains a muscarinic antagonist, an oxime and an anticonvulsant, namely, atropine, pralidoxime and avizafone (a diazepam pro drug). Atropine acts by blocking the action of acetylcholine at the muscarinic receptor and alleviates the muscarinic effects of nerve agent poisoning (Thiermann, et al., 2011). Oximes (Thiermann, et al., 1999;Kassa, 2002;Worek, et al., 2007) comprise a group of pyridinium ring containing compounds which react with phosphorylated acetyl cholinesterase, removing the phosphyl moiety from the active site thereby enabling the acetyl cholinesterase to resume its normal physiological function according to the reaction scheme:

$$Phosphylated\ AChE + Oxime \rightarrow AChE \ldots RS \quad 5$$

As acetylcholinesterase is regenerated by the oxime, the reliance on atropine blockading the effects of excess acetylcholine diminishes. Unfortunately, the efficacy of acetylcholinesterase regeneration by the oxime is nerve agent specific (Worek, et al., 2004) and governed by the time post nerve agent exposure it can be administered. It should be noted that soman is particularly resistant to oxime therapy due to aging effects. The final drug housed within the combopen is avizafone, a pro drug of the anticonvulsant, diazepam. Seizures attributed to nerve agent poisoning can be severe, resulting in permanent damage or death to the casualty (Myhrer, 2007). The use of an anticonvulsant can prevent or lessen the severity of seizures. After a casualty has received immediate treatment, been decontaminated and moved to suitable facilities, supportive care in the form of artificial ventilation with additional oxygen may be required along with further drug therapy (atropine, oxime, anticonvulsant) which can be tailored to the specific nerve agent if its identity is known (Zilker, 2005).

Ideally, medical countermeasures against nerve agents should be evaluated against all the nerve agents they are envisaged to be needed to protect against. Realistically, for the timescales of the current programme this would not have been technically feasible. Instead, representative agents from each class were chosen on the basis of those representing the greatest percutaneous toxicity. From the G series, soman (GD), was selected for evaluation.

1.5.5. Soman

Soman belongs to the “G” series of nerve agent and is commonly referred to as GD. This series of nerve agent were developed during the Second World War by German scientists, with soman first synthesised in spring 1944. A detailed history of the development of the “G” series of nerve agents has been compiled by Schmaltz, (Schmaltz, 2006). Although rare, a documented case of accidental poisoning in man by GD is cited in the literature (Sidell, 1974). The structure of GD is shown in Figure 1.6. It is important to note that GD possesses two chiral centres in the molecule , one at the carbon in the pinacolyl moiety and one at the phosphorous atom, it is therefore found as a mixture of four stereoisomer’s (same molecular formula and sequence of bonded atoms, differing only in the three dimensional orientations of their atoms).

Soman (GD)

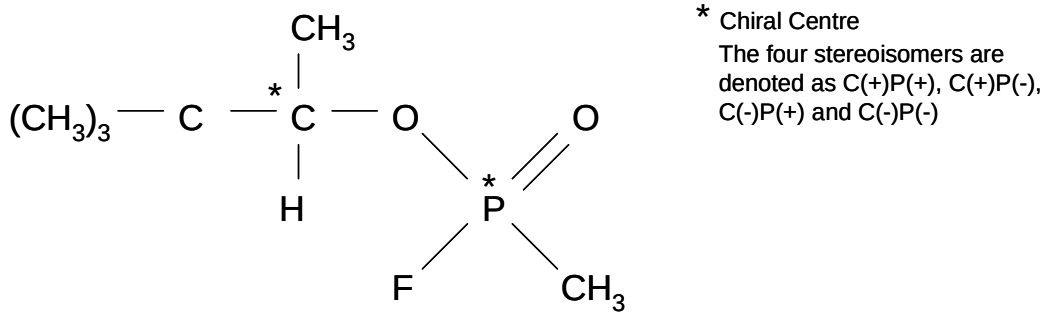

Pinacolyl methylphosphonoflouridate

Figure 1.6: Structural Formula for Soman including identification of chiral centres. As indicated, soman exists as four stereo isomers.

Under the Cahn-Ingold-Prelog priority rules (CIP) the stereoisomer's are designated R_CR_P, R_CS_P, S_cR_P and S_CS_P. The optical activity notation C(+)P(+), C(+)P(-), C(-)P(+) and C(-)P(-) may also be used, with C denoting chirality in the 1,2,2-trimethylpropyl moiety. The second notation system has been adopted for the purpose of this thesis. The isomers exhibit differing biological activities. The P(-) isomers have been found to exhibit a greater *in vivo* toxicity and more readily inhibit AChE than the P(+) isomers (Benschop, et al., 1981;Benschop, et al., 1984;Little, et al., 1989). The four stereoisomer's comprise of two pairs of enantiomer's (mirror image, but not super imposable) and two pair of diastereoisomer's (not a mirror image, not super imposable) shown in Figure 1.7.

1.5.5.1. Absorption of GD

At room temperature GD exists as a volatile liquid which is colourless and odourless in its pure state. The physicochemical properties of GD are shown in Table 1.4. As a chemical with a significant volatility, the most likely mode for exposure is scenario dependent, with absorption of GD likely to occur via the respiratory and percutaneous routes. This thesis particularly considers the dermal route of absorption.

1.5.5.1.1. Percutaneous absorption of soman

In the liquid phase, absorption of soman can occur across the skin to exert systemic toxicity without producing a local effect. The skin does, however, possess esterases which are able to metabolise GD whilst percutaneous absorption is in progress in a

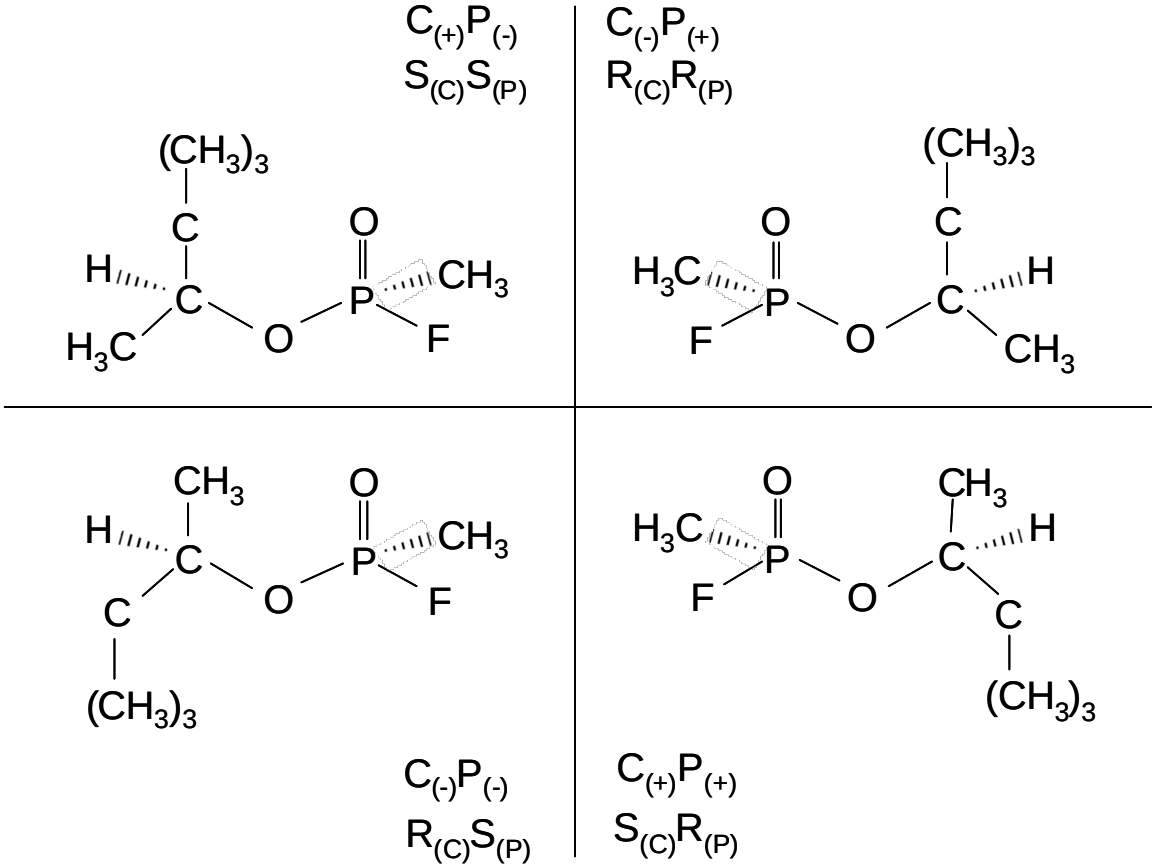

Figure 1.7: The four stereoisomer's of soman. The two pairs of enantiomer's are separated by the vertical line. The two pairs of diastereoisomer's are separated by the horizontal line. Both CIP and optical activity notation are used to describe each stereoisomer.

Soman (GD)				
Formula	**CAS No.**	**Mol. Wt.**	**State**	**Colour**
$C_7H_{16}FO_2P$	96-64-0	182.18	Liquid	Colourless
Melting Point	**Boiling Point**	**Density**	**Vapour Pressure**	**Volatility**
- 42 ºC	198 ºC	1.022 @ 25 ºC	0.40 @ 25 ºC	3900 mg m^{-3} @ 25 ºC
Vapour Density	**Water Solubility**	**Hydrolysis Rate**	**Log K_{ow}**	**Log K_{oc}**
6.3 (air =1)	21 g L^{-1} @ 20 ºC	45 h $T_{1/2}$ @ pH 6.6	1.78 a 1.824 b	1.17

Table 1.4: Identity and physicochemical properties of soman adapted from Munro (Munro, et al., 1999). Where, log K_{OW} is the log of the octanol water partition coefficient, log K_{OC} is the log of the organic carbon partition coefficient. Log K_{OW} value “a” obtained from (Benschop and Wesselman, 1989), Log K_{OW} value “b” obtained from (Czerwinski, et al., 1998).

number of species including mouse skin (van Genderen, et al., 1985), guinea pig skin (Fredriksson, 1969b;van Hooidonk, et al., 1980) and human skin (van Hooidonk, et al., 1980). Species differences in the rate of soman skin absorption have been shown, with human skin being less permeable than mouse skin (van Genderen, et al., 1985).

1.5.5.2. Mechanism of action

A number of esterases that are present in the blood and nervous tissues of mammals and are subject to inhibition by soman. These include butrylcholinesterase, erythrocyte cholinesterase and acetylcholinesterase. Although the inhibition of acetylcholinesterase gives rise to the clinical manifestations of soman poisoning, all of the named esterases are inhibited. The effect of soman acting on multiple esterase species means that it may be classified as a broad spectrum esterase inhibitor. One positive consequence of this, is the systemic removal of soman by esterases other than acetylcholinesterase, giving a reduction in the amount of soman being available to reach and subsequently bind and inhibit AChE to give deleterious toxic effects. Sterri and co-workers conducted a comparison of blood versus brain cholinesterase inhibition in the guinea pig after intravenous, subcutaneous and percutaneous exposure to soman (Sterri, et al., 1982). The results showed that total inhibition of erythrocyte cholinesterase was almost completed within 1 minute for an intravenous challenge, by 60 minutes for a subcutaneous challenge or between 90 to 120 minutes for percutaneous challenge. However, for all the exposure routes, brain acetylcholinesterase inhibition although high was not complete.

For soman that binds with acetylcholinesterase, soman rapidly loses a fluoride ion and phosphoylates the serine residue within the acetylcholinesterase active site. Of the nerve agents, soman is most subject to rapid aging (Section 1.5.4.2.). A phenomenon which results in permanent inactivation of acetylcholinesterase and for soman occurs within a few minutes of binding to AChE according to reaction scheme:

$$Phosphylated\ AChE \rightarrow Permanently\ deactivated AChE \ldots RS\ 6$$

Once aging has occurred, soman is no longer amenable to oxime therapy (Section 1.5.4.6.).

1.5.5.3. Distribution

Soman distribution to the blood supply from an intra muscular injection is rapid (Traub, 1985). From the vasculature, soman is primarily distributed to the highly vascularised organs including the liver, lung and kidney where it can remain for prolonged periods of time. Shih and co-workers were able to detect GD metabolites within the lung of rats for several days (Shih, et al., 1994). The binding of GD to tissue proteins in rats was determined to follow the order lung >> kidney > liver > brain > diaphragm (Fleisher and Harris, 1965). Due to its action as a broad spectrum esterase inhibitor, concentrations of soman in the brain are typically one hundred times lower than in the highly vascularised organs, however, even these amounts are sufficient to begin distributing to the cerebrospinal fluid (CSF) by two minutes. Traub

made the following observations whilst following the time course of soman interaction with the brain: By two minutes, brain nuclei were contaminated (indicating binding processing occurring from either GD or its metabolites). By thirty two minutes there was an observable shift from general neocortical and hippocampal labelling to a pattern that implicated cellular uptake rather than neutrophil uptake. At no point did the lipid rich sites (myelinated structures) accumulate GD or its metabolites. By 48 hours, soman was associated predominantly to caudate and accumbens nuclei (in comparison with other brain areas) (Traub, 1985).

1.5.5.4. Toxicity of soman

The toxic effects caused by soman have been studied in a number of species including rats, cats and cynomolgus monkeys (Petras, 1994). Across all these species the following symptoms have been observed; generalised muscle fasiculations and tremor, uncoordinated movements, convulsions, respiratory distress and excessive salivation. Soman induced seizures have been linked with muscarinic receptor activation (section 1.5.4.3.) which gives rise to a cascade of biochemical events that culminate in a glutamate driven limbic static epilepticus (Pazdernik, et al., 2001). As a result of this, brain damage has been found to be caused by soman in all species. It has been postulated that humans surviving GD exposure may experience long term nervous system damage with impairment of skilled movement, posture, locomotion, cognition, psychiatric disorders and autonomic regulation. It is likely that the mechanism for these neurotoxic effects are linked with ischemic hypoxia, cellular ischemia or direct soman neurotoxicity (Petras, 1981). Diurnal variation has

previously been observed with soman toxicity with lethality highest at 10am and lowest at 6pm. These timings correspond closely with periods of greatest and least physical activity. Perhaps unsurprisingly, brain cholinesterase levels were lowest at the time of greatest GD toxicity (Petras, 1994). The effect of environmental temperature can also modify soman toxicity, with conditions of thermal stress, both hot (31ºC) and cold (-1ºC) increasing soman toxicity (Wheeler, 1987;Wheeler, 1989). The likely reason for this is that the thermoregulatory system is effectively neutralised for multiple LD_{50} GD exposures, meaning that the body is unable to respond to temperature extremes whilst poisoned with GD.

1.5.5.5. Metabolism and elimination

The three major pathways for detoxification of soman include phosphylation of esterases and other proteins, enzymatic hydrolysis by phosphorylphosphatases and spontaneous hydrolysis (Reynolds, et al., 1985). The importance of each pathway for the four stereo isomers of GD have been studied by Benschop (Benschop, et al., 1987). Essentially, enzymatic hydrolysis was the major pathway for P(+) isomers whilst the more toxic P(-) isomers proceed via an irreversible phosphylation pathway. Work by Shih supports this theory, with P(+) isomers being metabolised quickly (enzymatic hydrolysis) (Shih, et al., 1994). Briefly, there was a slower hydrolysis phase for P(-) isomers with incomplete recovery (due to irreversible protein binding). Van Dongen studied soman metabolism using guinea pig, human and mouse skin homogenates. The data indicated that P(+) isomers were metabolised by skin enzymes, whereas, P(-) isomers were not (as they did not differ from spontaneous

hydrolysis rate constants) (van Dongen, et al., 1989). Soman administered subcutaneously in rats has been shown to be absorbed and distributed rapidly, with detoxification and elimination due to a combination of enzymatic and spontaneous hydrolysis combined with irreversible phosphorylation. Due to irreversible phosphylation, metabolite pharmacokinetics gave a slower, complex and incomplete elimination pattern when compared with sarin and GF (Shih, et al., 1994).

1.5.5.6. Decontamination of soman

Pathways for the decontamination of chemicals include hydrolysis, thermolysis and photolysis. Soman is moderately soluble in water with half lives of the order of 24 hours. GD breaks down into a number of hydrolysis products (Munro, et al., 1999), at a rate which is dependent upon factors including pH and temperature (Broomfield, et al., 1986). Between pH 4 and 6 hydrolysis is minimal and constant, however, below pH 4 the hydrolysis rate increases exponentially with a more concentrated solution degrading more rapidly than a dilute solution. For example, a 2 mg ml^{-1} solution in distilled water was 62% degraded by 24h (Shih and Ellin, 1984). Initially, hydrogen fluoride (molecular weight 20.01) is released to give pinacolyl methylphosphonic acid (molecular weight 180.18, Log K_{OW} 1.63). Subsequent cleavage results in breakdown to 3,3-dimethyl-2-butanol (molecular weight 102.18, Log K_{OW} 1.48) and methylphosphonic acid (molecular weight 96.02, Log K_{OW} 0.70) (Figure 1.8). As for thermolysis and photolysis, soman and its hydrolysis products are thermally stable at temperatures less than 49ºC and soman and its hydrolysis products exhibit no significant phototransformations in sunlight.

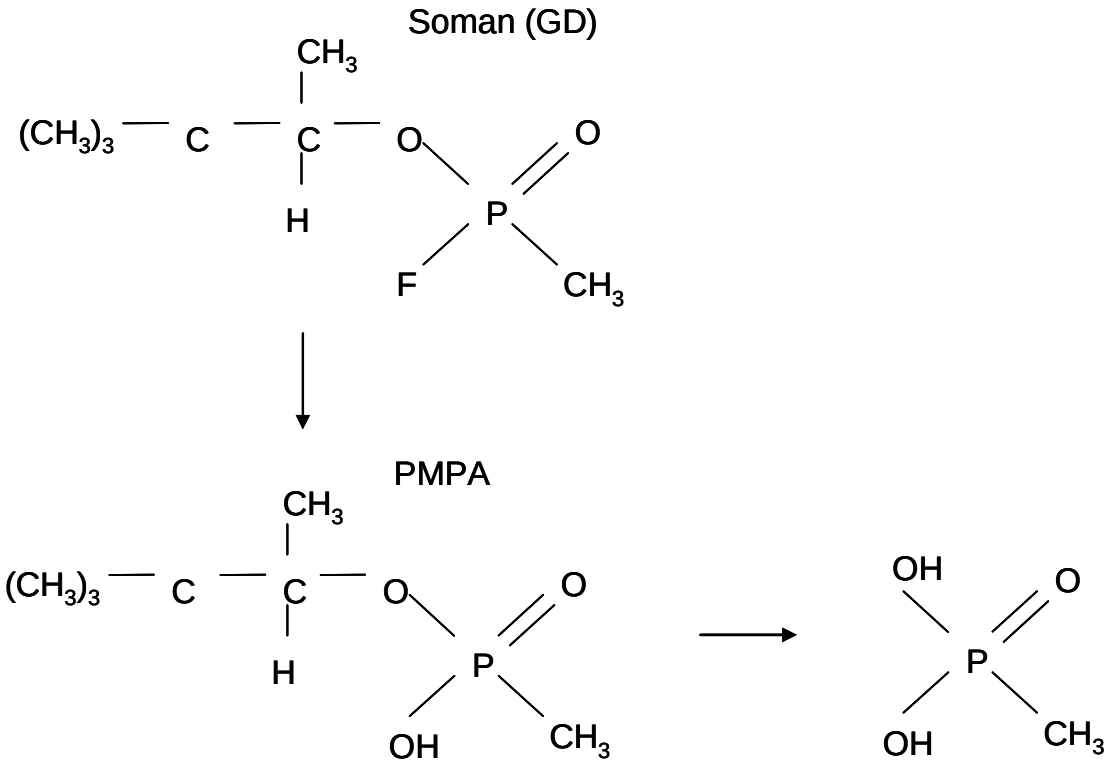

Figure 1.8: Hydrolysis pathway for soman. Initially, hydrogen fluoride is released to give pinacolyl methylphosphonic acid (PMPA). Subsequent cleavage results in breakdown to 3,3-dimethyl-2-butanol (not shown) and methylphosphonic acid.

1.6. Skin research methodology

The primary aim of the work conducted in this thesis was to evaluate the efficacy of existing commercial off the shelf (COTS) haemostatic products as skin decontaminants for chemical warfare agents. An effective product must have utility as a decontaminant not only on undamaged (normal) skin and physically damaged skin, but, also retain its haemostatic efficacy in haemorrhaging wounds. The toxic nature of chemical warfare agents ethically and morally precludes the use of human volunteers for such studies leading to the need to use other appropriate techniques. Such techniques can include *in vivo* animal models or *in vitro* models, ideally in combination so that the 3Rs (Reduction, Refinement and Replacement) of scientific animal experimentation can be strictly adhered to. This section will provide a review of the function and morphology of skin along with the techniques available for measuring percutaneous absorption.

1.6.1. The skin

The skin is the largest organ in the body by weight, representing around 4% of the bodies mass (Cevc and Vierl, 2010), and, at the simplest level, can be viewed as one of the major interfaces between an organism and the environment within which the organism is situated. In other words, the structure and function of the skin depends on the environment of the species. As a major interface with the environment, the skin has an important role not only in protecting the organism from external deleterious insults, but also, in the life support mechanism of the organism. These functions enable the prevention of systemic and widespread localised damage, but,

can be overwhelmed if severe damage is inflicted with the resultant manifestation of acute or chronic injury. The functions of the skin are many and diverse, but may be classified broadly into defensive and supportive functions. Defensive functions can be assigned as antimicrobial, immune, prevention of percutaneous penetration, physical, thermal and ultraviolet. Life support functions may be classified into temperature regulation and prevention of catastrophic water loss (Lee, et al., 2006).

Barrier function at the boundary with the environment is essential for the maintenance of both temperature (via sweat and arteriovenous anastomoses) and electrolyte and fluid balance (with water and nutrients being retained within the organism). Conversely, toxic environmental substances, viruses and bacteria are, to a certain extent, prevented entry. Where entry occurs, the skin is capable of xenobiotic metabolism.

The skin is a sensory organ (touch and pain) capable of surveillance and action, responding to mechanical force and transmitting contact with the external world. The skin synthesises, processes and metabolises proteins, lipids and signalling molecules and is an integral component of the immune, nervous and endocrine systems. Further important functions include protection from physical damage, protection from ultra violet light (via melanocytes), automatic repair (wound healing) by continuous cell turnover, acting as a blood reservoir and being the site for Vitamin D synthesis.

1.6.2. Skin morphology

Histologically, human skin can be subdivided into three main layers, namely the epidermis, dermis and hypodermis (Rushmer, et al., 1966), throughout which cutaneous appendages are spaced at irregular intervals (Figure 1.9). These in turn can be further subdivided into individual cell types and functions (Urmacher, 1990). The epidermis is the outermost layer of the skin, covering an area of 2 m^2 (Hadgraft, 2001) averaging between 0.06 and 0.1 mm thick across the human body except for the palm and sole where it exceeds 0.5 mm (Hsia, 1971). The epidermis comprises two distinct layers, the stratum corneum which comprises the upper 5 – 20 µm of the epidermis and the viable epidermis which comprises the lower 50 – 100 µm that is in direct contact with the dermis (Figure 1.10) (Holbrook and Odland, 1974). The dermis is a thicker layer of supportive, viable, connective tissue with nerve, lymphatic and vascular networks that on average is between one and two mm thick (although the boundary between this and the innermost layer of subcutaneous tissue is ill defined with no definite border, (Hsia, 1971)). The dermis is the source of cutaneous appendages such as hair follicles, sweat glands and sebaceous glands. The subcutaneous tissue (or hypodermis) is in direct contact with the dermis and averages a thickness of one to two mm and consists of lobules of fat cells. The morphology of the skin defines how the skin acts as an effective barrier to the percutaneous penetration of xenobiotics, with the outward facing stratum corneum representing a substantial barrier (Figure 1.11).

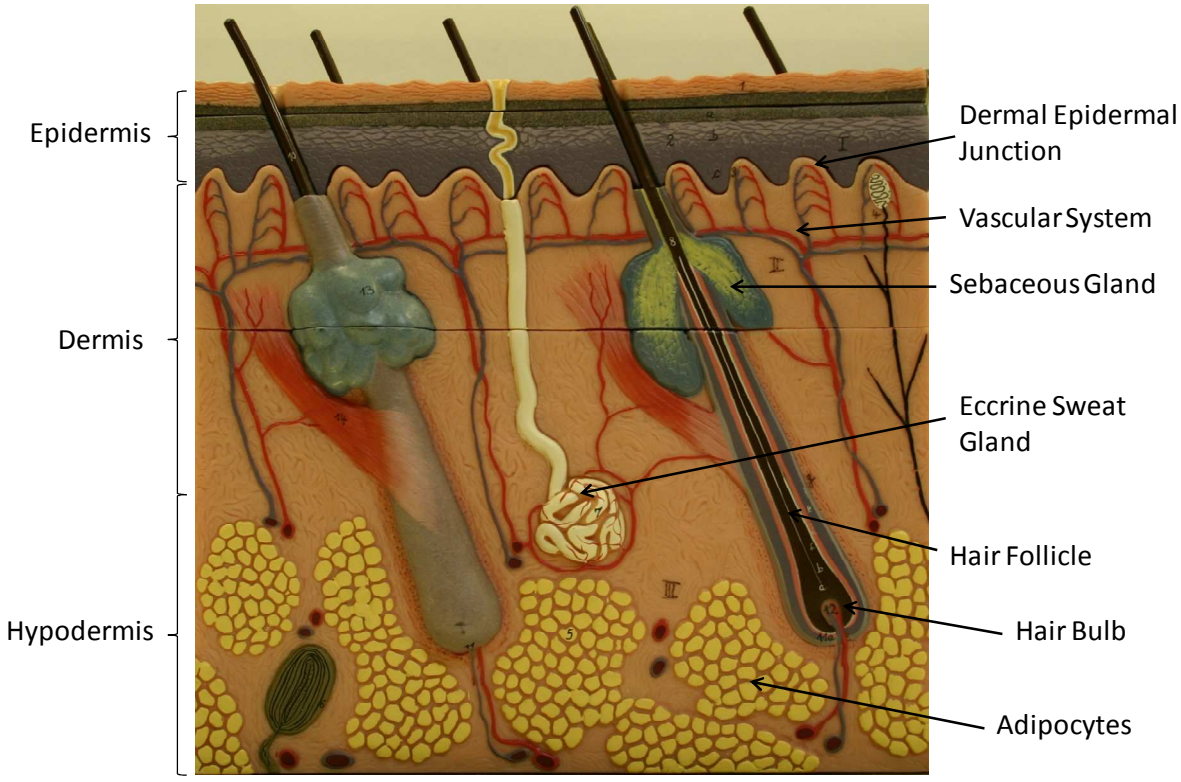

Figure 1.9: Schematic cross section through human skin. The subdivision into the three major layers: epidermis, dermis and hypodermis are indicated along with the major structural components. Photograph of Adam Rouilly skin section block model, Kent, UK.

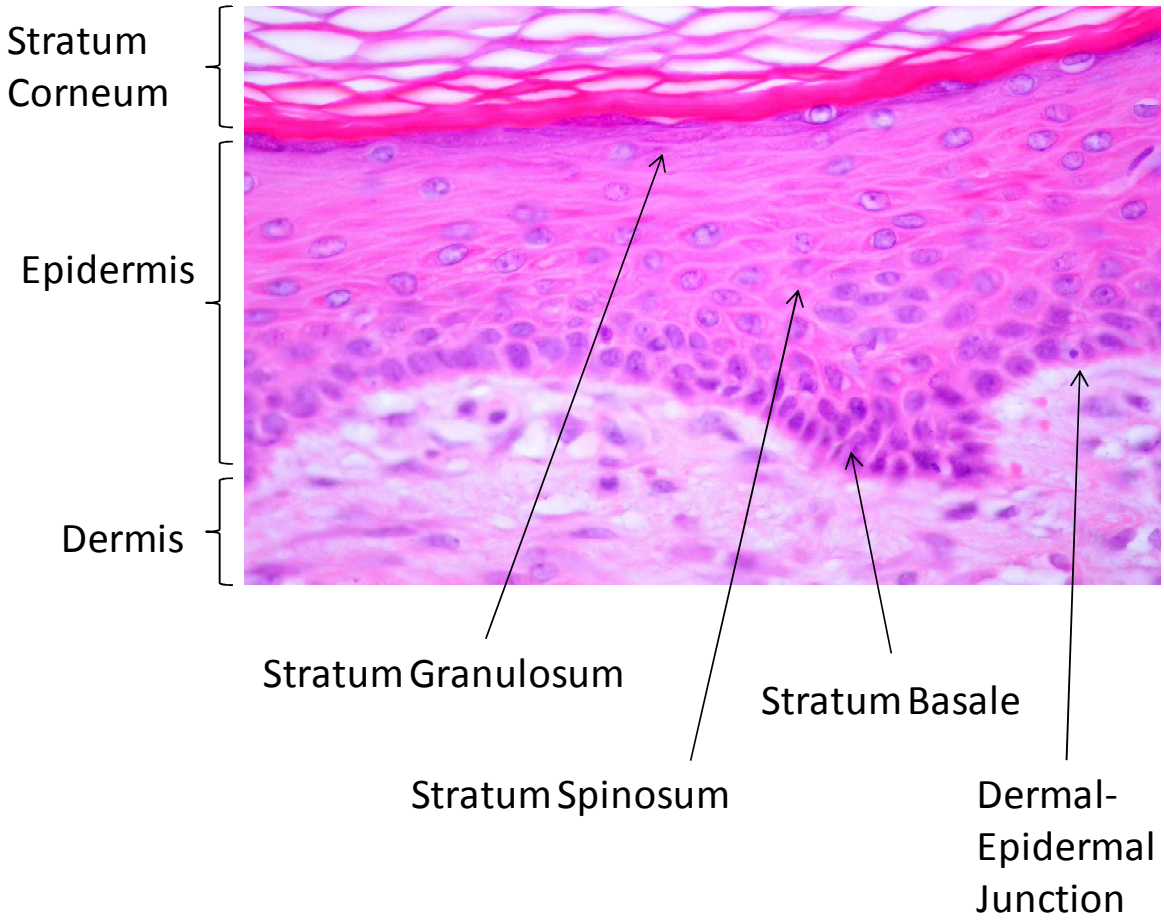

Figure 1.10: H&E staining of human skin. The main layers of the skin are indicated. Keratin and erythrocytes stain red, the cytoplasm stains pink and cell nuclei stain blue.

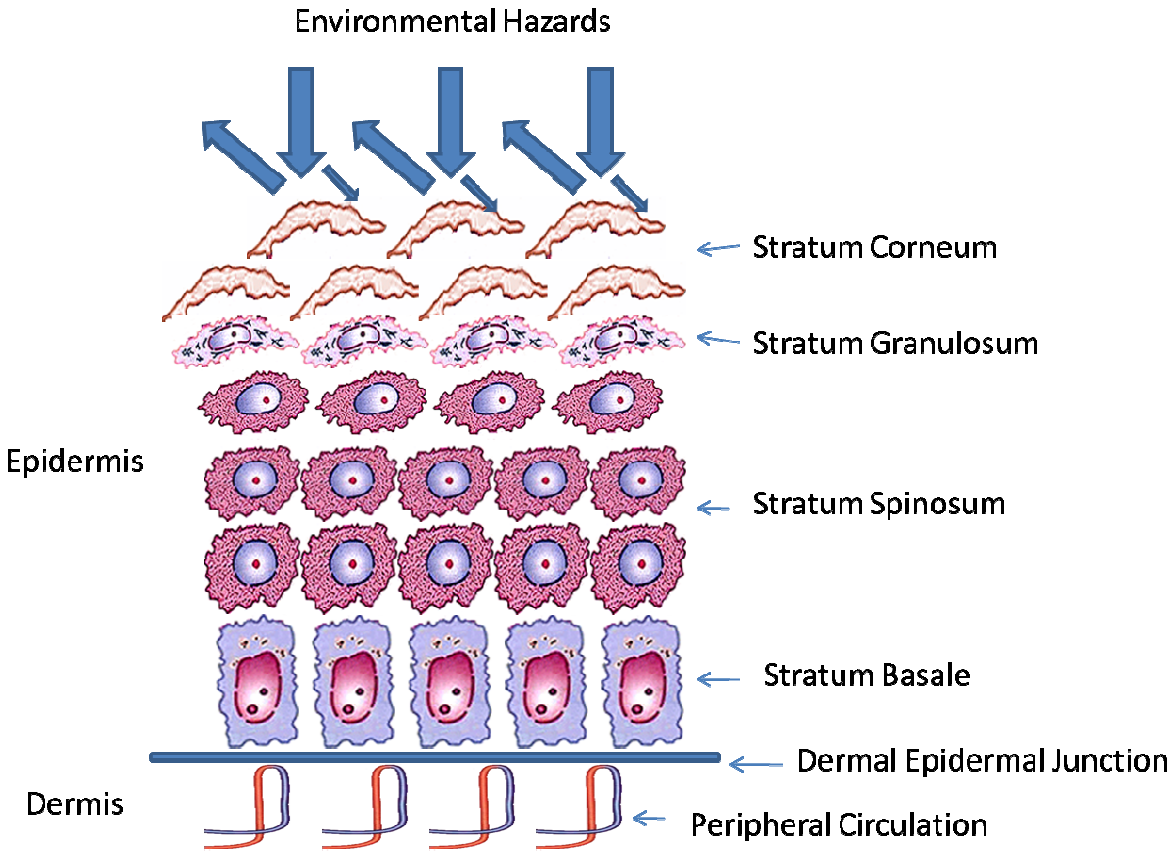

Figure 1.11: Simplified diagram of the epidermis (defining individual cell layers), dermal epidermal junction and upper dermis. For a hazardous chemical present in the environment to reach the peripheral circulation and from there systemic toxicity, the stratum corneum must first be breached. Note: skin appendages are not shown on this diagram.

1.6.3. The epidermis

The epidermis comprises keratinocytes, melanocytes, Langerhan's cells and Merkel cells, each of these cell types have specific roles in the maintenance or protective function of the epidermal layer. The keratinocytes synthesise the stratum corneum, via a process of apical migration and comprise approximately 95 % of the epidermal layer (Menon, 2002). Melanocytes are involved with the skins pigmentation (Wickett and Visscher, 2006), Langerhan's cells are involved with antigen presentation and immune responses (Callard and Harper, 2007) and Merkel cells are involved with sensory perception (Schaefer and Redelmeier, 1996).

1.6.3.1. The stratum corneum

The outermost extremity of the epidermis is the stratum corneum or horny layer. The stratum corneum is the non viable epidermis comprising a number of cell layers of flattened, stacked, hexagonal cornified cells (measuring 15-25 µm thick) that are in direct contact with the environment (Hadgraft, 2001). Anatomical location dictates the number of cell layers with genital skin having the least layers (4 to 8 layers) followed by the face, neck and scalp (7 to 14 layers) and extremities (12 to 19 layers). The palm and soles have (23 to 71 layers) and the heels have the greatest number of layers (50 to 122 layers) (Ya-Xian, et al., 1999). Individual corneocytes have a diameter of 20 to 40 µm and are 0.5µm thick (except for the palms and soles where the thickness increases by approximately 10 fold) and contain 70% insoluble bundled keratin by weight. The corneocytes origin can be traced back to an individual basal cell in the basal layer that is the interface between the epidermis and dermis (Cevc,

1996). Cell nuclei and other cellular organelles are absent in the stratum corneum. Skin hydration is low (10 – 30%) compared to that of the body (70%) (Menon, 2002).

The extracellular region surrounding each corneocyte contains a variety of lipids and desmosomes which allow for effective cohesion between corneocytes. Desmosomes are intercellular junctions that provide strong adhesion between cells (Garrod and Chidgey, 2008). Corneodesmosomes, the desmosomes that join the corneocytes differ from those that join epidermal keratinocytes by the addition of the protein corneodesmosine (Wickett and Visscher, 2006). These intercellular tight junctions provide strong adhesion between the corneocytes and give the stratum corneum its rigid structure. Corneodesmosomes are gradually digested by proteases (including desmosglein I and stratum corneum chromotryptic enzyme (SCCE) leading to desquamation (Wickett and Visscher, 2006). Both the corneocytes and the intercorneocyte lipids are derived from keratinocytes through the terminal differentiation process. For normal skin the process of desquamation, the time for complete turnover of epidermal cells, takes from two to three weeks, however, disease states such as psoriasis can lower this to two to four days leading to substantially impaired barrier function (Lebwohl and Herrmann, 2005).

The extracellular lipid matrix can be categorised into three main groups; cholesterol, ceramides and free fatty acids, accounting for approximately 90% of the lipid weight in the stratum corneum (Feingold, 2007). Cholesterol derivatives include cholesterol esters (2 - 5 % of SC lipids), free cholesterol (27 % of SC lipids) and cholesterol

sulphate (3% of SC lipids) (Wilkinson, 2008). Ceramides comprise over 40% of SC lipids and can be subdivided into a number of ceramide classes. The number of known ceramide classes have increased from nine (Bouwstra and Ponec, 2006) to eleven (Masukawa, et al., 2008) to the current number of twelve (van Smeden, et al., 2011), referred to as CER 1 to 12, they have small head groups that can form lateral hydrogen bonds with adjacent CERs. The tail groups of the CERs typically have a chain length of C24-C26 although a small fraction have a chain length of C16-C18 (Bouwstra, et al., 2003). Fatty acids account for a further 9 % of SC lipids with the remaining 11% accounted for by triglycerides and others (Wilkinson, 2008). The spatial arrangement of these lipids is to form bilayers with aqueous and lipid domains consisting of hydrophilic head groups and lipid tail groups of 6 nm and 13 nm periodicity, stacked as lamellae as defined in the sandwich model (Bouwstra, et al., 2003).

1.6.3.2. The viable epidermis

The stratum granulosum comprises increasingly flattened cells from one to three layers thick containing keratohyalin granules. The thickness of this layer can be seen as representative of the keratinisation rate, with the stratum granulosum largely absent in disease states such as psoriasis. Keratohyalin granules themselves are dense irregular amorphous deposits which lie along keratin filaments. They are found not only in the stratum granulosum but also the stratum spinosum, and comprise profilaggrin, loricin, cystatin A and keratins K1 and K10. Loricin and cystatin A are components used to construct the cornified cells. Profilaggrin, a highly

phosphorylated, histidine rich basic protein forms filaggrin within the granular layer (McGrath and Uitto, 2008). Filagrin aggregates along keratin filaments and undergoes proteolysis within the stratum corneum to release amino acids which act to retain epidermal moisture (Hsu, et al., 2008).

The stratum spinosum comprises layers of polyhedral cells which begin to flatten as they approach the stratum granulosum. The stratum spinosum is rich in desmosomes which connect adjacent cells, giving rise to the layers alternative name, the prickle cell layer. The process of keratinisation begins in this layer with the synthesis of keratin filaments K1 and K10. Lamellar bodies of size 0.1 x 0.5µm (also known as Odland bodies or keratosomes) appear within keratinocytes in the stratum spinosum layer and are the main source of skin lipids, occupying 20% volume of the keratinocyte. These lipids are arranged as striated sheets containing acyl ceramide, acylglucoceramides, phospholipids, free sterol and cholesterol sulphate. A number of enzymes are also present in the lamellar bodies and include acid hydrolase, sphingomyelinase and phospholipase A2.

The stratum basale comprises a single layer of cuboidal cells which adhere to the basement membrane via hemidesmosomes. In disease states this layer may be two or three layers thick. The stem cell keratinocyte population is contained in this layer along with melanoctyes which are primarily located in the stratum basale.

The basement membrane between the epidermis and dermis is an irregular layer due to upward indentations by dermal papillae and is typically 50 to 70 nm thick. It comprises two layers, the lamina densa and lamina lucida which contain type IV collagen (for mechanical stability) and laminin and bibronectin (for basal cell attachment). Nutritive, immune and support systems are provided by the dermis to the epidermis via this junction, with restriction on the transfer of solutes based on charge and size allowing normal migrating cells, such as melanocytes and Langerhan's cells, to pass. A major role of the dermal epidermal junction is to control keratinocyte production.

1.6.3.3. Epidermal renewal and keratin development

The epidermis undergoes continual turnover (known as apical migration) commencing at the stratum basale where a single layer of proliferative stem cells reside (Brouard and Barrandon, 2003) attached via hemi desmosomes to the dermal epidermal junction. These basal cells express several characteristic markers, including keratins and transcription factors (Fuchs, 2008). The basal epidermal stem cell periodically withdraws from the cell cycle, differentiates terminally to an epidermal keratinocyte, detaches from the basement membrane and begins the transit process through the epidermis leading to eventual sloughing from the skin surface as a corneocyte. The migration process is activated by protein kinase C and Ca^{++} which leads to the disintegration of the hemidesmosome and the formation of desmosomes. Within the basal layer there are low levels of the keratin filaments K5 and K14 which gives the keratinocyte some strength but still allows for cell division. As it migrates

upwards, the epidermal keratinocyte progresses through three differentiation phases which account for varying properties of each of the epidermal layers; spinosum, granulosum and corneum. The epidermal keratinocyte is forced towards the skins surface by the freshly produced epidermal keratinocytes beneath it. After leaving the stratum basale, the migration continues to the basale / spinosum layer transition. Here, changes in morphology and function occur with the synthesis of keratin by a shift in production from K5 and K14 keratin filaments to K1 and K10 keratin filaments. As the keratinocyte traverses the stratum spinosum, keratin accumulation reaches about 40% of the keratinocytes total protein (Rice and Cohen, 1996). The plasma membrane thickens in upper spinous regions at the same time as lamellar bodies and keratohyalin granules appear. At the stratum spinosum / granulosum interface, profillagrin synthesis begins within keratohyalin granules and the keratinocytes undergo morphological transformation. The transformation involves a flattening of the cells structure along with an increase in cell volume. The cell's plasma membrane, loses its phospholipid content to be replaced by sphingolipid, in the process becoming permeable, leading to a loss of the intracellular environment (Rice and Cohen, 1996). Without this environment, the keratin proteins extensively bond with each other through disulphide links. At the stratum granulosum / corneum interface, profillagrin begins to be converted into fillagrin leading to a zone of stable filaggrin. At this time the keratinocytes nucleus and other organelles undergo apoptosis and a cornified envelope is formed around the cell. The end product of these changes is the corneocyte which contains about 70% keratin and is surrounded by an intercellular lipid layer. After a time period of approximately a month from mitosis, the epidermal

keratinocyte reaches the surface of the stratum corneum where it is shed in the form of horny cell flakes (Fuchs, 2008).

In terms of genetic programming apical migration follows the sequence proliferation, differentiation, apoptosis. Apoptosis as the final program in the sequence maintains epidermal homeostasis by balancing cell death in the stratum granulosum with proliferation in the stratum basale. The key enzymes involved in apical migration are transglutaminases (soluble involucrin and cystatin A are early substrates to form a scaffold to which insoluble precursors such as the main protein loricin are added in latter stages). Involucrin, cystatin A and loricin are only a few of the structural proteins in the cornified envelope, others include elafin, small proline rich proteins, keratin intermediate filaments, trichohyalin and filaggrin.

1.6.4. The dermis

The dermis is a vascularised, innervated tissue with appendages interspersed throughout. Both elastic and compressible it supports and protects the epidermis. The dermis comprises cells, fibrous molecules and a ground substance (macromolecules filling the space between fibres and dermal cells) (Kanitakis, 2002). As with the epidermal layer, anatomical location determines the thickness of the dermis with the palms and the soles having the greatest depth. Structurally the dermis can be subdivided into the upper papillary dermis, mid reticular dermis and deep dermal layers. Contact between the papillary dermis and the epidermis is provided by dermal papillae which project upwards and alternate with epidermal rete

ridges. The dermis comprises an interstitial collagen framework (approximating to seventy percent of dry skin by weight (Schaefer and Redelmeier, 1996)) which acts as a skeleton that the other tissues of the dermis build on and gives the skin its mechanical resistance. The collagen fibres are arranged within loose bundles in the papillary layer and become more tightly bound within the deeper dermal layers. The skin's elastic properties are provided by elastic fibres (elastin) which become thicker in the deeper dermal layers. The dermis contains a number of cell types. Cell types of note are the fibroblasts (that produce the fibres and ground substance) and the monocytes involved in cellular defence systems including phagocytosis, immune responses and antimicrobial agent release (Schaefer and Redelmeier, 1996). Melanocytes, involved with skin pigmentation, are also present within the dermal layer. The dermis, in comparison with the epidermis, is more permeable and vascularised, forming the bulk component of the skin. The vascular system runs throughout the dermal layer and is responsible for provision of the skin's nutrients whilst at the same time allowing the body to thermally regulate itself. Functionally, the dermal layer contains the sense organs which detect pain and pressure perception along with cushioning and insulation. Appendageal support is also provided by the dermis.

1.6.5. The hypodermis

The deepest, innermost layer of the skin is the hypodermis which is mainly comprised of fat cells (adipocytes). Adipocytes are large (up to 100µm) rounded cells containing triglycerides and fatty acids within the cytoplasm (Kanitakis, 2002). Functionally, as

well as giving protection against mechanical injury the hypodermis is associated with insulation, thermoregulation and energy storage (Schaefer and Redelmeier, 1996).

1.6.6. Other structures and cells within the skin

Merkel cells (or touch cells) are present in the stratum basale layer of the epidermis and are involved with the sensory perception of pain, itch and temperature (Boulais and Misery, 2007). As such they are part of the peripheral nervous system, with Merkel cell-neurite complexes comprising sensory afferents and Merkel cells. The importance of Merkel cells to the somatosensory system has been recently confirmed (Maricich, et al., 2009). Langerhans cells are present in the stratum spinosum layer of the epidermis and are involved with the capture, uptake and processing of microbial antigens (Valladeau, 2006).

Hair follicles populate the entire cutaneous surface except for the soles of the feet and the palms of the hands. Functionally they provide insulation and sensory perception. Hair is morphologically and biologically different in different parts of the body, and varies in structure, rate of growth and response to stimuli (Giacomoni, et al., 2009). Hair types include lanugo (fetal hair), vellus and terminal (scalp, eyebrow and beard).

Sebaceous glands secrete sebum via the differentiation and disintegration of sebocytes (termed holocrine secretion as the whole excretory cell is secreted)

(Schneider and Paus, 2010). In the human sebaceous gland, sebum comprises; squalene 15%, wax esters 25%, cholesterol 2.5%, cholesterol esters 2%, triglycerides 42% and fatty acids 15% (Walters and Roberts, 2002). The majority of sebaceous glands are associated with hair follicles (to form the pilosebaceous unit), however, hair follicle free sebaceous glands are found in the eyelids, nipples, genitals and ears (Schneider and Paus, 2010). Functionally, the purpose of the sebaceous gland is to secrete sebum. Sebum itself aids in the maintenance of skin barrier function (Proksch, et al., 2008).

Sweat glands are located in the dermis and produce sweat which is secreted through ducts onto the skin surface. Sweat glands may be either eccrine (secretion is released from the cell without distintegration) or apocrine (secretion occurs via pinch off of outer cell parts) (Wilke, et al., 2007). However, sweat glands showing characteristics of both gland types (known as apoeccrine glands) have also been observed (Sato, et al., 1987). The apoeccrine sweat duct is present in axillary skin and active only after puberty. Eccrine sweat glands populate the entire cutaneous surface area except for muco-cutaneous junctions. By anatomical location, the approximate number of eccrine glands per square centimetre are; back 64, forearm 108, forehead 181, palms and soles 600 to 700 (Saga, 2002). A key function of the eccrine sweat gland is the thermoregulation of the body by sweating of an odourless, colourless hypotonic solution (pH 4.5 to 5.5) leading to evaporation and consequently cooling. Sweat is released from the eccrine sweat glands at a rate of 2 to 16 nl min^{-1} $gland^{-1}$ whilst sweating (Sato and Dobson, 1970). The secretory coil of the eccrine gland is 60 to 80µm in diameter and 2 – 5 mm in length (Saga, 2002). The apocrine

gland is a short duct gland sweat duct only active after puberty and restricted to hairy body areas (as it opens and secretes into the hair canal) (Wilke, et al., 2007). The secretion from the apocrine gland is oily and odourless containing lipids, protein and steroids. The milky appearance of apocrine sweat secretion may be due to mixing with sebum (due to the close proximity of the sebaceous gland) with any resulting odour due to bacterial action (Giacomoni, et al., 2009).

1.6.7. Xenobiotic metabolism in skin

The metabolising potential of the skin has been estimated to be approximately 2% that of the liver. One of the key differences between skin and liver metabolism is that of contact time, being long with skin enzymes and short with liver enzymes due to a blood flow of around 1 to 1.5 L min^{-1}. Metabolism can be classed as endogenous (metabolism of hormones, steroids and inflammatory mediators) or exogenous (metabolism of xenobiotics, including chemicals from accidental or deliberate release). Many of the enzyme systems found in liver are also present in the skin and include esterases, reductases, hydrolases, peptidases and oxidative enzymes. Specific Cytochrome P450 dependent monooxygenase located with the skin include CYP1A1, 1A2, 1B1, 2A6, 2B6, 2C9, 2C18, 2C19, 2D6, 2E1, 3A4 and 3A5 (Svennsson, 2009).

1.7. Xenobiotic percutaneous penetration

Section 1.6 has given a detailed description of the various skin layers and the structures and cells associated with them. Although the skin layers are capable of acting as a barrier to prevent the ingress of the vast majority of xenobiotics, environmental contaminants that possess the suitable physicochemical characteristics are able to penetrate through the skin. Of importance is work that has been carried out to determine the exact location within the skin of the main barrier to the ingress of xenobiotics and transport mechanisms through this barrier.

As early as 1853 researchers had determined that the skins layers were not equally permeable (as reviewed by Scheuplein) (Scheuplein, 1976). Defence research carried out during the First World War into sulphur mustard skin interactions determined that repeated swabbing of a contaminated area of skin with kerosene could prevent vesication (for an exposure time of less than 15 minutes). Their initial conclusion was “It is quite evident that the dichloroethylsulfide is at first rapidly taken up by some element on - or adjacent to - the surface of the skin, and for 2 to 3 minutes it may be completely removed, and for 10 to 15 minutes partially removed by prolonged washing with an organic solvent” (Smith, et al., 1919). The implication was that the skin barrier function must reside within the upper surface layers of the skin. Sulphur mustard extraction from the skin has since been evaluated *in vitro* with the conclusion that kerosene can remove sulphur mustard from the upper layers of the skin, supporting the conclusions of Smith (Hattersley, et al., 2008). Tape stripping studies were used to show that the barrier layer to the skin unequivocally resided within the stratum corneum (Blank, 1953). Since then more modern biophysical techniques such as transepidermal water loss (TEWL) have been in conjunction with

tape stripping to show that as the number of skin surface tape strips increase (and hence the removal of more surface skin layers) that TEWL also increased. TEWL is commonly used as a measure of skin barrier function although recent work has raised doubts to exactly how TEWL relates to the functionality of the skin barrier (Chilcott, et al., 2002). These studies confirm that the barrier to the ingress of xenobiotics resides within the stratum corneum. If the skin barrier is perturbed or removed by any form of damage, including blunt or penetrating trauma, the rate of absorption of xenobiotics from the surface of the skin will likely dramatically increase. Consequently, the employment of any dermal decontamination system would be more likely to prove less efficacious if applied to damaged skin rather than undamaged skin.

The morphology of the stratum corneum, comprising corneocytes containing densely packed keratin protein and intercellular spaces composed of lipid bilayers with both hydrophilic and lipophilic domains provides the skin with its barrier function. However, it does not provide a perfect barrier as xenobiotics are able to penetrate the skin, although they are subject to using skin transport mechanisms. For a substance to penetrate through the skin, a number of factors will determine the extent and magnitude of the penetration.

i. Solubility of the substance in the phase in which it is applied to the skin is of importance (unless the substance is applied in undiluted form).

ii. The ability of the penetrant to partition from the applied substance to the stratum corneum and, from there diffuse across the stratum corneum.

iii. The ability of the penetrant to partition from the stratum corneum and into the viable epidermis.

iv. Partitioning from the viable epidermis to the peripheral circulation within the papillary dermis.

1.7.1. Diffusion

Mathematically, diffusion processes through a single layer, simple membrane can be defined according to Fick's first law, which relates diffusive flux to concentration through the postulation that flux goes from regions of high concentration to low concentration such that:

$$J = -D\left(\frac{\delta C}{\delta x}\right)$$

Where, J is the flux per unit area, D is the diffusion coefficient (negative due to molecular transfer occurring in the opposite direction to the concentration gradient), C is the concentration gradient and x is the linear distance travelled.

Conventionally, Fick's first law is rewritten as:

$$J_{SS} = K_P \, x \, C_0$$

Where, J_{SS} is the steady state flux per unit area, K_p is the permeability coefficient for the penetrant (from a given vehicle, unless applied neat) and C_0 is the concentration

of the penetrant in the vehicle (assumed to be equal to the density of the penetrant if applied neat).

The permeability coefficient comprises a number of parameters and can be rewritten as:

$$K_p = \frac{\frac{K_M D_M}{V}}{h_M}$$

Where, $K_{M/V}$ is the partition coefficient of the penetrant between the membrane and vehicle, D_M is diffusion coefficient of the penetrant in the membrane and h_M is the diffusional path length of the membrane. The reciprocal of the permeability coefficient is known as the total barrier resistance, R, and takes the form:

$$R = \frac{1}{K_p}$$

Each barrier phase has its own resistance which is additive when a series of barrier phases are encountered. As an approximation, for the skin, this may be confined to the stratum corneum and the viable epidermis:

$$R_{Total} \cong R_{SC} + R_{VE}$$

Given that the skin cannot be regarded as a simple homogenous membrane, parameter value determinations for K_p and R are not simple tasks. However, permeability coefficients are experimentally determined parameters which inherently take into account the complexity of the membrane. The flux experiment allows experimental determination of the steady state flux (J_{SS}) from which K_p and R can be derived according to Fick's First Law, previously defined as:

$$J_{SS} = K_P \, x \, C_0$$

The J_{SS} is determined as the gradient of the steady state slope of the cumulative amount penetrated against time (Figure 1.12).

1.7.2. Location of the barrier within the stratum corneum

Transport of a penetrant through the skin can be broken down into a list of four likely possibilities (Figure 1.13), direct transport through the corneocytes (transcellular route), through the lipid bilayers surrounding the corneocytes (intercellular route), along hair follicles (transfollicular route) or through sweat glands (eccrine route). Barrier resistance is one of the evidence bases that have been used to confirm the most likely route for percutaneous penetration. The barrier resistance, R, has been experimentally derived for various compounds of increasing alkyl chain length including alkanols (Scheuplein and Blank, 1973). The alkanol studies showed that barrier resistance dropped exponentially with increasing alkyl chain length indicating that skin permeability increased as a function of alkanol hydrophobicity. It can be inferred therefore that the barrier resistance is lessened for environmental contaminants that can partition and diffuse across a lipid pathway. Further evidence for a primarily lipid pathway for skin diffusion is offered by the use of skin penetration enhancers that either dissolve lipids (organic solvents such as DMSO) or destabilise liquid crystalline phases (amphiphilics such as Azone (Engblom, et al., 1995)).

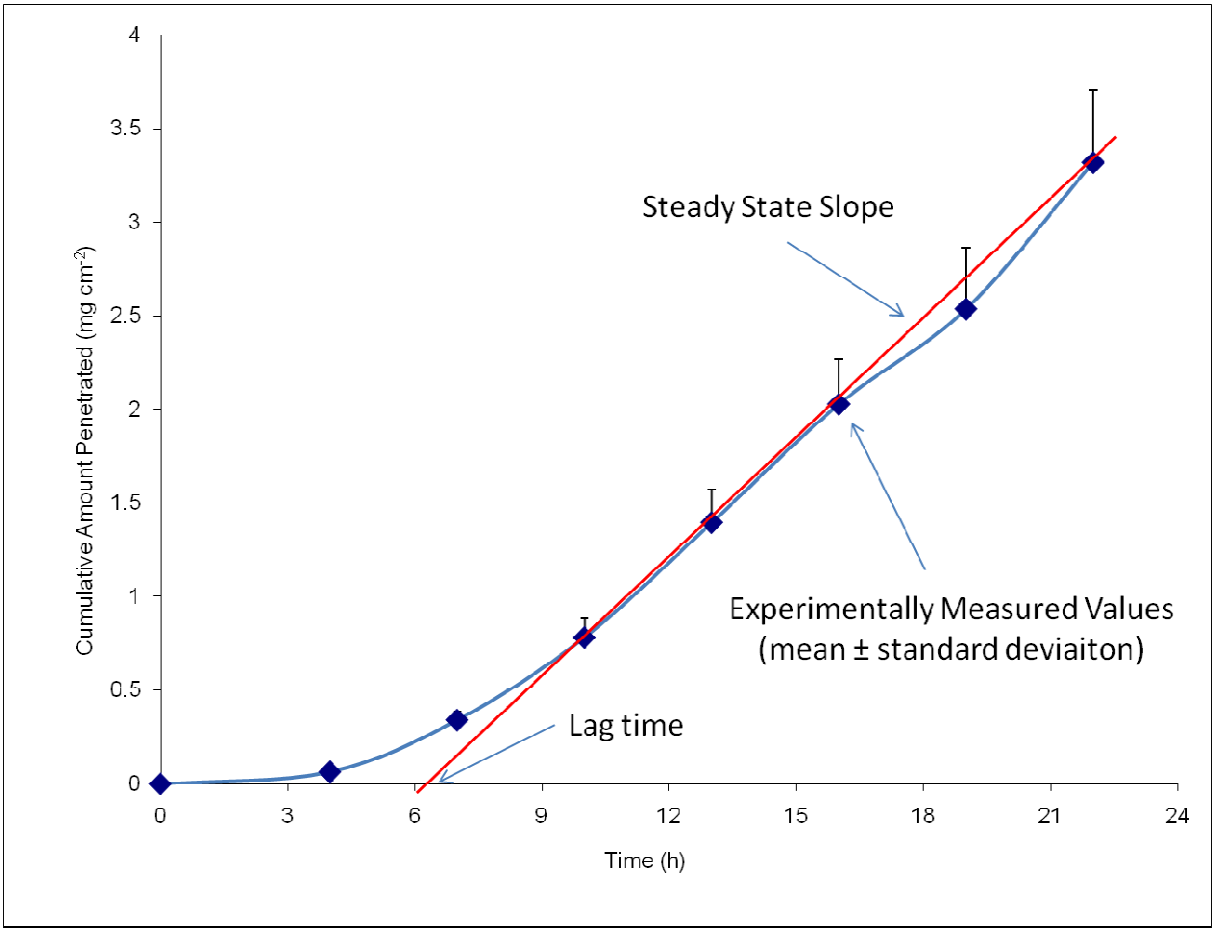

Figure 1.12: Example of experimental determination of the Steady State Flux (J_{SS}), taken as the gradient of the slope of cumulative amount penetrated against time (after the initial lag time has elapsed). Data shown is that of neat ^{14}C-VX penetration through dermatomed pig skin (mean ± standard deviation of n=6 animals) (Dalton, et al., 2006a). The J_{SS} was 207 ± 62 g cm^{-2} h^{-1} (x 10^{-6}) and the lag time was 6.3 ± 0.9 h.

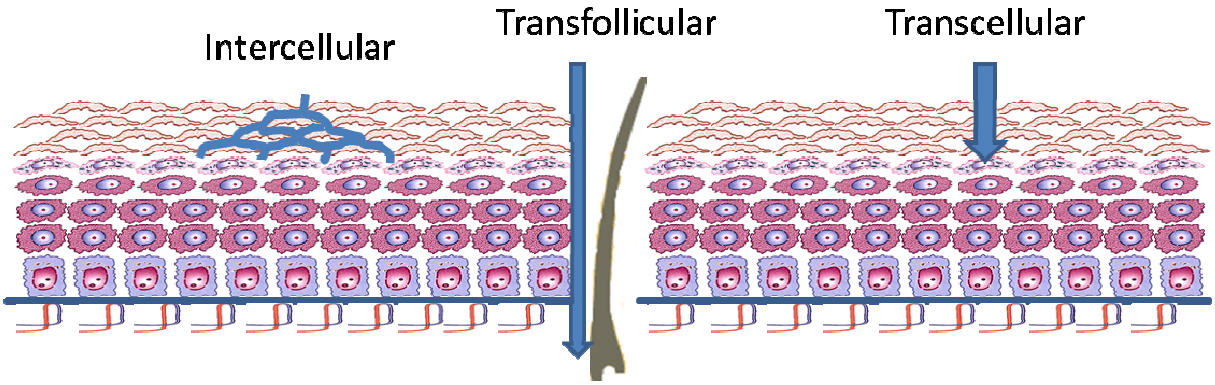

Figure 1.13: Potential routes of percutaneous penetration include the intercellular (penetration through the intercellular lipids), transfollicular (along hair follicles) and transcellular (direct transport through corneocytes) routes.

A popular analogy is to equate the properties of the stratum corneum to that of a brick wall, with the corneocytes taking on the role of the brick and the intracellular lipids taking on the role of the mortar. The bricks (that are ionic in nature) are comprised of dense protein and lack a lipid phase. The mortar, however, comprises lipid bilayers, and based upon the evidence, offers the likely route for the passage of the majority of penetrants when comparing the two.

This leaves the follicular and eccrine routes as possible percutaneous absorption pathways, although, it is important to note that hair follicles and sweat ducts are not evenly distributed across the skins surface, so any role they may play would likely be as a co-pathway alongside the intercellular route. The surface area occupied by hair follicles is small (up to 1% of skin surface area). Apocrine glands and hair follicles are co-located meaning that apocrine secretions mix with sebum within the hair follicle before the skin surface is reached. On this basis, the follicular route is a lipophilic route and cannot be ruled out as a potential co-pathway alongside the intercellular route. The surface area occupied by eccrine glands is small (approx 1/10 of that occupied by hair follicles), functionally eccrine glands are empty when inactive and express large volumes of water when active meaning that the eccrine route is not a lipid pathway and can be ruled out as a penetration pathway.

1.7.3. Factors affecting the penetration rate of a penetrant

Given that the intercellular route through the lipid bilayers offers the most likely explanation for skin transport through the stratum corneum, thought also needs to be

given to the penetrant itself. The ability of a penetrant to partition between the various phases required for skin transport relies on the penetrant having a suitable molecular weight, typically less than 500 Daltons, known as the rule of 500 (Bos and Meinardi, 2000) indicating that to some extent the stratum corneum acts as a molecular weight filter. Solubility parameters such as the octanol water partition coefficient should be within a suitable range, typically a negative log P value indicates that a substance will be too hydrophilic to penetrate the skin, whilst a log P value greater than three indicates that a substance will be too lipophilic and will be primarily retained within the stratum corneum. Charge on a penetrant will also impact the likelihood of percutaneous penetration. Generally, charged molecules will poorly penetrate the stratum corneum due to localised protein charges. It should be noted that this interaction can be overcome using iontophoretic techniques. The presence of hydrogen bonding groups on a penetrant will also limit percutaneous penetration due to interaction with hydrogen bonding groups present within the stratum corneum. The skin itself may also influence the penetration of the penetrant. Factors that may have a profound influence include anatomical location, age, gender, race, species, stress, disease states, follicular density, damage, regional blood flow and skin hydration status. The environment the skin is in will also have an influence on percutaneous penetration. Environmental temperature, diurnal variation, state of occlusion, vehicle (if any) that the penetrant is contained within are all factors that need consideration.

1.7.4. Predicting skin permeability

To summarise, the process of percutaneous penetration is complex and a wide range of factors need to be taken into account before prediction of skin penetration can be made. However, this has not stopped research groups from developing a number of models for predicting skin permeability. A number of models have been developed for predicting skin permeability coefficients including, by amongst others, Potts and Guy (Potts and Guy, 1992), Kasting (Kasting, et al., 2008) and Lee (Lee, et al., 2010). These models link the permeability coefficient (K_P) to the octanol water partition coefficient (K_{oct}) or the log of the partition coefficient (log K_{oct} or log P) and the molecular weight (MW) of the compound according to the equation:

$$log\ K_P = a\ log\ K_{oct} - b\ MW - c$$

Where, a, b and c are numerical values determined by the research group. The octanol-water partition coefficient is determined from the distribution of a chemical species between octanol and water and as such gives a measure of the chemicals lipophilicity.

The use of linear regression models allows for the development of *in silico* modelling techniques which allow the prediction of K_P values without the need to perform experimental studies.

1.8. Measuring percutaneous penetration

Models available for determining percutaneous penetration include; *in silico* mathematical models (used for both modelling existing data sets to extend to similar

compounds and for rank order correlations), *in vivo* animal models (used for evaluation of selected products), *in vitro* skin models (a variety of types including artificial, cultured, animal and human may be used depending on the study) and *in vivo* human models (the gold standard, however, ethical and moral constraints preclude use either entirely or until the pre clinical or clinical trials phase). Defence research, of the type this work aims to further, will not use an *in vivo* human approach, instead down selection of candidate products will be achieved using relevant *in vitro* techniques prior to validation of lead candidate(s) using a relevant animal model *in vivo*.

1.8.1. *In vitro* percutaneous penetration determination

The *in vitro* determination of percutaneous absorption offers a number of unique advantages not available when conducting *in vivo* studies. The precise control of experimental conditions (other than the skin membrane) is of immense value in obtaining reproducible data detailing both the permeation of a substance and its distribution within the skin. From the point of view of defence research seeking countermeasures against particularly toxic chemicals, *in vitro* human skin may be used to extrapolate how effective a countermeasure is likely to act in the *in vivo* human gold standard. Disadvantages with *in vitro* modelling are evident in the lack of a circulatory system and the inherent difficulties in preparing metabolically viable skin preparations. These disadvantages mean that pharmacokinetic effects (post skin penetration), pharmacodynamic effects (including vasodilation / vasoconstriction) and metabolic products resultant from transcutaneous metabolism are not elucidated.

Determination of percutaneous penetration is typically achieved using *in vitro* skin diffusion cell methodology (Figure 1.14). A variety of different diffusion cell designs have been developed using static and flow through techniques, however, the basic premise remains constant, that of a donor chamber in direct contact with the upper surface of a skin preparation and a receptor chamber in direct contact with the lower surface of the skin preparation. The penetrant of interest is placed onto the upper skin surface within the donor chamber and then time course samples are taken from a suitable receptor media within the receptor chamber.

1.8.1.1. Guidelines concerning percutaneous penetration studies

An understanding of what *in vitro* models can achieve is necessary before they can be used to determine experimental aims. To this end a number of protocols and guidelines have been assembled to enable skin researchers to execute studies that will be accepted by the wider scientific and non scientific communities. Perhaps the most useful of these is the Organisation for Economic Co-operation and Development (OECD) guideline 428 (OECD, 2004b), and its associated guidance documents (OECD, 2004a;OECD, 2010), which set the standard as to what is acceptable when conducting *in vitro* skin penetration studies using diffusion cells. These guidelines attempt to ensure that *in vitro* studies are carried out appropriately and aim to reduce variability from laboratories within different organisations.

Figure 1.14: *In vitro* static diffusion cells. Top left: From top - donor chamber, support or ‘frit’ for the skin sample. Magnetic stirrer bar which ensures even distribution of penetrant in the receptor fluid. Clamp which holds the ensemble together. Receptor fluid is subsequently collected via the sampling arm after removal of the ‘hat’. Top right: Jacketed variant – water is pumped through the outer jacket to maintain a constant receptor fluid temperature. Bottom: Bank of 9 jacketed diffusion cells *in situ* on a stirrer block. Visible to the rear are the tubing attachments for the heated jackets.

The OECD guidelines offer advice on all aspects of *in vitro* diffusion cell systems methodology, a detailed synopsis of which now follows due to the core of the research presented within this thesis, in either using or further validating, *in vitro* skin penetration techniques. The diffusion cell itself may be of the static or flow through type and should be constructed of inert materials and allow for good mixing of the receptor chamber. The membrane used within the diffusion cell should be maintained at 32 ± 1 ºC and ideally be human skin, but, animal skin may be used if necessary. The membrane preparation may be as epidermal membranes, full thickness skin or slice of skin prepared with a dermatome (to approx 500 µm). The receptor fluid bathing the underside of the skin preparation will ideally be a physiological buffer, however, the solubility of the penetrant within the receptor fluid should not be such that it is rate limiting. The penetrant exposure duration has a recommended maximum of 24 hours and should be applied as an application of up to 10 µl cm^{-2} (liquids) or up to 5 mg cm^{-2} (solids). The exception to these application amounts is when infinite dosing studies are being performed. Study replicates for an individual condition should be no less than four.

Even with a broad set of guidelines in place, inter laboratory (and even intra laboratory) skin diffusion cell experimental data are not always in agreement, even when similar protocols are followed, discrepancies between data sets are still encountered (Chilcott, et al., 2005a). An interesting point within the guidelines concerns the source of the skin, with human skin being the preferred option. However, animal skin may be the preferred option if *in vivo* work using the same animal model is required. It must be borne in mind, however, that to extrapolate any

results into man any variation in the penetration of a compound between the species must be accounted for, either with the addition of uncertainty factors or, ideally, with further studies using *in vitro* human skin. Examples of species difference in skin penetration are well documented (Barbero and Frasch, 2009). Also of interest is the choice of receptor medium, of utmost importance is that sink conditions for the penetrant are maintained for the duration of the study. Favoured, unless otherwise justified, is phosphate buffered saline at pH 7.4 to mimic physiological conditions. Lipophilic penetrants may require alternative receptor media for maintenance of sink conditions. Typically co solvents (ethanol) or binding proteins (bovine serum albumin, BSA) are used to increase solubility of the penetrant in this case.

1.8.1.2. Animal models for percutaneous absorption

Although, ideally human skin should be used for the determination of percutaneous penetration, work presented within this thesis uses skin from large white pigs. An animal model was chosen primarily due to the need to conduct a large number of diffusion cell studies for which insufficient human skin tissue was available. The use of animal models in toxicology studies will typically employ the most relevant model for subsequent data extrapolation to man (Simon and Maibach, 2000). In the case of skin penetration studies, the animal skin being used should exhibit properties close to that of human skin. However, availability and ease of handling and use also play a part which has led to a wide variety of laboratory animals including the mouse, rat, rabbit and guinea pig being used as animal models for percutaneous absorption. Perhaps the most relevant animal models for skin penetration research are the pig

and members of the primate family, as the skins from these animals most closely model human skin. However, the use of primates in skin research holds its own inherent difficulties and ethical constraints leaving the preferred animal model being the pig. There are similarities in the biochemistry, physiology and histology of human and pig skin, and, importantly, the permeability of pig skin is generally closest to that of human both *in vivo* (Bartek, et al., 1972) and *in vitro* (Bronaugh, et al., 1982;Chilcott, et al., 2001;Dick and Scott, 1992;Galey, et al., 1976;Gore, et al., 1998;Barbero and Frasch, 2009) . Another consideration is that an animal model should have similar responses to the chemical penetrant of interest, in the case of nerve agents, this includes signs of intoxication and measurable parameters such as cholinesterase inhibition. The majority of previous studies investigating the skin absorption of nerve agents have used rodent models such as the rat and guinea pig, as these animals have well characterised responses to anti-cholinesterase compounds. However, a number of studies have investigated the pig's response to nerve agent challenge (Chilcott, et al., 2003;Duncan, et al., 2002;Dorandeu, et al., 2007). As it is generally accepted that the most appropriate animal model for human skin absorption is the domestic pig (Sus scrofa) (Wester and Noonan, 1980;Simon and Maibach, 2000), the *in vitro* studies described in this thesis were carried out using pig skin to enable subsequent comparison with down selected haemostatic decontaminants in an *in vivo* pig model.

CHAPTER 2: INTERACTIONS OF GD WITH THE SKIN

2.1. Research goals

A detailed search of the literature indicated that only limited research had been conducted on the interactions of Soman (GD) with the skin. One of the major research goals of this thesis was to add to this knowledge base in a number of specific areas. These areas can be defined as:

2.1.1. Skin absorption kinetics of GD through porcine skin

The quantification of percutaneous penetration for any chemical measured using *in vitro* diffusion cell techniques requires use of the guidance offered by OECD guidelines (Section 1.8.1.1.). Of particular interest, is the choice of receptor fluid, due to the broad array of choices available. Phosphate Buffered Saline (PBS), PBS with added Bovine Serum Albumin (BSA) and an Ethanol Water solution were evaluated. Choice of skin preparation is also of interest; although the use of fresh skin is preferred, experimental constraints often make the freezing of tissue necessary. Work conducted as part of this thesis makes a comparison of fresh and frozen tissue in skin research.

2.1.2. Quantification of the GD skin reservoir

Previous work has alluded to the existence of a GD reservoir in a number of organs including the skin (Kadar, et al., 1985). Empirical knowledge of such a reservoir may be of importance to future work programmes seeking to develop medical countermeasures to dermal GD exposure. For example, exploitation of a removable GD reservoir could limit any subsequent systemic toxicity by removing not only surface contamination, but, also agent depots contained within the skin. The work presented here uses solvent extraction techniques, at a range of time points post GD exposure, as a proof of principle method to determine extractable fractions.

2.1.3. Quantification of GD skin surface spreading

One of the fundamental assumptions when measuring the penetration rate of a chemical through the skin is the knowledge of the surface area that the chemical has penetrated though. Without this information, amount per unit area penetration determinations cannot be made (although it is often assumed that a chemical will spread across the entire available surface area of a diffusion cell). Wrongful use of this assumption could potentially lead to gross underestimations in the true penetration rate.

2.1.4. Comparison of diffusion cell systems

Chronologically, work carried out initially used a commercially available water jacketed static diffusion cell system (Permegear™) (Figure 1.14 top right), whilst later work used an unjacketed Franz cell (Figure 1.14 top left). To ensure that both

systems gave comparable data for GD percutaneous penetration, they were evaluated simultaneously. The availability of two bespoke systems and the comparisons made allows for later discussion on implications for users of different systems in different laboratories both nationally and internationally.

2.1.5. Research purpose

The research presented within this section provides an assessment of the interaction of ^{14}C-GD with the skin *in vitro* and allows for the postulation of a ^{14}C-GD skin interaction scheme, from time of skin contact through to penetration into the receptor media. All of the work described makes use of Franz Static Diffusion Cells using either fresh or frozen skin samples.

2.2. Materials and methods

The synthesis, use and destruction of GD was conducted in accordance with the Chemical Weapons Convention (1996) to which the UK is a signatory state. Radiolabelled pinacolyl methylfluorophosphonate (GD) was synthesised by TNO (Rijswijk, Netherlands) and had a radiochemical purity >97% (as determined by radiometric HPLC analysis). The ^{14}C label was at the P-CH_3 moiety (see Figure 1.6). The chemical purity of labelled and unlabelled GD was >97% by NMR. Both radiolabelled and cold agent were mixed in appropriate proportions to give a nominal activity of approximately 0.5 µCi $µl^{-1}$. Tritium (^3H) labelled water was combined with non radiolabelled water to create a final dosing solution with a specific activity of approximately 5 µCi ml^{-1}. Liquid scintillation counting (LSC) materials (Soluene-350™, Ultima Gold and opaque plastic vials) were purchased from Perkin-Elmer (Chandler's Ford, Hampshire). All other chemicals were analytical grade and were purchased from the Sigma Chemical Company (Poole, Dorset) or VWR International (Lutterworth, Leicestershire).

The use of animals in this study was conducted in accordance with the Animals (Scientific Procedures) Act 1986. Weanling pigs (large white strain, weight range 20 - 30 kg) were purchased from a local supplier. Animals were pair-housed and given 24 h access to food and water. After one week acclimatisation, each animal was sedated with Hypnovel® (Midazolam, 6ml i.m., 5 mg ml^{-1}) and culled with an overdose of Euthatal™ (sodium pentobarbitol, 6ml i.v., 200 mg ml^{-1}). The whole abdominal skin flank (approximately 40 x 30 cm) was excised from each animal. The skin was

either prepared for use immediately or stored flat between sheets of aluminium foil at -20ºC for up to three months prior to use. Prior to study commencement, skin samples were removed from cold storage and thawed in a refrigerator at 5ºC for approximately 24 hours. The skin was close clipped and the subcutaneous fat removed before being dermatomed (Humeca Model D42, Eurosurgical Ltd, Guildford, UK) to a nominal thickness of 500 µm prior to insertion into diffusion cells.

Percutaneous absorption experiments were performed with Franz-type glass diffusion cells (Franz, 1975) of either unjacketed (Dstl engineering department, Wiltshire, UK) or jacketed (Permegear™, Hellertown, PA, USA) design. A 3 x 3 cm section of dermatomed pig skin was placed, epidermal side up, between the donor (upper) and receptor (lower) chamber. Each receptor chamber was filled with 5 ± 1 ml (unjacketed) or 14 ± 1 ml (Permegear™ jacketed type) receptor fluid to a level that ensured the meniscus of the receptor fluid in the sampling arm was level with the skin surface. Depending on the study type the receptor fluid was phosphate buffered saline (PBS), PBS with added 5% bovine serum albumin (BSA) or 50% aqueous ethanol. The unjacketed cells, once assembled, were placed into a metal holder incorporating a circulating water supply upon a magnetic stirrer block. The Permegear™ diffusion cells, once assembled, were placed into bespoke holders, incorporating a magnetic stirrer and water heater attachments. In both cases, stirring of the receptor fluid was achieved via a Teflon coated magnetic follower in the receptor chamber. The skin surface within each diffusion cell was maintained at a temperature of approximately 32ºC (as confirmed by infrared thermography; FLIR Model P640 camera, Cambridge, UK) using water pumped at approximately 37ºC

through either the metal holder (unjacketed) or through the diffusion cell jackets (Permegear™) via a circulating water heater (Model GD120, Grant Instruments, Cambridge, UK). All diffusion cells were set up in a Category C fume cupboard and once assembled, were allowed to equilibrate for approximately 24 hours. Baseline samples (100µl unjacketed type or 250µl Permegear™ type) were taken, with replacement by fresh receptor media, from each receptor chamber prior to commencement of the experimental protocol. Topical dosing was performed by the direct application of undiluted, ^{14}C-radiolabelled GD (100 µl (infinite dose studies) or 10 µl (finite dose studies)) onto the centre of the skin surface within the donor chamber. Depending on the protocol the following procedures were followed:

a) GD penetration through porcine skin under infinite dose conditions

The infinite dose study used abdominal flank skin from 8 individual pigs and was conducted using unjacketed diffusion cells with an area available for diffusion of 0.19 cm^2. Three pieces of skin were used from each animal. One piece of skin from an individual animal was mounted over 50% aqueous ethanol, PBS and PBS containing 5% BSA. A total of 24 diffusion cells were run, with 8 skin individual animal replicates for each receptor fluid type. Immediately after dosing with 100 µl neat ^{14}C-GD, the cells were occluded with a piece of tin foil which was affixed to the glass rim of the donor chamber using a layer of inert chemically resistant perfluorinated cream (Dstl, Wiltshire, UK).

b) GD penetration through porcine skin under finite dose conditions

The finite dose studies used abdominal flank skin from 11 individual pigs and were conducted using both unjacketed and jacketed (Permegear™) type diffusion cells. The area available for diffusion was 2.54 cm^2 and 1.76 cm^2 respectively. The receptor fluid used for this protocol was exclusively 50% aqueous ethanol. The donor chambers for all cells within the study group were left unoccluded for the duration of the experiment.

c) Studies using fresh versus frozen skin

The fresh versus frozen skin comparison study used abdominal flank skin from 6 individual pigs and was conducted using unjacketed diffusion cells with an area available for diffusion of 2.54 cm^2. Twelve pieces of skin were used from each animal, six of which had been frozen for a two week period at -20ºC and six of which were used fresh. All cells were mounted over 50% aqueous ethanol receptor fluid. A total of 72 diffusion cells were run, comprising six fresh and frozen skin individual animal replicates. Immediately after dosing with 1 ml ^3H_2O, the cells were occluded with a piece of tin foil which was affixed to the glass rim of the donor chamber using a layer of inert chemically resistant perfluorinated cream (Dstl, Wiltshire, UK).

For the infinite, finite and fresh versus frozen dose studies, following application of the agent, samples (100µl unjacketed or 250µl Permegear™) of receptor chamber fluid were removed into 5 ml of scintillation fluid (Ultima Gold, Perkin Elmer LAS (UK) Ltd, Buckinghamshire, UK) at regular intervals up to 24 h post exposure. Each

sample was replaced with an equivalent volume of fresh receptor fluid. Twenty four hours post-exposure a full dose distribution was performed as follows:

1. The receptor chamber fluid was removed from each diffusion cell.
2. For the occluded cells, the tinfoil was removed.
3. The skin surface was swabbed with cotton wool.
4. The skin from each diffusion cell was removed.

At each stage, the component removed was placed into a glass vial (with the skin containing vials being weighed). Cotton wool swabs and tin foil had 20 ml ethanol added to them and skins had 10 ml of Soluene-350™ added to them. Dose distribution vials were then stored at room temperature (with occasional shaking) until the skin had solubilised, after which aliquots (250 µl) were removed into 5 ml of scintillation fluid.

d) GD reservoir studies

The reservoirs study used abdominal flank skin from 8 individual pigs and was conducted using unjacketed diffusion cells with an area available for diffusion of 2.54 cm^2. Six pieces of skin were used from each animal for a total of 48 diffusion cells. The receptor fluid used for this protocol was exclusively 50% aqueous ethanol. The donor chambers for all cells within the study group were left unoccluded for the duration of the experiment. Eight cells (one from each animal) were dismantled at the following time points post GD exposure; 15, 30, 60, 180, 360 min and 24 hours. As for the infinite and finite dose studies, receptor fluids were collected and the skin surfaces were swabbed. To ensure all the surface GD had been removed, two swabs

were taken under this protocol. Swabs were placed into glass vials containing 20 ml ethanol. Skins were placed into glass vials and weighed prior to the addition of 20 ml acetonitrile. The skins were retained within the initial aliquot of acetonitrile for a period of 72 hours before being transferred to a second 20 ml of fresh acetonitrile for a further 72 hours and finally transferred to a third 20 ml of fresh acetonitrile for another 72 hours. At the end of this time, the skins were transferred into a fresh vial, weighed and had 10 ml of Soluene-350 added.

e) GD skin surface spreading studies

The skin surface spreading study used abdominal flank skin from 8 individual pigs and was conducted using unjacketed diffusion cells with an area available for diffusion of 2.54 cm^2. Six pieces of skin were used from each animal for a total of 48 diffusion cells. The receptor fluid used for this protocol was exclusively 50% aqueous ethanol. The donor chambers for all cells within the study group were left unoccluded for the duration of the experiment. Eight cells (one from each animal) were dismantled at the following time points post GD exposure; 15, 30, 60, 180, 360 min and 24 hours. Skins were gently dabbed with cotton wool to wick away any gross remaining surface contamination before being removed and placed into Kodak autoradiography cassettes (Sigma Chemical Company, Poole, Dorset) and frozen at -20ºC. Using dark room protocols, cassettes were opened and had autoradiography paper (Kodak Biomax) and intensifying screens inserted. After a period of 48 hours autoradiographs were developed by placing the paper into developing solution until spots could be visualised (less than one minute) and fixing for a period of 5 minutes.

Autoradiographs were then rinsed with distilled water and allowed to dry. All developing procedures took place in a category C fume cupboard.

For each study type described, the amount of radioactivity in each sample was measured using a Perkin Elmer Tri-Carb liquid scintillation counter (Model 2810 TR), using the manufacturer's ^{14}C-quench curve library set to exclude single-photon (non-radioactive) events. The amount of radioactivity in each sample was converted to amount of GD by comparison to standards (containing known quantities of ^{14}C-GD) prepared and measured simultaneously. For the infinite and finite dose studies, cumulative ^{14}C-GD penetration profiles for the 24 h study period were generated for each diffusion cell. Steady state (J_{SS}) or maximum penetration rates (J_{MAX}) were calculated by plotting the amount of ^{14}C-GD penetrated against time and calculating the gradient of the slope. Skins that had a ^{14}C-GD skin absorption rate with a correlation coefficient of < 0.98 or skins that had exhibited a large penetration of ^{14}C-GD during the diffusional lag-time were removed from the analysis as it was likely that the integrity of the skin had been compromised over the course of the study. Where applicable, statistical analysis was performed using a non-parametric ANOVA (Kruskal-Wallis test) with Dunn's multiple comparisons post-test. A predetermined alpha level of 0.05 was used for each statistical calculation.

2.3. Results

2.3.1. GD penetration through porcine skin under infinite dose conditions

The absorption profile of ^{14}C-GD (100µl, neat) through pig skin is shown in Figure 2.1. All values are mean ± standard deviation of n=8 diffusion cells with skin acquired from 8 individual pigs with samples being taken at the time points shown. Penetration of ^{14}C-GD into 50% aqueous ethanol receptor media increased steadily over the 24 hour study duration, whereas, for the other two receptor media types (PBS and PBS with BSA), there was an apparent reduction in penetration from 9 hours.

Due to the apparent biphasic nature of the cumulative penetration curves for the PBS receptor fluids, J_{SS} values and lag times were calculated between 12 and 24 hours (Table 2.1) and 3 and 9 hours (Table 2.2). The value of the J_{SS} for ^{14}C-GD skin penetration into the 50% aqueous ethanol receptor media was similar (439 ± 158 and 415 ± 250 µg.cm^{-2}.h^{-1}) for the two evaluated time ranges. Conversely, for the PBS receptor fluid, a statistical difference in J_{SS} (219 ± 195 and 119 ± 116 µg.cm^{-2}.h^{-1}) was shown between the evaluated time ranges. Although a similar trend in penetration rate reduction for the measured J_{SS} values for ^{14}C-GD penetration into the PBS-BSA receptor media was apparent (166 ± 176 and 84 ± 78 µg.cm^{-2}.h^{-1}), it was not statistically significant. The experimentally determined values of J_{SS} were used to determine the value of the permeability coefficient (K_P) and the skins total barrier resistance (R) (Section 1.7.1).

Comparison of ^{14}C-GD penetration into the three evaluated receptor fluids showed a significantly higher J_{SS} into 50% aqueous ethanol than for either of the PBS containing receptor fluids when measured between 12 and 24 hours. However, when the J_{SS} was evaluated between 3 and 9 hours, significance was only shown between 50% aqueous ethanol and PBS-BSA. The lag time measured for ^{14}C-GD penetration into each of the receptor fluids was similar when evaluated between 3 and 9 hours. Evaluation of lag times between 12 and 24 hours generated substantial negative lag times for the PBS containing receptor fluids, which whilst not realistic, are a consequence of the reduced penetration rates measured for these receptor fluids later in the experimental time course.

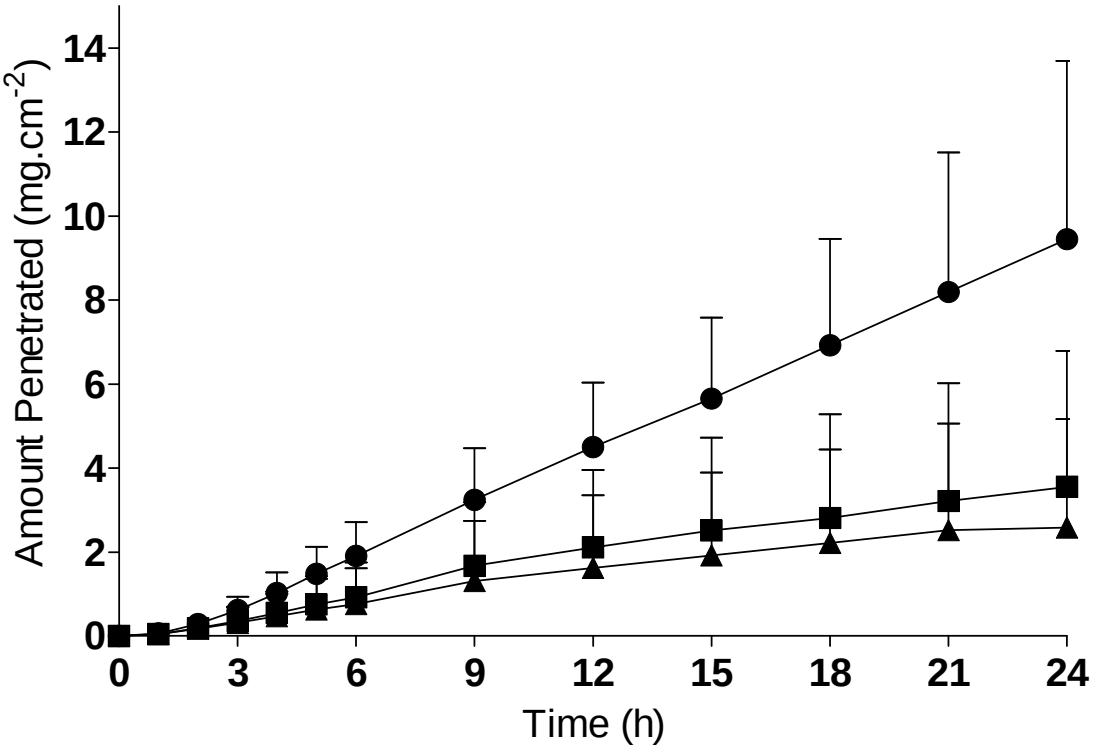

Figure 2.1: Cumulative amount of ^{14}C GD penetrated through undamaged abdominal flank pig skin using 3 different receptor media.Where, ●— = 50% Aqueous ethanol, ■— = Phosphate buffered saline (PBS) and ▲— = 5% Bovine Serum Albumin (BSA) in PBS. All values are mean ± standard deviation of n=8 diffusion cells. Study was carried out under infinite dosing conditions using an initialy applied dose of 100µl ^{14}C GD.

	Receptor Fluid Composition		
	50% Aqueous Ethanol	PBS	PBS with 5% BSA
J_{SS} ($g.cm^{-2}.h^{-1}$ $x10^{-6}$)	$415 \pm 250^{A,B}$	119 ± 116^{A}	84 ± 78^{B}
Lag time (h)	-0.4 ± 4.5	-6.5 ± 4.2	-4.6 ± 6.5
K_P ($cm.h^{-1}$ $x10^{-6}$)	406 ± 245	117 ± 113	82 ± 77
R ($h.cm^{-1}$ $x10^{-6}$)	3456 ± 2078	16756 ± 13941	29306 ± 26426

Table 2.1: Penetration rate (J_{SS}), lag time, permeability coefficient (K_P) and total barrier resistance (R) values for penetration of GD through 500 µm undamaged pig skin into 3 different types of receptor media (50% aqueous ethanol, phosphate buffered saline and phosphate buffered saline with 5% bovine serum albumin). Data obtained from measurements between 12 and 24 hours. For J_{SS} values, statistical significance ($P<0.05$) is indicated between same labelled parameters. Negative lag times are a consequence of the reduced calculated J_{SS} values later in the experimental time course. Study was carried out under infinite dosing conditions using an initially applied dose of 100 µl ^{14}C GD.

	Receptor Fluid Composition		
	50% Aqueous Ethanol	PBS	PBS with 5% BSA
J_{SS} ($g.cm^{-2}.h^{-1}$ $x10^{-6}$)	439 ± 158^{A}	219 ± 195	166 ± 176^{A}
Lag time (h)	1.7 ± 0.5	1.6 ± 0.3	1.7 ± 0.9
K_P ($cm.h^{-1}$ $x10^{-6}$)	429 ± 154	215 ± 191	163 ± 172
R ($h.cm^{-1}$)	2821 ± 1749	8829 ± 6780	16125 ± 13526

Table 2.2: Penetration rate (J_{SS}), lag time, permeability coefficient (K_P) and total barrier resistance (R) values for penetration of GD through 500 µm undamaged pig skin into 3 different types of receptor media (50% aqueous ethanol, phosphate buffered saline and phosphate buffered saline with 5% bovine serum albumin). Data obtained from measurements between 3 and 9 hours. For J_{SS} values, statistical significance ($P<0.05$) is indicated between same labelled parameters. Study was carried out under infinite dosing conditions using an initially applied dose of 100 µl ^{14}C GD.

The distribution of radiolabel within each diffusion cell was measured (Figure 2.2). Total recoveries of ^{14}C-GD after undamaged skin penetration were 96.0 ± 11.0 % (50% aqueous ethanol receptor fluid), 89.2 ± 10.5 % (PBS receptor fluid) and 95.7 ± 7.6 % (PBS with 5% BSA receptor fluid). In all cases, the majority (86.1 ± 15.9 %) of ^{14}C-GD was recovered from the surface of the skin indicating that infinite dosing conditions had been maintained throughout the study duration. Smaller amounts of ^{14}C-GD were recovered from within the skin and from the tin foil.

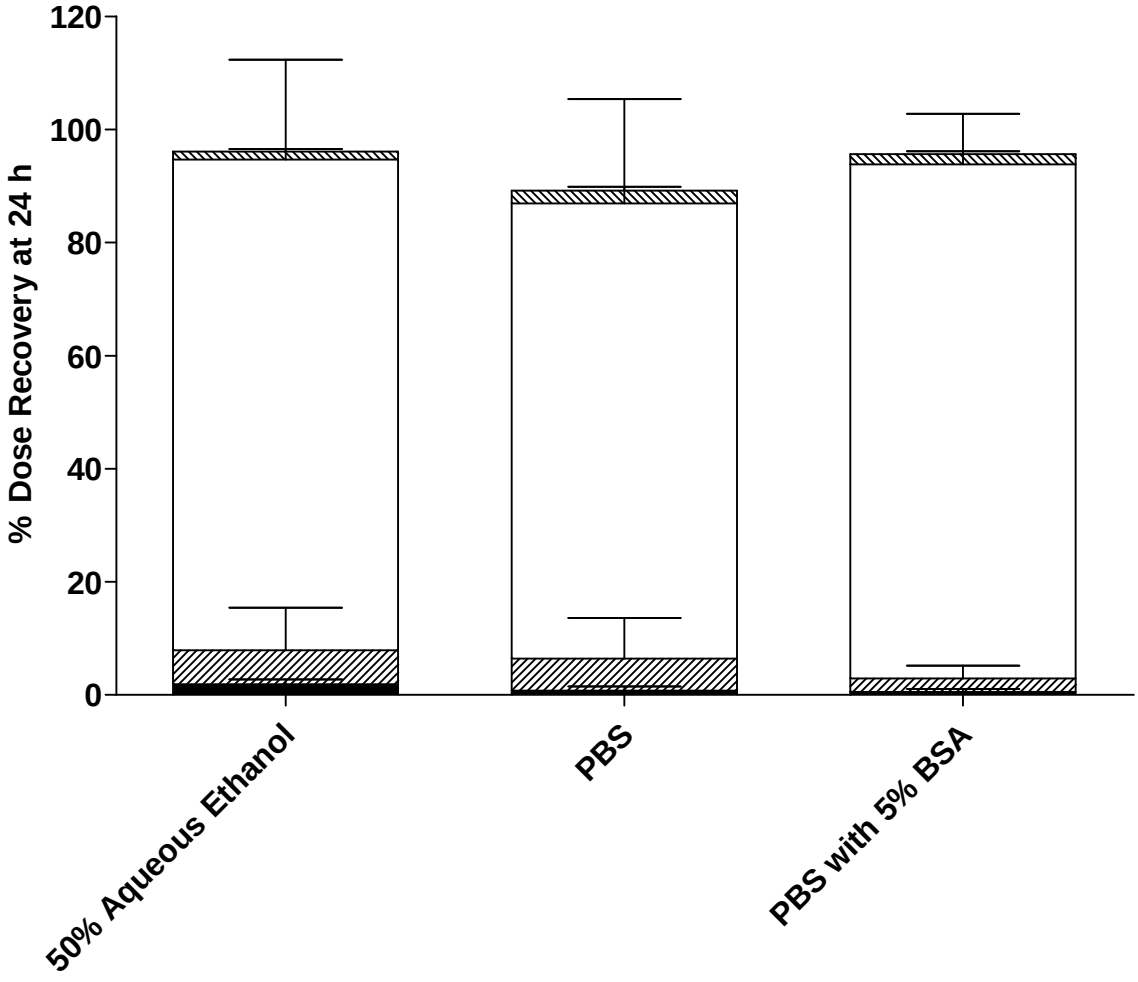

Figure 2.2: Dose distribution expressed as % recovery for ^{14}C GD recovered from; ☐ skin surface swab, ▨ within the skin, ▧ occlusive tin foil and ■ receptor fluid at 24 hours for each receptor media. All values are mean ± standard deviation of n=8 diffusion cells (each cell containing skin from a different animal). Study was carried out under infinite dosing conditions using an initialy applied dose of 100µl ^{14}C GD.

2.3.2. GD penetration through porcine skin under finite dose conditions

The absorption profile of ^{14}C-GD (10µl, neat) through pig skin for the two different types of diffusion cell used is shown in Figure 2.3. All values are mean ± standard deviation of n=16 (Dstl Franz type) or n=12 (Permegear^{TM}) diffusion cells with samples being taken at the time points shown. Values for the maximum penetration rates (J_{MAX}) and lag times of ^{14}C-GD through dermatomed abdominal flank skin for the two diffusion cell types are shown in Table 2.3. J_{MAX} values were determined between 2 and 6 hours, where correlation coefficients were >0.98.

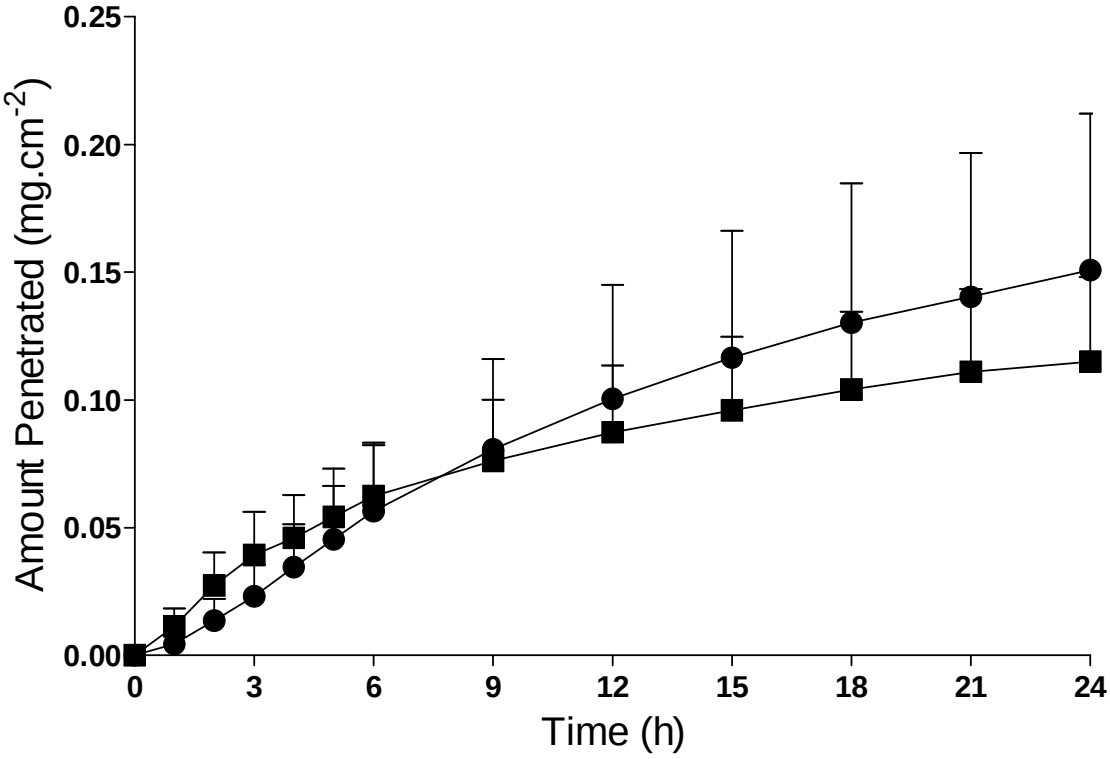

Figure 2.3: Cumulative amount of ^{14}C-GD penetrated through undamaged abdominal flank pig skin using two different types of static diffusion cell (Dstl Franz type (●) and Permegear™ (■)). All values are mean ± standard deviation of n=16 (Dstl Franz type) or n=12 (Permegear™) diffusion cells.Study was carried out under finite dosing conditions using an initially applied dose of 10 µl ^{14}C GD.

	Franz Diffusion Cell Type	
	Unjacketed (Dstl)	Jacketed (Permegear)
J_{MAX} ($g.cm^{-2}.h^{-1}$ $x10^{-6}$)	10.80 ± 4.78	8.49 ± 2.53

Table 2.3: Penetration rate (J_{MAX}) of ^{14}C-GD through 500 µm undamaged pig skin using two different types of Franz static diffusion cell. All values are mean ± standard deviation of n=16 (Dstl Franz type) or n=12 (Permegear™) diffusion cells. Data obtained from measurements between 2 and 6 hours. Study was carried out under finite dosing conditions using an initially applied dose of 10 µl ^{14}C GD.

2.3.3. GD reservoir studies

Two skin surface swabs were used to remove any remaining ^{14}C-GD surface contamination. The first swab consistently removed more than twice the contamination of the second swab for each of the reservoir assessment time points. Each skin was then subject to three acetonitrile extractions, in each case the majority of acetonitrile extractable ^{14}C-GD was recovered during the initial extraction, with only residual amounts being recovered during extractions two and three. The unextractable portion of ^{14}C-GD remaining within the skin after the three consecutive acetonitrile extractions was similar irrespective of the time at which the sample was taken. The amount of ^{14}C-GD that penetrated through the skin into the receptor media increased the longer the experimental duration to a maximum of approximately 5% by 24 hours (Figure 2.4).

Combination of the surface swab data to give total ^{14}C-GD present on the skin surface and amalgamation of the acetonitrile extraction data to give total ^{14}C-GD extractable from the skin are shown in Figure 2.5. Within the first 15 minutes of dosing the amount of ^{14}C-GD present on the skin surface approximated to 10% of the initially applied dose. This value dropped at later sampling time points. The amount of acetonitrile extractable ^{14}C-GD was similar to the amount of ^{14}C-GD fixed in the skin until one hour post GD challenge. By three hours and up to 24 hours post GD challenge the amount of extractable GD was statistically less than the amount of GD that remained unextractable within the skin.

Up to the one hour sampling time point total ^{14}C-GD recoveries were less than 50% of the originally applied dose, a value that had decreased to approximately 25% by 24 hours. Figure 2.6 takes the unrecovered fraction into account and simplifies the location of ^{14}C-GD into either on the skin surface, penetrated (whether extractable from the skin or not) and unrecovered. It is apparent that from 60 minutes post exposure the amount of ^{14}C-GD unrecovered remains constant.

The weight lost by skin samples upon extraction by acetonitrile was constant across the whole of this study, being in the region of 10-15% of the initial weight of the skin in most cases. Although this range was as large as 5-20% in some cases.

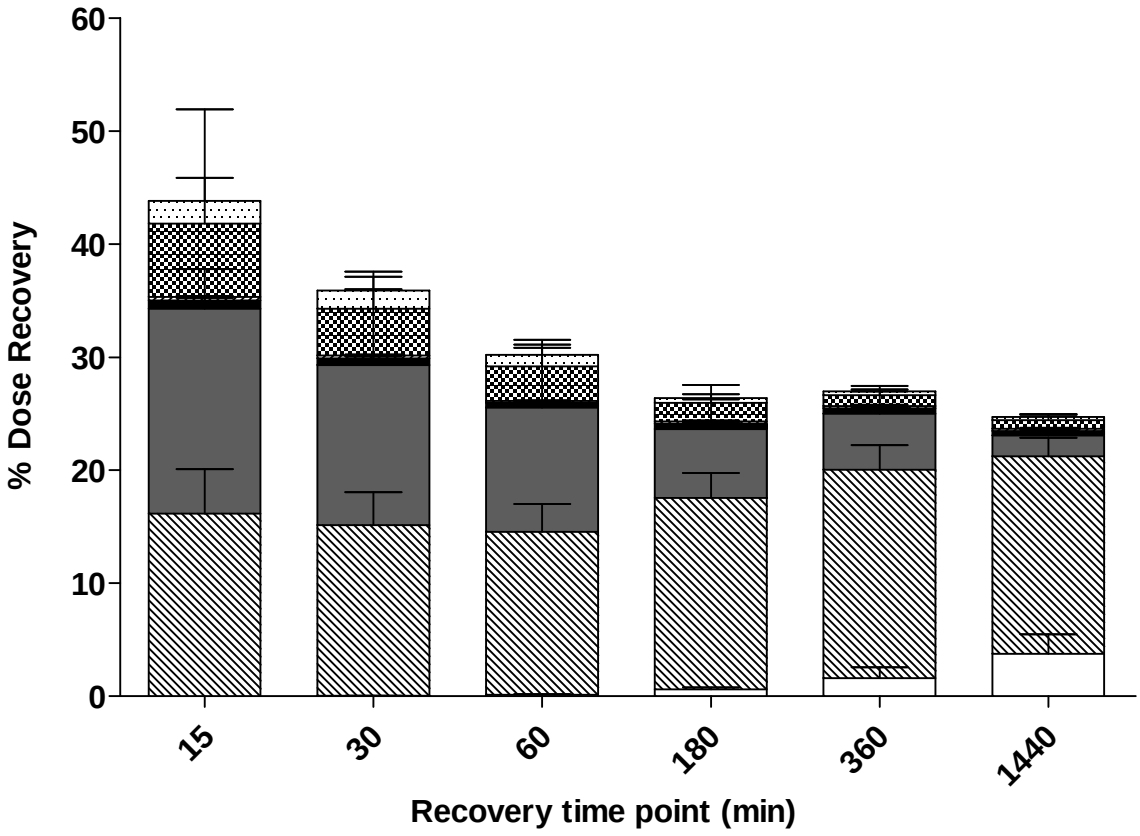

Figure 2.4: Percentage dose recovery of ^{14}C-GD from diffusion cells dismantled at the specified time points. Recovery was from the skin surface (swab 1 ▩ and swab 2 ⬚), extractable from the skin (acetonitrile extraction (AcN) 1 ■ , AcN extraction 2 ■ , AcN extraction 3 ▨), fixed within the skin ▨ or penetrated through the skin into the receptor fluid ☐ . All values are mean ± standard deviation of n=8 diffusion cells.

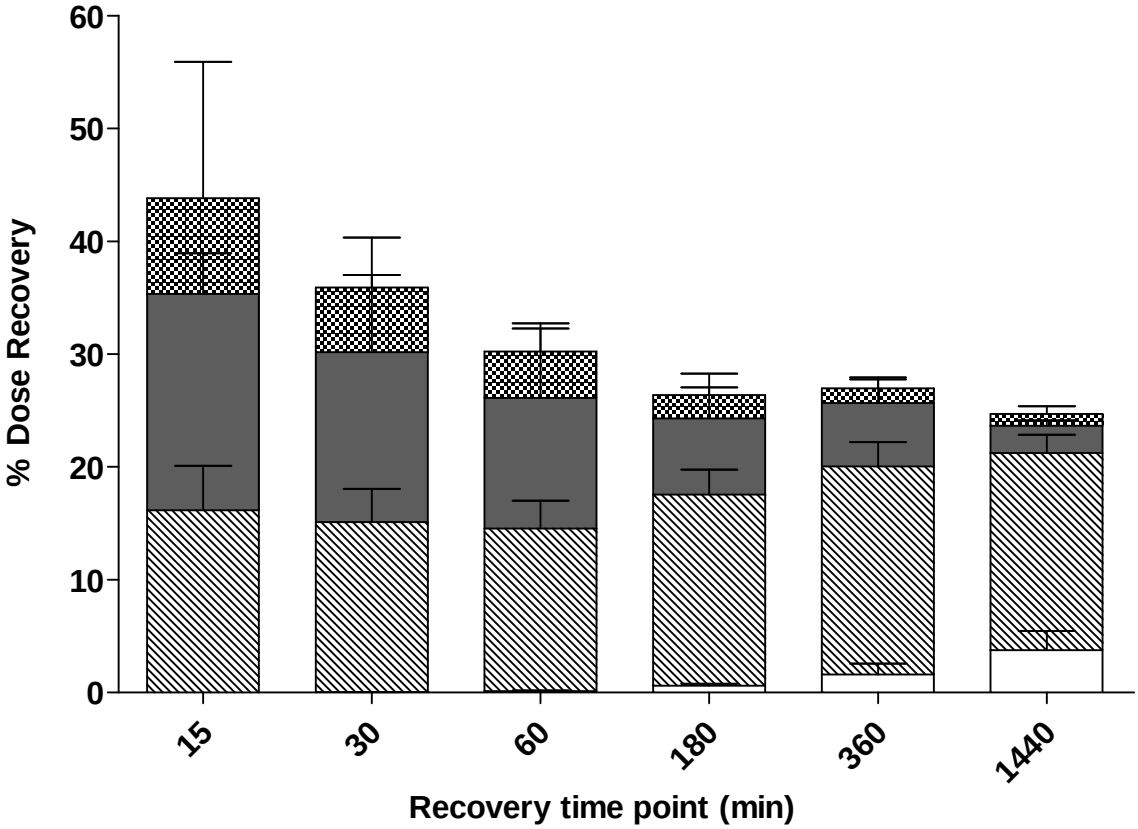

Figure 2.5: Percentage dose recovery of ^{14}C-GD from diffusion cells dismantled at the specified time points. Recovery was from the skin surface ▩ (2 surface swabs), extractable from the skin ■ (triple acetonitrile extraction), fixed within the skin ▨ or penetrated through the skin into the receptor fluid □ . All values are mean ± standard deviation of n=8 diffusion cells.

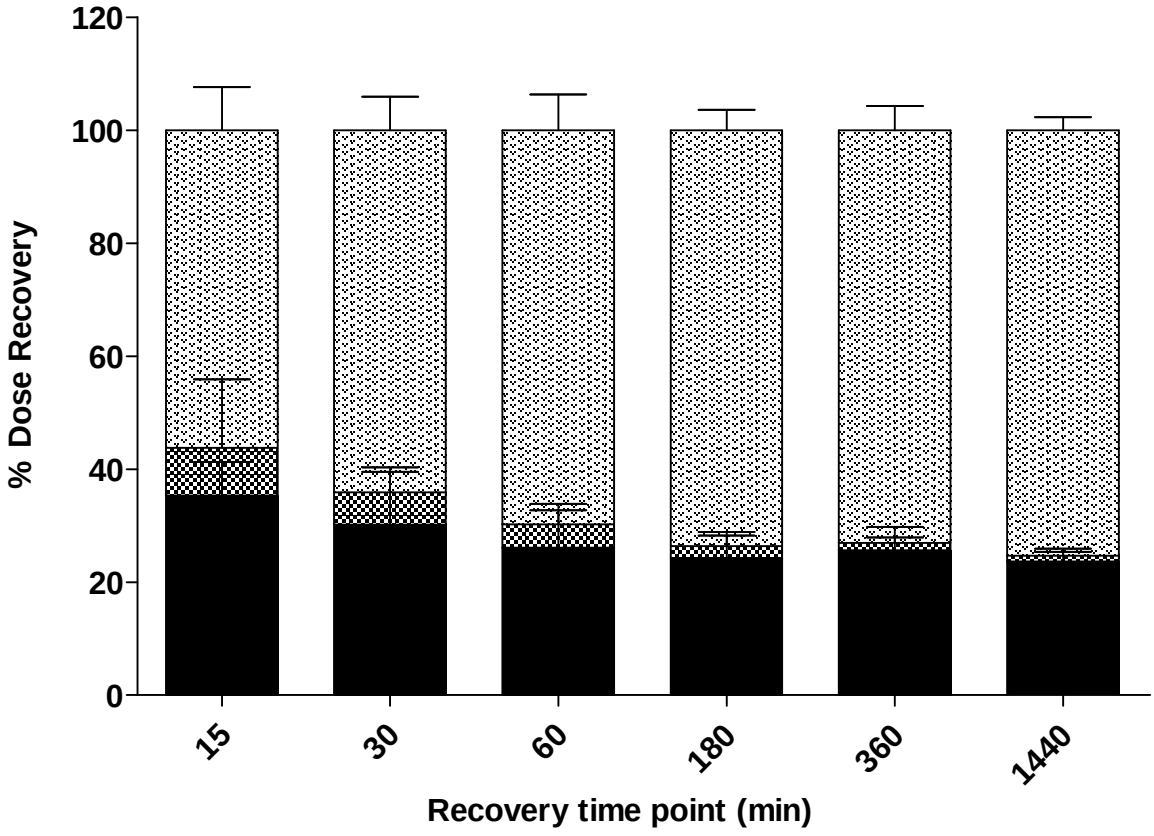

Figure 2.6: Percentage dose recovery of ^{14}C-GD from diffusion cells dismantled at the specified time points. Recovery was from the skin surface ▩ (2 surface swabs), within or pentrated through the skin ■ (summation of extractable, fixed and penetrated portions). The unrecovered fraction ▨ was taken as the difference between the initially applied dose and the total recovery. All values are mean ± standard deviation of n=8 diffusion cells.

2.3.4. GD skin surface spreading studies

Within 15 minutes of the application of a single 10 µl liquid GD droplet to the surface of undamaged pig skin, the ^{14}C-GD had spread to cover the entire diffusional surface area of the diffusion cell and beyond. The entire diffusional surface area was covered with ^{14}C-GD for the entire 24 hour study (Figure 2.7). A full dose distribution was carried out for all skins after autoradiographic procedures had been completed (Figure 2.8). Total recoveries were in the region of 25 and 30%, with the majority of ^{14}C-GD being recovered from within the skin. Any losses of radioactivity from the skin whilst being prepared for and undergoing autoradiography were not accounted for and were part of the unrecovered fraction.

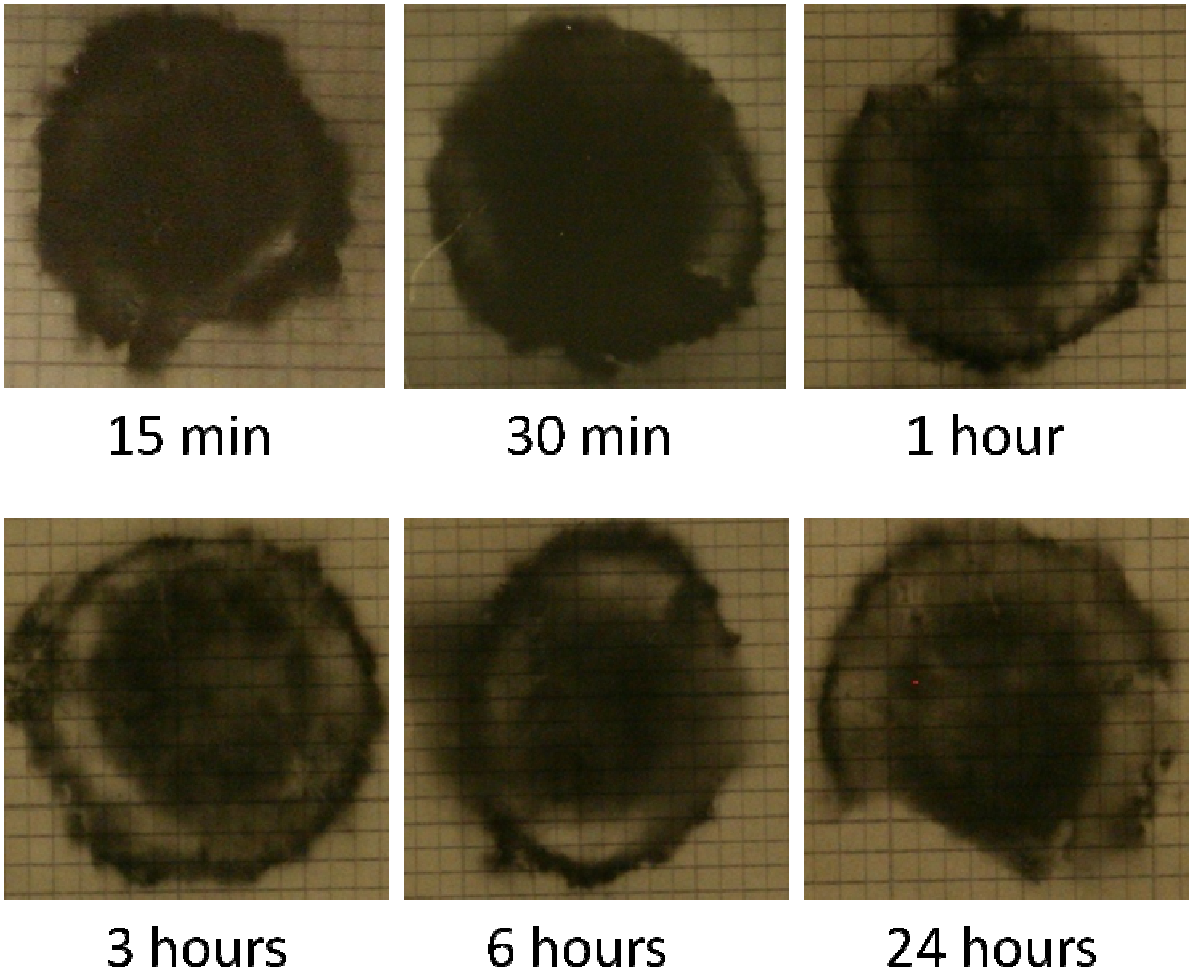

Figure 2.7: Representative skin autoradiographs showing skin surface spreading of ^{14}C-GD at each of the specified time points across unoccluded, undamaged pig skin with 50% aqueous ethanol receptor media. The central dark area (more easily visible at later time points) shows the area of skin bathed by the receptor fluid. The dark patches further out indicate that the GD was able to seep into the skin tissue clamped between the donor and receptor chamber. A total of n=8 diffusion cells were dismantled and skin surface spreading evaluated at each time point.

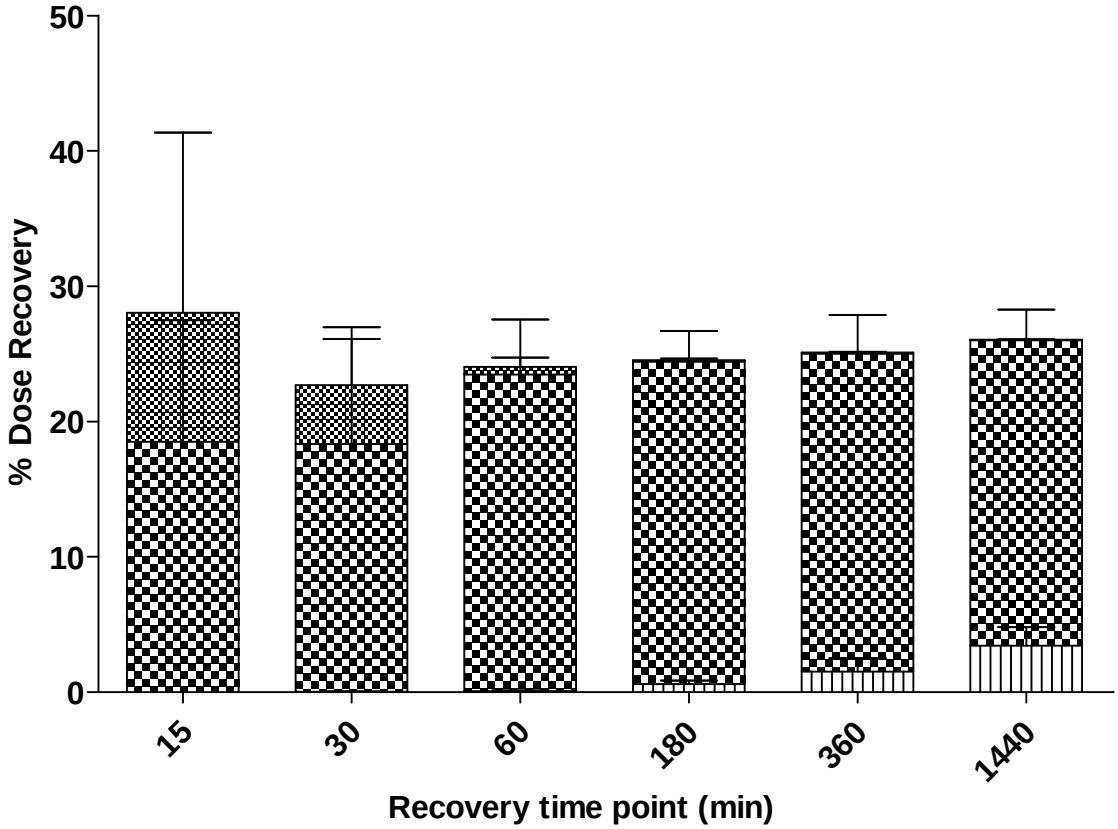

Figure 2.8: Percentage dose recovery of ^{14}C-GD from diffusion cells dismantled at the specified time points. Recovery was from the skin surface ▩ , within the skin ▩ or receptor fluid ▥ . All values are mean ± standard deviation of n=8 diffusion cells.

2.3.5. Fresh versus previously frozen skin studies

Cumulative penetration profiles of tritiated water through undamaged pig skin are shown in Figure 2.9. All values are mean ± standard deviation of n=36 diffusion cells (previously frozen skin) or n=33 diffusion cells (fresh skin), with skin acquired from 6 individual pigs with samples being taken at the time points shown. The penetration profiles were similar in both shape and magnitude. Values for the steady state penetration rates (J_{SS}) and lag times of tritiated water through dermatomed abdominal flank skin for both fresh and previously frozen skin are shown in Table 2.4. J_{SS} values were determined between 2 and 24 hours, where correlation coefficients were >0.98. The experimentally determined values of J_{SS} were used to determine the value of the permeability coefficient (K_P) and the skins total barrier resistance (R). Statistical analysis of the data revealed statistical significance ($p < 0.05$) between the J_{SS} values but not the lag times between fresh and frozen skin.

Individual animal J_{SS} values for each of the six animals used are shown in Figure 2.10. All values are mean ± standard deviation of n=6 diffusion cells (except for fresh skin for animals 1, 3 and 4, where n=5) with skin acquired from an individual pig. The contribution by each animal to the amalgamated skin permeability data (Table 2.4) is shown in Table 2.5. In general, the range of J_{SS} values were larger across animals for frozen skin than for fresh skin. Statistical analysis of this data showed significant differences ($p < 0.05$) between the J_{SS} values for fresh and frozen skin when skins from two of the individual animals (indicated in Table 2.5) were compared. Skins from animal 5 exhibited higher J_{SS} values whether fresh or frozen when compared to values from the other animals.

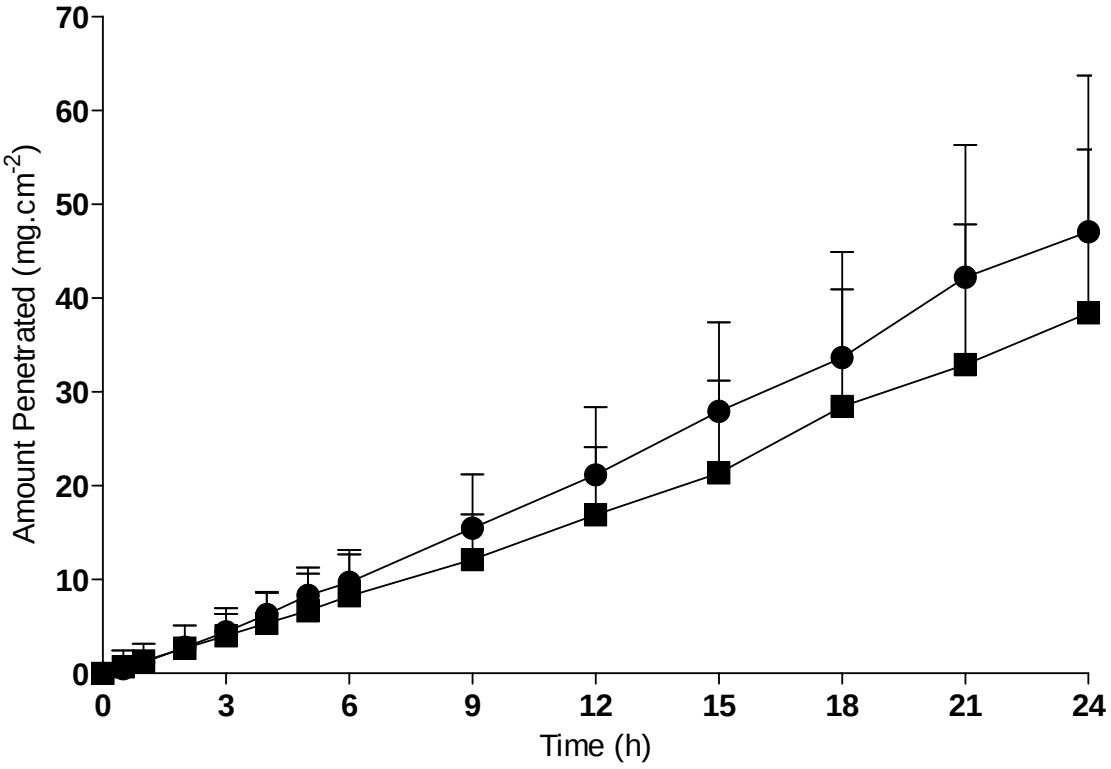

Figure 2.9: Cumulative amount of $^{3}H_2O$ penetrated through fresh -■- and previously frozen -●- abdominal flank pig skin. All values are mean ± standard deviation of n=36 (previously frozen) or n=33 (fresh) diffusion cells.

	Abdominal Flank Skin	
	Fresh	Frozen
J_{SS} ($g.cm^{-2}.h^{-1}$ $x10^{-6}$)	1644 ± 717*	2034 ± 698*
Lag time (h)	1.52 ± 0.93	1.11 ± 0.78
K_P ($cm.h^{-1}$ $x10^{-6}$)	1644 ± 717	2034 ± 698
R ($h.cm^{-1}$)	694 ± 220	556 ± 203

Table 2.4: Penetration rate (J_{SS}), lag time, permeability coefficient (K_P) and total barrier resistance (R) values for penetration of tritiated water through 500 µm undamaged fresh and previously frozen pig skin into 50% aqueous ethanol. All values are mean ± standard deviation of either n=36 (frozen) or n=33 (fresh) diffusion cells with skin taken from 6 individual animals. Data obtained from measurements between 2 and 24 hours. Statistical significance in the penetration of ^3H_2O through fresh and previously frozen skin is indicated (*).

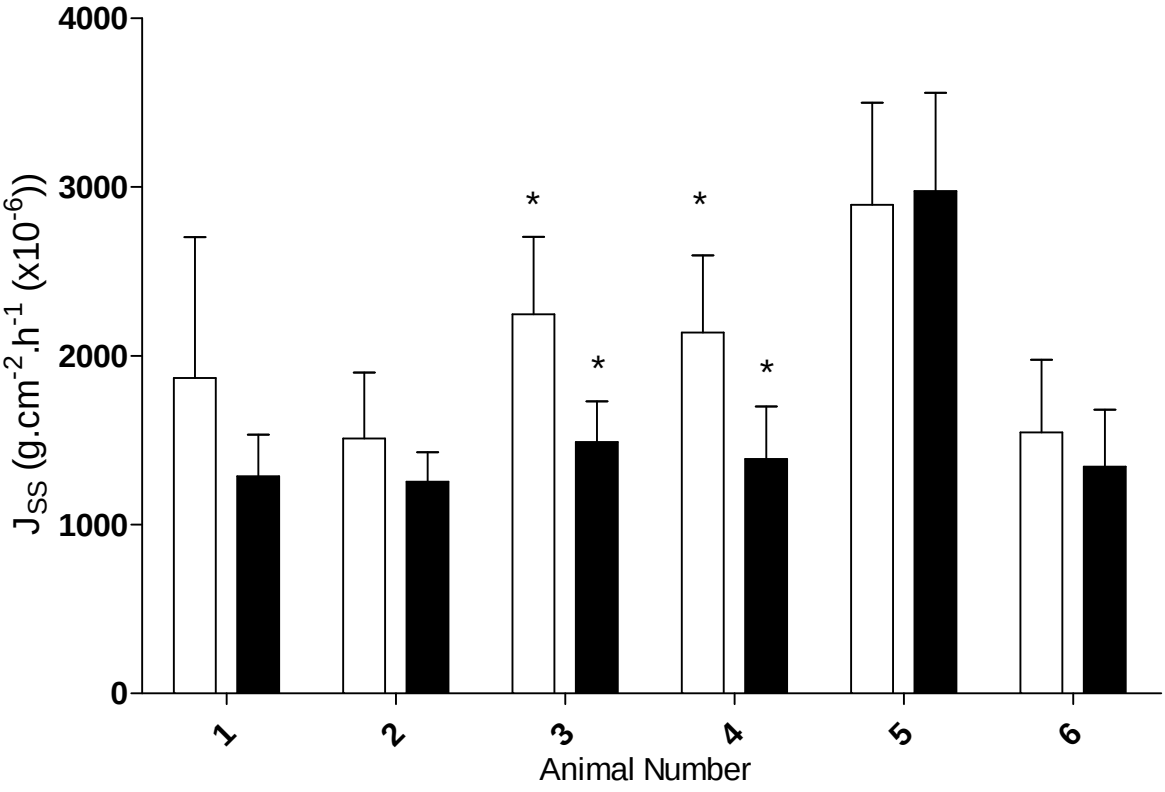

Figure 2.10: Average J_{SS} values for ^3H_2O penetration through fresh ■ or previously frozen □ abdominal flank skin from individual pigs. All values are mean ± standard deviation of n=6 diffusion cells (except for fresh skins from animals 1,3 and 4 where n=5).Statistical significance in the penetration of ^3H_2O through fresh and previously frozen skin from the same animal is indicated (*).

Abdominal Flank Skin – Frozen Skin

	1	2	3	4	5	6
J_{SS} ($g.cm^{-2}.h^{-1}$ $x10^{-6}$)	1870 ± 832	1511 ± 390	2245 ± 459*	2138 ± 456*	2894 ± 605	1547 ± 430
Lag time (h)	1.35 ± 0.92	1.03 ± 0.63	2.00 ± 0.60	0.60 ± 0.43	0.87 ± 0.81	0.7 9 ± 0.51
K_P ($cm.h^{-1}$ $x10^{-6}$)	1870 ± 832	1511 ± 390	2245 ± 459	2138 ± 456	2894 ± 605	1547 ± 430
R ($h.cm^{-1}$)	629 ± 264	703 ± 197	465 ± 118	490 ± 128	363 ± 102	684 ± 169

Abdominal Flank Skin – Fresh Skin

	1	2	3	4	5	6
J_{SS} ($g.cm^{-2}.h^{-1}$ $x10^{-6}$)	1287± 246	1254 ± 176	1490 ± 239*	1389 ± 310*	2975 ± 583	1343 ± 338
Lag time (h)	2.64 ± 1.81	1.47± 0.51	1.71 ± 0.52	0.95 ± 0.14	1.42 ± 0.59	1.07 ± 0.37
K_P ($cm.h^{-1}$ $x10^{-6}$)	1287± 246	1254 ± 176	1490 ± 239	1389 ± 310	2975 ± 583	1343 ± 338
R ($h.cm^{-1}$)	799 ± 144	812 ± 126	685 ± 111	754 ± 194	350 ± 84	787 ± 212

Table 2.5: Penetration rate (J_{SS}), lag time, permeability coefficient (K_P) and total barrier resistance (R) values for penetration of tritiated water through 500 µm undamaged fresh and previously frozen pig skin into 50% aqueous ethanol. These values are means of n=6 replicates for each animal (except for fresh skin studies for animals 1, 3 and 4 where n=5). Data obtained from measurements between 2 and 24 hours. Statistical significance in the penetration of ^3H_2O through fresh and previously frozen skin from the same animal is indicated (*). There was no significant difference in the lag times of ^3H_2O through fresh and previously frozen skin.

2.4. Discussion

2.4.1. Influence of receptor fluid choice in diffusion cell studies

One of the major considerations in the experimental design of an *in vitro* percutaneous penetration study is the choice of receptor fluid. The primary aim of the receptor fluid is to collect material that has penetrated the skin in a manner analogous as if a penetrant had absorbed through skin and into the peripheral vasculature *in vivo*. Absorption into the peripheral vasculature and from there into the rest of the body represents an “infinite sink” so the solubility of the penetrated material in the blood becomes largely irrelevant. However, in an *in vitro* diffusion cell to measure a biologically relevant penetration rate, “infinite sink” conditions are maintained by ensuring that the solubility of the penetrated material does not become rate limiting. For studies where the maintenance of viable skin is necessary, such as metabolism studies, the overriding factor is for a receptor fluid to be able to maintain skin viability within the diffusion cell system. Of equal importance, is a requirement that the penetrant must be adequately soluble within the chosen receptor media. Should this requirement not be met, it is likely that the receptor fluid could limit diffusion from the underside of the skin into the receptor fluid and lead to a gross underestimation in penetration rates. The current study used previously frozen, non viable tissue and, therefore, did not need to utilise receptor fluids that would maintain tissue viability. Of concern was whether GD, being a relatively hydrophobic compound, would exhibit suitable solubility characteristics within a traditional aqueous receptor fluid. The current study used both ethanol and bovine serum albumin (BSA) within the receptor fluid to increase penetrant solubility by offering a more lipophilic environment.

Previous work carried out into the percutaneous absorption of chemical warfare agents has used 50% aqueous ethanol as a receptor fluid to ensure that the receptor fluid did not become a rate limiting step in the diffusion process (Chilcott, et al., 2007;Dalton, et al., 2006a;Dalton, et al., 2006b). However, the skin penetration of GD has not previously been determined using *in vitro* diffusion cell methodology. The solubility of GD in water (21 $g.L^{-1}$) suggested that 5 ml of a standard phosphate buffered saline (PBS) receptor fluid may have offered sufficient sink conditions to be an appropriate receptor fluid for the 102 mg of applied GD (given that 86.1 ± 15.9 % of the applied GD was located on the skin surface upon study completion).

The absorption profiles indicated that of the three evaluated receptor fluids, only 50% aqueous ethanol offered suitable sink conditions for GD. Steady state (J_{SS}) flux was observed for GD penetrating into 50% aqueous ethanol after the initial lag phase, but, not for either of the PBS containing receptor fluids. For GD penetration into the PBS containing receptor fluids, the effect was similar, an initial flux of higher magnitude between 3 and 9 hours which then reduced over the twenty four hour time course, indicating that neither of the PBS based receptor fluids were able to solvate GD sufficiently. It should be noted that sufficient GD remained on the surface of each skin at the end of the each study so that diffusion should not have started to approach equilibrium (as it seemed to do with the PBS receptor media).

Of interest is why PBS with 5% BSA did not offer more suitable sink conditions for GD than PBS on its own. Studies by other researchers have shown the addition of BSA to the receptor media increases the solubility of lipophilic penetrants such as methyl paraben (Wilkinson, et al., 2007). Wilkinson and co-workers also evaluated an ethanolic receptor fluid alongside PBS and a BSA containing receptor fluid, with maximum absorption rates falling in the order of aqueous ethanol > BSA > PBS. The trend for the current study was aqueous ethanol > BSA = PBS. Explanation for the difference can only be due to the interaction of GD with ethanol and BSA. Ethanol is able to interact with and solvate lipophilic molecules due to its two carbon chain and is also able to hydrogen bond with hydrophilic molecules due to the presence of the hydroxyl group. This broad solvation ability allows ethanol to act as a general organic solvent for lipophilic compounds including GD. Conversely, the current study has shown that BSA is not a suitable solubility enhancing excipient for all organic molecules. BSA is typically chosen as a solubility enhancer for receptor fluids where it is necessary to maintain skin viability (Collier, et al., 1989). For studies where maintenance of skin viability is not of concern, this work has shown that ethanol water offers superior sink conditions, although, mention must also be made of other receptor fluids containing excipients such as polyethylene glycol (PEG) 20 oleyl ether that have recently been recommended to facilitate sink conditions for hydrophobic chemicals (Fasano and McDougal, 2008).

The current study has shown that use of an ethanol water receptor fluid gave an increased measured GD penetration rate compared to the GD penetration rates using PBS receptor fluids. Without knowledge of actual *in vivo* GD skin penetration

rates it is not possible to determine which penetration rate is correct. Should the penetration rate of GD into an ethanol water receptor fluid be correct, then the PBS receptor fluids underestimate dermal absorption. However, should the penetration rate of GD into PBS based receptor fluids be correct, then use of an ethanolic receptor fluid overestimates dermal absorption. Interestingly, previous work evaluating the skin penetration of the lipophilic chemical fluazifop-butyl into a range of receptor fluids showed that only an aqueous ethanol receptor fluid predicted *in vivo* skin absorption (Ramsey, et al., 1994). Guideline documentation (OECD, 2010) recognizes that although saline may be an adequate receptor fluid for hydrophilic compounds, it is likely to underestimate the percutaneous absorption of lipophilic compounds.

Questions have been raised as to whether an ethanolic receptor fluid disrupts the skins barrier layer and whether it is this disruption that leads to the observed increased penetration rates compared to PBS based receptor fluids. Previous work (Pershing, et al., 1993) indicates that ethanol concentrations have to exceed 75 % for penetration enhancement to be observed. Penetration rate enhancement by ethanol has been ascribed to lipid extraction (Van der Merwe and Riviere, 2005), however, this conclusion is not supported by the current study, as it would be expected that a disruption of this type would cause a reduction in the measured lag time when comparing aqueous ethanol to the PBS containing receptors fluids. In this study, all the lag times measured between 3 and 9 hours were similar suggesting that use of an ethanolic receptor fluid caused minimal barrier disruption. Given that use of a 50% aqueous ethanol receptor fluid in the current study was the only receptor fluid able to

maintain steady state flux for GD skin penetration suggests that the PBS receptor fluids were underestimating GD skin absorption.

Ultimately, as long as a receptor fluid is able to maintain skin viability (if appropriate) and suitable sink conditions, experimental choice as to the most appropriate receptor fluid comes down to achieving experimental aims. However, the potential effect of any excipient in the receptor solution on the partitioning of the penetrant into the stratum corneum should not be discounted. It should be noted that neither PBS nor ethanol is in contact with the barrier layer *in vivo* and so could alter the partitioning of the penetrant and its solubility in the skin layers. It may be concluded that any *in vitro* diffusion cell determined penetration rates will be different from those achieved under *in vivo* conditions; however, this does not make the results meaningless. Interpretation of *in vitro* penetration measurements need to be interpreted in the light of the differences between the *in vitro* and *in vivo* conditions. Using a receptor fluid such as 50% aqueous ethanol gives assurance that any determined penetration rate would not likely be an underestimate of *in vivo* penetration rates. This is particularly pertinent to the hazard assessment of toxic skin penetrants such as chemical warfare agents. In conclusion, the data from the current study has shown that the most suitable receptor fluid (from those evaluated) to use as a sink for GD was 50% aqueous ethanol.

2.4.2. Infinite dose studies with porcine skin

The infinite dose study uses occluded conditions to ensure that the penetrant within the donor chamber remains in excess for the duration of the study by eliminating any potential evaporation of the penetrant. When the penetrant is volatile, such as GD, this will lead to overestimation of the penetration rate compared to an application under unoccluded conditions. Furthermore, under realistic exposure conditions, it is unlikely that a contaminated area of skin would be bathed in a chemical warfare agent. As such the infinite dose studies carried out can be viewed as the worst case scenario, and while unrealistic, offers valuable insight into how effective a medical countermeasure ideally needs to be to cover the worst eventualities. An advantage of the infinite dose study is that it allows derivations of parameters such as Kp and R which finite dose studies do not.

The J_{ss} value for GD through dermatomed pig skin was determined to be 439 ± 158 $g.cm^{-2}.h^{-1}$ (x 10^{-6}). Work by van Hooidonk (1980) has previously determined that penetration rate of GD through human skin and guinea pig skin to be 210 $g.cm^{-2}.h^{-1}$ (x 10^{-6}) and 414 $g.cm^{-2}.h^{-1}$ (x 10^{-6}) respectively (van Hooidonk, et al., 1980). There are a number of important differences between these studies. The van Hooidonk study used full thickness tissue rather than split thickness. The use of full thickness skin may inhibit the penetration rate of lipophilic compounds due to the presence of extra dermis below the level of the peripheral vasculature which would not need to be crossed *in vivo*. It has been recommended that full thickness skin should be avoided in human skin *in vitro* diffusion experiments due to the generation of prohibitively long lag times (Henning, et al., 2009). A second difference was the choice of receptor fluid. The van Hooidonk study used a physiological salt solution (as metabolic

degradation was also being evaluated). As has been previously discussed, the use of a salt solution may have led to an underestimation of the true penetration rate. It is likely that the measured penetration rates in the van Hooidonk study would have been greater had split thickness skin and an ethanolic receptor fluid been used.

The van Hooidonk study also evaluated the penetration rate of VX through human skin and guinea pig skin to be 168 $g.cm^{-2}.h^{-1}$ (x 10^{-6}) and 516 $g.cm^{-2}.h^{-1}$ (x 10^{-6}) respectively. Previous work conducted by Dalton and co-workers has evaluated the steady state penetration rate of ^{14}C-VX through not only undamaged dermatomed pig skin, but, also human and guinea pig skin into a 50% aqueous ethanol receptor fluid (Table 2.6) (Dalton, et al., 2006a). A comparison of the VX penetration studies indicates that for both species, human and guinea pig, the methodology employed by van Hooidonk gave a lower penetration rate than the methodology employed by Dalton *et al*. The likely reasons, as discussed, between the values are due to differences in skin preparation and choice of receptor fluid.

Table 2.6 compares previous VX penetration studies to the current GD pig skin penetration studies. Using identical methodology, the penetration rate of GD through split thickness pig skin was approximately twice that of VX, furthermore, the lag time value was significantly less for GD than for VX. That GD is a more rapid skin penetrant than VX has implications in the design of countermeasures to treat percutaneous nerve agent intoxication. It would appear that the requirements of a medical countermeasure to treat percutaneous GD poisoning will likely require a

more rapid onset of action to ensure adequate removal of agent before penetration can occur.

OECD guidelines (Section 1.8.1.1) require that the success criteria for an *in vitro* diffusion cell study include a mass balance with a mean radioactivity recovery of 100 ± 10 % of the initially applied dose. The total recoveries at 24 h for all the infinite dose studies carried out achieved this criteria (94 ± 10 %), with the majority recoveries (86 ± 16%) being from the surface of the skin. Less than 5 % of the applied dose had penetrated through the skin and into the receptor fluid by 24h (Figure 2.2).

Using the infinite dosing technique as a method for determination of the likely worst case scenario for GD penetration through porcine skin has provided upper limit values that both current and future countermeasures ideally need to be able to protect against.

Nerve Agent	GD	VX		
Species	Pig	Pig	Human	Guinea Pig
J_{SS} ($g\ cm^{-2}\ h^{-1} \times 10^{-6}$)	439 ± 158	207 ± 62[A]	333 ± 226[B]	2406 ± 988[A,B]
K_p ($cm\ h^{-1} \times 10^{-6}$)	429 ± 154	205 ± 62[C]	330 ± 244[D]	2387 ± 980[C,D]
T_L (h)	1.7 ± 0.5	6.3 ± 0.9[E]	4.6 ± 1.2[F]	0.9 ± 0.2[E,F]

Table 2.6: Summary of the percutaneous absorption kinetics of ^{14}C-GD, topically applied as undiluted liquid through undamaged dermatomed pig skin and ^{14}C-VX, topically applied as undiluted liquid through undamaged dermatomed guinea pig, pig and human skin. In all cases the receptor fluid used was 50% aqueous ethanol. All values are average ± standard deviation. Steady-state fluxes for VX were measured between 2–24 h (guinea pig), 10–22 h (pig) and 9–24 h (human). Steady-state fluxes for GD were measured between 3–9 h (pig). Kinetic parameters were steady-state flux (J_{SS}), permeability coefficient (K_p) and lag time (T_L). Superscript capital letters indicate a significant difference ($p > 0.05$) between the same-labelled parameters. Kp assumes a liquid density of 1.008 g cm^{-3} at 25 ℃ for VX and 1.022 g cm^{-3} at 25 ℃ for GD.

2.4.3. Finite dose studies with porcine skin

The finite dose study offers a more realistic contamination scenario than that employed by infinite dosing methodology. Not only is the system unoccluded, allowing volatile chemicals to evaporate, rather than placing an unrealistic contamination density of the skin surface, only a small droplet is applied. The finite dose study may be viewed as a likely contamination scenario rather than the definitive worst case scenario and is typically the methodology employed when determining the efficacy of potential chemical warfare agent decontaminants.

The finite dosing methodology diffusion cell work presented in this thesis used two different types of static diffusion cells, while both of the Franz type, one was a commercially available system (PermeGear™) and the other an in house system. Static diffusion cells are used in laboratories both nationally and internationally and it is important that results generated in one laboratory are reproducible in another to enable confidence in the data generated. The guidelines and protocols that have been ratified go some way to affording data reproducibility. That laboratories have their own bespoke diffusion cell systems is accepted and reproducibility between laboratories has been evaluated using standardised protocols (Chilcott, et al., 2005a). This, however, is the first time that two systems have been compared within the same laboratory to look at differences whilst using the same operator. From the data generated, both the PermeGear^{TM} and Dstl in house system performed similarly, with no statistical difference in J_{MAX} values between the two. This gives confidence

that different systems do perform similarly and differences between laboratories are most likely due to the human operator, rather than the system itself.

The J_{MAX} value for GD through dermatomed pig skin was determined to be 10.8 ± 4.8 $g.cm^{-2}.h^{-1}$ (x 10^{-6}) for the Dstl in house diffusion cell system and 8.5 ± 2.5 $g.cm^{-2}.h^{-1}$ (x 10^{-6}) for the PermeGear^{TM} diffusion cell system. Comparison of GD skin penetration by infinite and finite dosing methodology showed an approximate 40 fold reduction in penetration rate. Other than the smaller volume of GD applied to the skin surface, another reason for the reduction in penetration rate was likely to be due to free evaporation of GD from the skin surface under finite dosing conditions (a situation deliberated prevented under infinite dose conditions and confirmed by a total recovery of (94 ± 10 %), (Section 2.4.2). Under unoccluded (finite) dosing conditions GD would be expected to volatilize with a half life of approximately 7.7 hours (Munro, et al., 1999) for GD not absorbed into the skin. Interestingly, however, there was no difference in lag time between infinite and finite dosing conditions indicating that even if evaporation of GD occurs, skin penetration is still rapid.

Dose distribution at 24 h showed a total recovery of approximately 25% of the applied dose. Given that the infinite dose study (section 2.4.2.) gave a total recovery of approximately 94% and the only difference (as far as the dose distribution was concerned) between the two studies was prevention of free evaporation, it is likely that the majority of the remaining 75% of the applied dose of GD evaporated from the skin surface over the 24 h study duration. As only negligible amounts of radioactivity

were recovered from the surface of the skin at 24 h (supporting the likelihood of evaporation under finite dosing conditions), the majority of the remaining 25% had penetrated into or through the skin. In terms of the actual amount penetrated, this equates to approximately 2.5 mg of GD or in terms of contamination density penetration, 1 $mg.cm^{-2}$. The majority of the GD contamination did not penetrate through to the receptor fluid and can be assumed to be bound to skin components and not available to induce systemic toxicity. Should the maximum GD skin penetration rate of approximately 11 $\mu g.cm^{-2}.h^{-1}$ have occurred through a contaminated surface area comprising the head, neck, arms and hands (those areas potentially left unclothed, and approximating to 3420 cm^2 of a total body surface area of 19000 cm^2 (Hettiaratchy and Papini, 2004;Mosteller, 1987)) then the dose per hour would equate to 37.6 mg h^{-1}. Given that the average person weighs 70 kg, this equates to 0.5 mg kg^{-1} h^{-1}. The estimated human LD_{50} value for GD has been quoted as being 5 mg kg^{-1} (or 350 mg) (Chauhan, et al., 2008). Using this value it would be expected for the LD_{50} threshold to be reached as little as 10 hours after exposure to GD exclusively via the percutaneous route in the absence of decontamination. However, it must be emphasised that the current study did not take metabolism into account, which has been previously been shown to be substantial (up to 80%) in human skin (van Hooidonk, et al., 1980).

2.4.4. GD reservoir studies

This study has shown that there is a reservoir of ^{14}C-GD in pig skin for up to 24 hours after contamination of the skin surface *in vitro* with liquid agent. A proportion of this

reservoir was extractable with the organic solvent acetonitrile, and the amounts of extracted GD represent more than 10% of the initially applied dose up to one hour post challenge. The proportion of liquid GD that remained on the skin surface lessened as recovery time points progressed (from 8 ± 12 % at 15 minutes to 1 ± 1 % at 24 hours) , conversely, the proportion of unaccounted for GD increased (from 56 ± 8 % at 15 minutes to 75 ± 2 % at 24 hours). The likelihood of the unrecovered fraction being due to evaporation from the skin surface is discussed in section 2.4.3. Interestingly, however, is the disparity in predicted half life time from the value of 7.7 hours (Munro, et al., 1999). The current study shows that the unrecovered fraction of the applied dose reaches its first half life within 15 minutes of application. The value of 7.7 hours is stated to have been derived from a linear deposition model. Full details of the model are unfortunately not available. Should the model have considered a lower surface temperature than the skin surface temperature of 32℃ used in the current study then that may explain the disparity. It should be noted that the current study does not directly measure evaporation, only the unrecovered fraction. At best this may be seen an indirect measure of evaporation, although, other losses such as lateral diffusion of GD in between the donor and receptor chambers of the diffusion cell and subsequent association into the ground glass joints cannot be discounted. The observation of lateral diffusion is discussed in section 2.4.5. Of the remaining 30 to 40% (depending on the reservoir quantification time point), a consistent 14 to 17% of the applied dose was fixed within the skin. The remaining extractable component represents the magnitude of the acetonitrile extractable GD skin reservoir. The extractable component was at a maximum at 15 minutes (19 ± 4 %) and reduced to 2.5 ± 0.5 % by 24 hours.

The fixed GD fraction can be assumed to be either irreversibly bound to intra- or intercellular constituents (such as keratin (Verstappen, et al., 2012)) within the skin or not amenable to extraction by acetonitrile. Assuming the former supposition is true, the fixed proportion of the applied dose (14 to 17 %) would be unavailable for the manifestation of any systemic toxicity. This being the case, 20% or less of the initial applied dose of liquid GD (the combination of GD present in the receptor fluid and the extractable GD skin reservoir) would have been available to cause any subsequent systemic toxicity. At 15 minutes post exposure the amount of GD available to cause systemic toxicity was 19 ± 4 % of the applied dose which dropped to 7 ± 3 % by 3 hours and to 6 ± 2 % by 24 hours. It would be expected for these values to remain similar throughout the study duration as any loss from the extractable reservoir should see a gain into the amount present in the receptor fluid. Explanation for this observation may be due to either the GD in the extractable skin reservoir diffusing back to the skin surface or that the GD was associated very closely with the upper skin layers and was not removable with dry swabbing (however, this would still be deemed as part of the reservoir). Either situation would then allow for evaporation from the skin surface (a process known as “off gassing”). It therefore seems likely that “off gassing” of GD from the skin reservoir occurs in tandem with skin penetration of GD from the skin reservoir. However, the magnitude of such an absorbed dose is more than sufficient to cause nerve agent toxicity. That back diffusion from within the skin occurs has important implications for the design and use of skin decontaminants. Early removal of a skin decontaminant may potentially result in secondary contamination of medical personnel from the GD skin reservoir.

It is questionable as to whether solvent extraction of the GD skin reservoir with acetonitrile was 100% efficient, as work with other chemical warfare agents, such as sulphur mustard, suggests that reservoirs cannot be completely removed using organic solvent extraction (Hattersley, et al., 2008). That the current study used sequential solvent extractions with minimal GD recovered in extractions 2 and 3 suggests that the acetonitrile extracted as much GD as it was able to. The observation that the unextractable (fixed) fraction was a consistent 14 to 17 % irrespective of reservoir quantification time point offers further evidence that the solvent extraction was as efficient as it was able to be. Solvent extraction is a commonly used technique to quantify the amount of a chemical within the skin, particularly for studies were radiolabel is not used. A recent example determining the percentage of a UV filter extractable by solvent extraction showed recoveries in excess of 94 % (Scalia, et al., 2011). It is likely that the reason that acetonitrile extraction was not completely effective for GD was due to irreversible binding to skin constituents; however, use of further solvents could be evaluated to ensure that this is indeed the case. Should the solvent extraction method used for the current study not have been 100% effective then the extractable skin reservoir of GD would have been underestimated. This would lead to a maximum underestimation of the extractable reservoir by 14 to 17%.

It is likely that a combination of back diffusion and skin penetration led to the extractable skin reservoir diminishing over time from 19 ± 4 % at 15 minutes to 2.5 ± 0.5 % by 24 hours. The decrease in the extractable reservoir over the 24 hour study duration was consistent with the hypothesis that GD forms a transient depot within

the skin during percutaneous absorption. The maximum percentage of applied dose within the skin was achieved up to one hour after exposure (with 50% of this being extractable at 15 minutes post exposure), indicating that this is the optimum time for any countermeasure based on removing the depot. The existence of GD reservoirs has been previously reported in a variety of tissues including the lung and skin (Kadar, et al., 1985;Benschop, et al., 1981;Clement, 1982;Nordgren, et al., 1985;Wolthuis, et al., 1981). In summary, the current work programme confirms the existence of GD reservoirs within the skin after a percutaneous exposure.

2.4.5. Skin surface spreading of soman

One of the key assumptions in the data interpretation of diffusion cell studies is that a penetrant diffuses across the entire surface area available for diffusion within the diffusion cell. Should this assumption be invalid and the penetrant diffuses across a smaller proportion of the available area then calculated penetration rates may substantially underestimate actual penetration rates.

The data provided by the series of skin surface spreading studies have shown that the spread of ^{14}C-GD either across the surface or within the upper skin layers (autoradiography being unable to distinguish between the two) is rapid, with complete coverage of the diffusional surface area within 15 minute of dosing. This allows for the appropriate conversion from amount of ^{14}C-GD penetrated per unit time to the amount per unit area of ^{14}C-GD penetrated per unit time. Complete coverage of the defined areas remained for the entire duration of each 24 hour study, although, it was

evident that for later time points the intensity of the radioactivity had diminished. The diminishing intensity correlated well with diminishing ^{14}C-GD on the skin surface observed during both the skin surface spreading studies and the reservoir quantification studies.

Interestingly, surface spread was not confined to the central area of the dosing chamber, with ^{14}C-GD laterally penetrating through the skin that was clamped between the donor and receptor chamber to the periphery of the skin section. The implication of this is that less of the ^{14}C-GD would have been available for skin penetration than previously thought, with evaporation not only taking place from the skin surface within the donor chamber, but, also from the skin periphery outside of the diffusion cell system. The contribution made to evaporation by GD from the peripheral tissue cannot be quantified from this series of studies, however, if the infinite (occluded) studies are taken into account, it can be seen that any periphery evaporation is negligible due to the approximate 100% dose recoveries made. It is likely therefore that although lateral diffusion takes place, it is limited and that the majority of laterally diffusing ^{14}C-GD remains within the skin tissue.

Comparison of these studies with the reservoir quantification studies (Section 2.4.4) showed that the amount of radioactivity fixed (not solvent extractable) for the reservoir studies correlated well with the amount of radioactivity found within the skin upon completion of autoradiography. The data suggests that the majority of the solvent extractable “free” GD evaporated from the skin surface during the

autoradiograph protocol. If this was the case, the hazard of secondary contamination to emergency responders cannot be under emphasised.

2.4.6. Use of fresh or previously frozen pig skin in diffusion studies

Freezing skin prior to use in diffusion cell studies is often a logistical necessity and is supported by OECD guidelines (although the preference would be to use fresh skin). This has led to the practice becoming commonplace (Barbero and Frasch, 2009;Bronaugh, et al., 1986;Davies, et al., 2004). Concern regarding potential degradation in skin barrier function using previously frozen skin in skin penetration studies has led a number of researchers to conduct comparison studies. Studies by Harrison (1984), Bronaugh (1986) and Hawkins (1986) evaluated the effect of freezing on human skin permeability (Harrison, et al., 1984;Bronaugh, et al., 1986;Hawkins and Reifenrath, 1986) with the conclusion that permeation did not increase through skin that had been stored frozen. However, more recent work by Ahlstrom (2007) has shown increased permeability of water through previously frozen tissue (Ahlstrom, et al., 2007). The current study was designed to clarify specifically whether freezing had a detrimental effect on the skin barrier integrity of pig skin. The penetrant used for this study was tritiated water (not ^{14}C-GD), the reason for this choice is that it is the standard penetrant for the evaluation of perturbation of skin barrier function (integrity testing), recommended by the OECD, prior to commencement of diffusion cell studies.

Storage of skin at -20ºC for 2 weeks produced a significant decrease in barrier function for 2 out of 6 animals when comparing individual animal data using tritiated water as a penetrant. For three of the other animals there seemed to be a trend for a reduced barrier function after freezing skin. There are a number of possible mechanisms which could explain reduced skin barrier function after freezing including perturbation of the lipid bilayers of the inter corneocyte lipids or potentially degradation of corneodesmosomes leading to reduced corneocyte adhesiveness (Sintov and Botner, 2006). Given that freezing has been shown to decrease pig skin barrier function means that this must be taken into account when evaluating penetration rate data from *in vitro* diffusion cell studies. The work reported supports the OECD guideline that the use of fresh skin is to be preferred, however, practically, use of fresh tissue is not often a realistic option (especially in the case of acquiring human *in vitro* skin). For studies of the type described in this thesis which use previously frozen skin, having a potential slight overestimation of penetration parameters may be viewed as beneficial as countermeasure research is generally interested in defining the worst case scenario to ensure that any countermeasure put into general service will be efficacious.

2.4.7. Summary of interactions of GD with skin

This work has investigated a number of aspects of GD skin penetration leading to the proposed interaction scheme in Figure 2.11. A droplet of GD coming into contact with the skin surface spreads rapidly either across the skin surface using the skin's micro relief to facilitate spreading or within the upper layers of the stratum corneum by

lateral diffusion (or more likely a combination of both). By 15 minutes auto radiographic techniques have shown that the entire surface area available for diffusion within the diffusion cell system was covered.

The amount of radioactivity removable from the skin surface with a dry swab at 15 minutes post contamination was less than 10% of the originally applied dose, whilst the amount of radioactivity that was associated with the skin (either within the microrelief or actually within the skin) was approximately 35% of the applied dose. The remaining unaccounted for 55% was assumed to have volatilised from the skin surface. Of the 35% associated with the skin, approximately 18% was solvent extractable and 17% was not solvent extractable.

The solvent extractable portion or “free” radioactivity was likely to have formed a depot or reservoir which would be available for percutaneous penetration whereas the “fixed”, non-extractable radioactivity would likely be bound to skin macromolecules and not available for skin penetration. It is likely, however, that the solvent extraction technique was not 100% efficient, so the approximate values for “free” and “fixed” should be interpreted with caution. The amount of “fixed” radioactivity remained constant for a 24 hour period whilst the amount of “free” radioactivity showed a steady decrease to around 2% of the applied dose at 24 hours. It is important to note that the majority of “free” radioactivity did not penetrate through the skin, with less than 5% of the applied dose being present in the receptor fluid at 24 hours. The difference between “free” and penetrated can be accounted for by an off gassing mechanism, with the majority of the “free radioactivity” dissociating

from the skin and assumed to volatilise from the skin surface. For this scenario to be valid, the depot of “free” radioactivity would likely be within the upper surface skin layers or associated with radioactivity within the skins microrelief. That auto radiographic data shows the presence of radioactivity associated with the upper skin layers for the entirety of the 24 hour study period supports this observation.

In the absence of volatilisation, using infinite dosing techniques, the steady state flux, J_{SS}, through abdominal flank pig skin was 439 ± 158 $\mu g.cm^{-2}.h^{-1}$ whereas for a finite, single 10µl droplet with volatilisation, the maximum penetration rate was 10.8 ± 4.8 $\mu g.cm^{-2}.h^{-1}$. These two values may be used to represent two different but specific scenarios, gross liquid contamination and small droplet contamination.

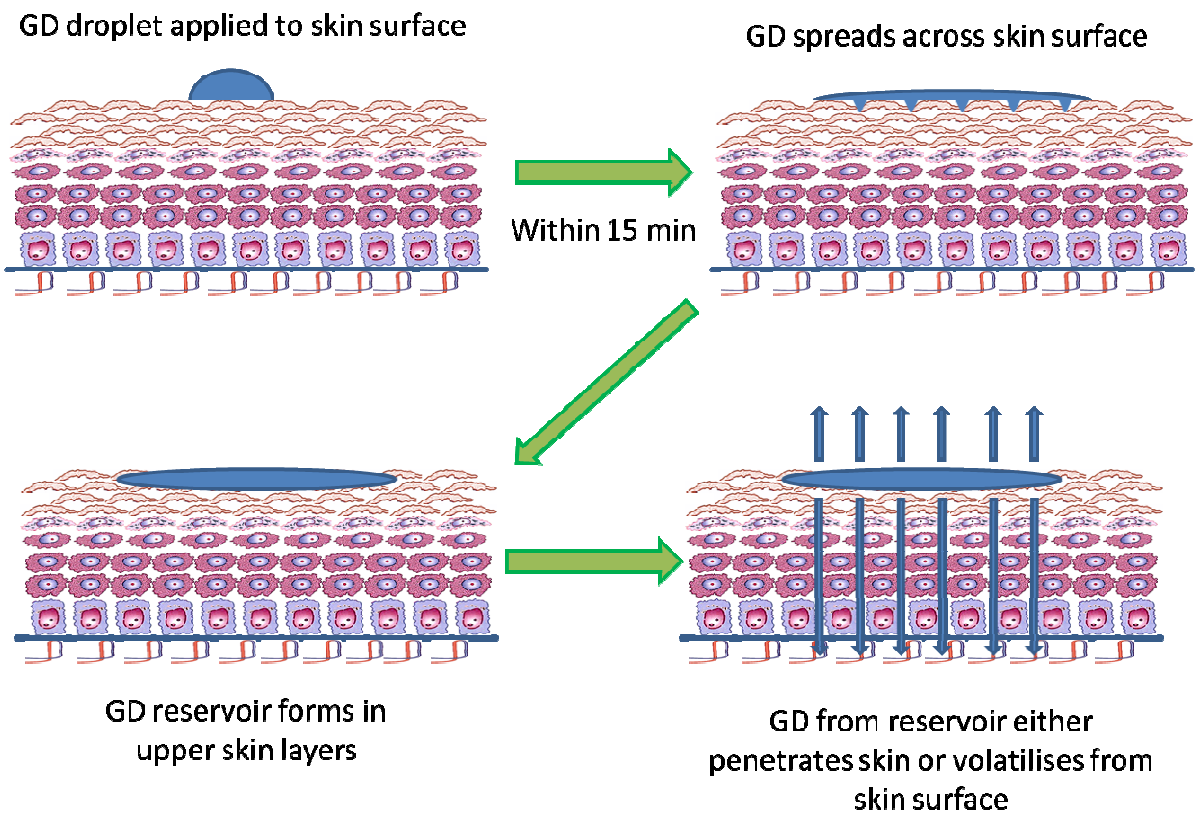

Figure 2.11: Summary representation of the interaction of GD with skin.

CHAPTER 3: EFFICACY TESTING OF HAEMOSTATIC PRODUCTS IN THE PRESENCE OF CHEMICAL WARFARE AGENTS: INTERACTIONS WITH GD

3.1. Introduction

The release of chemical warfare (CW) agent caused by an explosion may result in casualties presenting with contaminated, haemorrhaging wounds. There is an identified need to develop haemostatic products that can stop haemorrhage and decontaminate CW agents simultaneously (Section 1.1.). A number of commercial off the shelf (COTS) haemostatic products have been identified as potential candidates to fulfil a dual role as both haemostat and chemical warfare agent decontaminant (Section 1.3.) However, it is of vital importance that a potential haemostatic decontaminant should not have its haemostatic ability compromised in the presence of CW agent, otherwise, it will only fulfil the role of decontaminant. Should the CW agent compromise haemostatic ability then the haemorrhaging casualty would not stop bleeding and would rapidly deteriorate. It was therefore essential to ensure that a candidate COTS haemostatic therapy retains its haemostatic properties in the presence of CW agent.

The purpose of this *in vitro* study was to evaluate the effect of GD (Section 1.6) on the clotting efficacy of COTS haemostatic products. As the haemostatic decontaminant under development must display undiminished clotting ability in the presence of a range of CW agents, complementary studies have simultaneously

investigated the efficacy of the candidate haemostats in the presence of sulphur mustard and VX (Hall, et al., 2009).

3.1.1. Determination of clotting efficacy

A number of routine clinical methods are available to measure various clotting parameters including plasma thromboplastin (PT), partial thromboplastin time (PTT), platelet count, fibrinogen concentrations and thrombelastography (TEG). TEG offers the advantage of monitoring haemostasis as a whole dynamic process rather than as isolated endpoints (Mallett and Cox, 1992). Conventional clotting efficacy tests are generally performed at single time points in the blood coagulation process. As reviewed by Kashuk (Kashuk, et al., 2010), thrombelastography (TEG) was developed by Hartert in 1948 (Hartert, 1948) and allows haemostatic function to be assessed from a single blood sample. In comparison to other coagulation tests, the entire blood coagulation process from the initial platelet-fibrin interaction to eventual clot lysis may be observed. Standard coagulation tests tend to end with the formation of the first fibrin strands. TEG is being evaluated in both military and civilian settings to measure blood coagulation (Devlin and Gutierrez, 2010;Doran, et al., 2010;Dries, 2010), and for the purpose of the current study allowed for rapid selection of candidate treatments without the need for *in vivo* testing. Another advantage of TEG, making it the preferred option for the current study, was the ability to rapidly analyse a number of blood clotting parameters from CW agent contaminated samples in tandem with control samples.

3.1.2. Blood coagulation

Blood coagulation is an important defence mechanism against bleeding. Rupture of the endothelium that allows exposure of blood to the extravascular tissue triggers the response of the coagulation system (Dahlback, 2000). The blood coagulation system in humans comprises three general processes:

i. Immediate contraction of blood vessels at the site of vascular injury.
ii. Platelet plug formation.
iii. Platelet plug stabilisation via fibrin clot generation resulting from the interaction of tissue and plasma proteins primarily on the surface of activated platelets (Davie, 2003).

The generation of fibrin results from a series of reactions involving blood proteins which are in precursor or inactive forms. Activated platelets provide the necessary phospholipid to initiate the blood coagulation cascade (Figure 3.1). The blood coagulation cascade comprises two complementary pathways, the intrinsic and extrinsic. The extrinsic cascade is critical to the initiation of fibrin formation whilst the intrinsic cascade plays a role in the growth and maintenance of fibrin formation (Davie, et al., 1991). The final steps of the coagulation cascade see the conversion of Prothrombin to Thrombin, the enzyme responsible for conversion of fibrinogen to the insoluble fibrin clot. From initiation to termination, the coagulation cascade involves a large number of plasma proteins and cofactors (Davie, 1986).

3.1.3. The TEG® system

The TEG® system measures the properties of the forming clot through the use of a cylindrical cup which rotates through an angle of 45° over a 10 second period. Briefly, a pin is suspended in the blood held in the cup by a torsion wire. As the clot begins to form, the torque of the rotating cup is transmitted to the pin. In essence, the strength and rate of clot formation directly affects the extent of pin motion. The rotational movement of the pin is converted to an electrical signal that can be analysed by computer software to give a coagulation profile (Figure 3.2). Of importance for the current study were the “R time” which gives a measure of the time period from latency (time of sample placement) to initial fibrin strand formation. “K time” which gives a measure of the speed to reach a certain level (20 mm) of clot strength. “α” which gives a measure of the rapidity of fibrin build up and cross linking. “MA” or Maximum Amplitude which gives the ultimate strength of the fibrin clot. “TMA” or Time to maximum amplitude which gives the time to maximum clot strength and “CI” Coagulation Index, which describes the overall coagulation state as derived from the R, K, MA and α parameters.

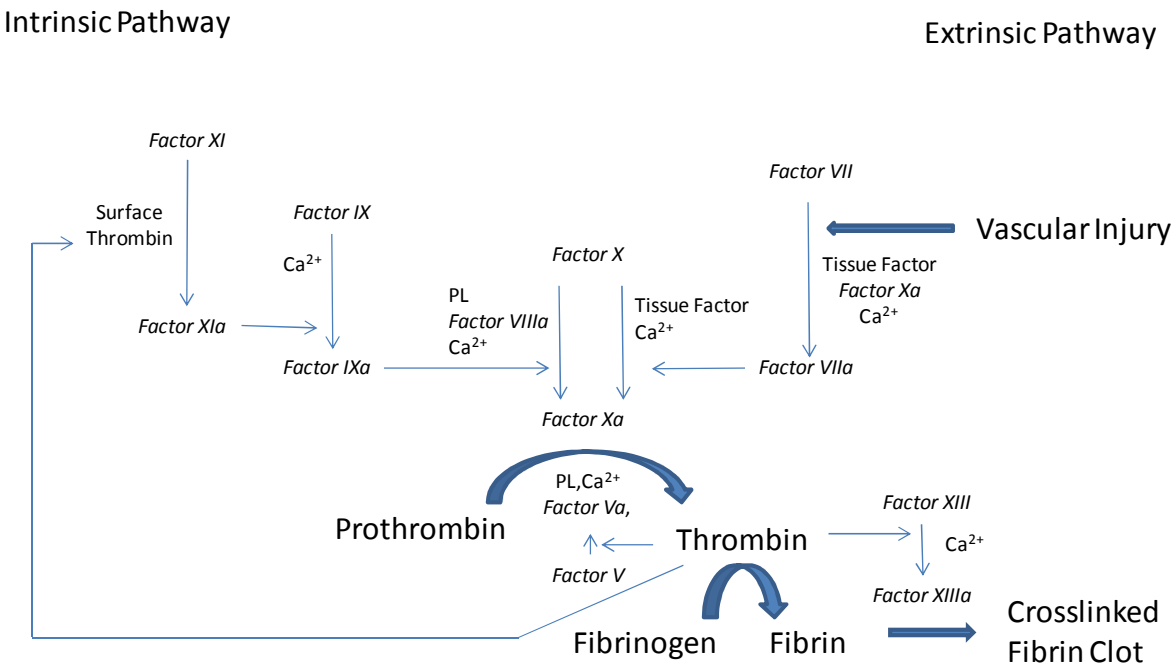

Figure 3.1: Coagulation cascade and fibrin formation, modified from the original by Davie (Davie, 2003). The importance of the extrinsic pathway in the initiation of blood coagulation following vascular injury and platelet plug formation is indicated. Tissue factor is an integral glycoprotein acting as a receptor for Factor VII only after vascular injury and in the presence of Ca^{2+}. PL refers to phospholipid provided by activated platelets.

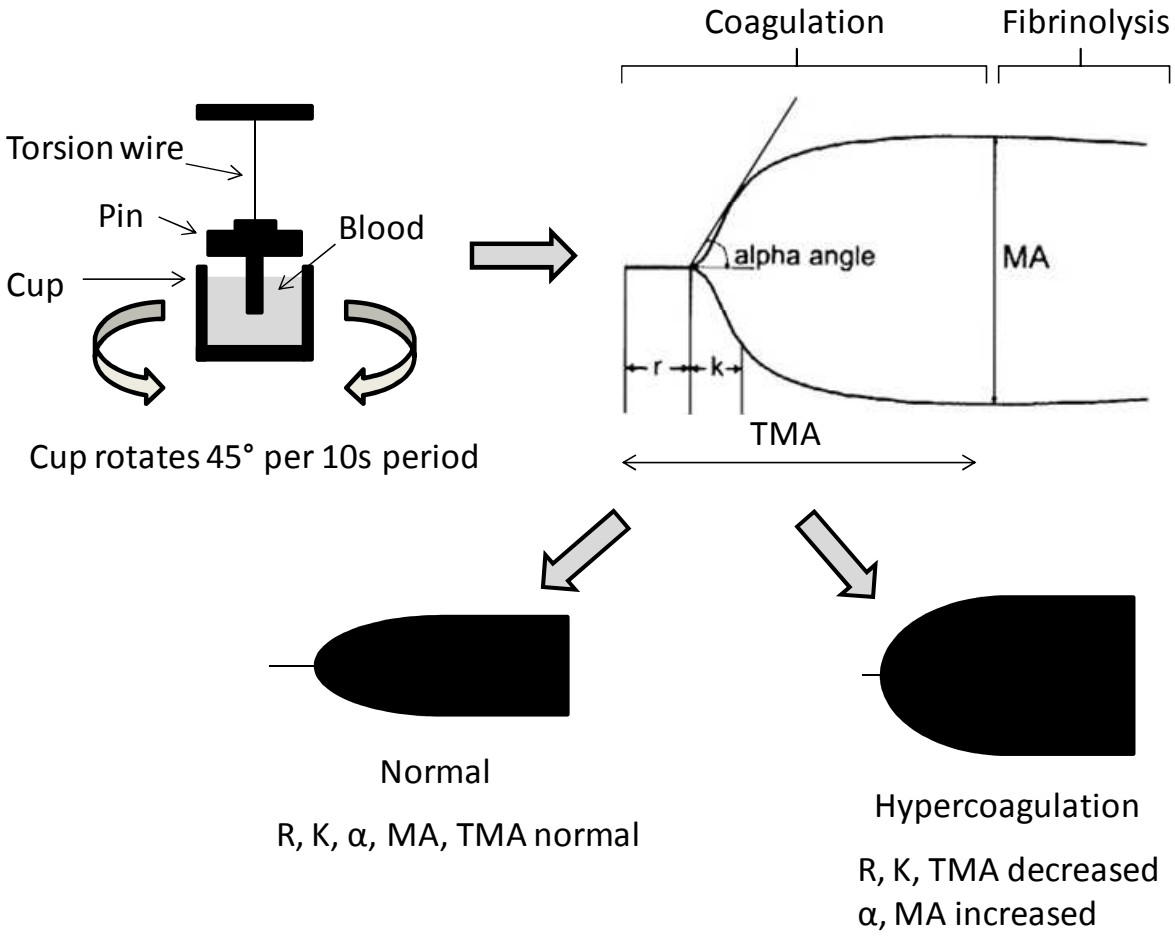

Figure 3.2: Thrombelastography. Top left: components. Top right: coagulation profile indicating parameter derivation for R-time, K-time, angle parameter, MA (Maximum amplitude) and TMA (Time to maximum amplitude). Bottom: Coagulation profiles for normal and hypercoaguable (for example after haemostat use) samples.

3.2. Materials and methods

Soman, GD (O-Pinacolyl methylphosphonofluoridate) was supplied by the Defence Science and Technology Laboratory (Dstl, Porton Down, UK) and was reported to be >98% pure by GC-MS. The storage and use of CW agents was in full compliance with the Chemical Weapons Convention (1986). Isofluorane-VET® (isofluorane; Merial Animal Health Ltd, Essex, UK), Hypnovel® (midazolam hydrochloride (5 $mg.ml^{-1}$); Roche Products Ltd., Hertfordshire, UK) and Dolethal® (sodium pentobarbitone (200 $mg.ml^{-1}$); Vetoquinol, Buckingham, UK were purchased from a registered UK supplier. Medical grade oxygen and nitrous oxide were obtained from BOC Ltd. (Surrey, UK). The haemostatic products evaluated were QuikClot Advanced Clotting Sponge plus® ("ACS^{+}"; Z-Medica, Wallingford, CT), WoundStat™ (TraumaCure, Inc., Bethesda, MD), Vitagel™ (Orthovita, Inc., Malvern, PA), HemCon® (HemCon Medical Technologies, Inc., Tigard, OR), Celox® (Medtrade Products Ltd., Crewe, UK), FastAct® (Wortham Laboratories Inc, Chattanooga, TN) and SuperQR (aka ProQR; Biolife, Sarasota, FL).

The use of animals in this study was authorised under the UK Animal (Scientific Procedures) Act (1986). A total of six healthy female pigs (*Sus scrofa*, large white strain; initial weight range 20 - 25 kg) were purchased from a local supplier and were housed in a controlled environment (22 ± 2 °C, 53 ± 2 % relative humidity) and allowed access to food and water *ad. lib*. The animals were allowed limited interaction (via sight and sound) with neighbouring animals. Pens were enriched with play items such as food cubes (International Market Supply, Cheshire, UK) and were

subject to a 12 h/12 h light/dark cycle. Authorisation for the use of animals was also obtained from the Animal Care and Use Review Office (ACURO) prior to the commencement of this work (protocol reference 07247002).

One blood sample (7.5 ml) was taken per animal per animal day to give a total of 6 blood samples daily. Samples were acquired from each animal following sedation with Hyponoval® (midazolam; 4 ml intramuscular administration) and induction and maintenance of anaesthesia (3 – 5 % isoflurane in 8 L min^{-1} O_2) as per an existing Home Office animal licence (PL 30/2421). Blood samples were drawn from the cephalic vein or cranial vena cava into dried polystyrene tubes containing 3.2% sodium citrate (Teklab Ltd, County Durham, UK) and were equilibrated (on a tube roller) at room temperature (22°C) for 30 minutes prior to use. The actual anatomical location from which venous samples were obtained was altered on a daily basis to ensure minimum discomfort to the animals. The animals were subject to frequent examination at least once a day by a veterinary surgeon.

Blood-clotting parameters were measured using an eight-channel thrombelastograph haemostasis system (TEG 5000®) purchased from Medicell Ltd, London, UK. The instrument was calibrated using quality control standards obtained from Haemoscope Corp. All other TEG consumables including cup/pins and 0.2 M calcium chloride ($CaCl_2$) were purchased from MediCell Ltd. Samples for TEG analysis were prepared from aliquots of equilibrated, citrated whole blood placed into polyethylene vials. Where applicable, the vials were pre-treated with haemostatic agent (to give 0.45%

w/v granular test products or 0.45% v/v liquid products) and/or GD (0.5 µl ml^{-1}). After 30 seconds of gentle mixing, aliquots (340 µl) of control (untreated) or treated blood samples were transferred to a TEG cup (containing 20 µl of $CaCl_2$) in each of the TEG channels and the analysis was conducted until acquisition of maximum clot amplitude or for a total of 45 minutes (whichever occurred first).

Statistical analysis was performed using the Kruskal-Wallis non-parametric, one-way ANOVA with Dunn's multiple comparisons post test. The level of significance was predetermined at 95% ($\alpha = 0.05$).

3.3. Results

3.3.1. Presence of candidate haemostats in pig blood

Pig blood treated with FastAct®, SuperQR, Vitagel™ and WoundStat™ showed increased haemostasis kinetics as measured by R-time, K-time and Angle parameter, compared to that of untreated pig blood. Conversely, pig blood treated with Celox®, Hemcon® and QuikClot ACS+® showed similar kinetics of haemostasis to that of untreated pig blood (Figures 3.3, 3.4 and 3.5). The ultimate clot strength (Figure 3.5) was similar between pig bloods treated with any haemostat or left untreated.

3.3.2. Presence of GD in pig blood

The presence of GD contamination in pig blood significantly increased the measured parameters of haemostasis kinetics, R-time, K-time and Angle parameter, Figures 3.3, 3.4 and 3.5 respectively. The reduction in R-time and K-time indicated that the onset of clotting was more rapid, whilst the increase in Angle parameter indicated that the overall rate of clot formation was increased. The ultimate clot strength was not affected by the presence of GD (Figure 3.6).

3.3.3. Candidate haemostats evaluated in the presence of GD

The presence of GD contamination in pig blood did not alter the haemostatic kinetics of any of the test products in terms of R-time (Figure 3.3), K-time (Figure 3.4) or

Angle parameter (Figure 3.5) compared to treatment in the absence of GD contamination. GD did, however, significantly affect the ultimate clot strength produced by Vitagel™ (Figure 3.6).

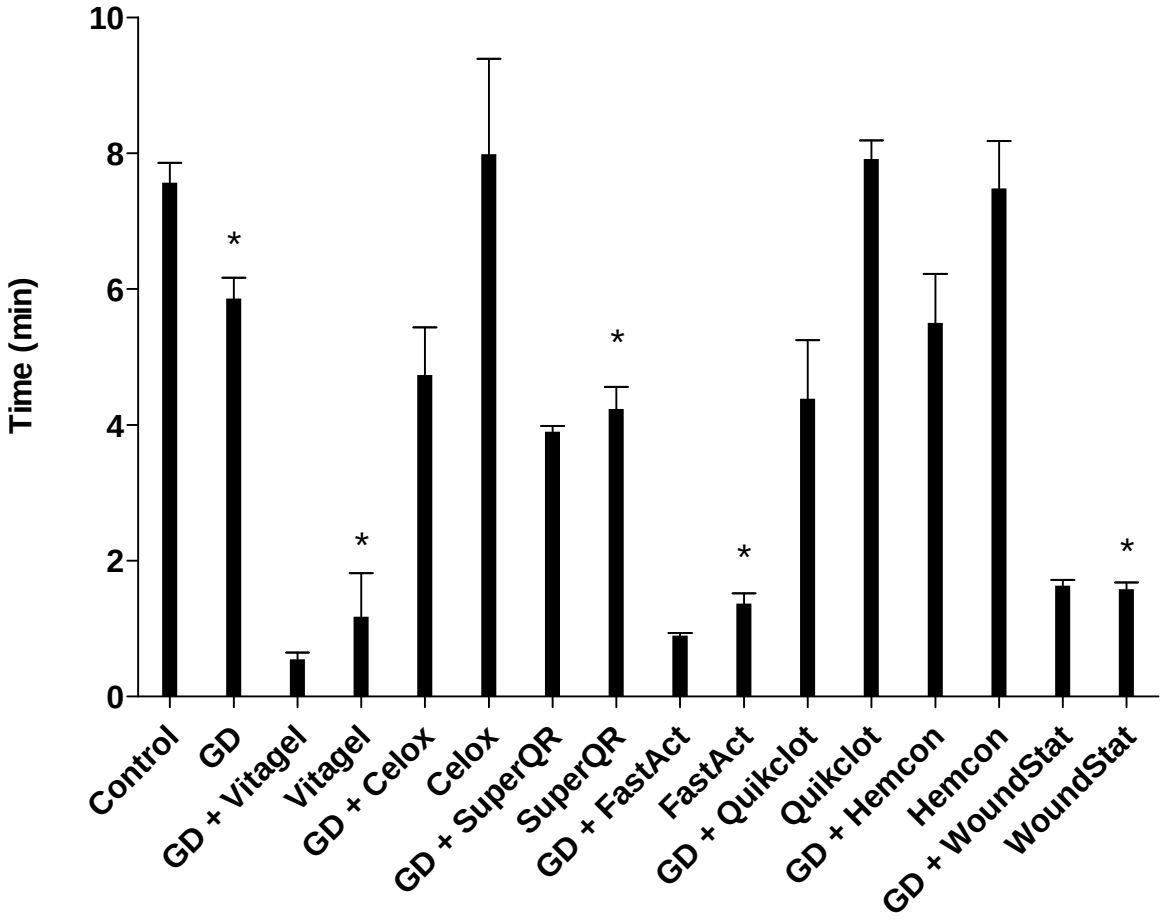

Figure 3.3: Effect of haemostatic agents on latency of clot formation in minutes (R-time) in the presence or absence of GD. Haemostats evaluated were: Celox®, SuperQR, WoundStat™, QuikClot ACS+® HemCon®, FastAct® and Vitagel™. All data are average ± standard error of n=6 (haemostats), n=42 (control) and n=42 (GD challenged control). Asterisks indicate that the value was significantly different from the n=6 (paired) controls measured simultaneously ($p<0.05$).

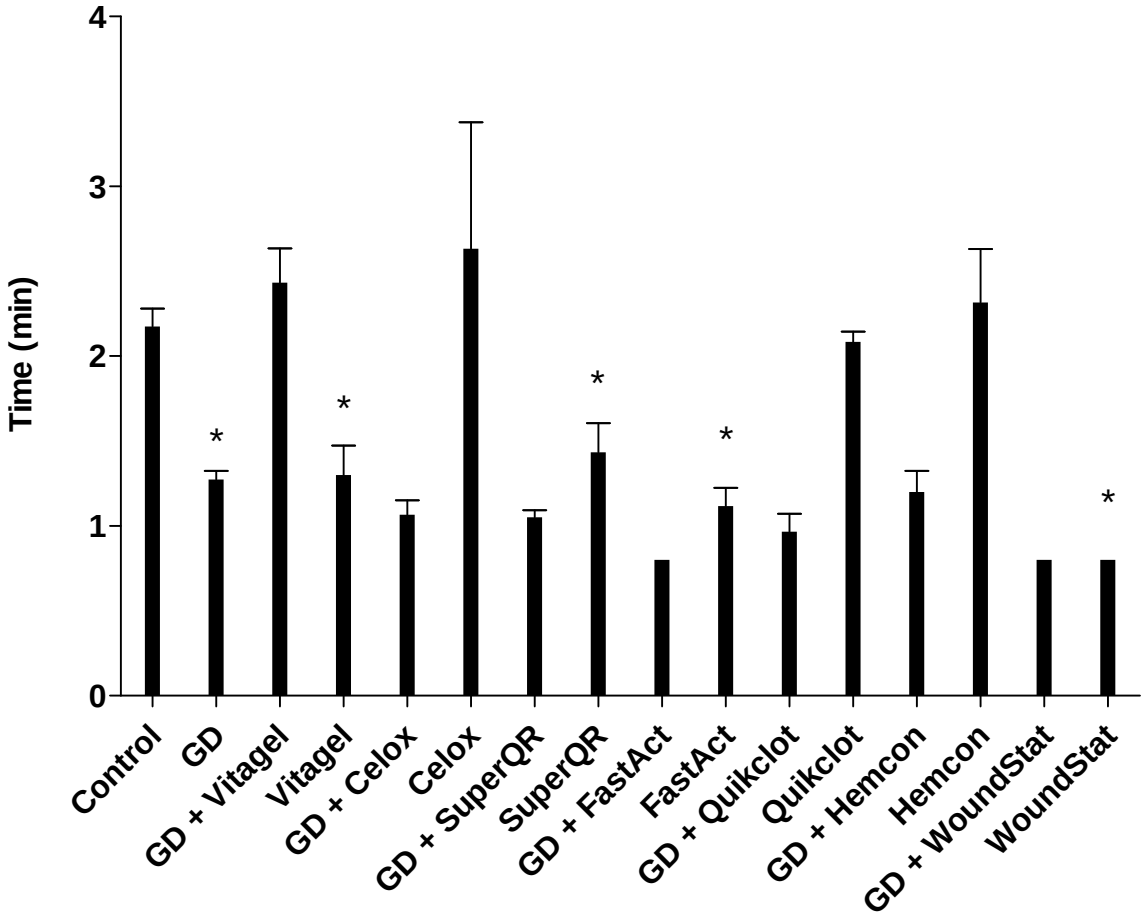

Figure 3.4: Effect of haemostatic agents on the rapidity to reach 20mm clot strength in minutes (K-time) in the presence or absence of GD. Efficacy of haemostatic products in the presence or absence of GD in terms of the "K Time" parameter. Haemostats evaluated were: Celox®, SuperQR, WoundStat™, QuikClot ACS+® HemCon®, FastAct® and Vitagel™. All data are average ± standard error of n=6 (haemostats), n=42 (control) and n=42 (GD challenged control). Asterisks indicate that the value was significantly different from the n=6 (paired) controls measured simultaneously ($p<0.05$).

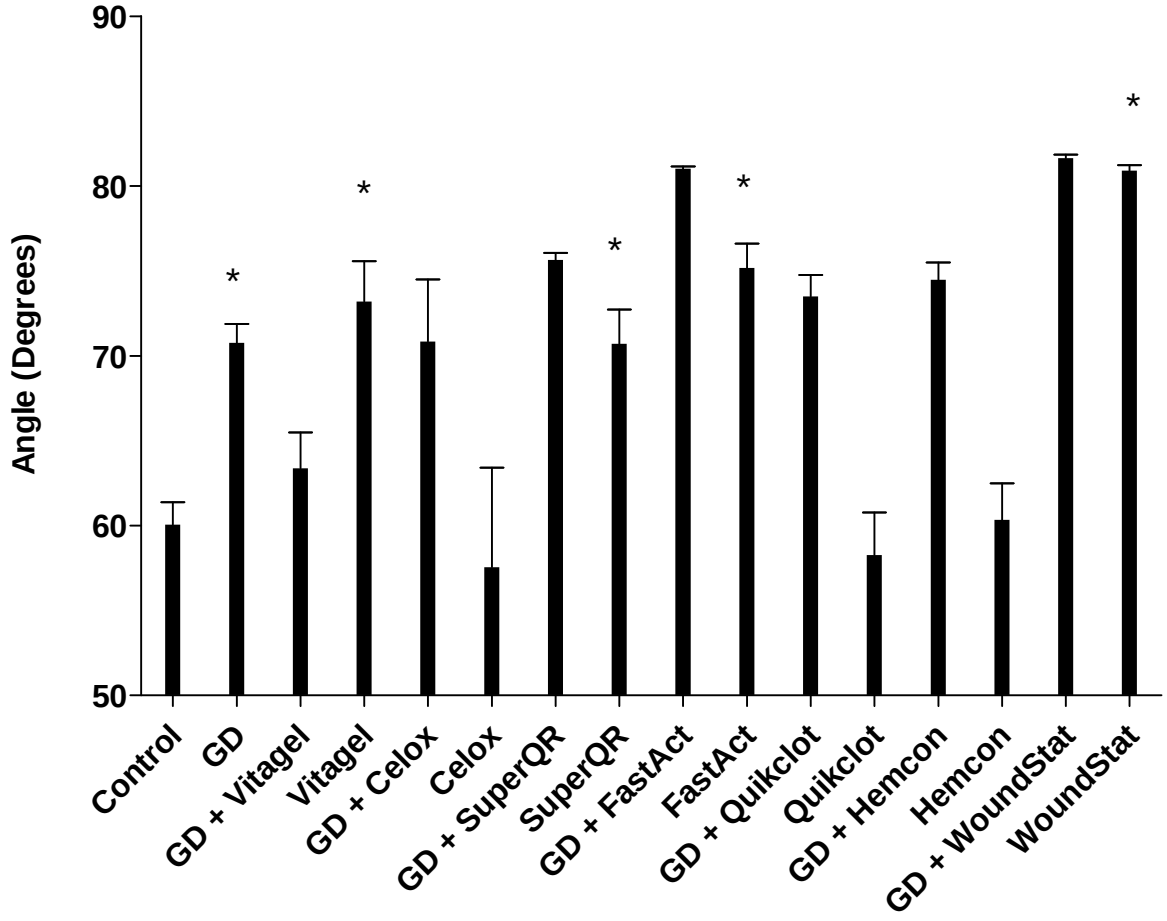

Figure 3.5: Effect of haemostatic agents on the rapidity of fibrin build up and cross-linking (clot strengthening kinetics) in terms of the "Angle" parameter in the presence or absence of GD. Haemostats evaluated were: Celox®, SuperQR, WoundStat™, QuikClot ACS+® HemCon®, FastAct® and Vitagel™. All data are average ± standard error of n=6 (haemostats), n=42 (control) and n=42 (GD challenged control). Asterisks indicate that the value was significantly different from the n=6 (paired) controls measured simultaneously ($p<0.05$).

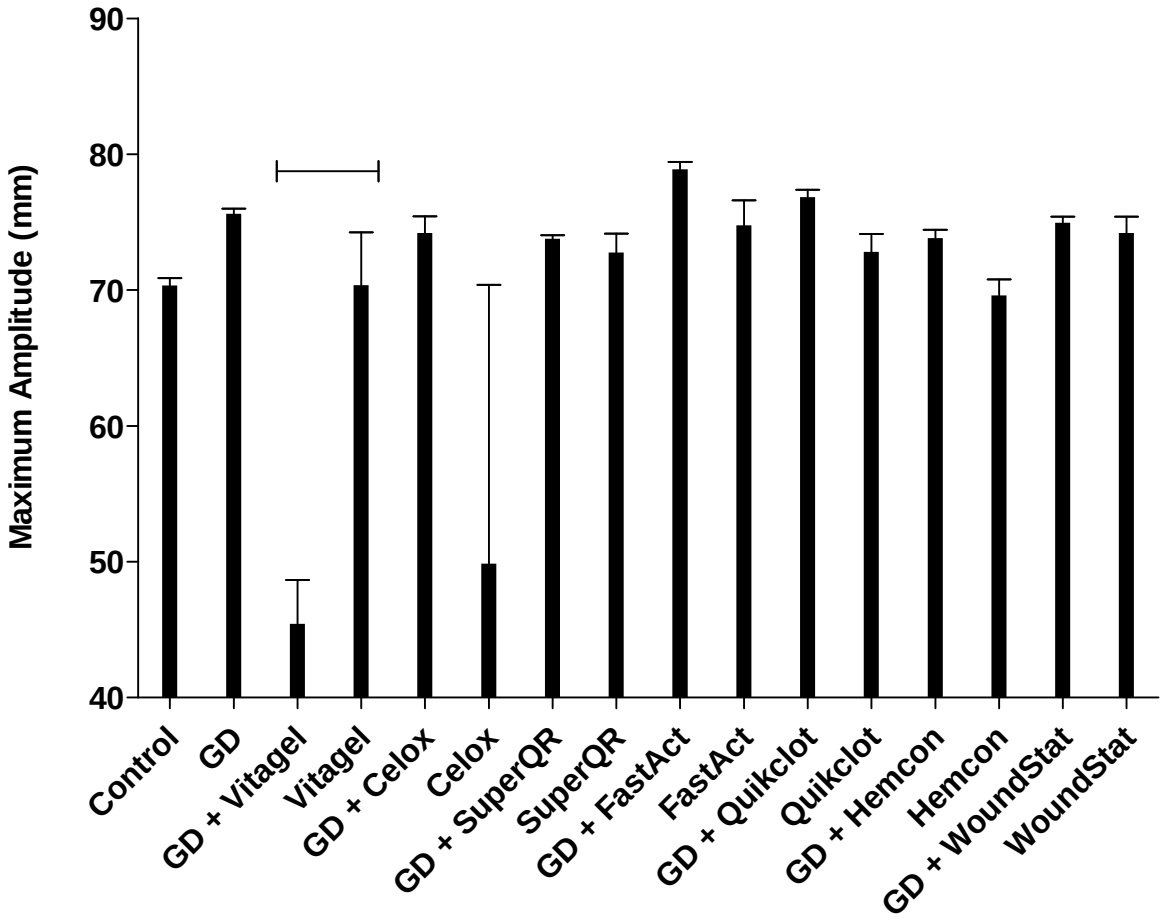

Figure 3.6: Effect of haemostatic agents on the ultimate strength of the fibrin clot in mm (Maximum Amplitude) in the presence or absence of GD. Haemostats evaluated were: Celox®, SuperQR, WoundStat™, QuikClot ACS+® HemCon®, FastAct® and Vitagel™. All data are average ± standard error of n=6 (haemostats), n=42 (control) and n=42 (GD challenged control). The bar indicates a significant difference between the haemostat Vitagel and Vitagel contaminated with GD ($p<0.05$).

3.4 Discussion

3.4.1. Overview

Seven candidate haemostats were assessed for haemostatic efficacy in the presence and absence of GD by thrombelastography (TEG). Three products showed no haemostatic ability in the TEG test system. Three products were not adversely affected by the presence of GD and one product showed unacceptable characteristics in the presence of GD.

3.4.2. Haemostats interaction with the TEG system

The four candidate treatments which performed as haemostats in the TEG system were WoundStat™, SuperQR, FastAct® and Vitagel™. Three of the haemostatic products (Celox®, Hemcon® and QuikClot ACS+®) showed similar haemostasis kinetics to untreated pig blood, indicating that they were not amenable to *in vitro* TEG analysis. This result has been shown previously (Kheirabadi, et al., 2008), with both Celox®, and QuikClot ACS+®. It must be stated that this lack of efficacy using TEG analysis is not necessarily representative of their *in vivo* efficacy. There are a number of possible reasons why the three candidates did not increase the clotting rate of pig blood in the TEG system, the most likely of which is that they require pressure to be applied to the wound site (not reproducible in this *in vitro* system). This requirement, however, makes them less suitable for use in a buddy aid situation (where it is desirable for the haemostat to work effectively with the minimum of intervention from

other personnel). However, QuikClot ACS$^{+®}$, WoundStat™ and SuperQR are thought to concentrate the clotting factors by absorbing water from the plasma. It is unlikely therefore that this is the mechanism of action by which haemostatic activity is being reduced, since it would affect all these agents, not just one. The data generated by this study indicate that TEG does not seem to be an appropriate test system for all haemostatic products.

3.4.3. GD contaminated blood

Perhaps most interestingly, GD itself had a haemostatic effect on pig blood. This finding has been reported by other researchers using an *in vivo* rabbit model (Lee and Clement, 1990) and so it is likely that the TEG analysis carried out is indicative of a real effect on haemostasis. It should be noted that Lee and Clement (1990) did not consider the pro-haemostatic effect to be of clinical relevance to nerve agent poisoning. The reason behind the observed pro haemostatic effect is currently unclear as the main mechanism of action of GD is inhibition of cholinesterase. However, recent studies have shown that organophosphates can increase cytokine release from the lymphocytes (Galloway and Handy, 2003;Kim, et al., 2007) therefore, it is feasible that the enhanced clotting rate observed is linked to this mechanism.

3.4.3.1 Effects of organophosphates on blood coagulation

Work on the effects of organophosphates on *in vivo* blood coagulation has been undertaken by a number of researchers. The results from these studies indicate that organophosphates can both activate (Lee and Clement, 1990) and inhibit (Murray, et al., 1994) blood coagulation. An *in vivo* study using Paraoxon showed that changes in blood coagulation after exposure were biphasic, with hypercoagulability evidenced in the early phase followed by hypocoagulability in the late phase (Petroianu, et al., 1999). Early phase effects were attributed to catecholamine release from the adrenal gland whilst late phase effects were attributed to inhibition of serine protease coagulation factors. Given that the current study was conducted *in vitro*, adrenal gland release does not offer a possible explanation for the observed hypercoagulability with GD. Interestingly, *in vitro* blood coagulation studies with paroxon have shown no coagulation activating effect (Petroianu, et al., 1997).

3.4.4. Effect of GD on haemostat clotting ability

GD had no statistically adverse affects on the blood clotting performance of WoundStat™, SuperQR and FastAct®, indicating that they were suitable candidates to potentially fill the role of haemostatic decontaminants from the point of view of interaction with GD (see also section 3.4.5. for interaction with VX and HD). However, one haemostatic product (Vitagel™), showed undesirable characteristics (decrease in ultimate clot strength) when contaminated with GD. Although, not determined to be statistically significant, there was an inconsistency between the K time and Angle parameter for Vitagel™ and Vitagel™ contaminated with GD when compared to the other evaluated haemostats. In general for the other haemostats, GD contaminated

pig blood caused a decrease in K time and increase in Angle parameter. For Vitagel™ however, the K time parameter increased and the Angle parameter decreased. It is likely that the decreased clotting rate attainable by Vitagel™ with GD contaminated pig blood when compared to normal pig blood offers explanation to the decrease in statistically observable ultimate clot strength.

3.4.5. Parallel studies using HD and VX

Two further chemical warfare agents, VX and HD (Section 1.5), where evaluated (Lydon, 2012;Hall, 2012) using the methodology described. Briefly, the addition of VX to pig blood gave similar results to that of GD with an observable decrease in R-time and K-time indicating that VX had a haemostatic effect on pig blood. In the presence of VX, a number of pro-haemostatic changes were observed for the candidate haemostats. These were; decreased R times for Vitagel™ and SuperQR and increased overall rates of clotting for Vitagel™, SuperQR, HemCon® and WoundStat™. In contrast, in the presence of HD, clotting parameters were not affected and HD did not affect the performance of the candidate haemostats.

3.4.6. Candidate haemostat down selection for use as a decontaminant

As three of the haemostats evaluated were not amenable to TEG methodology (Section 3.4.2.), it was not possible to make any definitive selections on the basis of the TEG studies alone. It was encouraging, however, that for those haemostats that

were amenable to TEG measurement, three out of the four showed no undesirable alteration in clotting characteristics in the presence of GD and two other CW agents.

CHAPTER 4: IN VITRO EFFICACY TESTING OF HAEMOSTATIC PRODUCTS AS CHEMICAL WARFARE AGENT DECONTAMINANTS

4.1. Introduction

Based on the initial review, a number of commercial off the shelf (COTS) haemostatic products are likely to be amenable to use as decontamination products, as, the mechanism of action of fluid absorption is similar to that of the mechanism of action of in service CW agent decontaminants such as the passive decontaminant fullers' earth (Section 1.3). Appropriately formulated liquid haemostats with excipients (such as cholinesterase (Gordon, et al., 1999)) may also be able to sequester GD and arrest bleeding simultaneously. The purpose of this series of studies was to evaluate a number of candidate haemostats for efficacy as potential skin decontaminants against the nerve agent soman, prior to further in vitro studies using favourable candidates in a damaged skin tissue model. To qualify for selection a number of essential criteria were defined as follows.

4.1.1. Skin decontamination efficacy

The candidate haemostatic decontaminant should approach the effectiveness of currently used military skin decontaminants (fullers' earth, M291 powder) when used on undamaged skin. Inability in this area would potentially rule out the option of replacing current military decontaminants with a haemostat based skin decontaminant system.

4.1.2. Agent desorption characteristics of decontaminant

The candidate haemostatic decontaminant should irreversibly sequester GD. Irreversible sequestration is of importance to first responders as off gassing from the haemostatic product could produce secondary casualties.

4.1.3. Damaged skin decontamination efficacy

The candidate haemostatic decontaminant should approach the effectiveness of current in service skin decontaminants when used on damaged skin. Inability in this area would lessen the likelihood of the candidate being efficacious in its main envisaged use of decontaminating haemorrhaging wounds.

4.2. Materials and methods

The synthesis, use and destruction of GD in this study was conducted in accordance with the Chemical Weapons Convention (1996) to which the UK is a signatory state. Radiolabelled pinacoyl methylfluorophosphonate (GD) was synthesised by TNO (Rijswijk, Netherlands) and had a radiochemical purity >97% (as determined by radiometric HPLC analysis). The ^{14}C label was at the P-CH_3 moiety (see Figure 1.6). The chemical purity of unlabelled GD was reported to be >97% (by NMR). Both radiolabelled and cold agent were mixed in appropriate proportions to give a nominal activity of approximately 0.5 µCi μl^{-1}. Liquid scintillation counting (LSC) materials (Soluene-350™, Ultima Gold and opaque plastic vials) were purchased from Perkin-Elmer (Chandler's Ford, Hampshire). All other chemicals were analytical grade and were purchased from the Sigma Chemical Company (Poole, Dorset). The haemostatic products evaluated were QuikClot Advanced Clotting Sponge plus® ("ACS^+"; Z-Medica, Wallingford, CT), WoundStat™ (TraumaCure, Inc., Bethesda, MD), Vitagel™ (Orthovita, Inc., Malvern, PA), HemCon® (HemCon Medical Technologies, Inc., Tigard, OR), Celox® (Medtrade Products Ltd., Crewe, UK), FastAct® (Wortham Laboratories Inc, Chattanooga, TN) and SuperQR (aka ProQR; Biolife, Sarasota, FL), "TOP", a mixture of Tetraglyme, Oxime and Polyethyleneimine (Walter Reid Army Institute of Research, MD, USA), Lupasol P, a high molecular weight ethylenimine homopolymer (BASF Aktiengesellschaft, Germany), KBDO (potassium butadiene monoximate) liquid (E-Z-EM Inc., Canada), M291 decontaminant (United States Army Medical Research institute of Chemical Defense, Maryland, USA) and fullers' earth (Sigma Chemical Co., Dorset, UK).

The use of animals in this study was conducted in accordance with the Animals (Scientific Procedures) Act 1986. Twelve weanling pigs (large white strain, weight range 20 - 30 kg) were purchased from a local supplier. Animals were pair-housed and given 24 h access to food and water. After one week acclimatisation, each animal was sedated with Hypnovel® (Midazolam, 6ml i.m., 5 $mg.ml^{-1}$) and culled with an overdose of Euthatal™ (sodium pentobarbitol, 6ml i.v., 200 $mg.ml^{-1}$). The whole abdominal skin flank (approximately 40 x 30 cm) was excised from each animal. The skin was stored flat between sheets of aluminium foil at -20ºC for up to three months prior to use. Prior to study commencement, a skin sample from one animal was removed from cold storage and thawed in a refrigerator at 5ºC for approximately 24 hours. The skin was close clipped and the subcutaneous fat removed before being dermatomed (Humeca Model D42, Eurosurgical Ltd, Guildford, UK) to a nominal thickness of 500 µm prior to insertion into diffusion cells. For the damaged skin studies, a thickness of 100 µm was removed from the epidermal side by dermatoming (Humeca Model D42, Eurosurgical Ltd, Guildford, UK). The 100µm slice was then discarded. The remaining 400 µm of skin was mounted in the diffusion cells.

Percutaneous absorption experiments were performed with Permegear™ Franz-type glass, water jacketed diffusion cells with an area available for diffusion of 1.76 cm^2. A 3 x 3 cm section of either tinfoil (agent desorption study) or undamaged (skin decontamination efficacy study) or damaged (damaged skin decontamination efficacy study) dermatomed pig skin was placed, epidermal side up, between the donor (upper) and receptor (lower) chamber. Each receptor chamber was filled with 14 ± 1

ml 50% aqueous ethanol receptor fluid to a level that ensured the meniscus of the receptor fluid in the sampling arm was level with the skin / tin foil surface. Once assembled, each diffusion cell was placed into a diffusion cell holder, incorporating a magnetic stirrer and water heater attachments. Stirring of the receptor fluid was achieved, via a Teflon coated iron bar situated within the receptor chamber. The skin surface within each diffusion cell was maintained at a temperature of approximately 32ºC (as confirmed by infrared thermography; FLIR Model P640 camera, Cambridge, UK) using water pumped at 36ºC through the diffusion cell jackets via a circulating water heater (Model GD120, Grant Instruments, Cambridge, UK). Once assembled, the diffusion cells were allowed to equilibrate for approximately 24 hours. For the decontamination efficacy studies, baseline samples (250µl) were taken, with replacement by fresh receptor media, from each receptor chamber prior to commencement of the experimental protocol. Due to space considerations within the fume cupboard, a maximum of 36 diffusion cells were set up for each study, allowing for 6 treatment regimes of n=6 diffusion cells.

Dependent on the study type the following protocols were followed:

(a) Skin decontamination efficacy

Topical dosing was performed by the direct application of undiluted, ^{14}C-radiolabelled GD (10 µl) onto the centre of the skin surface within the donor chamber. Decontamination using one of the test products (200 mg or volume equivalent) was carried out 30 seconds post GD exposure. Following application of the agent,

samples (250 µl) of receptor chamber fluid were removed into 5 ml of scintillation fluid (Ultima Gold, Perkin Elmer LAS (UK) Ltd, Buckinghamshire, UK) at regular intervals up to 24 h post exposure. Each sample was replaced with an equivalent volume of fresh receptor fluid. Twenty four hours post-exposure a full dose distribution was performed.

(b) Agent desorption

Topical dosing was performed by the direct application of undiluted, 14C-radiolabelled GD (10 µl) onto the centre of the tin foil surface within the donor chamber. If required, decontamination using one of the test products (200 mg) was carried out 30 seconds post GD exposure. Following application of the agent, the diffusion cells were left either unoccluded or were occluded with a piece of tin foil. Three hours post-exposure a dose distribution was performed. The agent desorption protocol was repeated at an elevated temperature of 45ºC.

A full dose distribution was carried out after each experimental protocol as follows: first, the receptor chamber fluid was removed from each diffusion cell. Second, the test product was gently removed from the skin or tin foil surface. Third, the skin / tin foil surface was swabbed with cotton wool. Finally, the skin / tin foil from each diffusion cell was removed. At each stage, the component removed was placed into a glass vial. Test products had 20 ml scintillation fluid added to them, cotton wool swabs had 20 ml ethanol added to them and skins had 10 ml of Soluene-350 added to them. Dose distribution vials were then stored at room temperature (with

occasional shaking) until the skin had solubilised, after which aliquots (250 µl) were removed into 5 ml of scintillation fluid. The amount of radioactivity in each sample was measured using a Perkin Elmer Tri-Carb liquid scintillation counter (Model 2810 TR), using the manufacturer's ^{14}C-quench curve library set to exclude single-photon (non-radioactive) events. The amount of radioactivity in each sample was converted to amount of GD by comparison to standards (containing known quantities of ^{14}C-GD) prepared and measured simultaneously. In this way, cumulative ^{14}C-GD penetration profiles for the 24 h study period were generated for each diffusion cell.

Maximum penetration rates (J_{MAX}) were calculated by interpolating the peak value obtained by plotting the amount of GD per unit time (under finite dose conditions) against time. Where applicable, statistical analysis was performed using a non-parametric ANOVA (Kruskal-Wallis test) with Dunn's multiple comparisons post-test. Differences between mean values were judged statistically significant at an alpha level of 0.05. Area under the curve analysis was carried out using GraphPad Prism 5 for each 24 hour penetration profile. To allow cross study comparison, each treatment cumulative penetration profile was normalised relevant to the study control cumulative penetration profile and converted to a percentage to give the parameter $\%CD_{AUC}$.

4.3. Results

4.3.1. Efficacy of decontamination from undamaged skin

There was a significant reduction in both the rate (J_{max}) and extent (total penetration at 24h) of ^{14}C-GD skin absorption though skins that had been treated with the standard powder CW agent decontaminants fullers' earth (J_{max} 0.5 ± 0.6 µg.cm^{-2}.h^{-1}, total penetration at 24h: 6.2 ± 7.8 µg.cm^{-2}) and M291 powder (J_{max} 0.7 ± 0.3 µg.cm^{-2}.h^{-1}, total penetration at 24h: 7.5 ± 3.3 µg.cm^{-2}) compared to untreated skins (J_{max} 3.7 ± 0.6 µg.cm^{-2}.h^{-1}, total penetration at 24h: 42.0 ± 8.7 µg.cm^{-2}). Similarly, there was a significant reduction in both the rate and extent of ^{14}C-GD skin absorption though skins that had been treated with the haemostatic powders, Super-QR (J_{max} 0.9 ± 0.4 µg.cm^{-2}.h^{-1}, total penetration at 24h: 10.3 ± 4.6 µg.cm^{-2}), WoundStat™ (J_{max} 0.6 ± 0.3 µg.cm^{-2}.h^{-1}, total penetration at 24h: 6.8 ± 3.2 µg.cm^{-2}) and QuikClot ACS+® (J_{max} 1.3 ± 0.7 µg.cm^{-2}.h^{-1}, total penetration at 24h: 16.0 ± 9.0 µg.cm^{-2}). One haemostatic powder (Celox®) did not decrease the skin absorption of ^{14}C-GD (Figure 4.1). For Celox® treated skin there was a qualitative increase in the amount of ^{14}C-GD penetrating the skin (J_{max} 5.8 ± 1.9 µg.cm^{-2}.h^{-1}, total penetration at 24h: 50.7 ± 15.2 µg.cm^{-2}), however, in comparison to the untreated control, this result was not significant.

Dose recovery of ^{14}C-GD (Figure 4.2) were in the region of 70 % for fullers' earth, Super-QR and WoundStat™ treatment with the majority of radioactivity recovered from the powders themselves rather than other compartments. Dose recoveries for

Celox® and QuikClot ACS+® were less than 10 % of the applied dose. Dose recovery for the positive control was less than 5 % of the applied dose. The unrecovered fractions of the dose recoveries were assumed to have volatilised from the skin surface due to the unoccluded conditions that were utilised for the test.

One product (HemCon®) fell into the wound dressing category, it caused a significant increase in the rate and extent of ^{14}C-GD penetrating the skin (J_{max} 22.8 ± 6.2 µg.cm^{-2}.h^{-1}, total penetration at 24h: 300 ± 97 µg.cm^{-2}) compared to untreated skin (J_{max} 9.3 ± 3.0 µg.cm^{-2}.h^{-1}, total penetration at 24h: 125 ± 40 µg.cm^{-2}) (Figure 4.3). Dose recovery of ^{14}C-GD (Figure 4.4) was in the region of 30 % for Hemcon® treatment with the majority of the radioactivity recovered from the dressing itself.

Compared to the untreated control, the standard liquid CW agent decontaminant, KBDO liquid significantly reduced both the rate (J_{max} 3.4 ± 1.4 µg.cm^{-2}.h^{-1} (KBDO liquid treated), J_{max} 11.5 ± 4.0 µg.cm^{-2}.h^{-1} (untreated control) and extent (penetration at 6h: 20.6 ± 8.4 µg.cm^{-2} (KBDO liquid treated), 71.4 ± 23.8 µg.cm^{-2} (untreated control) of ^{14}C-GD skin absorption for 6 hours post exposure. However, by 24 hours significantly more radiolabel had penetrated skin treated with KBDO liquid (total penetration 381 ± 109 µg.cm^{-2}) than had penetrated the untreated control skin (total penetration 125 ± 40 µg.cm^{-2}) (Figure 4.3).

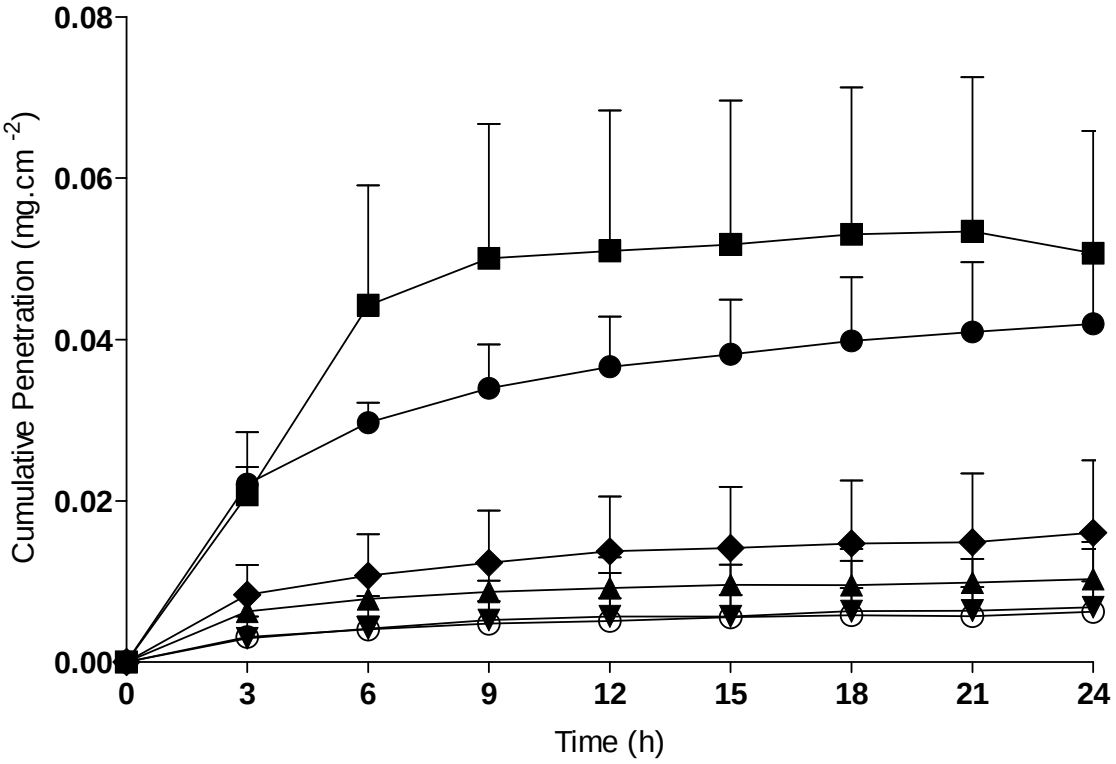

Figure 4.1: Cumulative ^{14}C-GD penetration through untreated (-●-) or treated pig skin over 24 hours from an initial topical 10µl dose at t = 0. Treatment was applied topically at 30 seconds post GD exposure using Celox® (-■-), SuperQR (-▲-), Woundstat™ (-▼-), QuikClot ACS+® (-◆-) or Fullers Earth (-⊖-). All values are mean ± standard deviation of n=6 diffusion cells. Fullers Earth, SuperQR, Woundstat™ and QuikClot ACS+® significantly reduced both the rate and extent of GD skin absorption compared to untreated skin.

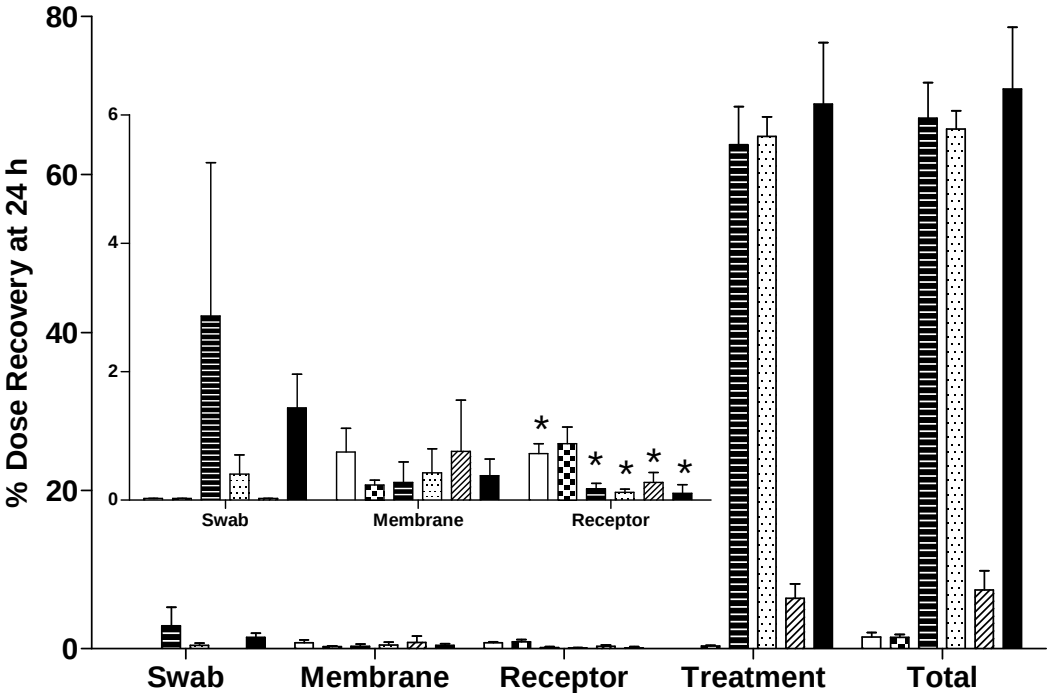

Figure 4.2: Dose recovery (%) at 24 hours of ^{14}C-GD remaining on the skin surface (swab), within the skin (membrane), sequestered into the test material (either haemostat or standard decontaminant) or penetrated into the receptor media. The skins were either untreated (□) or test materials (Celox® (⊠), SuperQR (▬), Woundstat™ (⊡), QuikClot ACS+® (▨) or Fullers Earth (■)) were placed onto the skin surface 30s after the skin had been contaminated with GD. Statistical significance between the extent of GD penetration at 24 hours though untreated and treated skins is indicated (*). There was no statistical significance between the amount of GD sequestered by Fullers Earth, SuperQR and Woundstat™.

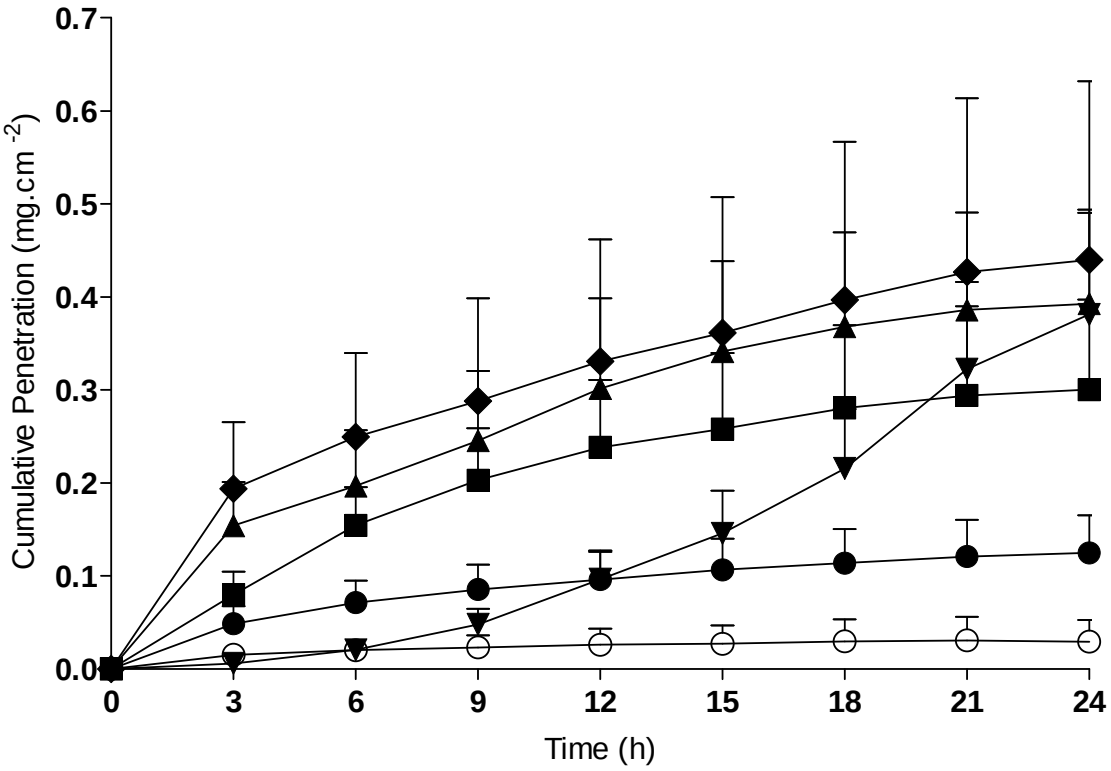

Figure 4.3: Cumulative ^{14}C-GD penetration through untreated (-●-) or treated pig skin over 24 hours from an initial topical 10µl dose at t = 0. Treatment was applied topically at 30 seconds post GD exposure using Hemcon® (-■-), FastAct® (-▲-), KBDO liquid (-▼-), Vitagel™ (-◆-) or Lupasol P (-⊖-). All values are mean ± standard deviation of n=6 diffusion cells. Hemcon®, FastAct® and Vitagel™ significantly increased the extent of GD skin absorption from 6 hours compared to untreated skin. Lupasol P and KBDO liquid significantly reduced the extent of GD skin absorption compared to untreated skin, however, for KBDO liquid by 24 hours the extent of absorption was increased compared to untreated skin.

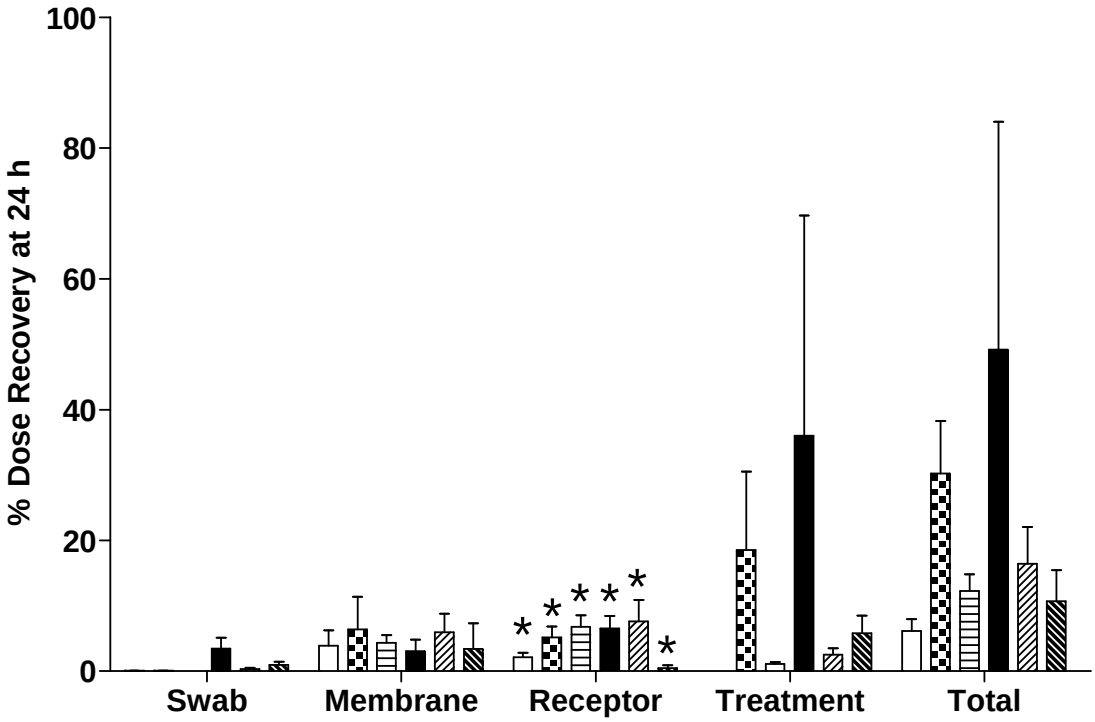

Figure 4.4: Dose recovery (%) at 24 hours of ^{14}C-GD remaining on the skin surface (swab), within the skin (membrane), sequestered into the test material (either haemostat or standard decontaminant) or penetrated into the receptor media. The skins were either untreated (□) or test materials Hemcon® (⊠), FastAct® (⊟), KBDO Liquid (■), Vitagel™ (▨) or Lupasol P (▧) were placed onto the skin surface 30s after the skin had been contaminated with GD. All values are mean ± standard deviation of n=6 diffusion cells. Statistical significance between the extent of GD penetration at 24 hours though untreated and treated skins is indicated (*).

Two haemostatic liquids (Vitagel™ and FastAct®) were investigated. Both caused a significant increase in the amount of ^{14}C-GD penetrating the skin from 6 hours (penetration at 6h: 249 ± 90 µg.cm^{-2} (Vitagel™), 197 ± 60 µg.cm^{-2} (FastAct®), 71.4 ± 23.8 µg.cm^{-2} (untreated control) (Figure 4.3). When Vitagel™ and FastAct® were used in conjunction with TOP the enhancement of skin penetration from 6 hours was prevented (penetration at 6h: 84.4 ± 12.9 µg.cm^{-2} (TOP + Vitagel™), 67.0 ± 15.1 µg.cm^{-2} (TOP + FastAct®), 53.2 ± 14.1 µg.cm^{-2} (untreated control). Treatment with TOP alone was initially similar to the untreated control, however, by 24h a significant reduction in ^{14}C-GD skin penetration was evident (penetration at 24h: 28.7 ± 2.6 µg.cm^{-2} (TOP), 105 ± 23 µg.cm^{-2} (untreated control) (Figure 4.5). Dose recovery of ^{14}C-GD for Vitagel™ and FastAct® treatment were in the region of 15 % (Figure 4.4) which increased to around 30 % when the haemostatic liquids were combined with TOP (Figure 4.6). Dose recoveries of ^{14}C-GD from the excipient only treatments (TOP and Lupasol P) were approximately 30 % and 10 % respectively.

Area under the curve analysis with normalisation relative to controls (Figure 4.7) allowed comparison between studies. Seven products significantly reduced ^{14}C-GD skin penetration compared to untreated controls.

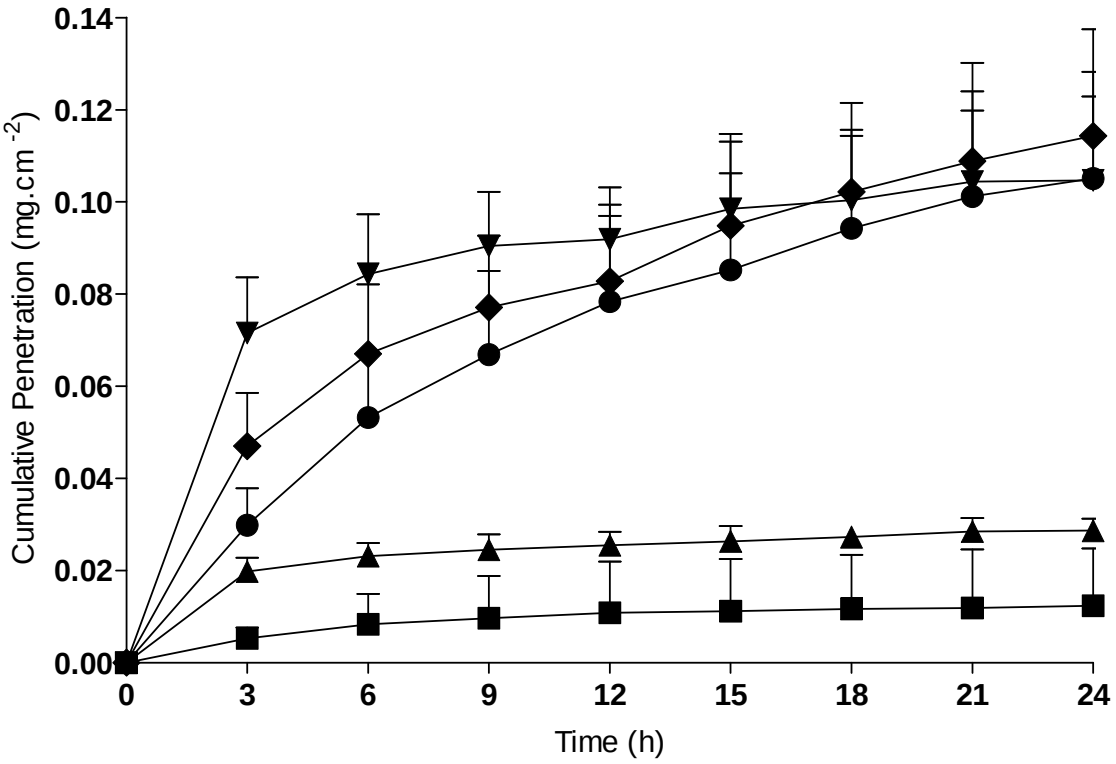

Figure 4.5: Cumulative ^{14}C-GD penetration through untreated (-●-) or treated pig skin over 24 hours from an initial topical 10µl dose at t = 0. Treatment was applied topically at 30 seconds post GD exposure using M291 Powder (-■-), TOP (-▲-), TOP + Vitagel™ (-▼-) or TOP + FastAct® (-◆-). All values are mean ± standard deviation of n=6 diffusion cells. Treatment with TOP and M291 powder significantly decreased the extent of GD skin absorption compared to untreated skin.

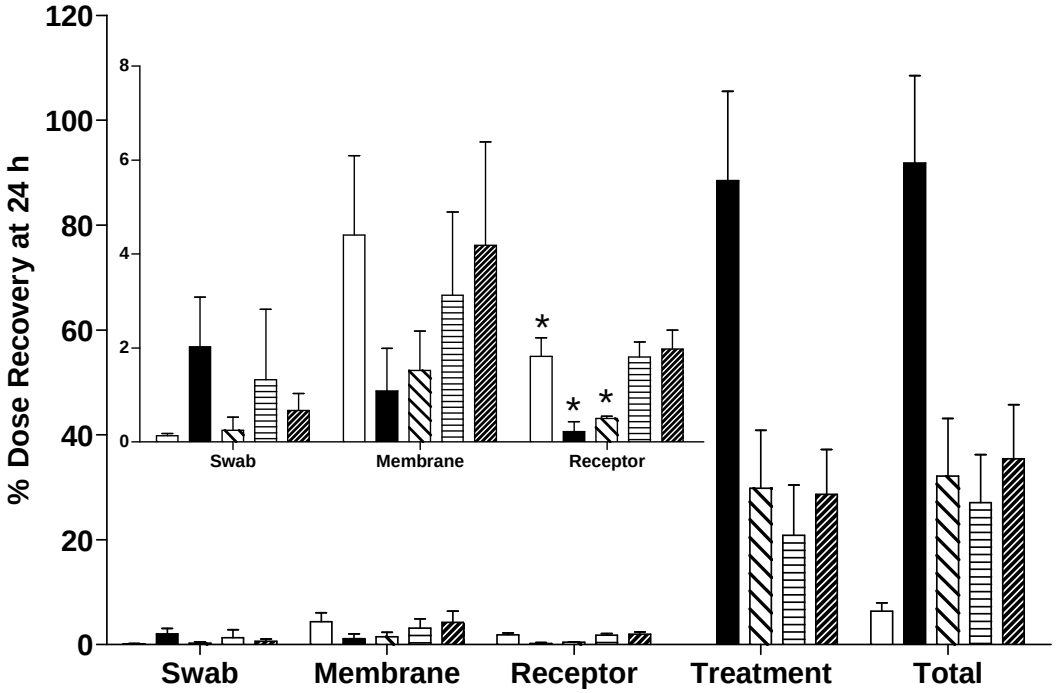

Figure 4.6: Dose recovery (%) at 24 hours of ^{14}C-GD remaining on the skin surface (swab), within the skin (membrane), sequestered into the test material (either haemostat or standard decontaminant) or penetrated into the receptor media. The skins were either untreated (☐) or test materials M291 Powder (■), TOP (⧅), TOP + Vitagel™ (▤) or TOP + FastAct® (▨) were placed onto the skin surface 30s after the skin had been contaminated with GD. All values are mean ± standard deviation of n=6 diffusion cells. Statistical significance between the extent of GD penetration at 24 hours though untreated and treated skins is indicated (*).

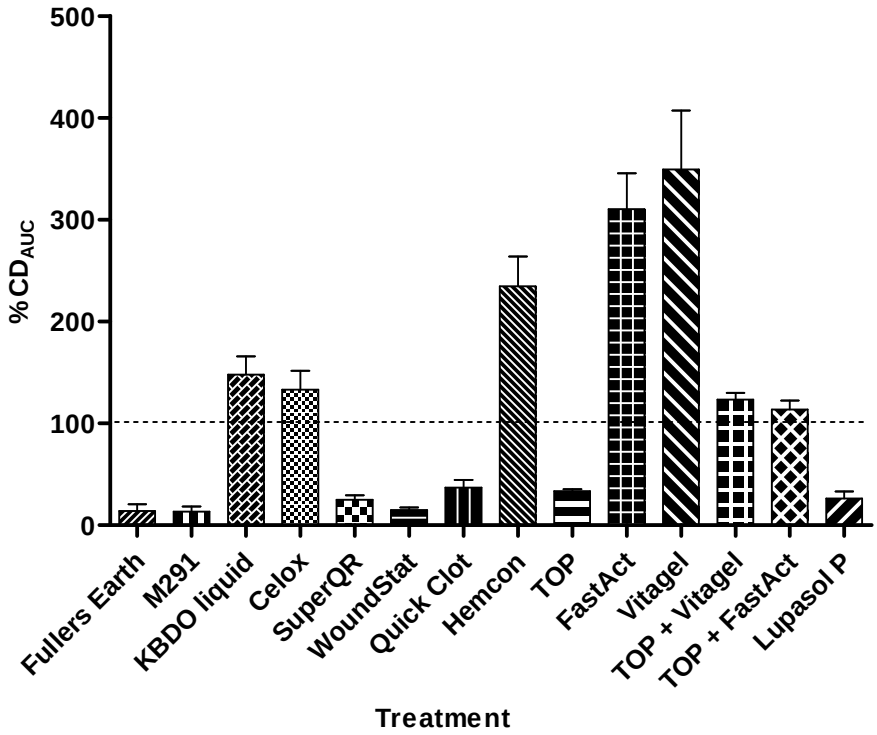

Figure 4.7: Skin penetration of ^{14}C-GD as a percentage of the control dose expressed in terms of the area under the curve value for the duration of the study. Decontamination was at 30 seconds post GD exposure using Fullers Earth, M291, KBDO liquid, Celox®, SuperQR, WoundStat™, QuikClot ACS+®, HemCon®, TOP, FastAct®, Vitagel™, TOP +Vitagel™, TOP + FastAct® or Lupasol P . All data are average ± standard error of n=6 diffusion cells.

4.3.2. Agent desorption characteristics from decontaminant

The agent desorption studies sought to determine whether or not candidate treatments could irreversibly sequester CW agent. As skin was not required to make this assessment, CW agent was placed onto a non absorbent tin foil surface, prior to treatment application. Over the three hour time period, none of the haemostatic products evaluated (Super-QR, WoundStat™ or QuikClot ACS+®) exhibited significant loss of ^{14}C-GD at ambient room temperature (comparing unoccluded to occluded conditions). Similarly, fullers' earth did not exhibit significant loss of ^{14}C-GD (Figure 4.8 and 4.9). This indicated that all the products tested irreversibly sequestered GD for the period of the test. In comparison, at ambient room temperature, the unoccluded control exhibited significant loss of ^{14}C-GD compared to the occluded control. At an elevated temperature of 45℃ neither WoundStat™ or fullers' earth exhibited significant loss of ^{14}C-GD. In contrast QuikClot ACS+® did exhibit significant loss of ^{14}C-GD (Figure 4.10 and 4.11). This indicated that only WoundStat™ and fullers' earth irreversibly sequestered GD for the period of the test at the elevated temperature. As for the ambient room temperature study, the unoccluded control exhibited significant loss of ^{14}C-GD compared to the occluded control.

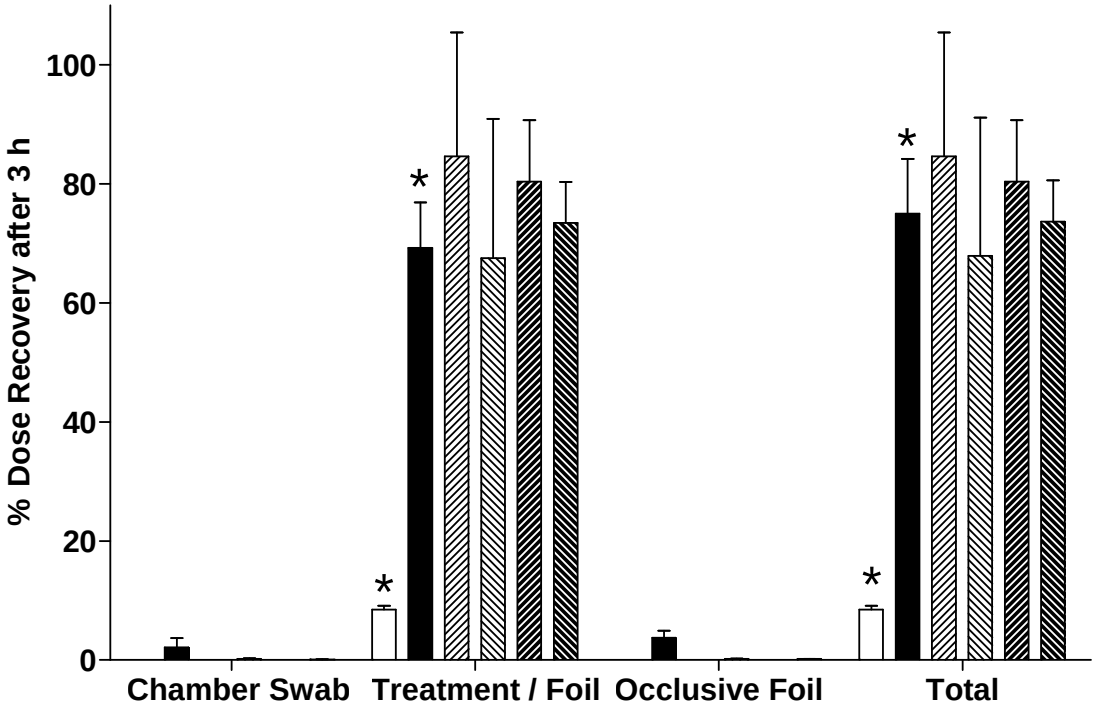

Figure 4.8: Dose recovery (%) at 3 hours of ^{14}C-GD placed onto tin foil at room temperature under both unnoccluded (□) and occluded (■) conditions. Treatments (Woundstat™ or Fullers Earth were applied 30 seconds post GD exposure under both unnocluded and occluded conditions. Where, ▨ = unnocluded Fullers Earth, ▧ = occluded Fullers Earth, ▨ = unoccluded Woundstat™ and ▧ = occluded Woundstat™. Compartments measured were; GD present on the donor chamber (Chamber swab), GD sequestered into the test material / remaining on tin foil surface (Treatment / Foil) or present on occlusive foil (occlusive conditions only). Statistical significance between GD recoveries comparing unoccluded and occluded conditions is indicated (*). All data are mean ± standard deviation of n=6 cells.

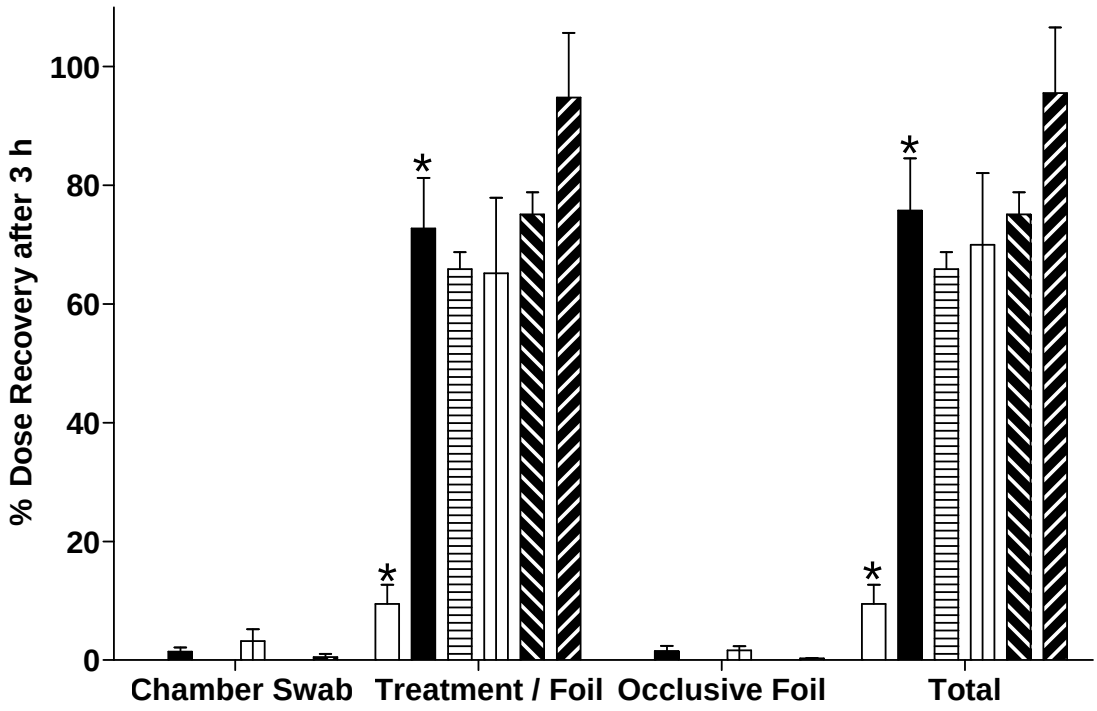

Figure 4.9: Dose recovery (%) at 3 hours of ^{14}C-GD placed onto tin foil at room temperature under both unnoccluded (□) and occluded (■) conditions. Treatments (SuperQR or QuikClot ACS$^{+®}$ were applied 30 seconds post GD exposure under both unnocluded and occluded conditions. Where, ▤ = unnocluded SuperQR, ◫ = occluded SuperQR, . ◹ = unoccluded QuikClot ACS$^{+®}$ and ◪ = occluded QuikClot ACS$^{+®}$. Compartments measured were; GD present on the donor chamber (Chamber swab), GD sequestered into the test material / remaining on tin foil surface (Treatment / Foil) or present on occlusive foil (occlusive conditions only). Statistical significance between GD recoveries comparing unoccluded and occluded conditions is indicated (*). All data are mean ± standard deviation of n=6 cells.

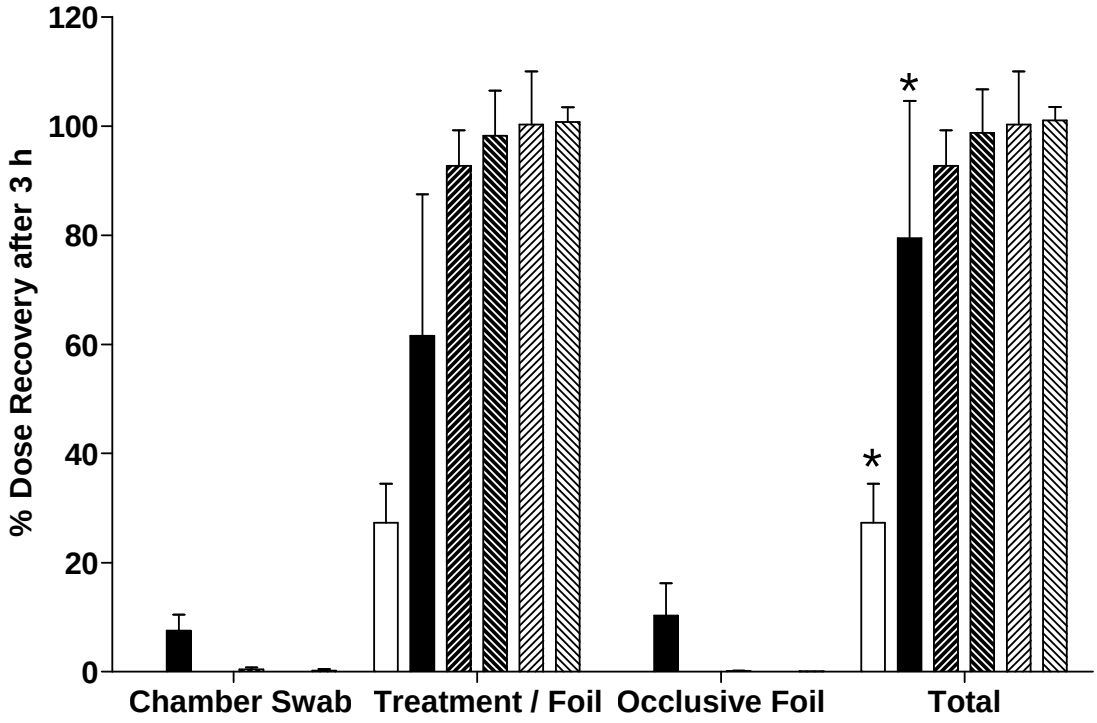

Figure 4.10: Dose recovery (%) at 3 hours of ^{14}C-GD placed onto tin foil at elevated (45°C) temperature under both unnoccluded (□) and occluded (■) conditions. Treatments (Woundstat™ or Fullers Earth were applied 30 seconds post GD exposure under both unnocluded and occluded conditions. Where, ▨ = unnocluded Fullers Earth, ▧ = occluded Fullers Earth, ▨ = unoccluded Woundstat™ and ▧ = occluded Woundstat™. Compartments measured were; GD present on the donor chamber (Chamber swab), GD sequestered into the test material / remaining on tin foil surface (Treatment / Foil) or present on occlusive foil (occlusive conditions only). Statistical significance between GD recoveries comparing unoccluded and occluded conditions is indicated (*). All data are mean ± standard deviation of n=6 cells.

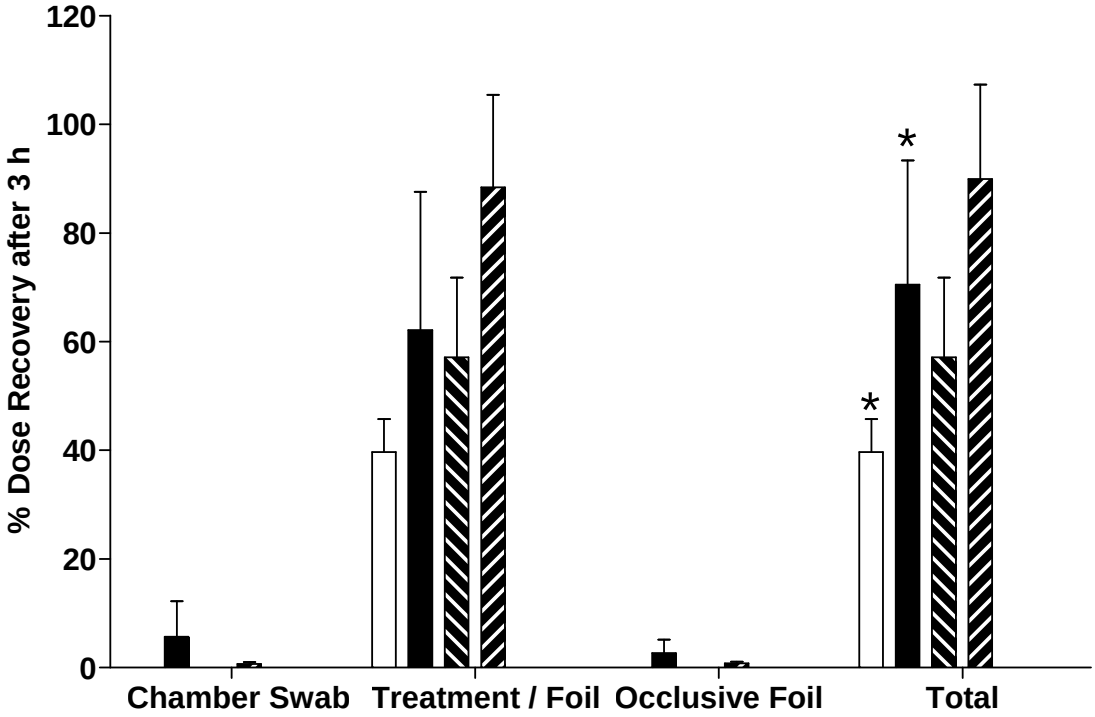

Figure 4.11: Dose recovery (%) at 3 hours of ^{14}C-GD placed onto tin foil at elevated (45°C) temperature under both unnoccluded (□) and occluded (■) conditions. Treatment (QuikClot ACS$^{+®}$) was applied 30 seconds post GD exposure under both unnocluded and occluded conditions. Where, ⬔ = unnocluded QuikClot ACS$^{+®}$, ◪ = occluded QuikClot ACS$^{+®}$. Compartments measured were; GD present on the donor chamber (Chamber swab), GD sequestered into the test material / remaining on tin foil surface (Treatment / Foil) or present on occlusive foil (occlusive conditions only). Statistical significance between GD recoveries comparing unoccluded and occluded conditions is indicated (*). All data are mean ± standard deviation of n=6 cells.

4.3.3. Efficacy of decontamination from damaged skin

There was a significant reduction in both the rate (J_{max}) and extent (total penetration at 24h) of ^{14}C-GD skin absorption though damaged skins that had been treated with the standard powder CW agent decontaminant fullers' earth (J_{max} 3.9 ± 5.1 µg.cm^{-2}.h^{-1}, total penetration at 24h: 28.2 ± 31.4 µg.cm^{-2}) compared to damaged untreated skins (J_{max} 183 ± 44 µg.cm^{-2}.h^{-1}, total penetration at 24h: 1280 ± 303 µg.cm^{-2}). Similarly, there was a significant reduction in both the rate and extent of ^{14}C-GD skin absorption though skins that had been treated with the haemostatic powders, Super-QR (J_{max} 15.1 ± 3.4 µg.cm^{-2}.h^{-1}, total penetration at 24h: 195 ± 39 µg.cm^{-2}) and WoundStat™ (J_{max} 27.3 ± 21.8 µg.cm^{-2}.h^{-1}, total penetration at 24h: 199 ± 148 µg.cm^{-2}). There was no statistical difference between the penetration of ^{14}C-GD though untreated and QuikClot ACS+® treated skin (J_{max} 85.0 ± 63.2 µg.cm^{-2}.h^{-1}, total penetration at 24h: 599 ± 439 µg.cm^{-2}) (Figure 4.12).

Super-QR and WoundStat™ were statistically comparable in performance to fullers' earth (Figure 4.12). Dose recovery (Figure 4.13) was in the region of 80% for fullers' earth, 70% for WoundStat™, 60% for SuperQR and 40% for QuikClot ACS$^{+®}$. In all cases the majority of radioactivity was recovered from the powders rather than other compartments. The unaccounted for portions of the dose recoveries were assumed to have volatilised from the skin surface due to the unoccluded conditions that were utilised for the test.

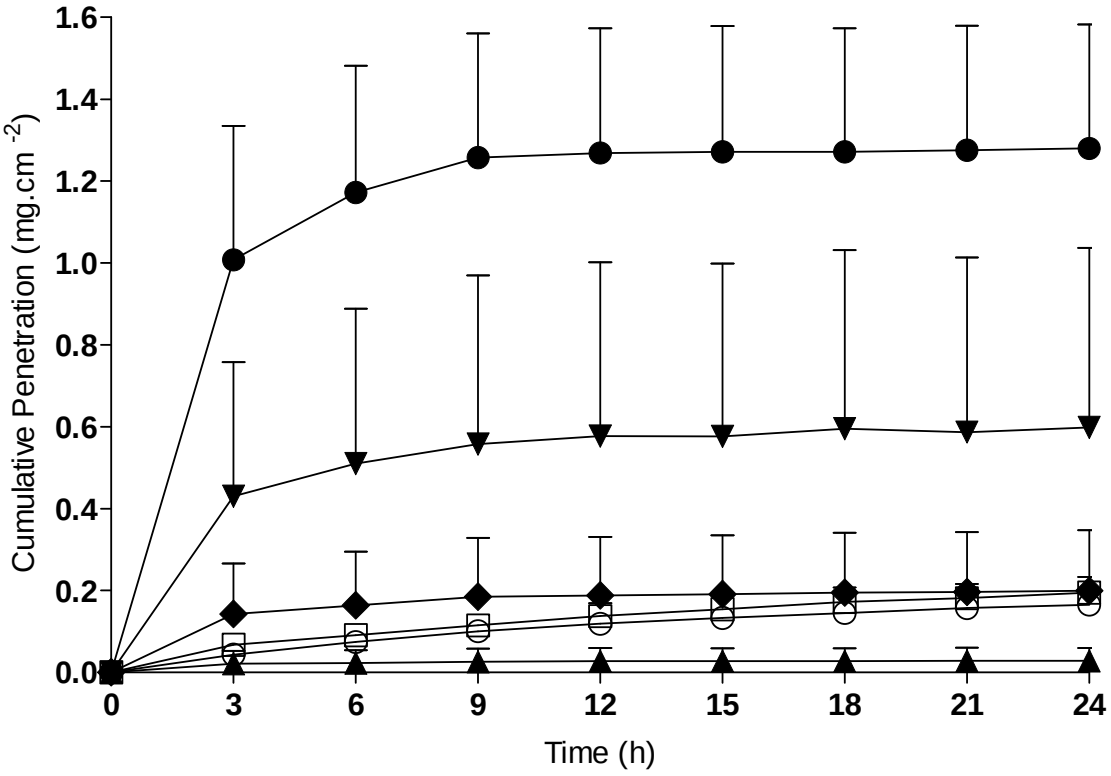

Figure 4.12: Cumulative ^{14}C-GD penetration through untreated (-●-) or treated damaged pig skin over 24 hours from an initial topical 10µl dose at t = 0. Treatment was applied topically at 30 seconds post GD exposure using Fullers Earth (-▲-), SuperQR (-⊟-), Woundstat™ (-◆-) or QuikClot ACS+® (-▼-). An untreated, undamaged skin control (-⊖-) was used also evaluated. All values are mean ± standard deviation of n=6 diffusion cells.

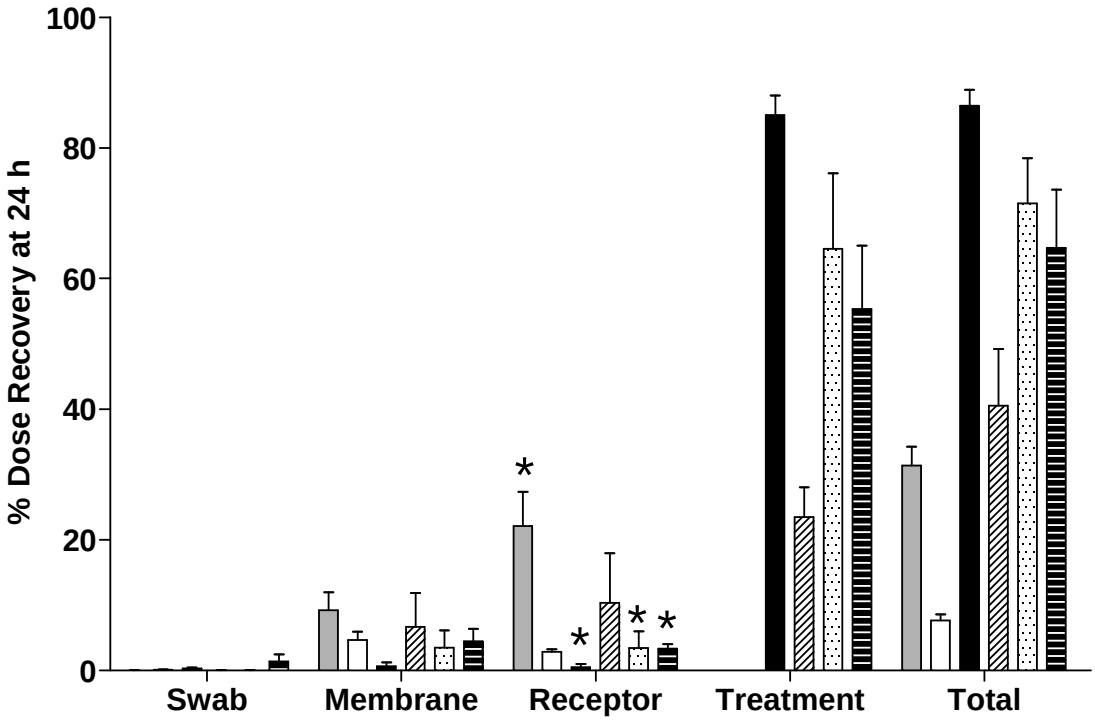

Figure 4.13: Dose recovery (%) at 24 hours of ^{14}C-GD remaining on the skin surface (swab), within the skin (membrane), sequestered into the test material (either haemostat or standard decontaminant) or penetrated into the receptor media. The skins were either untreated (damaged (▩), undamaged (□) or test materials (SuperQR (▤), Woundstat™ (⬚), QuikClot ACS+® (▨) or Fullers Earth (■)) were placed onto the skin surface 30s after the skin had been contaminated with GD. All values are mean ± standard deviation of n=6 diffusion cells. Statistical significance between the extent of GD penetration at 24 hours though damaged untreated and treated skins is indicated (*).

4.4. Discussion

4.4.1. Skin decontamination efficacy of haemostats

This *in vitro* study has shown that a number of COTS haemostatic products are potentially amenable to fulfil the role of skin decontaminants against GD when applied before 30 seconds after exposure. Standard military doctrine, however, indicates that decontaminant application should be completed by 2 minutes post exposure. In a battlefield scenario, 30 seconds approximates to the minimum likely time that would elapse before a haemostatic product would be applied to a haemorrhaging wound. The purpose of this study was to identify candidate test compounds that could both decontaminate and arrest haemorrhage. That being the case, a time delay of 30 seconds was deemed to be appropriate.

4.4.1.1. Haemostat category performance

Three broad categories of haemostat were investigated, powders, wound dressings and liquids. In general, the haemostatic powders were more effective than either haemostatic wound dressings or haemostatic liquids. The combination of haemostatic liquids with the potentially reactive excipient TOP (Tetraglyme, Oxime, Polyethyleneimine) did not significantly improve their performance as candidate decontaminants. The effectiveness of the haemostatic powders is most likely due to their absorptive mechanism of action: haemostasis achieved via fluid and low molecular weight compound removal from the blood. The haemostatic liquids (with or

without TOP) and wound dressing did not perform effectively as GD decontaminants. This ineffectiveness (and in some cases enhanced absorption of GD was evident) may have been due to their occlusive nature. It is well known that occlusion of volatile chemicals, such as GD, can enhance skin absorption via prevention of volatilisation of liquid away from the skin surface.

4.4.1.2. Standard military decontaminant performance

Three standard military decontaminants were included in the present study to provide a benchmark for the candidate test compounds to be compared against. As expected all three (Fullers Earth, M291 and KBDO liquid) were efficacious decontaminants, however, in the case of KBDO liquid, apparently only for six hours post exposure. A potential confounding factor is the underlying assumption that the radio labelled chemical is exclusively the parent compound (in this case GD) for the duration of the study and not a breakdown product. The mechanism of action of reactive decontaminants such as KBDO liquid is decontamination of CW agent to potentially less toxic breakdown products. Further investigation is required to determine which breakdown products subsequently penetrated through the skin.

4.4.1.3. Experimental design observations

When considering the study design involving medical countermeasures against CW agents, a typical stance, and the one employed here, is to test the worst case scenario. Worst case allows the identification and rejection of ineffective products at

an early stage in the study design. To this end a number of facets were incorporated including use of a receptor fluid consisting of 50% aqueous ethanol and leaving test products in contact with the skin surface for duration of the study (they would normally be removed after a suitable interval). The obvious benefit of leaving the test product in situ for the duration of the study is that it allows for any desorption characteristics to be elucidated. Just because a product is initially effective does not give the full picture. It is important to take into account any subsequent desorption which could potentially lead to an increase in dermal absorption. A robust approach eliminates the selection of potentially ineffective test compounds.

4.4.1.4. Parallel studies with VX and HD

The haemostatic products were also evaluated against HD and VX (Lydon, 2012;Hall, 2012). On undamaged skin, two products (Woundstat™ and QuikClot ACS+®) were effective against HD and eight products (SuperQR, Woundstat™, QuikClot ACS+®, Celox®, HemCon®, TOP, TOP +Vitagel™ and TOP + FastAct®) were effective against VX. On the basis of decontamination efficacy across all three chemical warfare agents, Woundstat™, QuikClot ACS+® and SuperQR were selected for further evaluation.

4.4.2. Agent desorption characteristics from haemostats

4.4.2.1. GD desorption from candidates at room temperature

At room temperature, all three of the selected haemostats irreversibly sequestered GD for the three hour study duration. A more rigorous test was to evaluate GD sequestration at elevated temperatures. It is not unreasonable to assume that the candidate product may be expected to perform well in temperatures approaching 45°C. Super-QR was not evaluated at elevated temperatures due to its withdrawal from the programme prior to this experimental aspect (Super-QR was withdrawn due a lack of efficacy against HD).

4.4.2.2. GD desorption from candidates at elevated temperature

Of the two remaining candidates, this *in vitro* study has shown that Woundstat™ irreversibly sequesters GD at both room temperature and elevated temperatures when applied by 30 seconds post exposure. Irreversible sequestration at both room and elevated temperature was also exhibited by fullers' earth. It has already been postulated that the effectiveness of the haemostatic powders is most likely due to their absorptive mechanism of action, a mechanism of action shared with fullers' earth. On the basis of this and earlier studies, it would seem that Woundstat™ and fullers' earth have similar absorptive properties.

4.4.2.3. Importance of irreversible sequestration

The ability of the selected haemostat to irreversibly sequester GD is of fundamental importance to the work programme. Secondary contamination from possible off gassing, either at the scene, or after evacuation, has the potential not to only further

injure the casualty, but also any attending medical personnel. Too reiterate, it would not be desirable for the selected candidate haemostat to only transiently absorb the chemical warfare agent.

4.4.2.4. Parallel Studies with VX and HD

The selected haemostatic products were also evaluated against HD and VX at both ambient and elevated temperatures (Lydon, 2012;Hall, 2012). There was no measurable loss of either VX or HD from Woundstat™ at ambient temperatures, however, at elevated temperature significant volatilisation (approximately 10%) was shown for both VX and HD. VX and HD were found to off gas from QuikClot ACS+® and SuperQR at both ambient and elevated temperatures.

4.4.3. Damaged skin decontamination efficacy of haemostats

This *in vitro* study has shown that all three selected COTS haemostatic products are potentially amenable to fulfil the role of skin decontaminants against GD *in vivo* when applied by 30 seconds post exposure onto damaged skin tissue.

4.4.3.1. Haemostat powder decontaminant performance

All three of the selected haemostats were powder based. It is likely that their absorptive mechanism of action was responsible for their effectiveness at sequestering the chemical warfare agents evaluated. On the basis of the current 24

hour study, it is reasonable to infer that GD is irreversibly sequestered within the haemostat (at a skin temperature of 32°C) as there is no evidence of increased absorption at any point during the study after the initial lag phase.

4.4.3.2. Military decontaminant performance

Fullers' earth was used as a positive control for both the undamaged and damaged skin *in vitro* diffusion cell studies. Fullers' earth was as effective against GD on damaged skin as it was on undamaged skin. It would seem that fullers' earth would be an ideal candidate to evaluate as a haemostat in its own right. However, the use of fullers' earth in wounds is contraindicated due to difficulties associated with the removal of fine particles from the wound site and the likelihood of any retained particles causing fibrosis and granuloma formation (Cooper, et al., 1994).

4.4.3.3. Parallel studies using HD and VX

The haemostatic products were also evaluated against HD and VX (Lydon, 2012;Hall, 2012). Woundstat™ and QuikClot ACS+® were effective decontaminants on damaged skin against both HD and VX, however, QuikClot ACS+® was qualitatively less effective than Woundstat™. SuperQR was ineffective against HD on damaged skin (although it was effective against VX).

4.4.3.4. Undamaged vs damaged skin absorption

Perhaps unsurprisingly, ^{14}C-GD penetrated through damaged skin more rapidly and to a greater extent (approximately 10 fold) than through undamaged skin (Figure 4.12). A number of researchers have investigated the skin permeability of a range of chemicals with differing log p values after damage from a variety of sources including mechanical damage (Bronaugh and Stewart, 1985;Gattu and Maibach, 2010). Gattu concluded that damage resulted in enhancement of absorption of molecules and that this enhancement was more pronounced for hydrophilic molecules compared to lipophilic molecules. Of interest was a 6 fold enhancement in the penetration of methyl paraben through mechanically abraded skin (methyl paraben and GD have similar log p values, measured at 1.96 and 1.8 respectively). Assuming that a ten fold difference in penetration rate between *in vitro* undamaged and damaged skin correlates to *in vivo* undamaged and damaged skin for GD, then a countermeasure developed for human *in vivo* use on contaminated damaged skin would likely have a requirement to be substantially more efficacious than if the countermeasure was only required to decontaminate undamaged skin.

4.4.4. Candidate haemostat selection for use as a decontaminant

The series of tests described were carried out as an assessment of the required performance criteria (Section 4.1) of the haemostatic decontaminant. In all tests and across all three chemical warfare agents used, Woundstat^{TM} consistently outperformed the other candidate haemostatic decontaminants. Furthermore, Woundstat^{TM} consistently performed as well as the standard in service powder

decontaminant fullers' earth. On this basis, Woundstat^{TM} was selected as the sole candidate for *in vivo* evaluation.

CHAPTER 5: IN VIVO EFFICACY TESTING OF HAEMOSTATIC PRODUCTS AS CHEMICAL WARFARE AGENT DECONTAMINANTS

5.1. Introduction

The use of *in vivo* animal models remains the method of choice to study whole body systemic interactions with nerve agents. The toxicity of nerve agents is such that it would be unethical to conduct nerve agent studies in human volunteers, although this does not preclude the use of less toxic simulants such as methyl salicylate. Although, traditionally smaller animal models such as the guinea pig have been extensively used for *in vivo* nerve agent studies, the pig is arguably a more relevant model for nerve agent exposure via the percutaneous absorption route.

5.1.1. The pig as an *in vivo* model

Percutaneous absorption through pig skin has been shown to be more representative as a model for human skin than that of rodents and has the advantage of allowing neat, rather than diluted chemical to be topically applied. Furthermore, for studies which also involve the withdrawal of multiple blood samples, a large animal model offers the advantage of a large circulating blood volume. Less well characterised is the response of the pig to nerve agent exposure after absorption has taken place (although for the characterisation of medical countermeasure efficacy, which operate on a pass / fail criteria, this may not be a major concern). Work to further characterise the pig for nerve agent exposures continues unabated both nationally and

internationally (Bjarnason, et al., 2008;Dorandeu, et al., 2007;Mikler, et al., 2011;Sawyer, et al., 2011;Sawyer, et al., 2012;Tenberken, et al., 2010;Chilcott, et al., 2005b).

5.1.2. Adherence to the 3R's

For the current study, adherence to the 3R's (refinement, replacement and reduction), has prompted the analysis of a substantial *in vitro* body of data to allow selection to the favoured test product. To this end, initial *in vitro* evaluation studies had been undertaken to answer a series of questions to allow effective product selection prior to *in vivo* evaluation. An effective candidate would retain haemostatic ability in the presence of a range of CW agents (nominally GD, VX and HD). This was seen as an essential quality due to the fact that that the haemostat would need to have continued efficacy when in intimate contact with CW agents. Thrombelastographic evaluation of CW agent spiked blood sample showed that this was the case for a number of test products. Of primary importance, was that an effective candidate would also have demonstratable efficacy as a CW agent skin decontaminant. This was shown to be the case for both normal and damaged skin *in vitro* using a range of CW agents including GD, VX, and HD. A final criterion was the desire that an effective candidate would irreversibly sequester any CW agent that it had absorbed from the skin surface. It is important to note that any re-release of CW agent from the test product would not only have potential consequences for the casualties, but, also for any attending medical personnel. A number of test products were shown to have this ability.

5.1.3. Haemostatic decontaminant for *in vivo* evaluation

From the initial *in vitro* studies (Chapter 4), the most efficacious product was determined to be Woundstat™. Although a number of test products were shown to be effective against GD challenge, only Woundstat™ consistently passed tests involving GD, VX and HD.

5.1.4. Study purpose

The purpose of the current study was to use a damaged skin *in vivo* pig model to evaluate Woundstat™, with the aim of determining whether a) it could both simultaneously act as a haemostat to prevent catastrophic blood loss after haemorrhaging injury, and b) whether it could effectively decontaminate a chemical warfare agent contaminated wound. As one of a suite of evaluation studies, this particular study was primarily concerned with the decontamination efficacy of the test product rather than its ability to induce haemostasis (a characteristic already proven for COTS haemostats). The definitive, final evaluation study will use a haemorrhaging wound model contaminated with CW agent to make the final efficacy evaluation. The current study also allowed for the clinical manifestations of GD poisoning to be defined and the absorption and distribution of ^{14}C-GD to be quantified.

5.2. Materials and Methods

The synthesis, use and destruction of GD in this study was conducted in accordance with the Chemical Weapons Convention (1996) to which the UK is a signatory state. Radiolabelled pinacolyl methylfluorophosphonate (GD) was synthesised by TNO (Rijswijk, Netherlands) and had a radiochemical purity >97% (as determined by radiometric HPLC analysis). The ^{14}C label was at the P-CH_3 moiety (see Figure 1.6). The chemical purity of unlabelled GD was reported to be >97% (by NMR). Both radiolabelled and cold agent were mixed in appropriate proportions to give a nominal activity of approximately 0.4 MBq μl^{-1}. WoundStat™ was purchased from TraumaCure, Inc. (Bethesda, MD). Batch WS-07-1200, expiry 03/12/10 was used for the procedure.

The use of animals in this study was conducted in accordance with the Animals (Scientific Procedures) Act 1986. Animal studies reported here were compliant with both UK Home Office and USAMRMC Animal Care and Use Review Office (ACURO) guidelines. Female pigs (sus scrofa) of weight range 15 to 25 kg were purchased form a local supplier. Each animal was habituated for a minimum of seven days and given 24 h access to food and water by animal technicians. After acclimatisation, each animal was sedated with Hypnovel® (Midazolam, 6ml i.m., 5 mg ml^{-1}) prior to induction of anaesthesia using up to 5% isofluorane delivered via a facemask. After a 15 minute stabilisation period, the pig was intubated with an endotracheal tube (7mm cuffed, lubricated with KY jelly). Surgery was conducted under isofluorane (1.5 to 3 %) respiratory anaesthesia.

Vital signs including pulse rate, ECG, arterial blood pressure, breathing rate, core temperature, CO_2 and SPO_2 monitored for the duration of the study using a Propaq Encore (Welch Allyn, USA) physiological monitoring system.

5.2.1. Surgery

Surgery was carried out under aseptic conditions to give arterial and venous access. The internal carotid artery and jugular vein were canulated using 2 mm catheters. All catheters were primed with sterile saline prior to introduction to the animal. Incisions were sutured using a vicryl straight needle suture. Anaesthesia was transitioned from respiratory isofluorane to intravenous Alfaxan (alphaxalone, Astra Zeneca) upon the completion of surgery. Alfaxan infusion rates were of between 12 to 24 $ml.hr^{-1}$ dependent upon clinical signs. Baseline samples and physiological measurements were taken during a 30 minute stabilisation period after transition onto intravenous anaesthesia. The pig was placed in a sling housed within a category C fume cupboard prior to preparation of the outer ear dosing site. The dorsal aspect of the left ear was secured to the sling with a flat piece of metal in a horizontal position. Skin damage (were required by experimental protocol) was achieved by dermatoming (Humeca Model D42, Serial No. 42116, Eurosurgical Ltd, Guildford, UK) a 3 cm^2 area of outer ear skin to a depth of 100 µm. Any bleeding from the wound was transient and was removed using sterile, saline soaked gauze. A dosing chamber constructed from a sawn off 20 ml syringe was glued over the wound site using Vetbond surgical adhesive. The animal remained within the fume cupboard until study completion.

5.2.2. Blood Sample Processing

Arterial blood samples were taken at various time points for determination of whole blood cholinesterase, clinical blood parameters, haematocrit levels, thrombelastography (TEG) and radioactivity quantification. Samples for clinical blood parameters were drawn into a blood gas syringe and run immediately on a GEM 3000 blood gas analyser, parameters obtained were pH, pCO_2, pO_2, Ca^{2+}, Na^{2+}, K^+, lactate, glucose and haematocrit. CO-Oximetry samples were run using a GEM OPL (Oxygen Portable Laboratory) to give the parameters THb (Total haemoglobin), O_2Hb, COHb, MetHb, RHb, SO_2m, FHb and SHb. Samples for whole blood cholinesterase and haematocrit were taken into sodium EDTA vials. Haematocrit sample were run immediately whilst whole blood cholinesterase samples were frozen at -20ºC prior to analysis to ensure lysis of the blood cells. Samples for TEG and radiometric analysis were taken into sodium citrated vials. TEG samples were run according to methodology in Chapter 3 whilst radiometric samples were collected and frozen at -20ºC for later analysis. Sample acquisition for an individual study was dependent on each individual study protocol.

5.2.3. Baseline parameter determination

Six animals were surgically prepared as described above before being monitored and sampled for 6 hours. Animals were euthanized prior to being subject to post mortem as described in the terminal procedures and post mortem section.

5.2.4. Determination of GD dosing volume

Eight animals were surgically prepared prior to receiving a GD dose of varying volume (0.3 µl kg^{-1} to 3 µl kg^{-1}) as a single droplet onto dermatome damaged ear skin within the dosing chamber using a Gilson positive displacement pipette. The droplet was left *in situ* without interference for the duration of the study. Animals were monitored and had blood sampled either until the animal suffered from terminal nerve agent effects or the maximum study duration of six hours was reached. Whether or not the animal died during the study, the euthanisation procedure was followed prior to post mortem (as described in the terminal procedures and post mortem section).

5.2.5. Determination of Woundstat™ efficacy

Twelve animals were dosed with a fixed volume of GD (0.3 µl kg^{-1}) as a single droplet onto dermatome damaged ear skin within the dosing chamber using a Gilson positive displacement pipette. Thirty seconds after GD challenge, six animals had an excess (2 g) of Woundstat™ placed onto the surface on the damaged skin site, completely covering the GD present on the skin surface. The applied Woundstat™ was left *in situ* for the study duration. Six control animals received no treatment after GD challenge with the droplet being left *in situ* with no interference. As with the dosing volume determination study, animals were sampled and monitored until the animal succumbed to the toxic affect of the nerve agent or the six hour maximum study duration was reached. The animal was then euthanized (irrespective of whether it had died due to nerve agent poisoning) prior to post mortem.

5.2.6. Terminal procedures and post mortem

Animals were culled with an intravenous overdose of Euthatal™ (sodium pentobarbitol, 6ml i.v., 200 mg ml^{-1}) prior to exsanguination using suction through the arterial line. The ear dosing site was excised and removed from the animal using a scalpel. For studies using Woundstat™, this was emptied into a glass vial with any remaining Woundstat™ being dry swabbed from the skin surface and retained in a separate vial. The dosing chamber was then removed and placed into a vial. The skin surface of the dosing site was swabbed with dry cotton wool with the swab being retained. After these operations had been completed, the ear dosing site was separated into 2 sections, the central dosing area and the periphery of surrounding skin tissue. The skins were placed into separate glass vials. A post mortem was performed, with organ weights being taken for brain, lungs, heart, spleen, pancreas and liver. Sections of these organs as well as diaphragm were retained for further analysis.

5.2.7. Cholinesterase activity determination

The Ellman method (Ellman, et al., 1961) was used to analyse samples of arterial whole blood that had been stored for a minimum of 30 minutes at -20°C. Aliquots of whole blood were incubated at 30°C using a hot plate, in cuvettes containing 5,5 – Dithiobis – (2 nitrobenzoic) acid (DTNB), sodium bicarbonate ($NaHCO_3$), acetylthiocholine iodide and a pH8 phosphate buffer. The reaction of these compounds was measured using a spectrophotometer (Ultrospec 6300 pro, Biochrom Ltd, Cambridge, UK) with an 8 cell holder at a wavelength of 412nm over a

10 minute period. Substrate blanks and sample blanks were run alongside each test sample. Preparation details for these solutions and amounts added to each cuvette are given below. Phosphate buffers at pH7 and pH8 were made up from 0.1M sodium dihydrogen orthophosphate ($NaH_2PO_4.2H_2O$), molecular weight 156.01 (weight of 7.8g made up to 500 ml with distilled H_2O) and 0.1M disodium hydrogen orthophosphate ($Na_2HPO_4.2H_2O$), molecular weight 177.99 (weight of 35.6 g made up to 2000 ml with distilled H_2O). For 1000 ml of the pH7 phosphate buffer, the required volumes were approximately 195 ml 0.1M sodium dihydrogen orthophosphate, 305 ml 0.1M disodium hydrogen orthophosphate and 500 ml distilled H_2O. For 2000 ml of the pH8 phosphate buffer, the required volumes were approximately 52 ml 0.1M sodium dihydrogen orthophosphate, 948 ml 0.1M disodium hydrogen orthophosphate and 1000 ml distilled H_2O. For both of the phosphate buffers, the pH was adjusted as necessary and checked using a calibrated pH meter. Buffers were stored at 4°C and checked daily until required. The DTNB solution comprised: 198 mg of 5,5 – dithiobis – (2 nitrobenzoic) acid (DTNB), molecular weight 396.35 added to 75 mg sodium bicarbonate ($NaHCO_3$), molecular weight 84.01, and made up to 50 ml with 0.1M pH7 phosphate buffer. From this stock solution, a DTNB working solution of 2.5 ml DTNB stock made up to 100 ml with distilled H_2O was made daily. Acetylthiocholine iodide, molecular weight 289.18, 44.1 mg was made up to 50 ml with distilled H_2O. Whole blood (25µl) that had previously been stored frozen at -20°C in EDTA tubes was diluted into 4.975 ml of pH8 phosphate buffer. The diluted blood was shaken gently to ensure thorough mixing prior to use.

5.2.7.1 Ellman assay procedure

Eight cuvettes were measured simultaneously; these were split into sample blanks, substrate blanks and whole blood test samples. Cuvettes for sample blanks contained 1 ml distilled H_2O, 1 ml diluted whole blood and 1 ml DTNB working solution. Cuvettes for substrate blanks contained 1 ml acetylthiocholine iodide solution, 1 ml pH 8 phosphate buffer and 1 ml DTNB working solution. Cuvettes for test samples contained 1 ml diluted whole blood, 1 ml acetylthiocholine iodide solution and 1 ml DTNB working solution. Each cuvette contained a total volume of 3 ml, with a total amount of blood within that volume (for test and sample blanks) of 5µl. The absorbance at 412 nm was measured for each solution every 30 seconds for 10 minutes. The absorbance output was exported to Microsoft Excel where the rate of reaction for the sample blank, substrate blank and test sample were determined. The reaction rate for each test sample was corrected by subtracting the sample and tissue blanks which had been run simultaneously. The percentage cholinesterase activity in each test sample post GD dosing was determined by reference to an assigned pre GD dosing sample of 100% activity.

5.2.8. Radiometric analysis

Radiometric dose distribution was carried out to quantify the amount of GD present in the following compartments at the conclusion of the study: within the skin at the dosing site, within the skin around the periphery of the dosing site, on the surface of the skin and within the dosing assembly. For Woundstat™ studies, the Woundstat™ was retained to quantify absorption efficiency. Each compartment was taken into a

vial as described earlier. Iso propyl alcohol was used to extract radioactivity from the skin cotton wool swabs and dosing chambers, skin samples were solubilised using soluene 350 and Ultima Gold liquid scintillation fluid was used to extract radiolabel from Woundstat^{TM} treated samples. After solubilisation of the skin tissue, all compartments were sampled into Ultima Gold liquid scintillation fluid. The amount of radioactivity in each sample was measured using a Perkin Elmer Tri-Carb liquid scintillation counter (Model 2810 TR), using the manufacturer's ^{14}C-quench curve library set to exclude single-photon (non-radioactive) events. The amount of radioactivity in each sample was converted to amount of GD by comparison to standards (containing known quantities of ^{14}C-GD) prepared and measured simultaneously.

5.3. Results

The results generated during the *in vivo* studies are grouped into a number of discrete sections beginning with baseline parameter determination (six animals), then GD dose ranging studies used to determine the clinical manifestations of GD poisoning (which comprised eight animals run sequentially) and finally twelve animals in the main study group which received a fixed (µl kg^{-1}) GD volume with or without Woundstat™ treatment. Animals in the main study group were challenged with ^{14}C-GD. The results are presented in three sections; clinical manifestations of GD poisoning (incorporating data from control animals), damaged skin absorption and distribution of ^{14}C-GD and efficacy of a haemostatic decontaminant candidate *in vivo*.

5.3.1. Clinical manifestations of GD poisoning

Data collecting during the dose ranging studies included observed signs, monitored physiological signs, whole blood cholinesterase, arterial blood gas analysis and thrombelastography (TEG). Together these gave a broad assessment of the clinical manifestations of GD poisoning following percutaneous damaged skin exposure in the large white pig. Animal usage for the study comprised a total of 14 animals; 6 negative controls and 8 animals that received various $mg.kg^{-1}$ challenges of GD (Table 5.1) onto damaged ear skin.

Challenge ($mg.kg^{-1}$)	Assigned	Physiological Signs	TTD (min)
3	High	Early / Intermediate / Late onset	12
0.3	Low	Early only	Survived
1	Medium	Early / Intermediate / Late onset	34
1	Medium	Early / Intermediate / Late onset	114
1	Medium	Early / Intermediate	Survived
1	Medium	Early / Intermediate / Late onset	15
0.75	Medium	Early / Intermediate / Late onset	11
0.3	Low	Early / Intermediate / Late onset	138

Table 5.1: GD challenges applied to damaged pig ear skin on individual animals. Doses were assigned at challenge levels of high (3 $mg.kg^{-1}$), medium (0.75 to 1 $mg.kg^{-1}$) or low (0.3 $mg.kg^{-1}$). The physiological signs (Section 5.3.1.1) and time to death (TTD) for each animal did not correlate with the assigned challenge level.

5.3.1.1. Physiological signs of GD poisoning

Physiological signs were either physically observed or measured using a ProPaq monitoring system. Observations were recorded throughout the time course of each study until either apnoea or euthanasia. Observable clinical signs in GD poisoned animals included miosis, mastication, fasiculations (both head and body), tremors, nasal secretions, salivation and body spasm, apnoea and death. The appearance of these overt signs (if present) was consistent in relation to the onset of apnoea. Regardless of the GD challenge, early signs of GD poisoning included mastication, fasiculations and tremor. Intermediate signs included miosis, salivation and nasal secretions. Late onset effects (just prior to apnoea) included lacrimation and body spasm. None of the signs were dose specific, with the time to onset of apnoea seemingly unrelated to the GD challenge received. The monitored physiological signs measured both pre-exposure and immediately preceding apnoea or euthanisation are shown in Table 5.2. Differences between pre exposure and end of study parameters for GD exposed animals were consistent with the onset of apnoea.

GD challenge ($mg.kg^{-1}$)	0		0.3		0.75		1		3	
	Pre exposure	End	Pre exposure	End	Pre exposure	End	Pre exposure	End	Pre exposure	End
Pulse Rate	163 ± 19	156 ± 31	163 ± 4	145 ± 33	144	66	153 ± 25	113 ± 90	167	93
Systolic Pressure (mmHg)	120 ± 9	106 ± 10	119 ± 3	155 ± 52	130	120	104 ± 10	92 ± 28	119	172
Diastolic Pressure (mmHg)	93 ± 7	79 ± 9	46 ± 73	58 ± 95	98	88	79 ± 9	62 ± 25	97	130
Mean Pressure (mmHg)	107 ± 6	93 ± 8	84 ± 33	104 ± 65	107	103	91 ± 11	74 ± 29	108	146
$C0_2$ (kPa)	6.2 ± 0.1	5.9 ± 0.7	5.8 ± 0.4	7.3 ± 1.6	6.4	0.7	6.1 ± 0.2	2.8 ± 4	5.9	0.5
Breathing Rate	36 ± 13	33 ± 9	36 ± 11	13 ± 12	52	0	50 ± 11	5 ± 11	52	0
$Sp0_2$ (%)	93 ± 3	92 ± 7	93 ± 3	49 ± 67	89	0	93 ± 4	54 ± 4	89	74
Body Temp (°C)	38.2 ± 0.6	38.1 ± 0.5	38.3 ± 0.9	34.6 ± 4.9	37.8	37.3	38.2 ± 0.4	37.3 ± 0.8	38.6	38.3

Table 5.2: Monitored physiological signs in pigs during steady state anaesthesia both pre GD exposure and at the end of the experiment (immediately preceding apnoea of euthanisation) at a range of challenge doses. Data from a total of 14 animals as follows; n=6 for GD challenge of 0 $mg.kg^{-1}$, n=1 for GD challenge of 0.75 and 3 $mg.kg^{-1}$, n=2 for GD challenge of 0.3 $mg.kg^{-1}$ and n=4 for GD challenge of 1.0 $mg.kg^{-1}$.

5.3.1.2. Whole blood cholinesterase

Whole blood cholinesterase did not significantly vary from the original cholinesterase value of 100% for the six hour study duration for the control group (Figure 5.1). In contrast, there was a rapid blood cholinesterase inhibition for GD poisoned animals. For all GD challenge levels, whole blood cholinesterase had decreased to less than 5% of the original value by 10 minutes post contamination. Whole blood cholinesterase levels generally remained below the 5% level until the onset of apnoea. For the challenge levels chosen, whole blood cholinesterase inhibition was independent of GD dose given, indicating that for the challenge levels used, extent of whole blood cholinesterase inhibition was not a reliable indicator of final clinical outcome. Similarly, the observed physiological signs (section 5.3.1.1.) did not indicate the rapidity and extent of the cholinesterase depression.

5.3.1.3. Blood parameters

Generally, exposure to GD caused an elevation in arterial blood gas parameters (except for pO_2 which decreased) immediately prior to apnoea (Table 5.3). Of particular interest was the increase in blood glucose after GD exposure. Changes in Co-Oximetry parameters are shown in Tables 5.3 and 5.4.

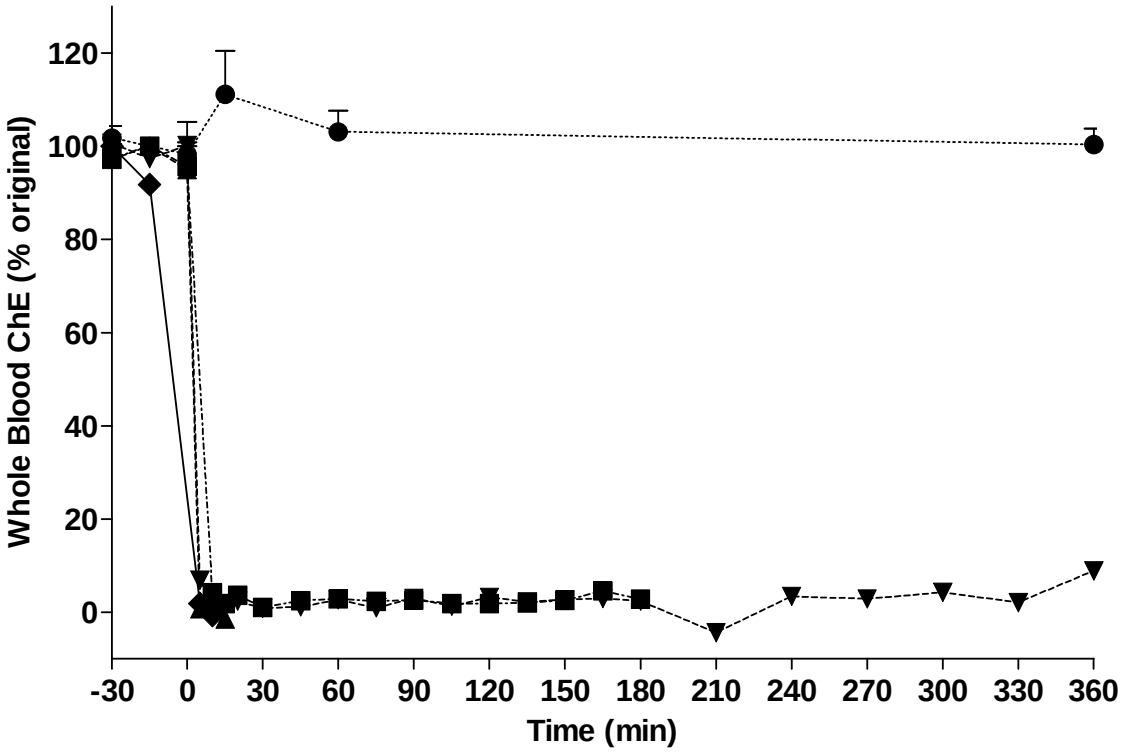

Figure 5.1: Total whole blood cholinesterase (ChE), shown as percentage of original (pre GD challenge) activity in anaeathetised pigs following damaged ear exposure to liquid GD. All values are mean ± standard deviation of up to 6 animals. GD challenge levels were 0 $mg.kg^{-1}$ (●, n=6), 0.3 $mg.kg^{-1}$ (■, n=2), 0.75 $mg.kg^{-1}$ (▲, n=1), 1 $mg.kg^{-1}$ (▼, n=4) and 3 $mg.kg^{-1}$ (◆, n=1).

.

GD challenge ($mg.kg^{-1}$)		0		0.3		0.75		1		3	
		Pre exposure	End	Pre exposure	End	Pre exposure	End	Pre exposure	End	Pre exposure	End
At 37oC	pH	7.5	7.5	7.5 ± 0	7.4 ± 0.1	7.5	7.1	7.5 ± 0	7.3 ± 0.1	7.5	7.3
	pCO_2 (kPa)	5.7	6.3	5.2 ± 0.1	8.4 ± 4	5.2	12.1	5.6 ± 0.3	7.9 ± 1.8	5.9	9.7
	pO_2 (kPa)	8.5	9.6	10.9 ± 2	5.2 ± 5.6	10.0	0.3	10.7 ± 1.1	5.1 ± 2.9	8.9	0.7
	Na^+ (mmol/L)	136.0	135.0	138.0 ± 1.4	139.0 ± 1.4	140.0	137.0	137.8 ± 2.2	138.3 ± 2.5	139.0	138.0
	K^+ (mmol/L)	3.9	3.5	4.1 ± 0.1	4.2 ± 0.7	3.9	10.1	4.0 ± 0.2	5.8 ± 1.5	3.8	7.4
	Ca^{++} (mmol/L)	1.4	1.3	1.4 ± 0	1.4 ± 0	1.6	1.5	1.4 ± 0.1	1.4 ± 0	1.4	1.4
	Glu (mmol/L)	4.9	4.7	3.8 ± 0.6	8.6 ± 2.9	3.6	3.6	4.7 ± 0.3	11.5 ± 7.7	3.5	3.2
	Lac (mmol/L)	0.7	0.3	1.1 ± 0.6	5.6 ± 0.4	0.6	5.5	0.8 ± 0.5	4.8 ± 3.8	0.7	3.8
	Hct (%)	30.0	28.0	29.0 ± 0	33.0 ± 1.4	27.0	36.0	28.0 ± 1.4	37.0 ± 2.6	32.0	35.0
Co-oximetry	THb (g/dL)	10.0	9.6	10.4 ± 0.4	11.1 ± 0.4	10.5	11.9	10.0 ± 0.3	12.9 ± 0.8	10.9	11.9
	O_2Hb (%)	92.4	93.8	95.3 ± 4	52.2 ± 56.1	92.4	8.8	95.2 ± 1.5	54.7 ± 33.6	92.5	10.8
	COHb (%)	0.0	0.1	0.2 ± 0.3	0.0 ± 0	0.0	0.1	0.0 ± 0	0.2 ± 0.2	0.0	0.0
	MetHb (%)	1.7	1.6	1.6 ± 0.4	1.1 ± 0.8	1.9	0.4	1.8 ± 0.8	1.7 ± 0.7	1.8	0.5
	HHb (%)	5.9	4.5	3.0 ± 4	46.7 ± 57	5.7	90.7	3.0 ± 1.6	43.5 ± 34	5.7	88.7
	SO_2 (%)	94.0	95.5	97.1 ± 4	53.0 ± 57.3	94.2	8.8	97.0 ± 1.5	55.8 ± 34	94.2	10.8

Table 5.3: Blood parameters measured in pigs during steady state anaesthesia both pre GD exposure and at the end of the experiment (immediately preceding apnoea of euthanisation) at a range of challenge doses. Data from a total of 9 animals as follows; n=1 for GD challenge of 0, 0.75 and 3 $mg.kg^{-1}$, n=2 for GD challenge of 0.3 $mg.kg^{-1}$ and n=4 for GD challenge of 1.0 $mg.kg^{-1}$.

GD challenge (mg.kg^{-1})		0		0.3		0.75		1		3	
		Pre exposure	End	Pre exposure	End	Pre exposure	End	Pre exposure	End	Pre exposure	End
Derived Parameters	HCO3- (mmol/L)	34.3	36.7	32.3 ± 0.6	34.0 ± 7.8	29.0	30.3	32.9 ± 0.7	31.5 ± 2	34.3	35.1
	HCO3std (mmol/L)	32.9	34.4	31.8 ± 0.2	29.4 ± 1.9	28.8	22.0	31.7 ± 0.4	27.1 ± 3.3	32.6	27.8
	TCO2 (mmol/L)	35.6	38.1	33.5 ± 0.6	36.0 ± 8.7	30.2	33.1	34.3 ± 0.8	33.3 ± 1.8	35.7	37.3
	BE(B) (mmol/L)	10.3	12.2	8.8 ± 0.4	7.0 ± 4.1	5.1	-1.0	8.8 ± 0.6	4.2 ± 3.9	10.0	6.3
	O2ct (ml/dL)	12.8	12.6	13.7 ± 0.1	7.9 ± 8.3	13.5	1.5	13.2 ± 0.6	9.5 ± 5.4	14.0	1.8
	O2cap (ml/dL)	13.6	13.2	14.2 ± 0.5	15.3 ± 0.7	14.3	16.5	13.6 ± 0.4	17.5 ± 1.2	14.8	16.4
	A-aDO2 (kPa)	2.4	2.0	1.2 ± 0.7	4.1 ± 1.4	2.8	5.1	1.0 ± 0.6	4.8 ± 3	2.3	6.7
	pAO2 (kPa)	12.1	12.0	13.1 ± 0.6	9.6 ± 4.6	13.3	5.3	12.5 ± 0.4	10.0 ± 2	12.1	7.3
	paO2/pA02	0.8	0.8	0.9 ± 0.1	0.5 ± 0.4	0.8	0.1	0.9 ± 0	0.5 ± 0.3	0.8	0.1
	CcO2 (ml/dL)	13.9	13.3	14.4 ± 0.4	15.4 ± 0.5	14.6	16.3	13.9 ± 0.5	17.7 ± 1.1	15.1	16.4

Table 5.4: Derived blood parameters measured in pigs during steady state anaesthesia both pre GD exposure and at the end of the experiment (immediately preceding apnoea of euthanisation) at a range of challenge doses. Data from a total of 9 animals as follows; n=1 for GD challenge of 0, 0.75 and 3 mg.kg^{-1}, n=2 for GD challenge of 0.3 mg.kg^{-1} and n=4 for GD challenge of 1.0 mg.kg^{-1}.

5.3.1.4. TEG measurements

The coagulation profile for pig blood with GD contamination at a range of challenge doses was determined by Thrombelastography (TEG) to enable an *in vivo* comparison to be drawn against pig blood contaminated with GD *in vitro* (Section 3.3.2.). For a GD challenge of 0.3 $mg.kg^{-1}$ the clotting time was decreased as indicated by the decreased “R-time” and increased “angle parameter” compared to pre-exposure measurements, an observation consistent with the *in vitro* studies. However, at a higher GD challenge (1 $mg.kg^{-1}$) there was no difference between the end of study values and the pre-exposure measurements (Table 5.5).

GD challenge ($mg.kg^{-1}$)	0.3		1		3	
	Pre exposure	End	Pre exposure	End	Pre exposure	End
R(min)	8.8 ± 1.7	4.7 ± 0.4	7.1 ± 3.6	8.3 ± 2.6	4.2	7.3
K(min)	1.9 ± 1.3	1.1 ± 0.2	1.5 ± 5.3	2.6 ± 1.3	1.0	1.3
Angle(deg)	65.0 ± 1.4	73.7 ± 0.3	70.6 ± 3.4	62.7 ± 1.3	77.0	72.3
MA(mm)	72.7 ± 6.0	76.4 ± 2.8	74.8 ± 23.7	72.1 ± 6.5	79.3	77.2

Table 5.5: Thrombelastography (TEG) parameters, R Time, K Time, Angle Parameter and Maximum Amplitude (defined in Section 3.1.3) measured in pigs during steady state anaesthesia both pre GD exposure and at the end of the study (immediately preceding apnoea or euthanisation) at a range of challenge doses. Data from a total of 9 animals as follows; n=1 for GD challenge of 3 $mg.kg^{-1}$, n=2 for GD challenge of 0.3 $mg.kg^{-1}$ and n=4 for GD challenge of 1.0 $mg.kg^{-1}$.

5.3.2. *In Vivo* damaged skin absorption and distribution of GD in the domestic white pig.

The data was split two discrete sets, absorption profiles (Figure 5.2), determined from regular blood sampling during each study (Section 5.3.2.1) and distribution profiles (Figures 5.3 to 5.5), determined from analysis of radioactivity after post mortem (Section 5.3.2.2). The data is presented as both individual animal data and as the average ± standard error mean of n=6 animals.

5.3.2.1. Absorption

Absorption of radiolabelled GD varied markedly between animals and the measured blood concentrations were directly related to the animals survival time (Figure 5.2). Early deaths had a direct impact on the dose distribution determined post mortem. In all the animals, ^{14}C-GD was detectable within the systemic circulation consistently by 10 minutes post challenge (Figure 5.2). As there was negligible activity detected within the dosing template and in the periphery of skin (Figure 5.4), the ^{14}C-GD did not spread beyond the central dosing area. This indicated a maximum absorptive area of 3.14 cm^2. The apparent (measured) absorption rate for ^{14}C-GD into the systemic circulation was 37 ± 12 $\mu g.h^{-1}$. As the measured appearance of ^{14}C-GD in the systemic circulation did not allow for distribution to internal organs, a further determination of absorption rate was calculated taking internal dose distribution data into account. The apparent absorption rate taking all sampled organs into account was 287 ± 120 $\mu g. h^{-1}$. It should be noted that as 36% of the radioactivity could not be

accounted for (Section 5.3.2.2.) it is not known how much of the applied dose was in the body of the animal and how much evaporated, hence the use of the term apparent.

5.3.2.2. Distribution

The total measured systemic recovery was 1.95 ± 0.24 % of the original applied dose, with the majority of radioactivity located within the blood, liver or kidney (Table 5.6, Figure 5.3). Local recovery at the skin dosing site accounted for 43.0 ± 9.3 % of the ^{14}C-GD application (Table 5.6, Figure 5.4). Unabsorbed radioactivity accounted for a further 18.67 ± 8.89 % of the applied dose (Table 5.6, Figure 5.4). This gave a total recovered radioactivity of 63.62 ± 8.33 %. The unaccounted for radioactivity represented 36.38 ± 8.33 % of the applied dose (Table 5.6, Figure 5.5) and can be assumed to have either volatilised or been present in unsampled tissues. The proportion of radioactivity recovered locally, unabsorbed or unaccounted for seemed primarily to be dependent on the time to death of the animal (Figure 5.5).

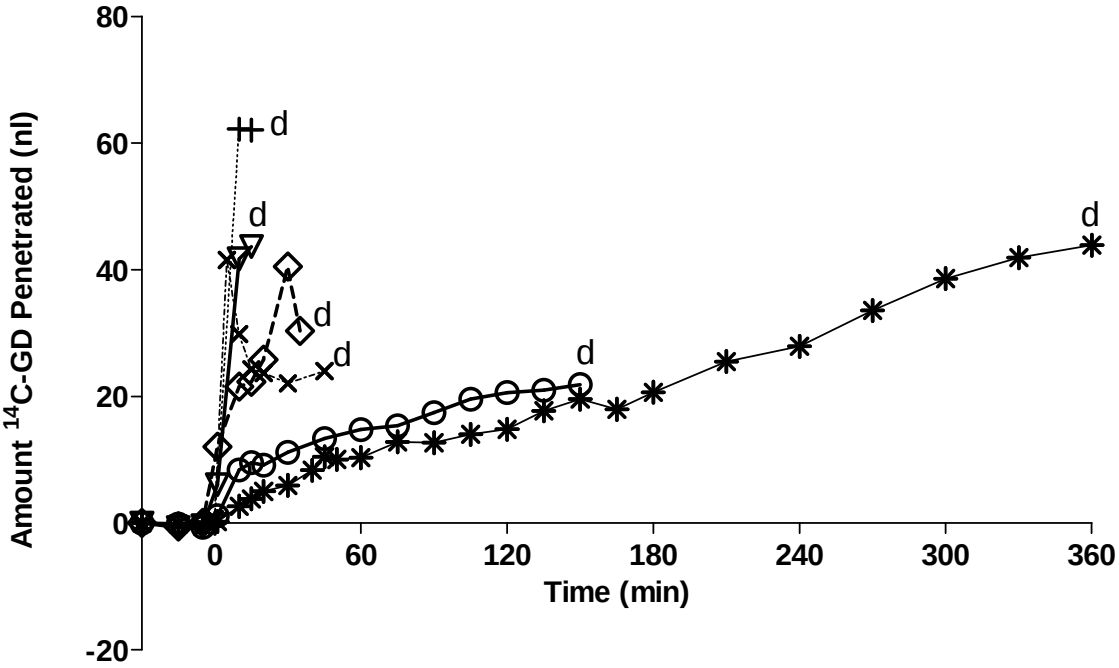

Figure 5.2: ^{14}C-GD penetration into the system circulation of the large white pig after application onto damaged ear skin. Each data set represents penetration determinations from an individual animal. Where, ✕ = animal 1, + = animal 2, ◇ = animal 3, ▽ = animal 4, ○ = animal 5 and ✳ = animal 6. Animal 6 survived for the maximum study duration of 6 hours. Those animals with larger amounts of ^{14}C-GD penetrated earlier in the time course (animals 1 -4) succumbed to the toxic effects of GD within 45 minutes of challenge (death indicated by "d"). Each animal received a GD dose at t=0 of 0.3 mg.kg^{-1}.

Compartment	Location	% Recovery	^{14}C GD (ng) /g tissue
Unabsorbed	Dosing chamber	1.99 ± 1.60	
	On skin surface	16.7 ± 8.5	
Local recovery	Skin dosing site	42.7 ± 9.3	
	Periphery of dosing site	0.33 ± 0.08	
Systemic recovery	Brain	0.04 ± 0.004	39.3 ± 4.8
	Heart	0.09 ± 0.005	44.7 ± 2.8
	Lung	0.16 ± 0.019	42.8 ± 3.8
	Spleen	0.03 ± 0.002	33.0 ± 1.7
	Pancreas	0.02 ± 0.003	41.5 ± 3.5
	Liver	0.74 ± 0.123	70.6 ± 10.8
	Kidney	0.11 ± 0.014	104.5 ± 10.3
	Blood	0.76 ± 0.093	33.9 ± 4.3
Total Recovery	Unabsorbed / Local / Systemic	63.6 ± 8.3	
Unaccounted	Volatilised or in unsampled organs	36.4 ± 8.3	

Table 5.6: ^{14}C GD recovery expressed as percentage recovery of the initial applied dose. Recovery is assigned to one of four major compartments, namely unabsorbed, local recovered, systemic recovered and unaccounted for. Unabsorbed material was assigned as the percentage of material residing on the dosing chamber or on the skin surface at the end of the study. Local recovery was designated as the percentage of ^{14}C GD located either within the skin under the dosing site or at the periphery of the dosing site. Systemic recovery was the percentage recoveries of radioactivity located in the named internal organs and within the blood. Summation of the radioactivity within all these compartments gave the total radioactivity recovery. Unaccounted for radioactivity was ascribed as either having volatilised from the dosing site or being located in unsampled organs. For the tissue recoveries, the amount of GD ng g^{-1} tissue was also calculated. All values are average ± standard error mean of n=6 animals. Each animal received a GD dose of 0.3 $mg.kg^{-1}$.

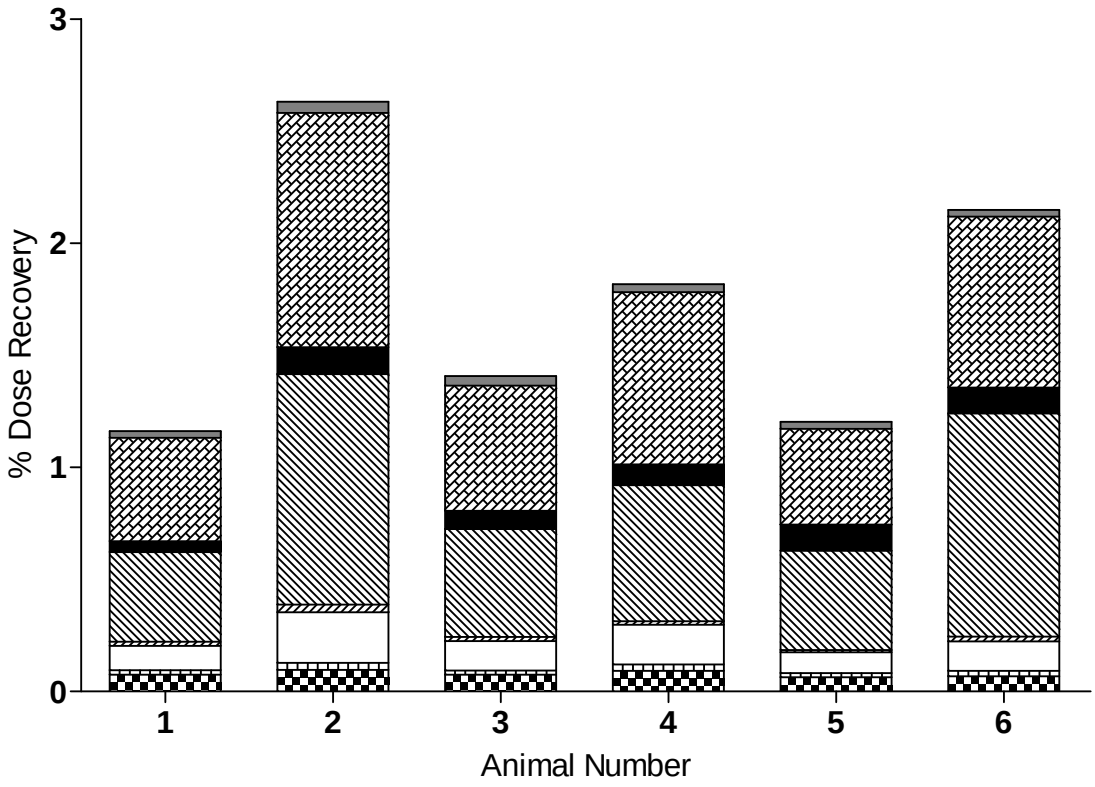

Figure 5.3: ^{14}C-GD distribution in sampled internal organs in individual animals after a 0.3 mg.kg^{-1} damaged ear skin exposure, expressed as percentage of the applied dose. Organs sampled were: heart, spleen, lung, pancreas, liver, kidney, blood and brain. Organs were harvested after either the animal had succumbed to GD toxicity or upon completion of the 6 hour study duration. Recovery from within the systemic circulation was determined from the final blood sample taken prior to the end of each study.

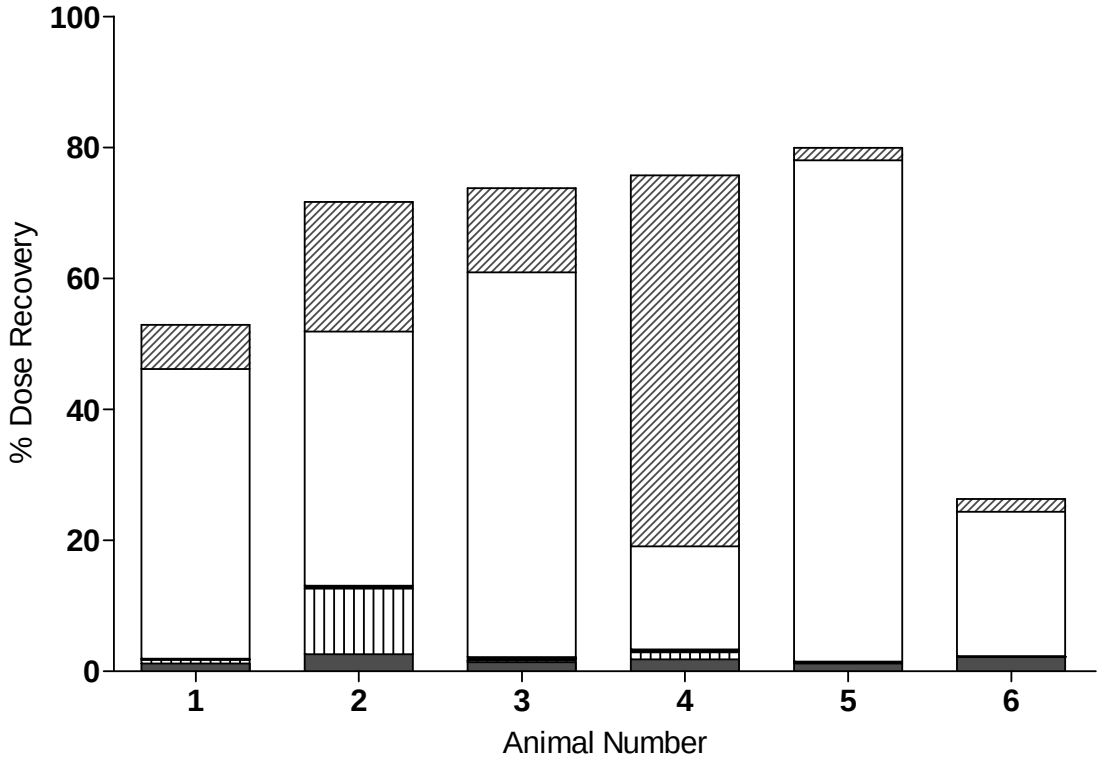

Figure 5.4: ^{14}C-GD distribution for individual animals after a 0.3 mg.kg^{-1} damaged ear skin exposure, expressed as percentage of the applied dose. Sampled compartments were: ▨ GD remaining on damaged skin surface, □ GD present with the skin directly under the dosing site, ■ GD present within the skin adjacent to the dosing site, ◫ GD absorbed into the dosing assembly and ■ GD recovered from sampled organs (detailed in Figure 5.3). Compartments were sampled after either the animal had succumbed to GD toxicity or upon completion of the 6 hour study duration.

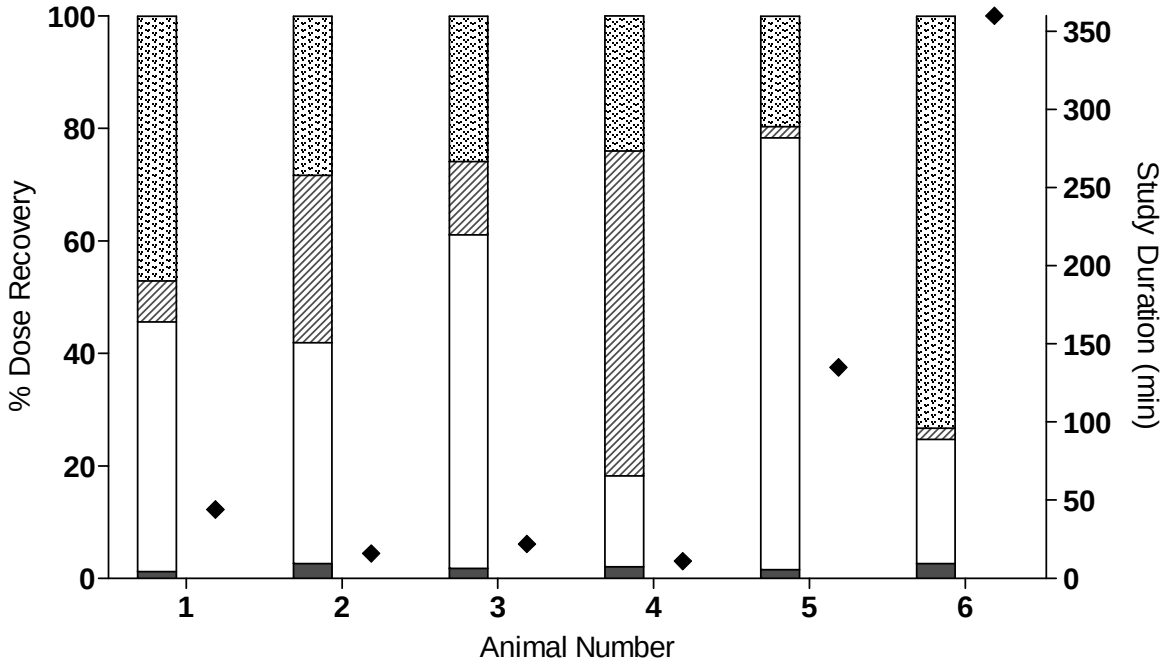

Figure 5.5: ^{14}C-GD distribution for individual animals after a 0.3 mg.kg^{-1} damaged ear skin exposure, expressed as percentage of the applied dose. Sampled compartments were: ▨ unabsorbed GD, □ locally recovered GD and ■ systemically recovered GD. The compartment, ⁙ "unaccounted" was taken as being 100 - the total measured recovery. A full description of the sampled locations contributing to each compartment is given in Table 5.6. Study duration (◆) is displayed on the secondary y axis to relate the time taken for each animal to succumb to GD toxicity to compartment recoveries.

5.3.3. Efficacy of a haemostatic decontaminant candidate *in vivo*

Data collecting included observed signs, monitored physiological signs, total blood cholinesterase and radiological analysis. Together these gave a broad assessment of the efficacy of the haemostatic decontaminant against percutaneous GD poisoning through damaged skin in the large white pig. Animal usage for the study comprised a total of 18 animals; 6 negative controls (no GD challenge, no treatment), 6 positive controls (GD challenge, no haemostat treatment) and 6 treatment animals (GD challenge, haemostat treatment). All animals were weighed prior to study commencement to enable determination of the GD challenge (Figure 5.6). The 6 negative control animals were the same animals used for comparison in the dose ranging study.

5.3.3.1. Distribution of GD in treated and untreated pigs

The direct quantification of localisation of radioactivity was quantified externally, locally and internally (Figure 5.7) with internal localisation broken down by organ type (Figure 5.8). For the untreated group, the majority of recovered radioactivity was located either on the skin surface or within the skin at the dosing site with a smaller portion of radioactivity recovered from the periphery of the dosing site. Internal recovery was approximately 1.75% of the initially applied dose. For the Woundstat^{TM} treatment group, the majority of the radioactivity (approximately 70%) was sequestered by Woundstat^{TM}. Smaller portions of radioactivity were recovered from the skin surface or within the skin at the dosing site. As with the untreated group, a

small portion of radioactivity was recovered from the periphery of the dosing site. Internal recovery was approximately 1% of the initially applied dose for the treated animals.

5.3.3.2. Absorption kinetics of GD in treated and untreated pigs

The amount of ^{14}C-GD in pig blood was quantified at regular time points for the study duration of each animal (Figure 5.9). For both study groups the maximum amount of GD in the blood was measured within 10 minutes of GD challenge. By 20 minutes the amount of GD in the blood had halved and remained constant at this level for the study duration for the treatment group. In contrast, for the untreated group, the amount of GD in the blood steadily increased as the study progressed. The irregular, highly variable initial phases for each group can be primarily attributed to the study duration for each animal. Animals that succumbed to GD toxicity early in the time course had higher GD blood recoveries than for animals that either succumbed later or survived.

5.3.3.3. Whole blood cholinesterase in treated and untreated pigs

Whole blood cholinesterase did not significantly vary from the original cholinesterase value decrease in whole of 100% for the six hour study duration for the control group (Figure 5.10). In contrast, there was a rapid blood cholinesterase depletion for all GD poisoned animals. For the untreated animals, whole blood cholinesterase decreased to less than 5% of the original value by 15 minutes post contamination and remained

at this level until the onset of apnoea or until euthanisation. For the treatment group, whole blood cholinesterase levels decreased to less than 10% of the original value by 15 minutes post contamination and gradually decreased until the onset of apnoea or until euthanisation. Whole blood cholinesterase measurements and the amount of ^{14}C-GD in the blood determined at the same time point were plotted to show the effect of nerve agent blood concentration on whole blood cholinesterase (Figure 5.11). A non linear regression least squares fit analysis was used to curve fit the data.

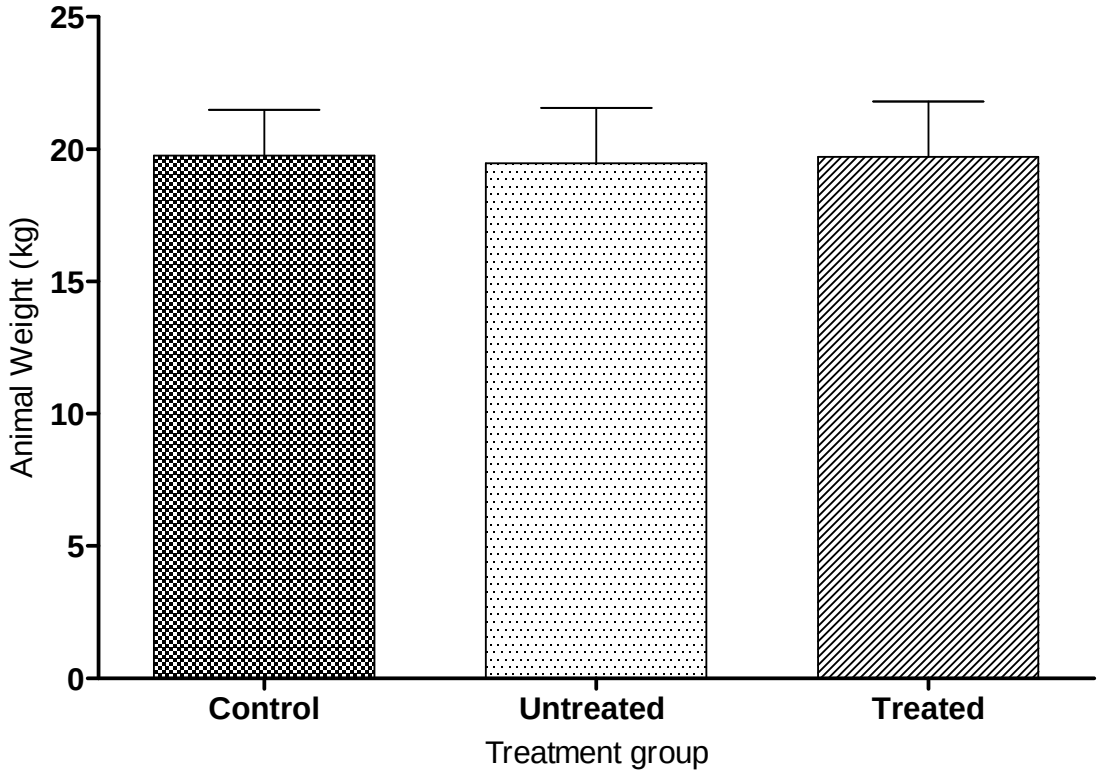

Figure 5.6: Animal weights taken immediately prior to study commencement. All groups comprised 6 animals with the untreated and treated animals receiving a 0.3 $mg.kg^{-1}$ GD challenge onto damaged ear skin. The treated animal group received Woundstat^{TM} treatment at 30 seconds post GD contamination. All values are mean ± standard deviation of n=6 animals.

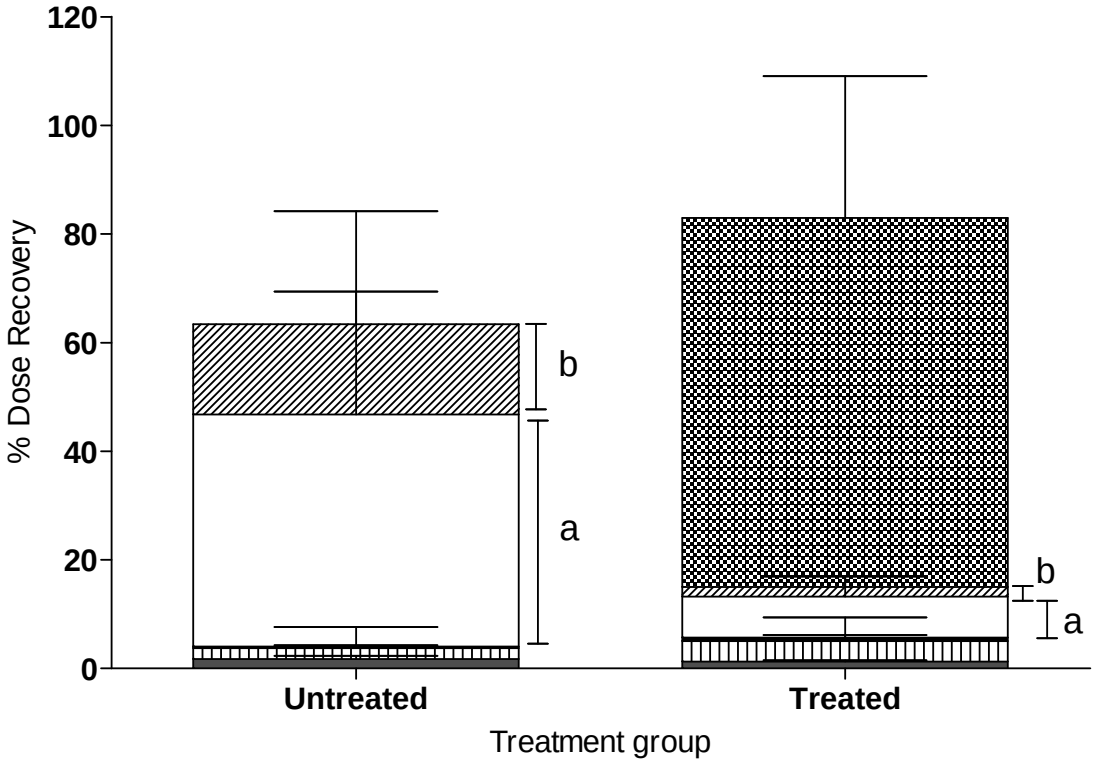

Figure 5.7: ^{14}C-GD distribution for Woundstat^{TM} treated and untreated animals after a 0.3 mg.kg^{-1} damaged ear skin exposure, expressed as percentage of the applied dose. Sampled compartments were: ▩ Woundstat^{TM} sequestered (treated animals only), ▨ GD remaining on damaged skin surface, □ GD present with the skin directly under the dosing site, ■ GD present within the skin adjacent to the dosing site, ◫ GD absorbed into the dosing assembly and ■ GD recovered from sampled organs (detailed in Figure 5.8). All values are mean ± standard deviation of n=6 animals. Compartments were sampled after either the animal had succumbed to GD toxicity or upon completion of the 6 hour study duration. Statistical significance between same labelled paramaters is indicated.

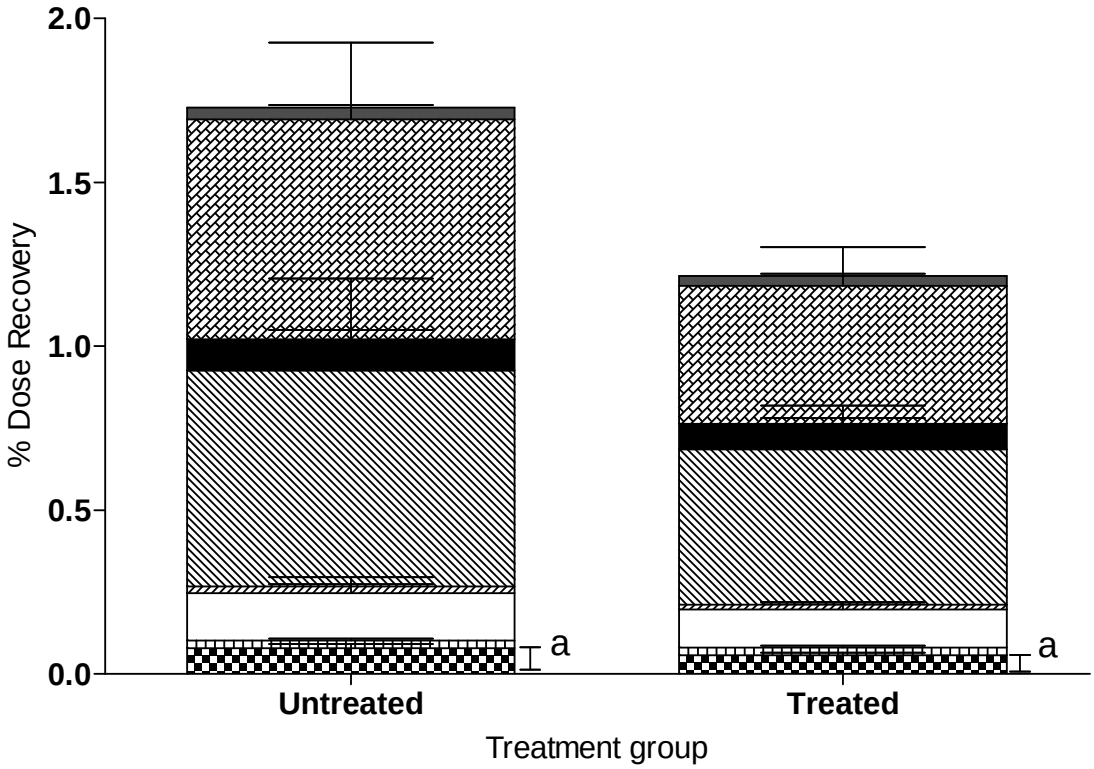

Figure 5.8: ^{14}C-GD internal organ distribution for Woundstat^{TM} treated and untreated animals after a 0.3 mg.kg^{-1} damaged ear skin exposure, expressed as percentage of the applied dose. Sampled internal organs were: ▩ heart, ◫ spleen, □ lung, ▨ pancreas, ▧ liver, ■ kidney, ▨ blood and ■ brain. Organs were harvested after either the animal had succumbed to GD toxicity or upon completion of the 6 hour study duration. Recovery from within the systemic circulation was determined from the final blood sample taken prior to the end of each study. All values are mean ± standard deviation of n=6 animals.Statistical significance between same labelled paramaters is indicated.

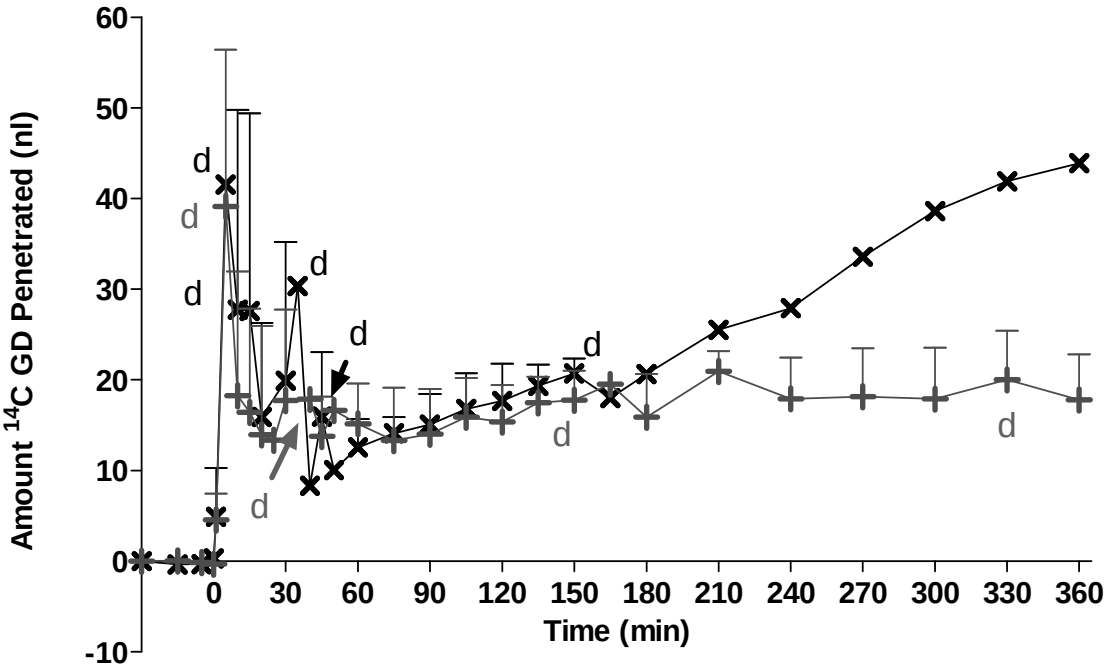

Figure 5.9: ^{14}C-GD penetration into the system circulation of the large white pig after application onto damaged ear skin for untreated (✕) and Woundstat™ treated (+) animals. One animal in the untreated group and two animals in the treated group survived for the maximum study duration of 6 hours. Those animals with larger amounts of ^{14}C-GD penetrated earlier in the time course succumbed to the toxic effects of GD within 45 minutes of challenge. Each animal received a GD dose at t=0 of 0.3 mg.kg^{-1}. All pre GD challenge values are mean ± standard deviation of n=6 animals which decreased as animals succumbed to GD toxicity over the study duration.

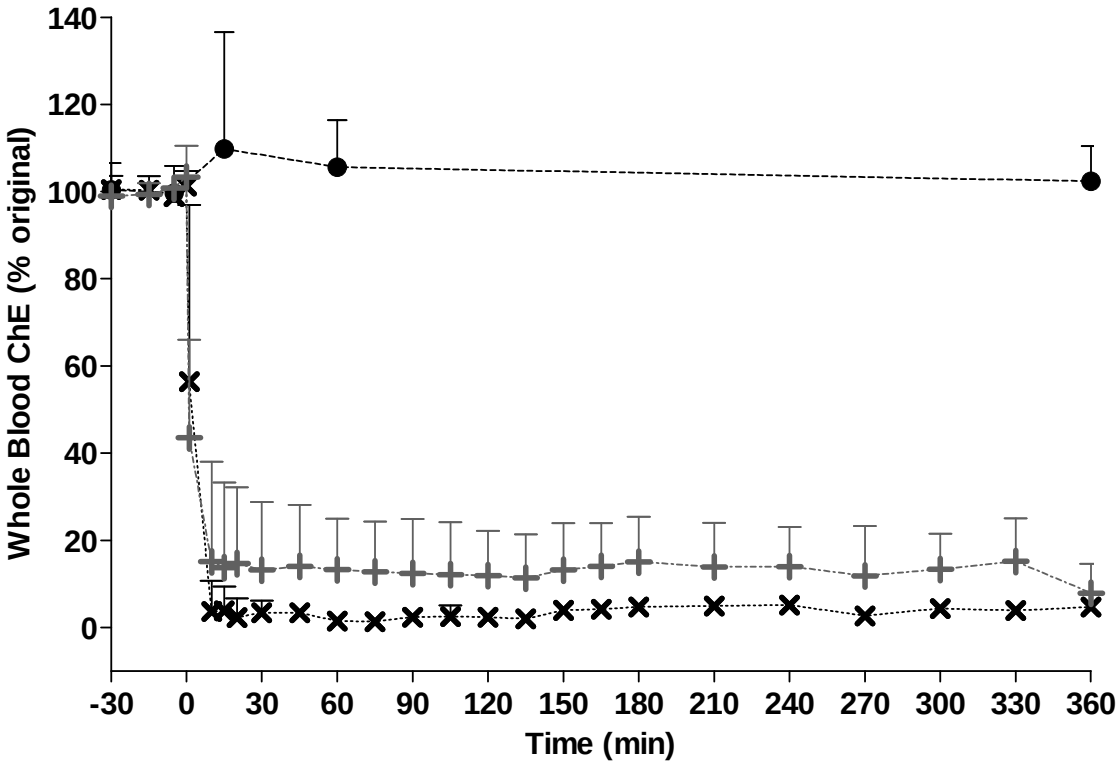

Figure 5.10: Total whole blood cholinesterase (ChE), shown as percentage of original (pre GD challenge) activity in anaeathetised pigs following damaged ear exposure to liquid GD. All values are mean ± standard deviation of up to 6 animals. All groups comprised 6 animals with the untreated (-✕-) and treated animals (-✚-) receiving a 0.3 mg.kg^{-1} GD challenge onto damaged ear skin. The treated animal group received Woundstat^{TM} treatment at 30 seconds post GD contamination. The control group (-●-) were not exposed to GD and did not receive treatment.

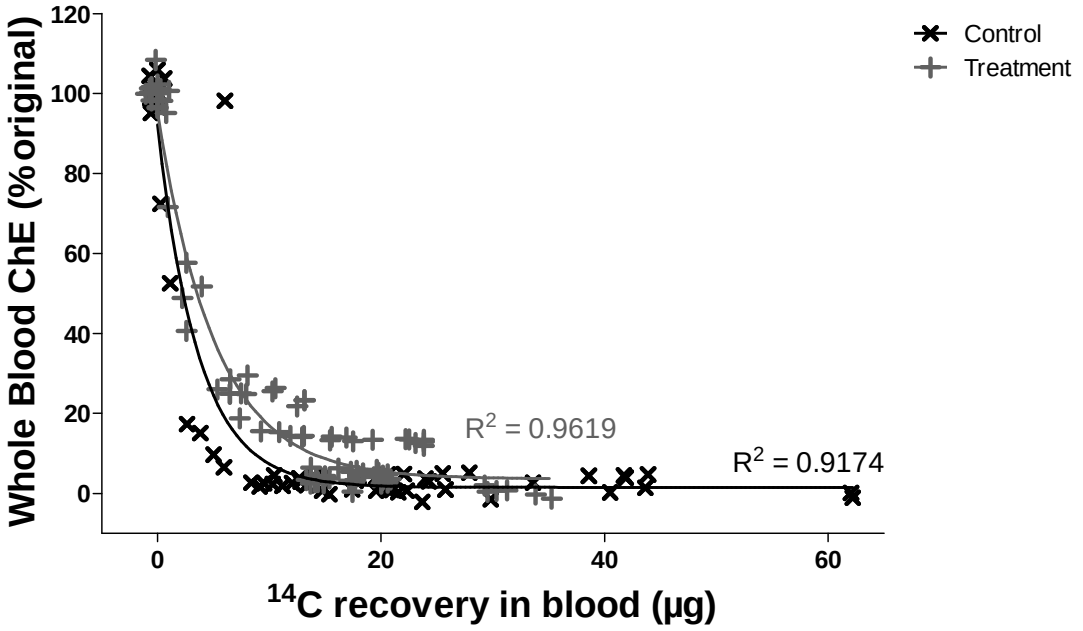

Figure 5.11: Comparison of whole blood cholinesterase (% of original) and the amount of ^{14}C-GD (or breakdown products) in the blood (determined from quantification of radiolabel) for untreated and Woundstat^{TM} treated animals. Each animal received a GD dose 0.3 mg.kg^{-1}onto damaged ear skin. A least squares fit non linear regression analysis was used to curve fit the data for each group.

5.3.3.4. Haematocrit

Haematocrit measurements taken from whole blood samples throughout each experimental time course (Figure 5.12) remained stable at 34 ± 2 % for control animals. For GD challenged animals, whether untreated or treated with Woundstat^{TM}, haematocrit values were elevated after exposure compared to pre exposure values and remained elevated for the study duration (Figure 5.13).

5.3.5.5. Physiological signs of GD poisoning

Observable clinical signs (miosis, mastication, fasiculations, tremor, convulsion, hypersalivation and apnoea) in each experimental group are shown in Table 5.7. One animal from the negative control group showed signs (mastication, fasciculation, hypersalivation), which could have been mistaken for mild GD poisoning. All animals from both the untreated and treated groups showed a number of observable signs (with similar times to onset), of GD poisoning. The differences between the untreated and treated groups were a lack of observable tremor / convulsions (Frequency treated group = 0; frequency untreated group =4) in the treated group. The frequency of mastication (treated 3; untreated 4), head / face / neck fasciculation (treated 5; untreated 6), limbs / rest of body fasciculation (treated 1; untreated 3), hypersalivation (treated 4; untreated 5) and apnoea (treated 6; untreated 4) was less in the treated group. Monitored physiological signs for each experimental group were pulse rate (Figure 5.14), blood pressure (Figure 5.15), exhaled CO_2 (Figure 5.16),

breathing rate (Figure 5.17), blood oxygenation (Figure 5.18) and core temperature (Figure 5.19). With the exception of core temperature (which declined over the study duration for GD poisoned animals), alterations of physiological parameters were linked to the onset of apnoea for each animal (Table 5.8). The combination of all observed and measured signs for each animal were categorised into an overall severity level of no effect, mild, severe or fatal (Figure 5.20). For all animals exposed to GD the assigned severity level was either severe or fatal. Where effects resulted in fatality, time to death is shown (Figure 5.20). For each of the experimental groups, the average survival time and final whole blood cholinesterase values were plotted for comparison (Figure 5.21).

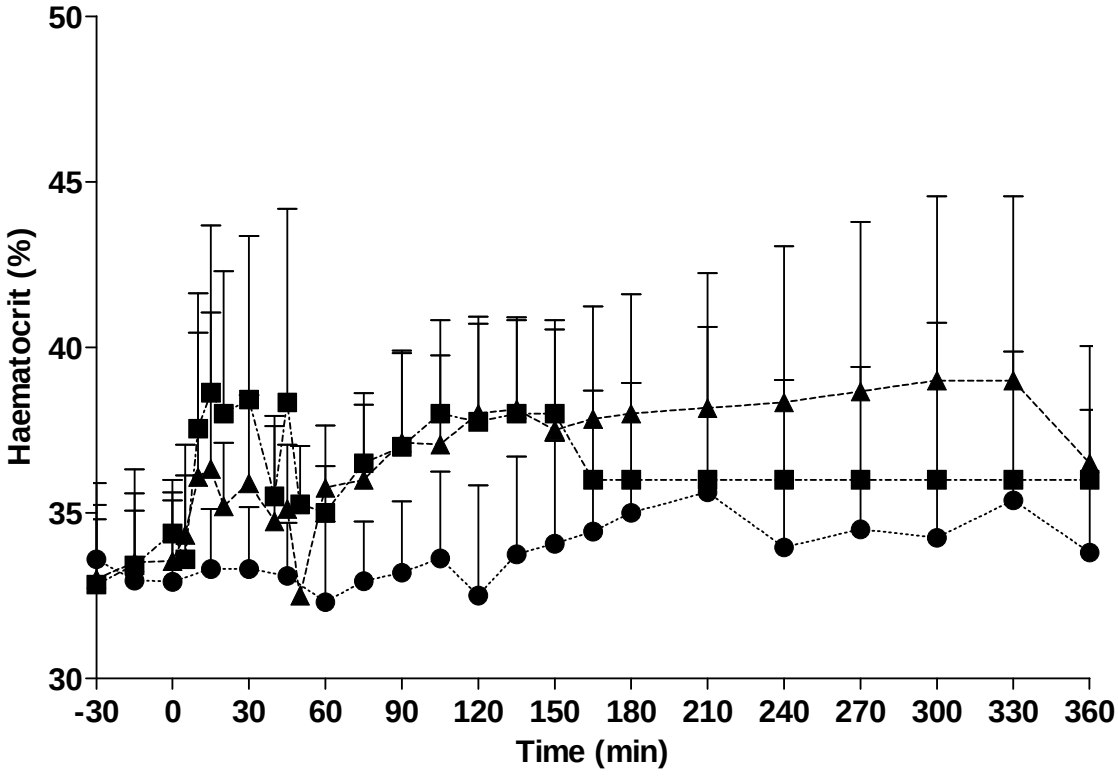

Figure 5.12: Total whole blood haematocrit (%) in anaesthetised pigs following damaged ear exposure to liquid GD. All values are mean ± standard deviation of up to 6 animals. All groups comprised 6 animals with the untreated (-▲-) and treated animals (-■-) receiving a 0.3 $mg.kg^{-1}$ GD challenge onto damaged ear skin with measurements recorded until either the study duration (6 hours) or until an individual animal had succumbed to GD toxicity. The treated animal group received Woundstat^{TM} treatment at 30 seconds post GD contamination. The control group (-●-) were not exposed to GD and did not receive treatment.

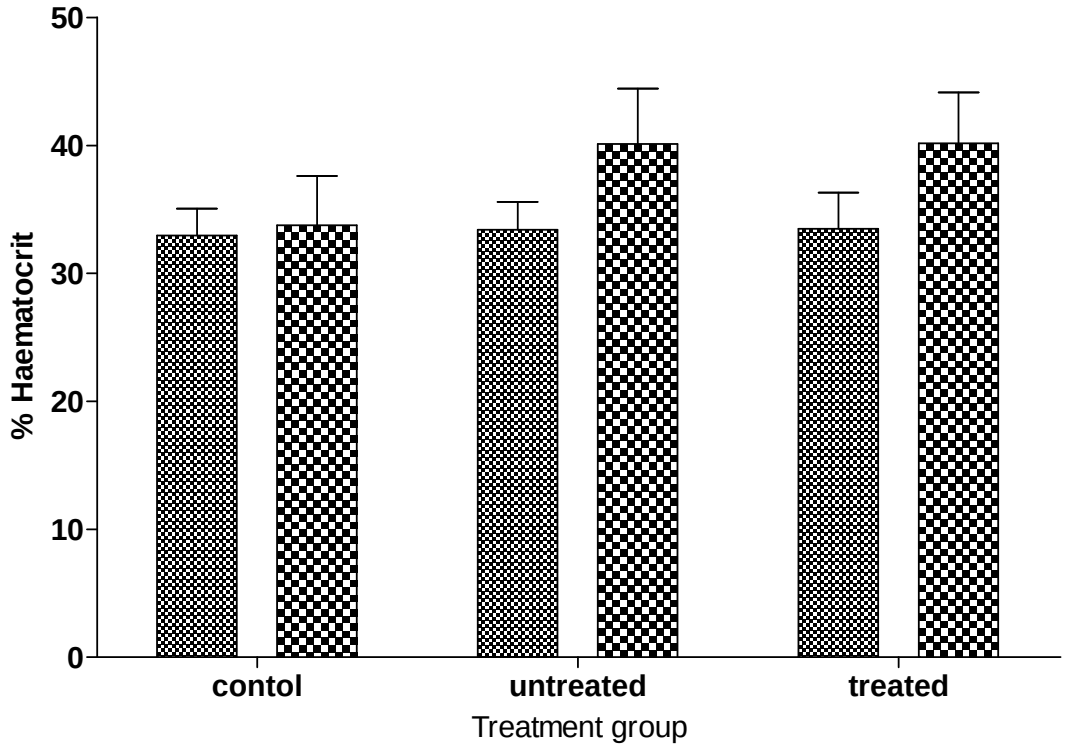

Figure 5.13: Total whole blood haematocrit (%) in anaesthetised pigs pre (▩) and post (▩) exposure to liquid GD onto damaged ear skin. Pre exposure values were taken immediately prior to GD exposure whilst the post exposure values were taken immediatley prior to either the animal succumbing to GD toxicity or upon completion of the 6 hour study duration. The treated animal group received Woundstat^{TM} treatment at 30 seconds post GD contamination. The control group were not exposed to GD and did not receive treatment.All values are mean ± standard deviation of 6 animals.

		Control	Untreated	Treated
Miosis	Frequency Time to onset (min)	0 N/A	2 25 ± 18	4 71 ± 126
Mastication	Frequency Time to onset (min)	1 42	4 6 ± 1	3 7 ± 3
Fasiculation (head/face/neck)	Frequency Time to onset (min)	0 N/A	6 7 ± 9	5 11 ± 12
Fasiculation (limbs and rest of body)	Frequency Time to onset (min)	1 21	3 6 ± 1	1 13
Tremor / Convulsion	Frequency Time to onset (min)	0 N/A	3 33 ± 38	0 N/A
Hypersalivation	Frequency Amount (g)	1 3.84	5 19.4 ± 19.9	4 22.6 ± 18.4
Apnoea	Frequency Time to onset (min)	0 N/A	6 80 ± 101	4 127 ± 153

Table 5.7: Observed signs of GD poisoning in the anaesthetised large white pig for the three experimental groups (Control (no GD, no treatment), Untreated (GD, no treatment), Treated (GD with Woundstat^{TM} treatment 30 seconds post GD application). Each group contained 6 animals, where, frequency is the number of animals in the group that displayed the observable sign with the either the time to onset of the sign or the amount of saliva produced. Values are mean ± standard deviation of the frequency of the occurrence.

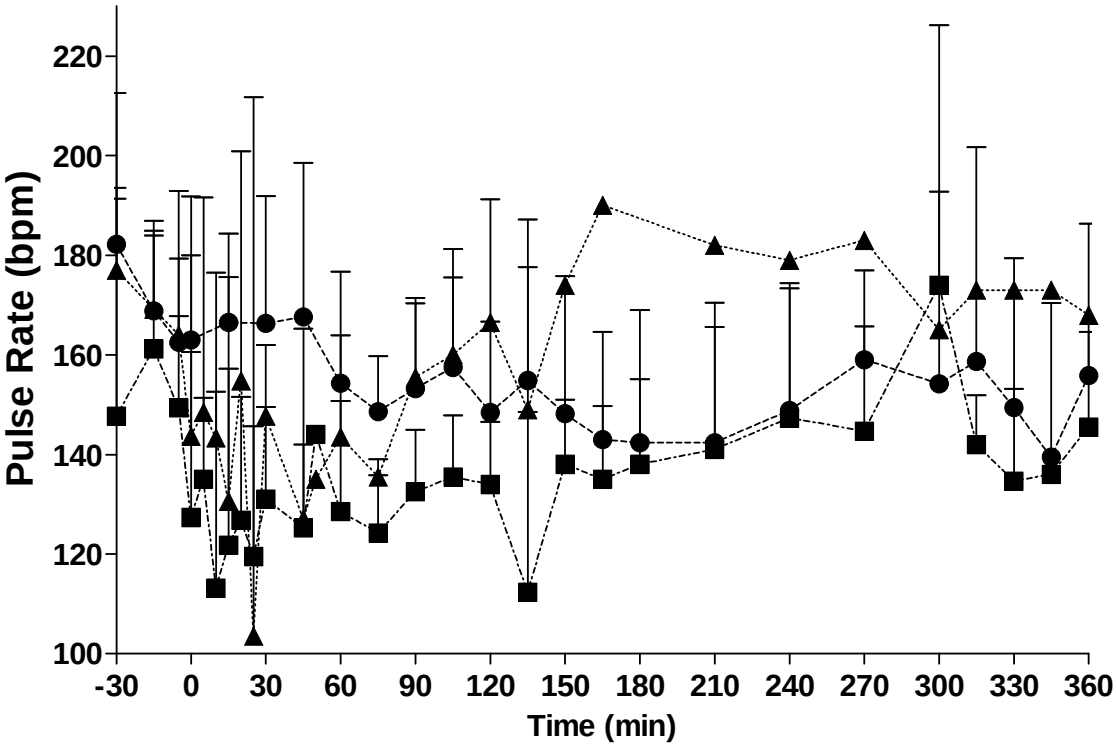

Figure 5.14: Pulse Rate (beats per minute, bpm), in anaesthetised pigs following damaged ear exposure to liquid GD. All values are mean ± standard deviation of up to 6 animals. All groups comprised 6 animals with the untreated (▲) and treated animals (■) receiving a 0.3 $mg.kg^{-1}$ GD challenge onto damaged ear skin with measurements recorded until either the study duration (6 hours) or until an individual animal had succumbed to GD toxicity. The treated animal group received Woundstat™ treatment at 30 seconds post GD contamination. The control group (●) were not exposed to GD and did not receive treatment.

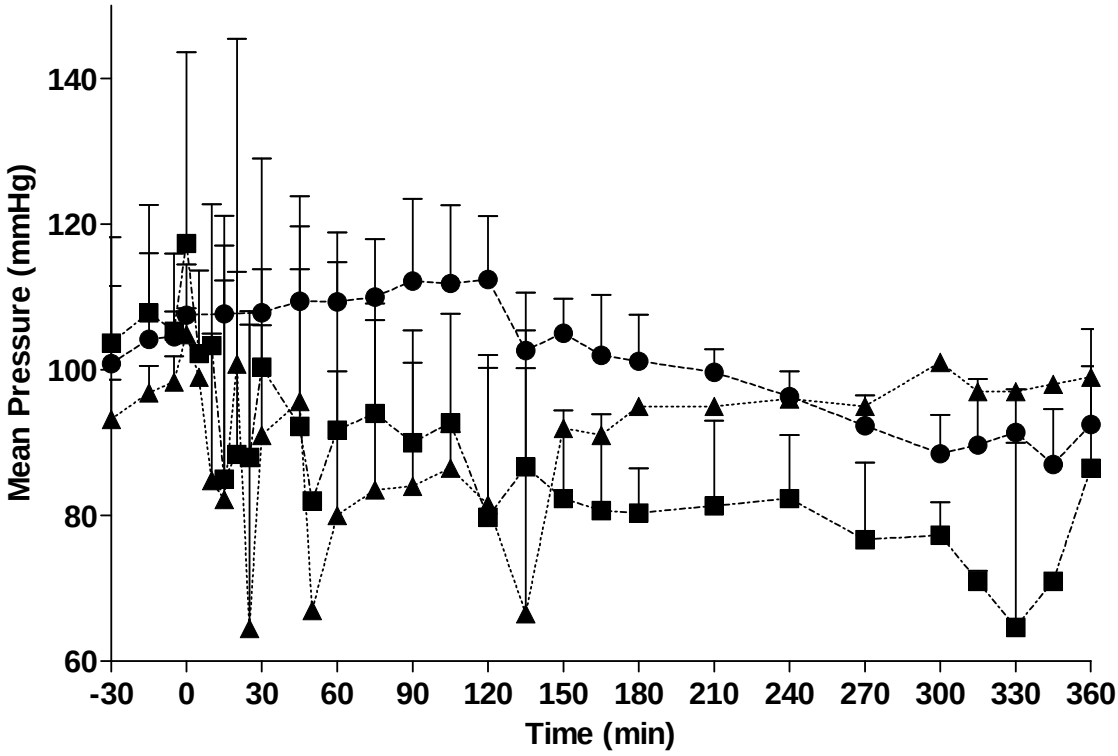

Figure 5.15: Mean arterial pressure (mmHg), in anaesthetised pigs following damaged ear exposure to liquid GD. All values are mean ± standard deviation of up to 6 animals. All groups comprised 6 animals with the untreated (···▲···) and treated animals (-■-) receiving a 0.3 $mg.kg^{-1}$ GD challenge onto damaged ear skin with measurements recorded until either the study duration (6 hours) or until an individual animal had succumbed to GD toxicity. The treated animal group received Woundstat^{TM} treatment at 30 seconds post GD contamination. The control group (-●-) were not exposed to GD and did not receive treatment.

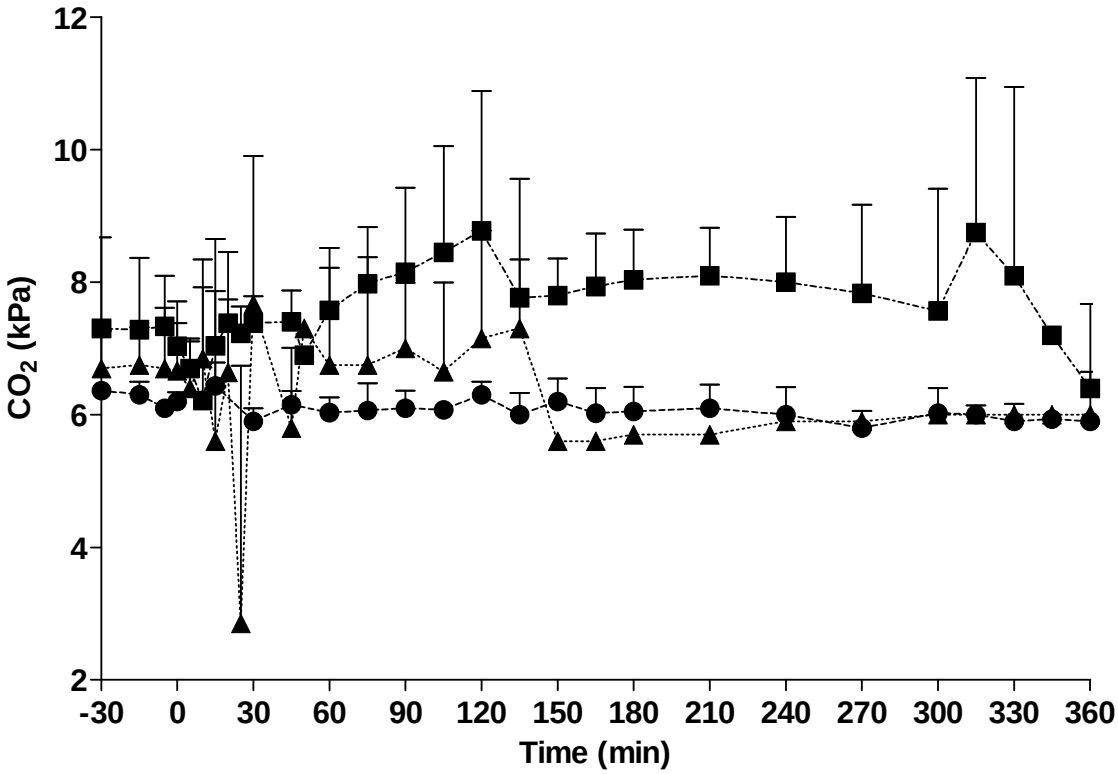

Figure 5.16: Carbon dioxide (kPa) in anaesthetised pigs following damaged ear exposure to liquid GD. All values are mean ± standard deviation of up to 6 animals. All groups comprised 6 animals with the untreated (▲) and treated animals (■) receiving a 0.3 $mg.kg^{-1}$ GD challenge onto damaged ear skin with measurements recorded until either the study duration (6 hours) or until an individual animal had succumbed to GD toxicity. The treated animal group received Woundstat™ treatment at 30 seconds post GD contamination. The control group (●) were not exposed to GD and did not receive treatment.

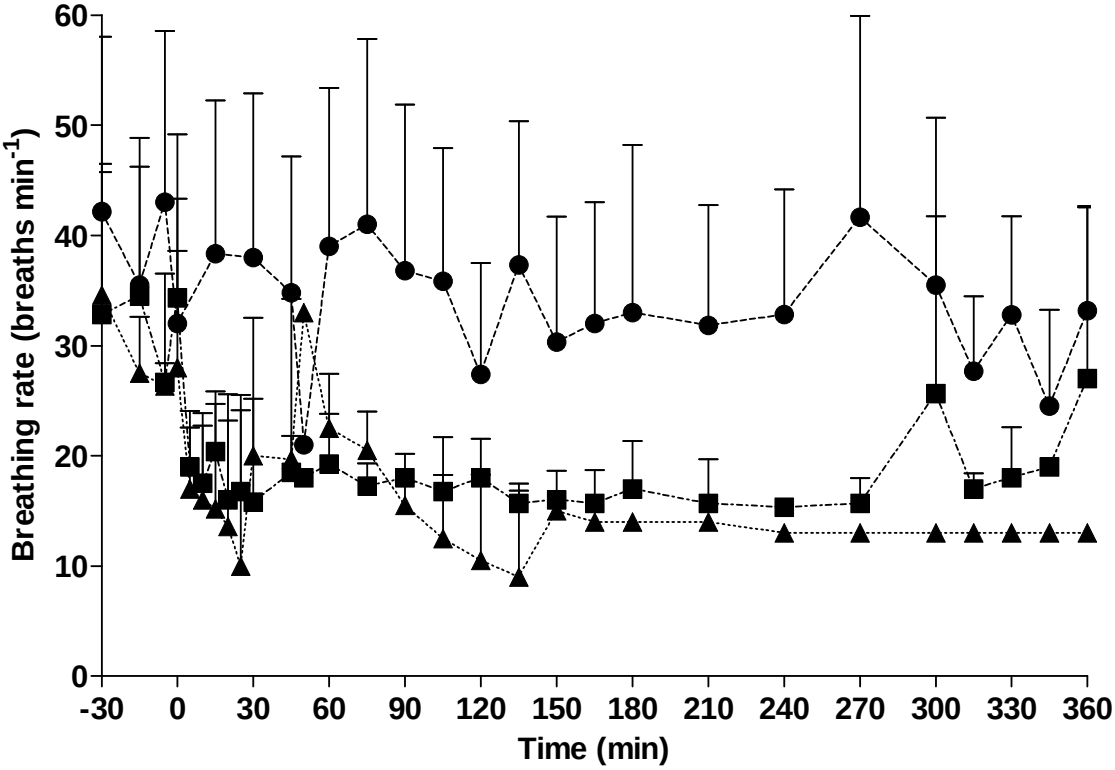

Figure 5.17: Breathing rate (breaths min^{-1}) in anaesthetised pigs following damaged ear exposure to liquid GD. All values are mean ± standard deviation of up to 6 animals. All groups comprised 6 animals with the untreated (▲) and treated animals (■) receiving a 0.3 $mg.kg^{-1}$ GD challenge onto damaged ear skin with measurements recorded until either the study duration (6 hours) or until an individual animal had succumbed to GD toxicity. The treated animal group received Woundstat™ treatment at 30 seconds post GD contamination. The control group (●) were not exposed to GD and did not receive treatment.

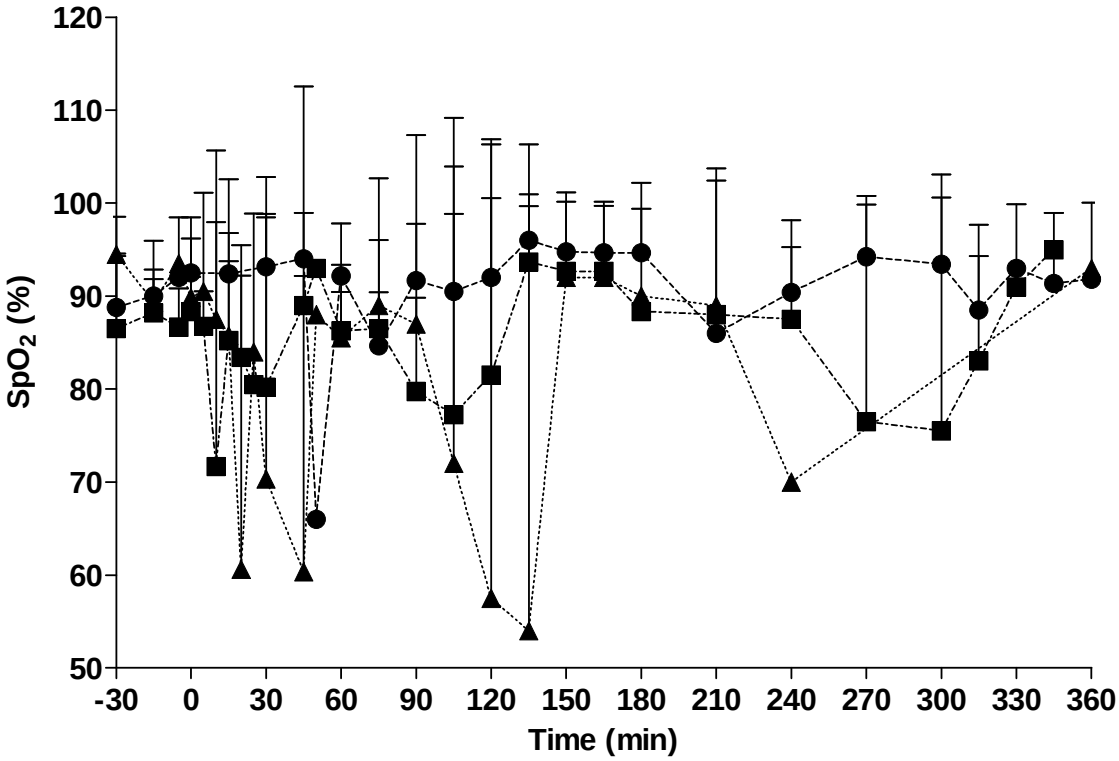

Figure 5.18: Percent oxygen saturation (SpO_2) in anaesthetised pigs following damaged ear exposure to liquid GD. All values are mean ± standard deviation of up to 6 animals. All groups comprised 6 animals with the untreated (▲) and treated animals (■) receiving a 0.3 $mg.kg^{-1}$ GD challenge onto damaged ear skin with measurements recorded until either the study duration (6 hours) or until an individual animal had succumbed to GD toxicity. The treated animal group received Woundstat™ treatment at 30 seconds post GD contamination. The control group (●) were not exposed to GD and did not receive treatment.

.

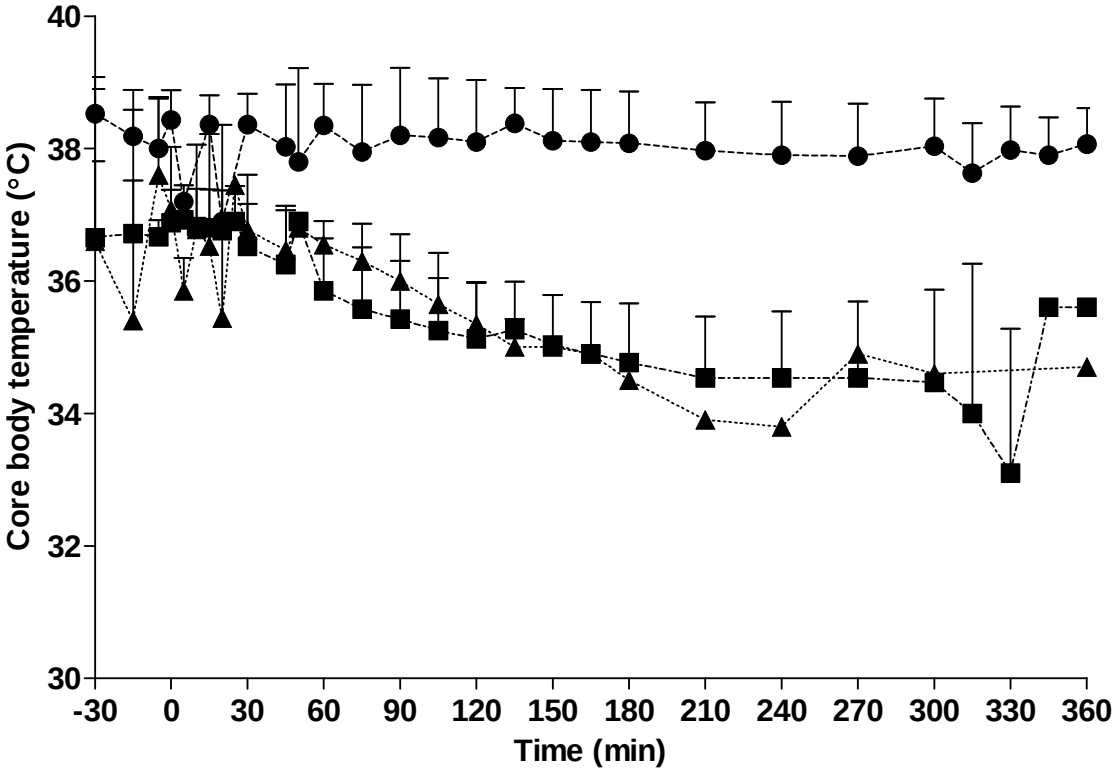

Figure 5.19: Core body temperature (°C) in anaesthetised pigs following damaged ear exposure to liquid GD. All values are mean ± standard deviation of up to 6 animals. All groups comprised 6 animals with the untreated (▲) and treated animals (■) receiving a 0.3 mg.kg^{-1} GD challenge onto damaged ear skin with measurements recorded until either the study duration (6 hours) or until an individual animal had succumbed to GD toxicity. The treated animal group received Woundstat^{TM} treatment at 30 seconds post GD contamination. The control group (●) were not exposed to GD and did not receive treatment.

		Control	Untreated	Treated
Pulse Rate	Pre exposure	163 ± 19	163 ± 30	146 ± 34
	End	156 ± 31	115 ± 71	130 ± 24
Systolic Pressure (mmHg)	Pre exposure	120 ± 9	113 ± 7	122 ± 18
	End	106 ± 10	88 ± 36	108 ± 40
Diastolic Pressure (mmHg)	Pre exposure	93 ± 7	84 ± 7	93 ± 15
	End	79 ± 9	51 ± 36	70 ± 38
Mean Pressure (mmHg)	Pre exposure	107 ± 6*	99 ± 6	109 ± 18
	End	93 ± 8*	65 ± 38	87 ± 39
CO_2 (kPa)	Pre exposure	6.2 ± 0.1	6.7 ± 0.6	7.2 ± 1.0
	End	5.9 ± 0.7	4.6 ± 3.7	7.5 ± 3.7
Breathing Rate (min^{-1})	Pre exposure	36 ± 13	29 ± 9*	33 ± 13*
	End	33 ± 9	6 ± 5*	17 ± 12*
SpO_2 (%)	Pre exposure	93 ± 3	91 ± 7*	88 ± 5
	End	92 ± 7	46 ± 40*	61 ± 36
Body Temperature (℃)	Pre exposure	38.2± 0.6	36.5 ± 2.2	36.7 ± 0.8*
	End	38.1± 0.5	36.6 ± 1.5	34.4 ± 2.2*

Table 5.8: Monitored physiological signs in pigs during steady state anaesthesia both pre GD exposure and at the end of the study (immediately preceding apnoea or euthanisation) for the three experimental groups (Control (no GD, no treatment), Untreated (GD, no treatment), Treated (GD with Woundstat^{TM} treatment 30 seconds post GD application). Values are mean ± standard deviation of n=6 animals. Statistical significance between values is indicated (*) between pre exposure and end of study results.

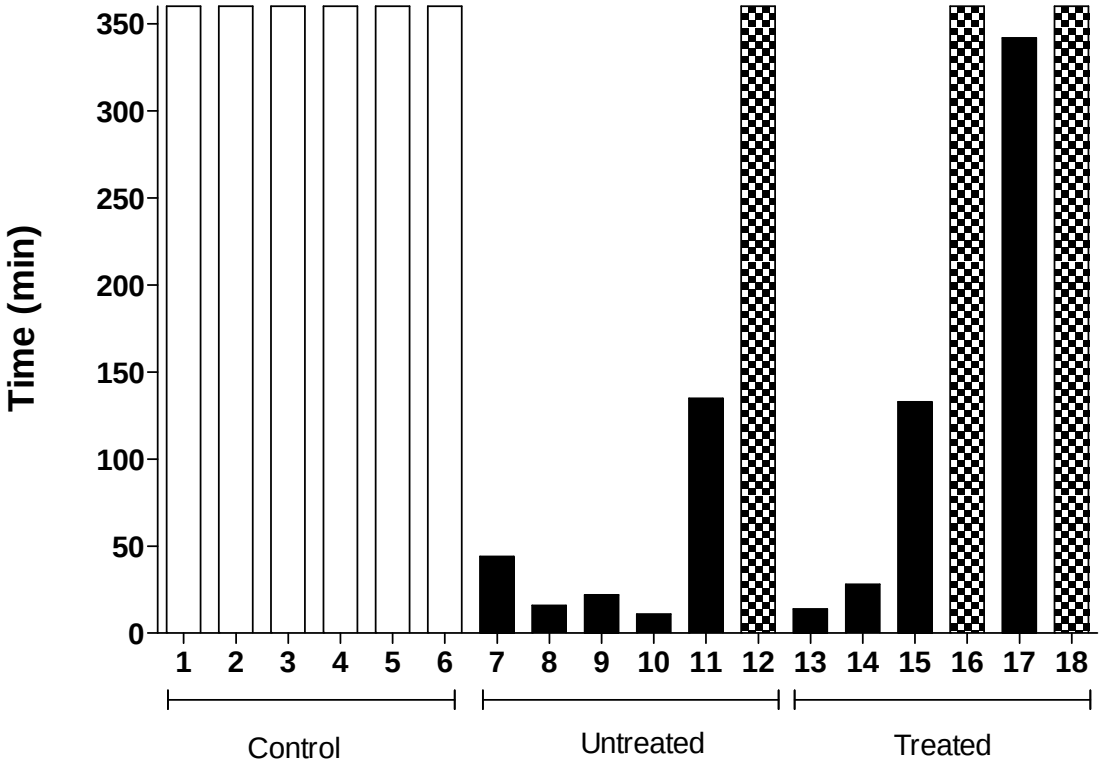

Figure 5.20: Survival time for individual animals in each study group All groups comprised 6 animals with the untreated and treated animals receiving a 0.3 $mg.kg^{-1}$GD challenge onto damaged ear skin. The treated animal group received Woundstat™ treatment at 30 seconds post GD contamination. The control group were not exposed to GD and did not receive treatment. Physiological effects were ranked according to severity and assigned as no effect (□), mild (▨), severe (▩) and fatal (■).

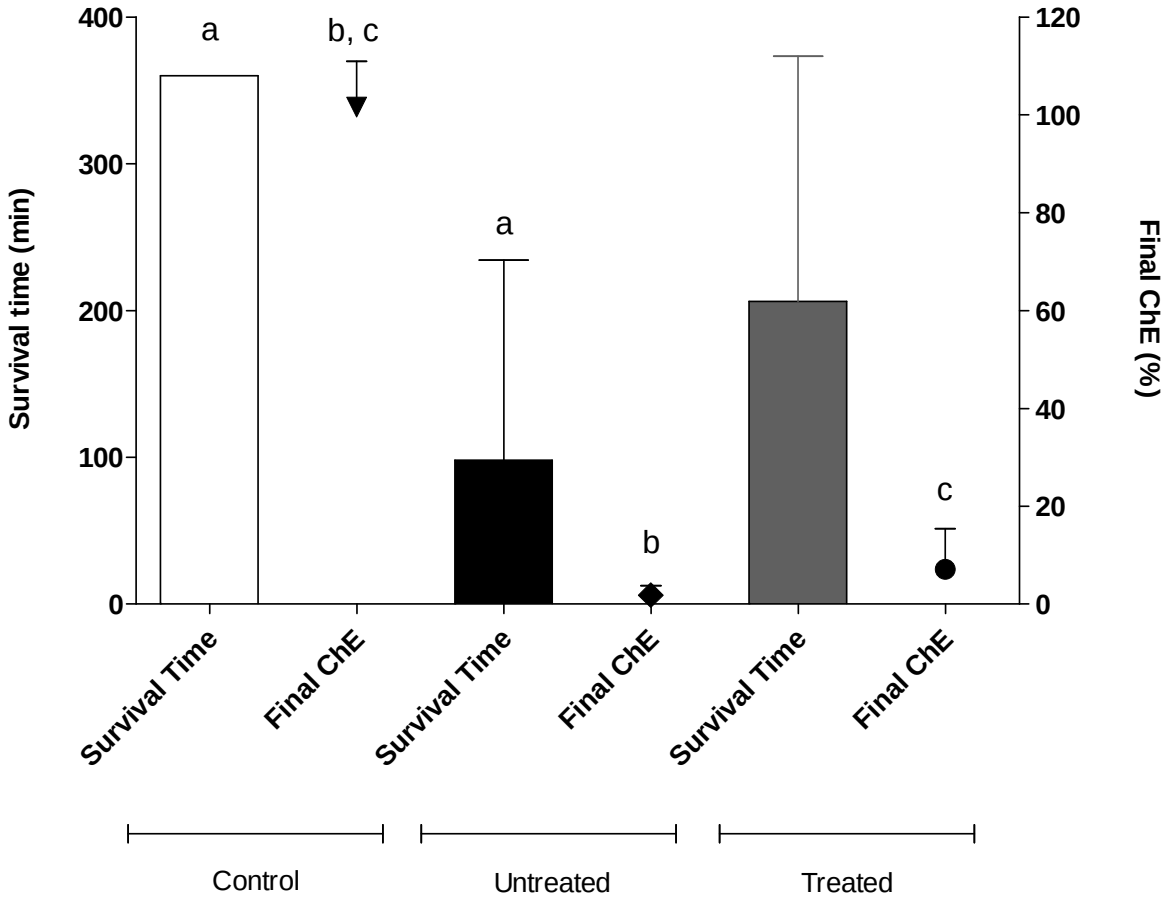

Figure 5.21: Comparison of survival time (min) and final ChE activity for each study group. Values are mean ± standared deviation of n=6 animals.All groups comprised 6 animals with the untreated and treated animals receiving a 0.3 $mg.kg^{-1}$GD challenge onto damaged ear skin. The treated animal group received Woundstat^{TM} treatment at 30 seconds post GD contamination. The control group were not exposed to GD and did not receive treatment. Statistical significance between same labelled paramaters is indicated.

5.4. Discussion

All *in vivo* work was conducted used a terminally anaesthetised large white pig model, with the GD challenge, were appropriate, applied to the ear of the animal. This model and dosing site has been previously used for the assessment of countermeasures against nerve agents (Chilcott, et al., 2005c;Duncan, et al., 2002). In contrast to previous studies, the skin was damaged to allow a more rapid ingress of chemical warfare agent, as the likely mode of use of a haemostatic decontaminant would be application to damaged skin. Although the skin was damaged, this series of studies did not evaluate efficacy of the haemostat in a contaminated haemorrhaging model of injury. The haemorrhaging model was evaluated in subsequent studies at the United States Army Medical Research Institute of Chemical Defense (USAMRICD). The model described in this chapter may be described as a contaminated injury model. For the initial *in vivo* studies with the selected haemostat this methodology was used to enable a rigorous test of the haemostats decontaminating ability as opposed to its haemostatic ability.

5.4.1. Clinical manifestations of GD poisoning

The use of animals to acquire clinical information that may be relevant to human exposures necessitates that the chosen animal species is relevant. In the case of exposure to nerve agents, the guinea pig has been used previously as it gives a comparable physiological response to humans. There are a number of drawbacks associated with the guinea pig for dermal exposure assessment after nerve agent

poisoning including differences in skin absorption rates (Dalton, et al., 2006a) and difficulties associated with dosing small volumes of nerve agent (due to the guinea pigs size) which often requires the dilution of the nerve agent in a solvent vehicle (Murnford and Troyer, 2011). Vehicle effects have been shown to influence skin penetration rates (Baynes, et al., 1997;Mills, 2007) meaning that the researcher must bear this in mind when considering solvent choice. The pig has neither of these potential drawbacks and is generally accepted to be the most suitable model for human skin absorption (Simon and Maibach, 2000). The pigs' larger size means that nerve agents can be easily applied without the need for dilution in solvent.

The current study considered an application of GD onto damaged pig ear skin in a terminally anaesthetised animal. Differences in permeability have been previously shown between application sites for nerve agent percutaneous absorption studies (Duncan, et al., 2002), however, as GD deposition was onto damaged skin for the current study, it is likely that these differences would be less marked than for an undamaged skin percutaneous exposure.

A total of four challenge doses (3 $\mu l.kg^{-1}$, 1 $\mu l.kg^{-1}$, 0.75 $\mu l.kg^{-1}$ and 0.3$\mu l.kg^{-1}$) were used. The upper dose was based on previous percutaneous LD_{50} determinations on undamaged skin (Knezevic, et al., 1993), whilst the lowest challenge was evaluated for the observed 10 fold difference between damaged and undamaged skin penetration in vitro (Dalton, et al., 2010). However, the data indicated that of the

doses of GD applied to damaged pig ear skin there was no easily definable dose response relationship between the challenge levels and it can be inferred that a challenge dose of 0.3µl.kg^{-1} or above of GD applied onto damaged pig ear skin will give severe clinical manifestations of GD poisoning within a six hour time frame. Instead, “time to death” was used as a marker to normalise the chronology of events in the clinical manifestations of GD poisoning. Early signs of GD poisoning included mastication, fasiculations and tremor. Intermediate signs included miosis, salivation and nasal secretions. Late onset effects (just prior to apnoea) included lacrimation and body spasm. All of these gross clinical signs occurred concurrently with a measured rapid depletion of whole blood cholinesterase levels. Recent work determining inhibition of cholinesterase in blood following intra muscular injection in guinea pigs (Bajgar, et al., 2011) showed a remarkably similar cholinesterase depletion profile for an LD_{50} dose of GD and indicates that application of GD onto damaged skin is more akin to an intramuscular challenge rather than a percutaneous challenge.

In clinical practice, suspected exposure to organophosphate cholinesterase inhibitors may be confirmed and the extent of exposure quantified through the measurement of plasma and / or erythrocyte cholinesterase activities. Whole blood cholinesterase assessment as measured in the current study allowed the contribution of cholinesterase depletion in both fractions to be rapidly measured and required a minimum of sample preparation. Although cholinesterase determinations are routinely made for patients presenting with signs and symptoms of nerve agent

poisoning (Evison, et al., 2002), the current study has shown that although rapid depletion of whole blood cholinesterase (to less than 5% of pre soman application values) did indicate nerve agent poisoning, final clinical outcome for each animal could not be correlated with the decrease in whole blood cholinesterase. This finding is in agreement with previous work that has shown that in the case of nerve agent exposures, cholinesterase activity should only be deemed an indicator of poisoning, not a prognostic aid (Chilcott, et al., 2003). Whole blood cholinesterase measurement is used as a surrogate for AChE measurement within the nervous system. As the action of GD on AChE in the central nervous system defines final clinical outcome it must be reiterated that whole blood ChE gives only an indication of what inhibition may occur for central nervous system AChE.

The current study indicated that a number of haematological and blood biochemistry parameters were elevated after GD exposure including carbon dioxide, potassium, glucose, lactate and haematocrit and haemoglobin. Conversely, a number of parameters were lower than controls including pO_2 and O_2Hb. Previous work using swine has shown that percutaneous exposure to high doses of GD (15.8 mg kg^{-1} (Hanford miniature swine) and 25 mg kg^{-1} (Chester White / Yorkshire cross swine)) caused hyperglycemia in swine that survived for more than 2 hours (James, et al., 1987). Work evaluating biochemical changes in rats following soman intoxication has also shown elevation of glucose concentrations (Jovic, 1974). The current study was in agreement with these findings with elevated levels of glucose shown for those animals surviving for more than 2 hours. It has been previously postulated that

hyperglycaemia may be attributed to a failure of the peripheral tissues to respond to insulin (James, et al., 1987). In reported human cases of acetylcholinesterase poisoning, hyperglycaemia has been observed (Meller, et al., 1981). However, previous work assessing the percutaneous absorption of the nerve agent VX showed that VX did not significantly affect glucose utilisation in the pig (Chilcott, et al., 2003). Although rare, cases of accidental human poisoning with nerve agents have been reported (Sidell, 1974). In contrast to the current study, blood parameters such as haematocrit, haemoglobin, calcium, potassium and carbon dioxide were all within normal limits for the accidental human poisoning case study, although, it should be noted that the patient made a full recovery. The elevated haematocrit and haemoglobin levels observed in the current study may be due to dehydration caused by excessive salivation whilst the increased carbon dioxide, potassium and lactate levels may be ascribed to major organ dysfunction caused by soman intoxication. Studies (Chapter 3) using pig blood contaminated with GD *in vitro* indicated that GD had a pro haemostatic effect. Samples analysed using the same methodology but from samples withdrawn after GD application *in vivo* did not replicate the *in vitro* result. Obviously the concentration of GD in the blood samples between the two methods varied enormously and it may be concluded that a pro haemostatic effect is only produced in blood contaminated with large concentrations of GD.

In the case of nerve agent intoxication, given that cholinesterase monitoring can only be used to give a broad indication of the severity and not as a prognostic indicator, it has previously been stated that the principle should be to treat the patient not the

depression of the cholinesterase (Evison, et al., 2002). Detailed accounts on the medical management of nerve agent casualties are available in Chapter 1 of this thesis.

In summary, after application of GD onto damaged pig ear skin, the onset of clinical manifestations was rapid leading to a number of fatalities within 15 minutes of exposure. Whole blood cholinesterase inhibition was similarly rapid with 95% inhibition of pre GD exposure values within 5 minutes of exposure. Measurable changes in blood parameters, notably haematocrit and blood glucose, were observed.

5.4.2. *In vivo* damaged skin absorption and distribution of GD in the domestic white pig

This study has shown that ^{14}C-GD (0.3 mg.kg^{-1}) penetrated though damaged pig ear skin *in vivo* and entered the systemic circulation at an apparent rate of 37 ± 12 µg.h^{-1}. This value is not dissimilar to a value obtained for *in vivo* undamaged cat skin penetration of 16.2 µg.cm^{-2}.h^{-1} (Fredriksson, 1969b). Fredriksson noted, for his study, that the value obtained denoted only the absorption of active soman into the blood stream from the topical deposit and did not take into account any detoxification processes (such as hydrolysis (Fredriksson, 1969a)) that may have occurred in the skin. It was postulated that the real value might be considerably higher. Similarly, the

current study, using ^{14}C radiolabel, does not discriminate against soman and any breakdown products (as it is radiolabel that has been quantified and not soman itself).

The value of 37 ± 12 $\mu g.h^{-1}$ potentially underestimates the skin penetration rate of ^{14}C-GD as it is an equilibrium value between the amount penetrating into the blood and the amount being removed from the blood into internal organs. Another method to determine the penetration rate from *in vivo* radiometric data is to consider the amount of radiolabel within the internal organs and blood at the culmination of a study as described by Chilcott and Dalton (Chilcott, et al., 2005c). Using this methodology, a derived penetration rate of 287 ± 120 $\mu g.h^{-1}$ was obtained. However, this is also likely to be an underestimate as lag time (assumed to be negligible for damaged skin) along with radioactivity present in unsampled organs (such as the digestive system, fat and muscle) are not taken into account. Due to the premature deaths in the majority of animals, apparent penetration rates were determined between different time points for each animal, generally between 15 and 60 minutes, (unless death occurred earlier).

In vitro static diffusion cell systems (Franz, 1975;Friend, 1992), have been used extensively for the determination of skin penetration rates of numerous chemicals, including chemical warfare agents (Chilcott, et al., 2000;Chilcott, et al., 2001;Dalton, et al., 2006a). A previous study, using damaged pig skin gave a direct measure of

penetration rate for ^{14}C GD of 337 ± 107 µg cm^{-2} h^{-1} (Dalton, et al., 2010). This *in vitro* value is free from potential artefacts such as metabolism and distribution to unsampled organs. Given that the derived *in vivo* value does not take unsampled organs into account, it is not surprising that this value is slightly lower than the *in vitro* value. Comparison of the *in vitro* and *in vivo* studies shows that the derived penetration rate of GD into the blood was 287 ± 120 µg.h^{-1} whilst the *in vitro* penetration rate was 337 ± 107 µg cm^{-2} h^{-1}. The maximum absorptive area *in vivo* was assessed as having been up to 3.14 cm^{2}, although the rapid ingress of GD, applied as a single droplet, through the damaged skin site likely indicates that the area of penetration was much less than this. Difference between the *in vitro* and *in vivo* value can be ascribed to unsampled organs and / or lack of knowledge regarding the exact skin surface spread area of GD *in vivo*.

The concentration of ^{14}C-GD in blood increased over the time course of each study (with the exception of animal 1 which appeared to have received a bolus dose. Explanation for this may be due to more rapid blood organ partitioning or due to a reduction in partitioning from the skin into the peripheral circulation). In the case of those animals succumbing to the toxic effects of GD more rapidly, the concentrations of ^{14}C-GD where generally higher earlier than for those animals that survived for longer. This observation means that initial concentrations of GD in the systemic circulation could be used as an indicator of likely final clinical outcome. That ^{14}C-GD concentrations increased throughout each study indicates that there was not a complete depletion of surface ^{14}C-GD (or that the agent was rapidly absorbed into

the surface layers and continued to be delivered to the circulation from there) during the study and that the systemic circulation had not become saturated with ^{14}C-GD.

Previous studies (Chilcott, et al., 2005c) using an *in vivo* pig ear skin model (albeit not damaged) have shown the penetration rate of VX (a nerve agent of lower volatility) to be approximately 512 µg cm^2 h^{-1} (taking into account distribution into sampled organs). It is interesting to note that the rate of penetration of VX though undamaged skin was higher than GD through damaged skin using a similar animal model. The volatilities of these nerve agents differ substantially (GD has a volatility of 3900 mg m^{-3} whilst VX has a volatility of 10.5 mg m^{-3} (Munro, et al., 1999)) and offers likely explanation for this observation). Between the two nerve agents there is a 300 fold difference in volatility, and, it has been shown that evaporation from the skin surface for percutaneously applied chemicals can significantly impact the dose absorbed (Reifenrath and Robinson, 1982).

The high volatility of GD means that the location of the unrecovered fraction of the applied dose is not easily identified from the data presented here. For low volatility agents, such as VX, it can be reasonably assumed that any unrecovered radioactivity would have been present in unsampled tissues. For GD, the unrecovered radioactivity was either in the unsampled tissues or had volatilised from the skin surface. Obviously, any volatilised material would not be available for skin penetration. From the current studies, a large proportion of ^{14}C-GD was unaccounted

for (36.4 ± 8.3 % of the applied dose). The standard error can be directly related to the survival times of the animals. Typically, animals that succumbed quickly had a lower unrecovered fraction than those that survived longer. Logically, this should be the case as there would be less time for the GD to volatilise away from the skin surface for short duration studies. Interestingly, internal organ recoveries were similar for each animal regardless of study duration, with the majority of radioactivity located within the blood, liver, lung or kidney, with a lower amount of radioactivity located in the brain. It can be inferred that radiolabel located within the liver and kidney are likely to be detoxification products which do not contribute to systemic toxicity. Whole body auto radiographic studies using ^{3}H soman in a mouse model (Kadar, et al., 1985) showed similar results, with high concentrations of radioactivity being seen in the blood, heart, kidney, lung and skin of mice. Kadar (Kadar, et al., 1985) quantified the distribution of soman across the entire animal and observed that radioactivity was located in the nasal cavities, lachrymal and sweat glands, striated muscle, bladder, intestinal lumen and gallbladder at two hours post challenge. As these sites were not sampled during the current study, a portion of the unaccounted for radioactivity may have resided in these tissues. The current study also confirmed the findings of Kadar that low concentrations of radioactivity were located in the brain. As soman is known to severely affect the central nervous system, it shows how small a percentage of the applied dose is actually required to reach the target organ to realise its lethal toxic effects.

Recovery of ^{14}C GD from within the skin exposure site was 43.0 ± 9.3 % of the applied dose. This recovery was substantially larger than that found internally within the animal. Should the animal have survived the initial intoxication, the dose still present within the skin would have continued to be absorbed into the systemic circulation or been metabolised in the skin (assuming that the remaining ^{14}C GD was free and not bound to tissue components or hydrolysed to a hydrolysis product). The existence of a "reservoir" has been previously reported for GD (Kadar, et al., 1985;Benschop, et al., 1981;Clement, 1982;Nordgren, et al., 1985;Wolthuis, et al., 1981) and ascribed to potential locations such as skin, lung, muscles, liver and plasma. The current study supports the theory of the dermal reservoir in the case of dermal exposures. Dermal reservoirs tend to be formed by highly lipophilic chemicals (GD has a log P value of approximately 1.824 (Czerwinski, et al., 1998)) which have passed through the lipophilic stratum corneum and encountered the more aqueous lower skin layers (lower epidermis and dermis), the penetration of the lipophilic chemical then slows leading to a reservoir build up. As the current study examined penetration through damaged skin, reservoir effects were limited to either the dermis or subcutaneous fat. Dermal reservoirs have been shown for other chemical warfare agents (Hattersley, et al., 2008) and offer a target for medical countermeasures aimed at limiting systemic absorption after confirmed contamination.

In conclusion, the current study has shown that ^{14}C-GD can rapidly penetrate through damaged skin *in vivo* into the systemic circulation and from there preferentially distribute into the liver and kidney. The percentage of ^{14}C-GD measured in brain

tissue was 0.04 ± 0.004 of the applied dose which equated to 39.30 ± 4.79 ng ^{14}C-GD per gram of tissue. Animal survival time was directly related to the measured blood concentrations of ^{14}C-GD.

5.4.3. Efficacy of a haemostatic decontaminant candidate *in vivo*

The purpose of the study was to determine whether Woundstat^{TM} could be used to decontaminate damaged skin that had been contaminated with GD 30 seconds prior to Woundstat^{TM} application. Assessment of decontamination efficacy was made using a range of techniques including radioactivity, whole blood cholinesterase and haematocrit quantification alongside examination of observed and measured physiological signs. The combination of these techniques allowed for quantification of the internally absorbed dose responsible for the observed and measured physiological signs, whole blood cholinesterase and haematocrit levels.

Woundstat^{TM} treatment 30 seconds post GD challenge sequestered 68 ± 26 % of the applied ^{14}C-GD. Of the remaining 32% it is likely that a proportion was absorbed prior to treatment application and was therefore not available for absorption by Woundstat^{TM}. Similar levels of Woundstat^{TM} ^{14}C-GD sequestration were measured in the initial *in vitro* studies for both damaged and undamaged skin (Chapter 4) indicating that decontamination must be carried out as rapidly as possible to limit percutaneous absorption of GD. A greater proportion of ^{14}C-GD was recovered for the treated animals (83 ± 24%) compared to the untreated animals (63 ± 20%) This

result was not unexpected as the Woundstat™ treatment would occlude the GD on the skin surface and would sequester ^{14}C-GD volatilising from the skin surface. In the case of the untreated animals, ^{14}C-GD was free to volatilise from the skin surface. Treatment with Woundstat™ substantially reduced the amount of ^{14}C-GD remaining on the skin surface (1.8 ± 1.9 %, treated and 16.7 ± 20.8 %, untreated) and remaining localised within the skin under the dosing site (7.5 ± 3.8 %, treated and 42.7 ± 22.7 %, untreated). Although it can be assumed that the GD recovered from these compartments would not impact upon systemic toxicity, it would have a bearing on contamination spread prevention to first responders and others in the medical chain. Any observable or measurable parameters of systemic toxicity including cholinesterase inhibition should be directly related to the internally recovered dose of GD. Woundstat™ treatment resulted in a reduction of internally measured GD by approximately 0.5 % (1.2 ± 0.3 %, treated and 1.7 ± 0.6 %, untreated). This equates to a 30% reduction in systemically recovered material.

The absorption of ^{14}C-GD through damaged ear skin and into the systemic blood supply had a similar absorption profile whether or not treatment had been given. Both groups had animals that had high initial levels of ^{14}C-GD in the blood. These animals did not survive for more than 45 minutes into the exposure period. For the animals that had a lower initial ^{14}C-GD blood concentration, survival times were lengthened, in a number of cases out to the full study duration. In treated animals that survived the initial period, ^{14}C-GD absorption rates stabilised by 30 minutes and remained constant for the study duration. Conversely, for those animals in the untreated group

which survived the initial period, ^{14}C-GD penetration rates steadily increased until death or study termination.

Woundstat™ treatment was not able to reduce the rapid decline in whole blood cholinesterase, although there was a slight reduction in the amount of the depletion compared to the control animals. However, the slight increase in cholinesterase activity was not sufficient to reduce the assigned severity level from “severe” or “fatal” to a lower category. The increased cholinesterase in the Woundstat™ treatment group as measured at 15 minutes gradually decreased, and by 6 hours was at the same level as the untreated group. The small difference in cholinesterase activity between the two groups allowed the Woundstat™ treated animals to survive for a longer time period than the control animals and demonstrates the benefit of performing decontamination. The increased survival time period would allow a longer therapeutic window for further, nerve agent specific, medical countermeasures to be employed. For both the untreated and the Woundstat™ treated groups, haematocrit levels increased steadily over the exposure duration, whereas for the negative control group haematocrit levels were consistently lower and remained constant. There were no observable differences between the two groups in terms of physiological signs, indicating that sufficient GD had penetrated systemically to cause nerve agent poisoning.

The current study has shown that use of Woundstat™ as a decontaminant on damaged (non haemorrhaging) pig ear skin was able to increase animal survival time, however, it was unable to fully protect against GD toxicity. Most importantly, use of Woundstat™ did not enhance the toxicity of GD.

Further note: A complimentary study using the same experimental protocol with challenge by VX was however able to offer 100% survival (Lydon, 2012). The difference between these observations may lie with the increased penetration observed between GD and VX though damaged and undamaged skin. It is likely that sufficient GD was able to penetrate through the damaged skin in the initial 30 seconds prior to Woundstat™ application to have considerable impact on the final experimental result. Importantly, the fact that Woundstat™ did not increase the toxicity of the evaluated nerve agents allowed it to progress to final evaluation stage outlined in Chapter 6.

CHAPTER 6: GENERAL DISCUSSION

The work undertaken in support of this PhD thesis comprised a series of studies that enabled a range of COTS haemostats to be evaluated for potential use as a decontaminant for GD, with associated programmes evaluating the haemostats against VX and HD (Lydon, 2012;Hall, 2012). It was hypothesised that it would be possible to identify structures with combined haemostatic and decontaminant features. Use of *in vitro* methodologies allowed for selection of candidates with the required parameters (maintenance of haemostatic properties, effective CW agent decontamination ability on both undamaged and damaged skin and the ability to irreversibly sequester CW agent) whilst minimising animal use in accordance with the 3R's. Validation of the *in vitro* static diffusion cell methodology used was required to evaluate haemostatic efficacy against GD (skin surface spreading to allow correct penetration rate determination and choice of receptor media to ensure that GD was adequately soluble). The existence of GD skin reservoirs was shown *in vitro,* and offers potential scope for the development of future medical countermeasures.

The final *in vivo* studies, evaluating the one, most favourable, candidate from the *in vitro* studies showed that whilst use of Woundstat^{TM} as a single medical countermeasure did not give 100% survival, it did potentially offer an increased therapeutic window where specific nerve agent therapy adjuncts could be employed. Recent work by Joosen (Joosen, et al., 2013) supports the rationale of

decontamination prior to medical treatment in the case of percutaneous poisoning by nerve agent. Importantly, use of Woundstat™ on damaged skin contaminated with GD did not increase GD toxicity. One of the major reasons for the initiation of the programme was the concern that use of a haemostatic product in a wound contaminated with CW agent would increase the toxicity of the CW agent. Due to the potential life threatening nature of haemorrhaging injury it would not be acceptable to not give preventative aid, however, it would be nugatory to give aid that would stop the haemorrhage but would then increase the toxicity of the CW agent. The output of this programme has shown that use of Woundstat™ did not increase the absorption of a range of CW agents on either undamaged or injured skin.

This programme has shown that Woundstat™ can be used as a decontaminant, without loss of haemostatic ability. The final evaluation was an assessment of Woundstat™ efficacy in a CW agent contaminated haemorrhaging injury model. This work was carried out by the United States Army Medical Research Institute of Chemical Defense (USAMRICD) (Smith, et al., 2011). The study protocol involved the creation of an axial pocket (approximately 5 cm in length and 100 ml volume) in a terminally anaesthetised large white pig. Chemical warfare agent (VX only, 5 LD_{50} challenge) was applied onto the exposed rib cage approximately half way up the height of the pocket. The axialary vein was immediately transected and Woundstat™ was applied 45 seconds later in sufficient quantity to arrest the haemorrhage. Those animals that survived until the maximum study duration (360 minutes) were culled by anaesthetic overdose. A total of 9 animals were challenged with VX of which 4 were

treated with Woundstat™. All the animals that did not receive Woundstat™ treatment succumbed to VX toxicity (time to death 58 ± 43 minutes). Out of the treatment group one animal survived for the study duration. The average time to death for the Woundstat™ treatment group was 263 ± 85 minutes. As with the GD studies on damaged non haemorrhaging skin none of the animals received any specific nerve agent adjunct therapy. In conclusion, the USAMRICD studies indicated that although use of Woundstat™ as a standalone treatment did not offer 100% survival, it did offer an increased therapeutic window where specific nerve agent therapies could be employed. Importantly, the haemorrhaging studies showed that Woundstat™ remained an effective haemostat in the presence of VX and, also, did not increase the toxicity of VX.

Future investigations into haemostatic decontaminants, should, ideally concentrate on the increased therapeutic window and adjunct, chemical warfare agent specific therapies that could be given. In the case of nerve agents, the combopen (Section 1.5.6.2) is available for rapid deployment on the battlefield. However, it is of importance to note that the combopen contains atropine, a muscarinic receptor antagonist which can cause an increase in heart rate. An increased heart rate could potentially cause issues with blood clots formation at the site of traumatic injury.

Woundstat™ was developed for use as a haemostatic agent for complex traumatic wounds to fill the perceived shortcomings of tourniquet placement. Approved for use

by the FDA in 2007 and fielded for use by the U.S. Army in 2008. The Committee on Tactical Combat Casualty Care (CoTCC) voted to recommend that Woundstat™ should be third in the line of treatment for haemorrhage control after the traditional tourniquet and Combat Gauze (a gauze type haemostatic agent rather than a powder or granule). It was perceived that Woundstat™ could be of use where the characteristics of the wound would make a granular agent preferable. In 2009 an All Army Activity Message stated that "The risk inherent in WS (Woundstat™) use outweighs its benefits as a back-up agent hemostatic agent to Combat Gauze" (Abramson, 2009). Although by this point Woundstat™ was a lead candidate in the haemostatic decontaminant programme, the customer requested (as the programme was well underway) that work on its use a potential haemostatic decontaminant continue. The work reported within this thesis can, therefore, be viewed as proof of principle that the development of haemostatic decontaminants is feasible. It is interesting to note that research evaluating Woundstat™ against other haemostatic agents has also continued (Littlejohn, et al., 2011) despite the U.S. Army withdrawing the product from use.

Tourniquet use is typically restricted to limb haemorrhage and is not suitable for use on junctional haemorrhage (axillary and inguinal). Management of junctional haemorrhage led to the requirement for deployable haemostatic agents in a combat setting. Front line deployable haemostats are found as impregnated gauzes or as granules based on the mechanism of action of either absorption (zeolites and smectites) or tissue sealant characteristics (chitosan). In situations where tourniquet

use is impractical, Combat Gauze and Woundstat™ have been shown to the most effective topical products for the cessation of junctional haemorrhage. Given that Woundstat™ has currently been withdrawn due to safety concerns over its potential to cause intravascular clotting and embolism, this leaves Combat Gauze alone as the fielded second line treatment.

Although Combat Gauze was not evaluated during the studies reported here as to its efficacy as a haemostatic decontaminant, the previous generation of this product, Quikclot ACS+ was. The results showed that Quikclot ACS+ significantly reduced both the rate and extent of ^{14}C-GD skin absorption (although not as effectively as Woundstat™). However, the active constituents between the two generations of product are different. Quikclot ACS+ uses a zeolite, whereas, Combat Gauze uses a smectite (Kaolin). It cannot therefore be inferred that Combat Gauze has the potential to be as effective a CW agent decontaminant as Quikclot ACS+. Interestingly, the most effective haemostatic decontaminant shown by this research (Woundstat™), was also smectite based. It is feasible that Combat Gauze could have similar decontaminating properties to Woundstat™. As a priority, future work in this area should evaluate the CW agent decontaminating abilities of Combat Gauze.

Woundstat™ is a solid material composed of mineral smectite (Figure 6.1). The general formula for smectites is $2Al_2O_3.8SiO_2.2H_2O.nH_2O$ (however, the aluminium may be substituted for either iron or magnesium). These clay minerals comprise two

silica tetrahedral sheets with a central alumina octahedral sheet which possess a net negative charge. The interlayer H_2O and exchangeable cations (Calcium, Sodium, Potassium) balance the negative charge (Vallenzuela Diaz and de Souza Santos, 2001). It is recognized that clay minerals have hydrophilic surfaces and that such surfaces are not ideal for the absorption of organic molecules, leading to the development of organo-clays for this purpose (Boyd, et al., 1988). However, it has been shown that potassium and calcium saturated smectite clays can adsorb a range of pesticides (Sheng, et al., 2001) including parathion, a nerve agent simulant. Work by Li (Li, et al., 2004) indicated that the pesticide adsorption ability of soil clays was influenced by the exchangeable cation present with potassium demonstrating the strongest affinity for pesticides. Smectite interlayer hydration status has also been shown to influence Atrazine sorption, with air dried smectite adsorbing more Atrazine than native smectite (Chappell, et al., 2005). More recent work has shown that smectites are effective adsorbents for the hydrophobic dibenzo-p-dioxins (Liu, et al., 2009). Given that smectites are primarily hydrophilic, the ability of GD and other chemical warfare agents to adsorb into Woundstat™ is determined by the direct interaction of the agent with exchangeable cation and the level of interlayer swelling. The fine particulate nature of Woundstat™ gives a large surface area making the exchangeable cations readily available.

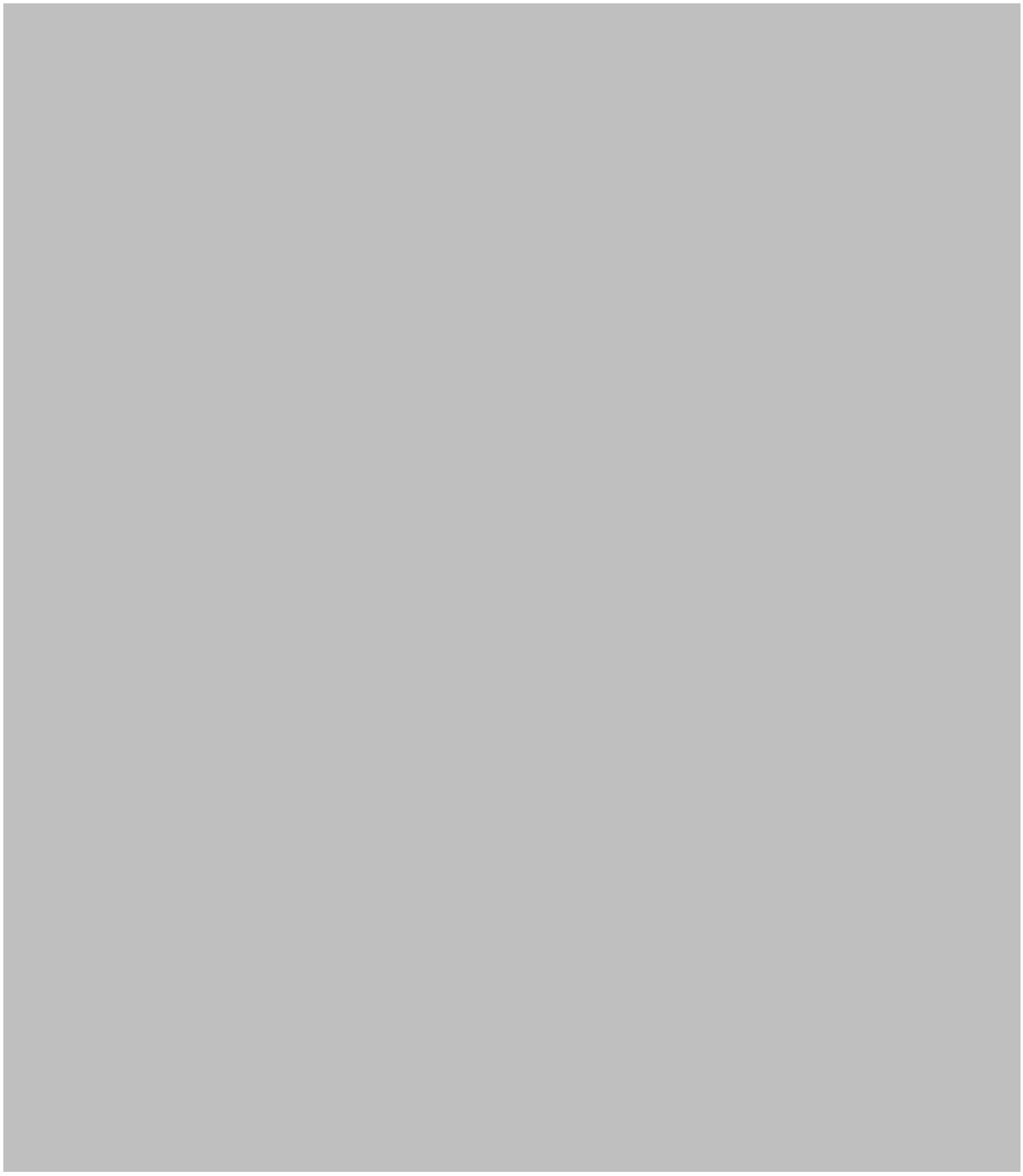

Figure 6.1: Woundstat^{TM}. A solid granular powder composed of mineral smectite. Work in this thesis has shown the ability of Woundstat^{TM} to effectively adsorb GD and other chemical warfare agents. Images property of TraumaCure.

Recent developments in haemostatic materials have seen a number of new products receiving FDA approval in addition to Combat Gauze. Celox-A (the original Celox reformatted into an applicator for delivery deep into a penetrating wound), Chitoflex (based on the original HemCon, but with a less rigid structure) have most recently been evaluated (Littlejohn, et al., 2011). Emerging products include hydrophobically modified chitosan (Dowling, et al., 2011) and Hemostatic multilayer coatings (Shukla, et al., 2012), indicating that interest in haemostatic materials remains undiminished.

In summary, the work reported here had two main themes, firstly, the *in vitro* skin penentration of ^{14}C-GD was characterised in terms of appropriate receptor fluid use, rapidity of skin surface spread and reservoir development, which allowed postulation of a mechanism of interaction of GD with the skin. Such characterisation has wider implications on the relevance of the extrapolation of *in vitro* to *in vivo* data. Rapid skin surface spread of GD may have implications when extrapolating *in vitro* to *in vivo* penetration rates (where the area available for skin penetration is not artificially limited). Rapid reservoir formation within the skin surface layers has implications not only in decontamination regimens, but, also for emergency responders who may suffer secondary exposure. Secondly, a number of haemostats were evaluated for potential use as decontaminants in GD contaminated environments. A logical progression from *in vitro* to *in vivo* experimentation enabled efficient selection of promising materials whilst minimising animal use. The rapid development of improved and novel haemostatic materials means that further assessments of these products should be made before they are used in CW agent contaminated wounds.

The methodology explored and developed in this thesis will serve as a basis for this work to continue. The smectite based Woundstat^{TM} was shown to effectively adsorb GD both *in vitro* and *in vivo* and retained haemostatic ability even after gross GD contamination. It is recommended that the use of specific nerve agent medical countermeasures (such as the Combopen) be evaluated in conjunction with haemostatic decontaminant application, as work evaluating the combined use of skin decontaminants and nerve agent medical countermeasures are currently showing positive results (Joosen, et al., 2013).

PUBLICATIONS ARISING FROM WORK IN THIS THESIS

Dalton, C.H., Graham, S.J., Payne, O.J., Chipman, J.K., Chilcott, R.P. and Jenner, J. "Influence of Receptor Media on GD Skin Penetration *In Vitro*" Advances in Dermatological Sciences, Volume 1. Eds. Brain, K.R. and Chilcott, R.P. RSC Publishing, 2013.

Dalton, C.H., Payne, O.J., Graham, S.J., Chilcott, R.P. and Jenner, J. "The skin reservoir of the nerve agent soman (GD) *in vitro*" Poster presented at Stratum Corneum VII, Cardiff, UK (September 2012)

Smith, K.H., Hall, C.A., Lydon, H.L., **Dalton**, C.H., Graham, J.S., Railer, R.F., Stevenson, R.S., Deckert, R.R., Devorak, J.L., Boecker, J.D., Braue, E.H., Lumpkin, H.L., Doxzon, B.F., Chilcott, R.P. and Clarkson, E.D. "Testing the Ability of Haemostatic Products to Protect Against the Chemical Warfare Agent VX" Poster presented at the 18th Biennial Medical Chemical Defense Bioscience Review, Maryland, USA (May 2012).

Dalton, C.H., Graham, S.J., Payne, O.J., Chipman, J.K., Chilcott, R.P. and Jenner, J. "Influence of Receptor Media on GD Skin Penetration *In Vitro*" Poster presented at Perspectives in Percutaneous Penetration, Montpellier, France (April 2012).

Clarkson, E.D., Smith, K.H., Hall, C.A., Lydon, H.L., **Dalton**, C.H., Graham, J.S., Railer, R.F., Stevenson, R.S., Deckert, R.R., Devorak, J.L., Boecker, J.D., Braue, E.H., Lumpkin, H.L., Doxzon, B.F. and Chilcott, R.P. "Testing the Ability of WoundStat(tm) to Protect against the Chemical Warfare Agent VX". The Toxicologist 120 (2): 433 (2011)

Dalton, C.H., Hall, C.A., Lydon, H.L., Chipman, J.K., Chilcott, R.P. and Graham, J.S. "Absorption of GD through damaged and undamaged pig skin in vitro" Poster presented at Perspectives in Percutaneous Penetration, Montpellier, France (April 2010)

Hall, C. A., Lydon, H.L., **Dalton**, C.H., Chipman, J.K., Chilcott, R.P. and Graham, J.S. "The in vitro efficacy of haemostatic products in the presence of chemical warfare agents-Sulphur mustard (HD) and VX" Toxicology 262 (1): 9-10 (2009)

LIST OF REFERENCES

Abramson M. Army halts use of WoundStat. Stars and Stripes. 23-9-2009.

Ahlstrom LA, Cross SE and Mills PC (2007) The effects of freezing skin on transdermal drug penetration kinetics. *Journal of Veterinary Pharmacology and Therapeutics* **30**:456-463.

Alam HB, Burris D, DaCorta JA and Rhee P (2005) Hemorrhage control in the battlefield: Role of new hemostatic agents. *Military Medicine* **170**:63-69.

Arrowsmith JE (2007) The neuromuscular junction. *Surgery* **25**:105-111.

Bajgar J, Kassa J, Pohanka M, Karasova JZ, Novotny L, Fusek J and Blaha V (2011) Inhibition of blood and tissue cholinesterases by soman in guinea pigs in vivo. *Journal of Applied Biomedicine* **9**:35-41.

Balali-Mood M and Hefazi M (2005) The pharmacology, toxicology, and medical treatment of sulphur mustard poisoning. *Fundamental & Clinical Pharmacology* **19**:297-315.

Barbero AM and Frasch H (2009) Pig and guinea pig skin as surrogates for human in vitro penetration studies: A quantitative review. *Toxicology in Vitro* **23**:1-13.

Bartek MJ, Labudde JA and Maibach HI (1972) Skin Permeability In-Vivo - Comparison in Rat, Rabbit, Pig and Man. *Journal of Investigative Dermatology* **58**:114-123.

Baynes RE, Halling KB and Riviere JE (1997) The influence of diethyl-m-toluamide (DEET) on the percutaneous absorption of permethrin and carbaryl. *Toxicology and Applied Pharmacology* **144**:332-339.

Benschop HP, Berends F and de Jong LP (1981) GLC-analysis and pharmacokinetics of the four stereoisomers of Soman. *Fundam Appl Toxicol* **1**:177-182.

Benschop HP, Bijleveld EC, de Jong LP, Van Der Wiel HJ and van Helden HP (1987) Toxicokinetics of the four stereoisomers of the nerve agent soman in atropinized rats--influence of a soman simulator. *Toxicol Appl Pharmacol* **90**:490-500.

Benschop HP, Konings CA, van GJ and de Jong LP (1984) Isolation, in vitro activity, and acute toxicity in mice of the four stereoisomers of soman. *Fundam Appl Toxicol* **4**:S84-S95.

Benschop HP and Wesselman HC (1989) Pharmacokinetics of the soman simulant 1,2,2-trimethylpropyl dimethylphosphinate (PDP) in rats. *Arch Toxicol* **63**:238-243.

Bijani K and Moghadamnia AA (2002) Long-term effects of chemical weapons on respiratory tract in Iraq-Iran war victims living in Babol (North of Iran). *Ecotoxicology and Environmental Safety* **53**:422-424.

Bjarnason S, Mikler J, Hill I, Tenn C, Garrett M, Caddy N and Sawyer TW (2008) Comparison of selected skin decontaminant products and regimens against VX in domestic swine. *Human & Experimental Toxicology* **27**:253-261.

Blank IH (1953) Further Observations on Factors Which Influence the Water Content of the Stratum Corneum. *Journal of Investigative Dermatology* **21**:259-271.

Bos JD and Meinardi MMHM (2000) The 500 Dalton rule for the skin penetration of chemical compounds and drugs. *Experimental Dermatology* **9**:165-169.

Boulais N and Misery L (2007) Merkel cells. *Journal of the American Academy of Dermatology* **57**:147-165.

Bouwstra JA, Honeywell-Nguyen PL, Gooris GS and Ponec M (2003) Structure of the skin barrier and its modulation by vesicular formulations. *Progress in Lipid Research* **42**:1-36.

Bouwstra JA and Ponec M (2006) The skin barrier in healthy and diseased state. *Biochimica et Biophysica Acta-Biomembranes* **1758**:2080-2095.

Boyd SA, Shaobai S, Lee JF and Mortland MM (1988) Pentachlorophenol Sorption by Organo-Clays. *Clays and Clay Minerals* **36**:125-130.

Brennan RJ, Waeckerle JF, Sharp TW and Lillibridge SR (1999) Chemical warfare agents: Emergency medical and emergency public health issues. *Annals of Emergency Medicine* **34**:191-204.

Bronaugh RL and Stewart RF (1985) Methods for Invitro Percutaneous-Absorption Studies .5. Permeation Through Damaged Skin. *Journal of Pharmaceutical Sciences* **74**:1062-1066.

Bronaugh RL, Stewart RF and Congdon ER (1982) Methods for Invitro Percutaneous-Absorption Studies .2. Animal-Models for Human-Skin. *Toxicology and Applied Pharmacology* **62**:481-488.

Bronaugh RL, Stewart RF and Simon M (1986) Methods for Invitro Percutaneous-Absorption Studies .7. Use of Excised Human-Skin. *Journal of Pharmaceutical Sciences* **75**:1094-1097.

Broomfield CA, Lenz DE and MacIver B (1986) The stability of soman and its stereoisomers in aqueous solution: toxicological considerations. *Arch Toxicol* **59**:261-265.

Brouard M and Barrandon Yybc (2003) Controlling skin morphogenesis: Hope and despair. *Current Opinion in Biotechnology* **14**:520-525.

Brown FJ (1968) *Chemical Warfare a Study in Restraints*. Princeton University Press, Conneticut.

Callard RE and Harper JI (2007) The skin barrier, atopic dermatitis and allergy: a role for Langerhans cells? *Trends in Immunology* **28**:294-298.

Cannard K (2006) The acute treatment of nerve agent exposure. *Journal of the Neurological Sciences* **249**:86-94.

Carr MEJ (2004) Monitoring of hemostasis in combat trauma patients. *Military Medicine* **169**:11-14.

Cevc G (1996) Transfersomes, liposomes and other lipid suspensions on the skin: Permeation enhancement, vesicle penetration, and transdermal drug delivery. *Critical Reviews in Therapeutic Drug Carrier Systems* **13**:257-388.

Cevc G and Vierl U (2010) Nanotechnology and the transdermal route A state of the art review and critical appraisal. *Journal of Controlled Release* **141**:277-299.

Chappell MA, Laird DA, Thompson ML, Li H, Teppen BJ, Aggarwal V, Johnston CT and Boyd SA (2005) Influence of smectite hydration and swelling on atrazine sorption behavior. *Environmental Science & Technology* **39**:3150-3156.

Chauhan S, Chauhan S, D'Cruz R, Faruqi S, Singh K, Varma S, Singh M and Karthik V (2008) Chemical warfare agents. *Environmental Toxicology and Pharmacology* **26**:113-122.

Chilcott RP, Barai N, Beezer AE, Brain SI, Brown MB, Bunge AL, Burgess SE, Cross S, Dalton CH, Dias M, Farinha A, Finnin BC, Gallagher SJ, Green DM, Gunt H, Gwyther RL, Heard CM, Jarvis CA, Kamiyama F, Kasting GB, Ley EE, Lim ST, Mcnaughton GS, Morris A, Nazemi MH, Pellett MA, Du Plessis J, Quan YS, Raghavan SL, Roberts M, Romonchuk W, Roper CS, Schenk D, Simonsen L, Simpson A, Traversa BD, Trottet L, Watkinson A, Wilkinson SC, Williams FM, Yamamoto A and Hadgraft J (2005a) Inter- and intralaboratory variation of in vitro diffusion cell measurements: An international multicenter study using quasi-standardized methods and materials. *Journal of Pharmaceutical Sciences* **94**:632-638.

Chilcott RP, Dalton CH, Emmanuel AJ, Allen CE and Bradley ST (2002) Transepidermal water loss does not correlate with skin barrier function in vitro. *Journal of Investigative Dermatology* **118**:871-875.

Chilcott RP, Dalton CH, Hill I, Davidson CM, Blohm KL and Hamilton MG (2003) Clinical manifestations of VX poisoning following percutaneous exposure in the domestic white pig. *Human & Experimental Toxicology* **22**:255-261.

Chilcott RP, Dalton CH, Hill I, Davison CM, Blohm KL, Clarkson ED and Hamilton MG (2005b) Evaluation of a barrier cream against the chemical warfare agent VX using the domestic white pig. *Basic & Clinical Pharmacology & Toxicology* **97**:35-38.

Chilcott RP, Dalton CH, Hill I, Davison CM, Blohm KL, Clarkson ED and Hamilton MG (2005c) In vivo skin absorption and distribution of the nerve agent VX (O-ethyl-S-[2(diisopropylamino)ethyl] methylphosphonothioate) in the domestic white pig. *Human & Experimental Toxicology* **24**:347-352.

Chilcott RP, Jenner J, Carrick W, Hotchkiss SAM and Rice P (2000) Human skin absorption of bis-2-(chloroethyl)sulphide (sulphur mustard) in vitro. *Journal of Applied Toxicology* **20**:349-355.

Chilcott RP, Jenner J, Hotchkiss SAM and Rice P (2001) In vitro skin absorption and decontamination of sulphur mustard: Comparison of human and pig-ear skin. *Journal of Applied Toxicology* **21**:279-283.

Chilcott RP, Dalton CH, Ashley Z, Allen CE, Bradley ST, Maidment MP, Jenner J, Brown RF, Gwyther RJ and Rice P (2007) Evaluation of barrier creams against sulphur mustard: (II) in vivo and in vitro studies using the domestic white pig. *Cutaneous and Ocular Toxicology* **26**:235-247.

Clay JG, Grayson J and Zierold MD (2010) Comparative Testing of New Hemostatic Agents in a Swine Model of Extremity Arterial and Venous Hemorrhage. *Military Medicine* **175**:280-284.

Clement JG (1982) Plasma aliesterase--a possible depot for soman (pinacolyl methylphosphonofluoridate) in the mouse. *Biochem Pharmacol* **31**:4085-4088.

Clifford CC (2004) Treating traumatic bleeding in a combat setting. *Military Medicine* **169**:8-4.

Collier SW, Sheikh NM, Sakr A, Lichtin JL, Stewart RF and Bronaugh RL (1989) Maintenance of Skin Viability During Invitro Percutaneous Absorption-Metabolism Studies. *Toxicology and Applied Pharmacology* **99**:522-533.

Cooper GJ, Ryan JM and Galbraith KA (1994) The surgical management in war of penetrating wounds contaminated with chemical warfare agents. *Journal of the Royal Army Medical Corps* **140**:113-118.

Czerwinski SE, Maxwell DM and Lenz DE (1998) A method for measuring octanol : water partition coefficients of highly toxic organophosphorus compounds. *Toxicology Methods* **8**:139-149.

Dahlback B (2000) Blood coagulation. *Lancet* **355**:1627-1632.

Dalton CH, Hall CA, Lydon HL, Chipman JK, Chilcott RP and Graham JS. Absorption of GD through damaged and undamaged pig skin in vitro. Twelfth International

Perspectves in Percutaneous Penetration Conference. Perspectives in Percutaneous Penetration 12, 121. 2010. Cardiff, UK, STS Publishing. 10.

Dalton CH, Hattersley IJ, Rutter SJ and Chilcott RP (2006a) Absorption of the nerve agent VX (O-ethyl-S-[2(di-isopropylamino)ethyl] methyl phosphonothioate) through pig, human and guinea pig skin in vitro. *Toxicology in Vitro* **20**:1532-1536.

Dalton CH, Maidment MP, Jenner J and Chilcott RP (2006b) Closed cup vapor systems in percutaneous exposure studies: What is the dose? *Journal of Analytical Toxicology* **30**:165-170.

Davie EW (1986) Introduction to the Blood-Coagulation Cascade and Cloning of Blood-Coagulation Factors. *Journal of Protein Chemistry* **5**:247-253.

Davie EW (2003) JBC Centennial 1905-2005 - 100 years of biochemistry and molecular biology - A brief historical review of the waterfall/cascade of blood coagulation. *Journal of Biological Chemistry* **278**:50819-50832.

Davie EW, Fujikawa K and Kisiel W (1991) The Coagulation Cascade - Initiation, Maintenance, and Regulation. *Biochemistry* **30**:10363-10370.

Davies DJ, Ward RJ and Heylings JR (2004) Multi-species assessment of electrical resistance as a skin integrity marker for in vitro percutaneous absorption studies. *Toxicology in Vitro* **18**:351-358.

Devlin JJ and Gutierrez MA (2010) Primum Non Nocere: Limitations of Military-Derived Transfusion Recommendations in Civilian Trauma. *Journal of Emergency Medicine* **39**:342-343.

Dick IP and Scott RC (1992) Pig Ear Skin As An Invitro Model for Human Skin Permeability. *Journal of Pharmacy and Pharmacology* **44**:640-645.

Doran CM, Woolley T and Midwinter MJ (2010) Feasibility of Using Rotational Thromboelastometry to Assess Coagulation Status of Combat Casualties in a Deployed Setting. *Journal of Trauma-Injury Infection and Critical Care* **69**:S40-S48.

Dorandeu F, Mikler J, Thiermann H, Tenn C, Davidson C, Sawyer T, Lallement G and Worek F (2007) Swine models in the design of more effective medical countermeasures against organophosphorus poisoning. *Toxicology* **233**:128-144.

Dowling MB, Kumar R, Keibler MA, Hess JR, Bochicchio GV and Raghavan SR (2011) A self-assembling hydrophobically modified chitosan capable of reversible hemostatic action. *Biomaterials* **32**:3351-3357.

Dries DJ (2010) The contemporary role of blood products and components used in trauma resuscitation. *Scandinavian Journal of Trauma Resuscitation & Emergency Medicine* **18**.

Duncan EJS, Brown A, Lundy P, Sawyer TW, Hamilton M, Hill I and Conley JD (2002) Site-specific percutaneous absorption of methyl salicylate and VX in domestic swine. *Journal of Applied Toxicology* **22**:141-148.

Ellman GL, Courtney KD, Andres V and Featherstone RM (1961) A New and Rapid Colorimetric Determination of Acetylcholinesterase Activity. *Biochemical Pharmacology* **7**:88-&.

Engblom J, Engstrom S and Fontell K (1995) The Effect of the Skin Penetration Enhancer Azone(R) on Fatty Acid-Sodium Soap-Water Mixtures. *Journal of Controlled Release* **33**:299-305.

Engelbrecht G. Ricin plot father is jailed for 10 years. The Northern Echo . 15-5-2010.

Evison D, Hinsley D and Rice P (2002) Chemical weapons. *British Medical Journal* **324**:332-335.

Fasano WJ and McDougal JN (2008) In vitro dermal absorption rate testing of certain chemicals of interest to the Occupational Safety and Health Administration: Summary and evaluation of USEPA's mandated testing. *Regulatory Toxicology and Pharmacology* **51**:181-194.

Feingold KR (2007) The role of epidermal lipids in cutaneous permeability barrier homeostasis. *Journal of Lipid Research* **48**:2531-2546.

Fleisher JH and Harris LW (1965) Dealkylation As A Mechanism for Aging of Cholinesterase After Poisoning with Pinacolyl Methylphosphonofluoridate. *Biochemical Pharmacology* **14**:641-&.

Franz TJ (1975) Percutaneous Absorption - Relevance of Invitro Data. *Journal of Investigative Dermatology* **64**:190-195.

Fredriksson T (1969a) Hydrolysis of Soman and Tabun (two organophosphorus cholinesterase inhibitors) in cutaneous tissues. *Acta Derm Venereol* **49**:490-492.

Fredriksson T (1969b) Percutaneous absorption of Soman and Tabun, two organophosphorus cholinesterase inhibitors. *Acta Derm Venereol* **49**:484-489.

Friedewald VE (2008) *Clinical Guide to Bioweapons and Chemical Agents*. Springer-Verlag, London.

Friend DR (1992) Invitro Skin Permeation Techniques. *Journal of Controlled Release* **18**:235-248.

Fries AA and West CJ (1921) *Chemical Warfare*. McGraw-Hill Book Company, New York.

Fuchs E (2008) Skin stem cells: rising to the surface. *Journal of Cell Biology* **180**:273-284.

Galey WR, Lonsdale HK and Nacht S (1976) Invitro Permeability of Skin and Buccal Mucosa to Selected Drugs and Tritiated-Water. *Journal of Investigative Dermatology* **67**:713-717.

Galloway T and Handy R (2003) Immunotoxicity of organophosphorous pesticides. *Ecotoxicology* **12**:345-363.

Garrod D and Chidgey M (2008) Desmosome structure, composition and function. *Biochimica et Biophysica Acta-Biomembranes* **1778**:572-587.

Gattu S and Maibach HI (2010) Enhanced Absorption through Damaged Skin: An Overview of the in vitro Human Model. *Skin Pharmacology and Physiology* **23**:171-176.

Genovese RF, Benton BJ, Oubre JL, Fleming PJ, Jakubowski EM and Mioduszewski RJ (2008) Determination of miosis threshold from whole-body vapor exposure to Sarin in African green monkeys. *Toxicology* **244**:123-132.

Ghanei M and Vosoghi AA (2002) An epidemiologic study to screen for chronic myelocytic leukemia in war victims exposed to mustard gas. *Environmental Health Perspectives* **110**:519-521.

Giacomoni PU, Mammone T and Teri M (2009) Gender-linked differences in human skin. *Journal of Dermatological Science* **55**:144-149.

Gordon RK, Feaster SR, Russell AJ, LeJeune KE, Maxwell DM, Lenz DE, Ross M and Doctor BP (1999) Organophosphate skin decontamination using immobilized enzymes. *Chemico-Biological Interactions* **119-120**:463-470.

Gore AV, Liang AC and Chien YW (1998) Comparative biomembrane permeation of tacrine using Yucatan minipigs and domestic pigs as the animal model. *Journal of Pharmaceutical Sciences* **87**:441-447.

Hadgraft J (2001) Skin, the final frontier. *International Journal of Pharmaceutics* **224**:1-18.

Hall CA. Haemostatic Products as a Potential Therapy for Vesicant-Contaminated Wounds. PhD Thesis . 2012. University of Birmingham.

Hall CA, Lydon HL, Dalton CH, Chipman J, Chilcott RP and Graham JS (2009) The in vitro efficacy of haemostatic products in the presence of chemical warfare agents-Sulphur mustard (HD) and VX. *Toxicology* **262**:9-10.

Hamilton MG, Hill I, Conley J, Sawyer TW, Caneva DC and Lundy PM (2004) Clinical aspects of percutaneous poisoning by the chemical warfare agent VX: Effects of application site and decontamination. *Military Medicine* **169**:856-862.

Hamilton MG and Lundy PM (2007) Medical countermeasures to WMDs: Defence research for civilian and military use. *Toxicology* **233**:8-12.

Harrison SM, Barry BW and Dugard PH (1984) Effects of Freezing on Human-Skin Permeability. *Journal of Pharmacy and Pharmacology* **36**:261-262.

Hartert H (1948) Blutgerinnungsstudien Mit der Thrombelastographie, Einem Neuen Untersuchungsverfahren. *Klinische Wochenschrift* **26**:577-583.

Hattersley I, Jenner J, Dalton C, Chilcott R and Graham J (2008) The skin reservoir of sulphur mustard. *Toxicology in Vitro* **22**:1539-1546.

Hawkins GS and Reifenrath WG (1986) Influence of Skin Source, Penetration Cell Fluid, and Partition-Coefficient on Invitro Skin Penetration. *Journal of Pharmaceutical Sciences* **75**:378-381.

Henning A, Schaefer UF and Neumann D (2009) Potential pitfalls in skin permeation experiments: Influence of experimental factors and subsequent data evaluation. *European Journal of Pharmaceutics and Biopharmaceutics* **72**:324-331.

Hettiaratchy S and Papini R (2004) ABC of burns - Initial management of a major burn: II - assessment and resuscitation. *British Medical Journal* **329**:101-103.

Holbrook KA and Odland GF (1974) Regional Differences in Thickness (Cell Layers) of Human Stratum-Corneum - Ultrastructural Analysis. *Journal of Investigative Dermatology* **62**:415-422.

Hsia SL (1971) Potentials in exploring the biochemistry of human skin. *Essays in biochemistry* **7**:1-38.

Hsu CK, Akiyama M and Shimizu H (2008) Filaggrin: An emerging star in atopic march. *Journal of the Formosan Medical Association* **107**:429-431.

James JT, Manthei JH, Goodwin BS, Heitkamp D and Liebenberg SP (1987) Clinical chemistry reference values in two breeds of swine and their changes during percutaneous exposure to soman. *Am J Vet Res* **48**:284-288.

Joosen MJA, van der Schans MJ, Kuijpers WC, van Helden HPM and Noort D (2013) Timing of decontamination and treatment in case of percutaneous VX poisoning: A mini review. *Chemico-Biological Interactions* **203**:149-153.

Joosen MJ, van der Schans MJ and van Helden HP (2008) Percutaneous exposure to VX: Clinical signs, effects on brain acetylcholine levels and EEG. *Neurochemical Research* **33**:308-317.

Jovic RC (1974) Correlation between signs of toxicity and some biochemical changes in rats poisoned by soman. *Eur J Pharmacol* **25**:159-164.

Kadar T, Raveh L, Cohen G, Oz N, Baranes I, Balan A, Ashani Y and Shapira S (1985) Distribution of 3H-soman in mice. *Arch Toxicol* **58**:45-49.

Kanitakis J (2002) Anatomy, histology and immunohistochemistry of normal human skin. *European Journal of Dermatology* **12**:390-400.

Kashuk JL, Moore EE, Sawyer M, Le T, Johnson J, Biffl WL, Cothren C, Barnett C, Stahel P, Sillman CC, Sauaia A and Banerjee A (2010) Postinjury Coagulopathy Management Goal Directed Resuscitation via POC Thrombelastography. *Annals of Surgery* **251**:604-614.

Kassa J (2002) Review of oximes in the antidotal treatment of poisoning by organophosphorus nerve agents. *J Toxicol Clin Toxicol* **40**:803-816.

Kasting GB, Miller MA and Bhatt VD (2008) A spreadsheet-based method for estimating the skin disposition of volatile compounds: Application to N,N-diethyl-m-toluamide (DEET). *Journal of Occupational and Environmental Hygiene* **5**:633-644.

Kembro RJ, Horton JD and Wagner M (2008) Use of Recombinant Factor VIIa in Operation Iraqi Freedom and Operation Enduring Freedom: Survey of Army Surgeons. *Military Medicine* **173**:1057-1059.

Kheirabadi BS, Edens JW, Terrazas IB, Estep JS, Klemcke HG, Dubick MA and Holcomb JB (2009) Comparison of New Hemostatic Granules/Powders With Currently Deployed Hemostatic Products in a Lethal Model of Extremity Arterial Hemorrhage in Swine. *Journal of Trauma-Injury Infection and Critical Care* **66**:316-328.

Kheirabadi BS, Estep JS and Dubick MA. Assessment of efficacy of new haemostatic agents in a model of extremity arterial hemorrhage in swine. Final Report to the US Army Institute of Surgical Research. 2008. Fort Sam, Houston, Texas.

Kim HS, Eom JH, Cho HY, Cho YJ, Kim JY, Lee JK, Kim SH and Park KL (2007) Evaluation of immunotoxicity induced by pirimiphos-methyl in male balb/c mice following exposure to for 28 days. *Journal of Toxicology and Environmental Health-Part A-Current Issues* **70**:1278-1287.

Knezevic DL, Tadic V and Cetkovic S (1993) The efficacy of different decontaminants in rats and pigs percutaneously poisoned with organophosphates. *Vet Hum Toxicol* **35**:403-405.

Lebwohl M and Herrmann LG (2005) Impaired skin barrier function in dermatologic disease and repair with moisturization. *Cutis; cutaneous medicine for the practitioner* **76**:7-12.

Lee MJ and Clement JG (1990) Effects of soman poisoning on hematology and coagulation parameters and serum biochemistry in rabbits. *Mil Med* **155**:244-249.

Lee PH, Conradi R and Shanmugasundaram V (2010) Development of an in silico model for human skin permeation based on a Franz cell skin permeability assay. *Bioorganic & Medicinal Chemistry Letters* **20**:69-73.

Lee SH, Jeong SK and Ahn SK (2006) An update of the defensive barrier function of skin. *Yonsei Medical Journal* **47**:293-306.

Li H, Teppen BJ, Laird DA, Johnston CT and Boyd SA (2004) Geochemical modulation of pesticide sorption on smectite clay. *Environmental Science & Technology* **38**:5393-5399.

Little JS, Broomfield CA, Fox-Talbot MK, Boucher LJ, MacIver B and Lenz DE (1989) Partial characterization of an enzyme that hydrolyzes sarin, soman, tabun, and diisopropyl phosphorofluoridate (DFP). *Biochem Pharmacol* **38**:23-29.

Littlejohn LF, Devlin JJ, Kircher SS, Lueken R, Melia MR and Johnson AS (2011) Comparison of Celox-A, ChitoFlex, WoundStat, and Combat Gauze Hemostatic Agents Versus Standard Gauze Dressing in Control of Hemorrhage in a Swine Model of Penetrating Trauma. *Academic Emergency Medicine* **18**:340-350.

Liu C, Li H, Teppen BJ, Johnston CT and Boyd SA (2009) Mechanisms Associated with the High Adsorption of Dibenzo-p-dioxin from Water by Smectite Clays. *Environmental Science & Technology* **43**:2777-2783.

Lydon H. Investigations of a Possible Novel Decontamination Role for a Haemostatic Product: Studies with S-[2-Diisopropylamino ethyl]-O-ethylmethylphosphonothioate (VX). PhD Thesis . 2012. University of Birmingham.

Malhotra RC, Ganesan K, Sugendran K and Swamy RV (1999) Chemistry and toxicology of sulphur mustard - A review. *Defence Science Journal* **49**:97-116.

Mallett SV and Cox DJA (1992) Thrombelastography. *British Journal of Anaesthesia* **69**:307-313.

Marchan EM and Andrews DW (2009) The Effective Use of the Hemostatic Agent Vitagel in Sealing Ependymal Breaches in Tumoral Resections That Involve the Ventricular System. *Neuro-Oncology* **11**:695.

Maricich SM, Wellnitz SA, Nelson AM, Lesniak DR, Gerling GJ, Lumpkin EA and Zoghbi HY (2009) Merkel Cells Are Essential for Light-Touch Responses. *Science* **324**:1580-1582.

Marrs TC, Maynard RL and Sidell FR (1996) Organophosphate Nerve Agents, in *Chemical Warfare Agents: Toxicology and Treatment* (Marrs TC, Maynard RL and Sidell FR eds) pp 83-100, John Wiley and Sons Ltd, Chichester.

Masson P (2011) Evolution of and perspectives on therapeutic approaches to nerve agent poisoning. *Toxicology Letters* **206**:5-13.

Masukawa Y, Narita H, Shimizu E, Kondo N, Sugai Y, Oba T, Homma R, Ishikawa J, Takagi Y, Kitahara T, Takema Y and Kita K (2008) Characterization of overall ceramide species in human Stratum corneum. *Journal of Lipid Research* **49**:1466-1476.

Maxwell DM, Brecht KM, Koplovitz I and Sweeney RE (2006) Acetylcholinesterase inhibition: does it explain the toxicity of organophosphorus compounds? *Arch Toxicol* **80**:756-760.

McGrath JA and Uitto J (2008) The filaggrin story: novel insights into skin-barrier function and disease. *Trends in Molecular Medicine* **14**:20-27.

Meller D, Fraser I and Kryger M (1981) Hyperglycemia in Anticholinesterase Poisoning. *Canadian Medical Association Journal* **124**:745-&.

Menon GK (2002) New insights into skin structure: scratching the surface. *Advanced Drug Delivery Reviews* **54**:S3-S17.

Mikler J, Tenn C, Worek F, Reiter G, Thierrnann H, Garrett M, Bohnert S and Sawyer TW (2011) Immobilization of Russian VX skin depots by localized cooling: Implications for decontamination and medical countermeasures. *Toxicology Letters* **206**:47-53.

Mills PC (2007) Vehicle effects on the in vitro penetration of testosterone through equine skin. *Veterinary Research Communications* **31**:227-233.

Mosteller RD (1987) Simplified Calculation of Body-Surface Area. *New England Journal of Medicine* **317**:1098.

Munro NB, Talmage SS, Griffin GD, Waters LC, Watson AP, King JF and Hauschild V (1999) The sources, fate, and toxicity of chemical warfare agent degradation products. *Environ Health Perspect* **107**:933-974.

Murdock D (2008) Trauma: when there's no time to count. *AORN journal* **87**:322-328.

Murnford H and Troyer JK (2011) Post-exposure therapy with recombinant human BuChE following percutaneous VX challenge in guinea-pigs. *Toxicology Letters* **206**:29-34.

Murray JC, Stein F, Mcglothlin JC and Mcclain KL (1994) Prolongation of the Prothrombin Time After Organophosphate Poisoning. *Pediatric Emergency Care* **10**:289-290.

Myhrer T (2007) Neuronal structures involved in the induction and propagation of seizures caused by nerve agents: Implications for medical treatment. *Toxicology* **239**:1-14.

Naguib M (2003) The Pharmacology of Commonly Used Chemical Agents. *Seminars in Anaesthesia, Perioperative Medicine and Pain* **22**:230-238.

National Health Service. Emergency care on the battlefield. http://www.nhs.uk/Livewell/Militarymedicine/Pages/Survivingbattlefield.aspx . 12-6-2011.

National Research Council (U.S.) and Committee on Toxicology (1997) *Review of acute human-toxicity estimates for selected chemical-warfare agents*. National Academy Press.

Neuffer MC, McDivitt J, Rose D, King K, Cloonan CC and Vayer JS (2004) Hemostatic dressings for the first responder: A review. *Military Medicine* **169**:716-720.

Nordgren I, Lundgren G, Puu G, Karlen B and Holmstedt B (1985) Distribution and elimination of the stereoisomers of soman and their effect on brain acetylcholine. *Fundam Appl Toxicol* **5**:S252-S259.

OECD (2004a) Guidance Document for the Conduct of Skin Absorption Studies. OECD Series on Testing and Assessment Number 28. *Paris, Organisation for Economic Co-operation and Development*.

OECD (2004b) Test Guideline 428: Skin Absorption: *in vitro* Method. *Paris, Organisation for Economic Co-operation and Development*.

OECD (2010) OECD Guidance Notes on Dermal Absorption. *Paris, Organisation for Economic Co-operation and Development*.

Pazdernik TL, Emerson MR, Cross R, Nelson SR and Samson FE (2001) Soman-induced seizures: limbic activity, oxidative stress and neuroprotective proteins. *J Appl Toxicol* **21 Suppl 1**:S87-S94.

Pershing LK, Parry GE and Lambert LD (1993) Disparity of In-Vitro and In-Vivo Oleic Acid-Enhanced Beta-Estradiol Percutaneous-Absorption Across Human Skin. *Pharmaceutical Research* **10**:1745-1750.

Petras JM (1981) Soman neurotoxicity. *Fundam Appl Toxicol* **1**:242.

Petras JM (1994) Neurology and neuropathology of Soman-induced brain injury: an overview. *J Exp Anal Behav* **61**:319-329.

Petroianu G, Toomes M, Maleck W, Bergler W and Rufer R (1997) In vitro paraoxon (E 600) exposure: No activating effect on human blood coagulation. *Toxicology* **119**:167-173.

Petroianu G, Toomes M, Maleck W, Bergler W and Ruefer R (1999) Intravenous paraoxon (POX) exposure: Coagulation studies in mini pigs. *Chemico-Biological Interactions* **119-120**:489-495.

Plurad DS (2011) Blast Injury. *Military Medicine* **176**:276-282.

Pope C, Karanth S and Liu J (2005) Pharmacology and toxicology of cholinesterase inhibitors: uses and misuses of a common mechanism of action. *Environmental Toxicology and Pharmacology* **19**:433-446.

Potts RO and Guy RH (1992) Predicting Skin Permeability. *Pharmaceutical Research* **9**:663-669.

Prentiss AM (1937) *Chemicals in War*. McGraw Hill Book Company, New York.

Proksch E, Brandner JM and Jensen JM (2008) The skin: an indispensable barrier. *Experimental Dermatology* **17**:1063-1072.

ProteinBoxBot. Acetylcholinesterase. PDB rendering based on 1b41 structure. www.pdb.org . 2007.

RamaRao G and Bhattacharya BK (2012) Multiple signal transduction pathways alterations during nerve agent toxicity. *Toxicology Letters* **208**:16-22.

Ramirez JG and Bacon DR (2003) Modern Chemical Warfare Agents: The Anesthesiologist's Perspective. *Seminars in Anaesthesia, Perioperative Medicine and Pain* **22**:239-246.

Ramsey JD, Woollen BH, Auton TR and Scott RC (1994) The Predictive Accuracy of In-Vitro Measurements for the Dermal Absorption of A Lipophilic Penetrant (Fluazifop-Butyl) Through Rat and Human Skin. *Fundamental and Applied Toxicology* **23**:230-236.

Rang HP, Dale MM and Ritter JM (1999) Cholinergic transmission, in *Pharmacology* (Simmons B ed) pp 110-138, Churchill Livingstone, Edinburgh.

Reifenrath WG and Robinson PB (1982) Invitro Skin Evaporation and Penetration Characteristics of Mosquito Repellents. *Journal of Pharmaceutical Sciences* **71**:1014-1018.

Reynolds ML, Little PJ, Thomas BF, Bagley RB and Martin BR (1985) Relationship between the biodisposition of [3H]soman and its pharmacological effects in mice. *Toxicol Appl Pharmacol* **80**:409-420.

Rice RH and Cohen DE (1996) Toxic responses of the skin, in *Casarett & Doull's Toxicology, The Basic Science of Poisons* (Klaassen CD ed) pp 529-546, McGraw-Hill, New York.

Riley B (2003) The toxicology and treatment of injuries from chemical warfare agents. *Current Anaesthesia & Critical Care* **14**:149-154.

Robinson K (2004) Controlling bleeding in the field: hemostatic powders and dressings debut in the prehospital setting. *Journal of emergency nursing: JEN : official publication of the Emergency Department Nurses Association* **30**:160-161.

Rushmer RF, Buettner KJ, Short JM and Odland GF (1966) Skin. *Science* **154**:343-&.

Saga K (2002) Structure and function of human sweat glands studied with histochemistry and cytochemistry. *Progress in Histochemistry and Cytochemistry* **37**:323-+.

Sakorafas GH and Peros G (2008) Principles of war surgery: current concepts and future perspectives. *American Journal of Emergency Medicine* **26**:480-489.

Sato K and Dobson RL (1970) Regional and Individual Variations in Function of Human Eccrine Sweat Gland. *Journal of Investigative Dermatology* **54**:443-&.

Sato K, Leidal R and Sato F (1987) Morphology and Development of An Apoeccrine Sweat Gland in Human Axillae. *American Journal of Physiology* **252**:R166-R180.

Sawyer TW, Mikler J, Tenn C, Bjarnason S and Frew R (2012) Non-cholinergic intervention of sarin nerve agent poisoning. *Toxicology* **294**:85-93.

Sawyer TW, Mikler J, Worek F, Reiter G, Thiermann H, Tenn C, Weatherby K and Bohnert S (2011) The therapeutic use of localized cooling in the treatment of VX poisoning. *Toxicology Letters* **204**:52-56.

Scalia S, Coppi G and Iannuccelli V (2011) Microencapsulation of a cyclodextrin complex of the UV filter, butyl methoxydibenzoylmethane: In vivo skin penetration studies. *Journal of Pharmaceutical and Biomedical Analysis* **54**:345-350.

Schaefer H and Redelmeier TE (1996) Structure and Dynamics of the Skin Barrier, in *Skin barrier: Principles of percutaneous absorption* (Schaefer H and Redelmeier TE eds) pp 1-42, S. Karger, Basel, Switzerland.

Scheuplein RJ (1976) Percutaneous Absorption After 25 Years - Or Old Wine in New Wineskins. *Journal of Investigative Dermatology* **67**:31-38.

Scheuplein RJ and Blank IH (1973) Mechanism of Percutaneous Absorption .4. Penetration of Nonelectrolytes (Alcohols) from Aqueous-Solutions and from Pure Liquids. *Journal of Investigative Dermatology* **60**:286-296.

Schmaltz F (2006) Neurosciences and research on chemical weapons of mass destruction in Nazi Germany. *J Hist Neurosci* **15**:186-209.

Schneider MR and Paus R (2010) Sebocytes, multifaceted epithelial cells: Lipid production and holocrine secretion. *International Journal of Biochemistry & Cell Biology* **42**:181-185.

Schwartz M (2009) Dr. Jekyll and Mr. Hyde: A short history of anthrax. *Molecular Aspects of Medicine* **30**:347-355.

Sheng GY, Johnston CT, Teppen BJ and Boyd SA (2001) Potential contributions of smectite clays and organic matter to pesticide retention in soils. *Journal of Agricultural and Food Chemistry* **49**:2899-2907.

Shih ML and Ellin RI (1984) Stability of aqueous solutions of sarin and soman: influence of concentration and an equation for determining concentration. *Bull Environ Contam Toxicol* **33**:1-5.

Shih ML, McMonagle JD, Dolzine TW and Gresham VC (1994) Metabolite pharmacokinetics of soman, sarin and GF in rats and biological monitoring of exposure to toxic organophosphorus agents. *J Appl Toxicol* **14**:195-199.

Shukla A, Fang JC, Puranam S, Jensen FR and Hammond PT (2012) Hemostatic Multilayer Coatings. *Advanced Materials* **24**:492-+.

Sidell FR (1974) Soman and Sarin - Clinical Manifestations and Treatment of Accidental-Poisoning by Organophosphates. *Clinical Toxicology* **7**:1-17.

Silman I and Sussman JL (2005) Acetylcholinesterase: 'classical' and 'non-classical' functions and pharmacology. *Current Opinion in Pharmacology* **5**:293-302.

Simon GA and Maibach HI (2000) The pig as an experimental animal model of percutaneous permeation in man: Qualitative and quantitative observations - An overview. *Skin Pharmacology and Applied Skin Physiology* **13**:229-234.

Sintov AC and Botner S (2006) Transdermal drug delivery using microemulsion and aqueous systems: Influence of skin storage conditions on the in vitro permeability of diclofenac from aqueous vehicle systems. *International Journal of Pharmaceutics* **311**:55-62.

SIPRI (1971) *The Rise Of CB Weapons*. Almquist and Wiksell, Stockholm.

Smith HW, Clowes GHA and Marshall EK (1919) On dichloroethylsulfide (mustard gas) IV. The mechansim of absorption by the skin. *Journal of Pharmacology and Experimental Therapeutics* **13**:1-30.

Smith K, Hall C, Lydon H, Dalton C, Graham J, Railer R, Stevenson R, Deckert R, Devorak J, Boecker J, Braue E, Lumpkin H, Doxzon B, Chilcott R and Clarkson E (2011) Testing the Ability of Hemostatic Products to Protect against the Chemical Warfare Agent VX. *Journal of the American Association for Laboratory Animal Science* **50**:801.

Soreq H and Seidman S (2001) Acetylcholinesterase - new roles for an old actor. *Nature Reviews Neuroscience* **2**:294-302.

Stalker A, Ollerton J, Everington S, Russell R, Walker C and White S (2011) A three-year review of emergency department admissions--Op HERRICK 4 to 9. *Journal of the Royal Army Medical Corps* **157**:213-217.

Sterri SH, Kloster O and Valdal G (1982) Reduction of blood cholinesterase activities following administration of soman by different routes in guinea-pig. *Acta Pharmacol Toxicol (Copenh)* **50**:326-331.

Subcommittee on Acute Exposure Guideline Levels, Committee on Toxicology and National RC (2003) *Acute Exposure Guideline Levels for Selected Airborne Chemicals:Volume 3*. The National Academies Press, Washigton DC.

Svennsson CK (2009) Biotransformation of Drugs in Human Skin. *Drug Metabolism and Disposition* **37**:247-253.

Szinicz L (2005) History of chemical and biological warfare agents. *Toxicology* **214**:167-181.

Tenberken O, Mikler J, Hill I, Weatherby K, Thiermann H, Worek F and Reiter G (2010) Toxicokinetics of tabun enantiomers in anaesthetized swine after intravenous tabun administration. *Toxicology Letters* **198**:177-181.

Thiermann H, Szinicz L, Eyer F, Worek F, Eyer P, Felgenhauer N and Zilker T (1999) Modern strategies in therapy of organophosphate poisoning. *Toxicology Letters* **107**:233-239.

Thiermann H, Steinritz D, Worek F, Radtke M, Eyer P, Eyer F, Felgenhauer N and Zilker T (2011) Atropine maintenance dosage in patients with severe organophosphate pesticide poisoning. *Toxicology Letters* **206**:77-83.

Tokuda Y, Kikuchi M, Takahashi O and Stein GH (2006) Prehospital management of sarin nerve gas terrorism in urban settings: 10 years of progress after the Tokyo subway sarin attack. *Resuscitation* **68**:193-202.

Traub K (1985) In vivo distribution of 14C radiolabeled soman [3,3-dimethyl-2-butoxy)-methylphosphorylfluoride) in the central nervous system of the rat. *Neurosci Lett* **60**:219-225.

Tuyet LTN and Johansson A (2001) Impact of chemical warfare with agent orange on women's reproductive lives in Vietnam: A pilot study. *Reproductive Health Matters* **9**:156-164.

Urmacher C (1990) Histology of Normal Skin. *American Journal of Surgical Pathology* **14**:671-686.

Vale A, Bradbury S, Rice P and Marrs TC (2003) Chemical Warfare and Terrorism. *Medicine* **31**:26-29.

Vale A, Marrs TC and Rice P (2007) Chemical terrorism and nerve agents. *Medicine* **35**:573-575.

Valladeau J (2006) The Langerhans cell. *M S-Medecine Sciences* **22**:144-148.

Vallenzuela Diaz FR and de Souza Santos P (2001) Studies on the acid activation of Brazilian smectitic clays. *Quim Nova* **24**:345-353.

Van der Merwe D and Riviere JE (2005) Comparative studies on the effects of water, ethanol and water/ethanol mixtures on chemical partitioning into porcine stratum corneum and silastic membrane. *Toxicology in Vitro* **19**:69-77.

van Dongen CJ, de LJ and van GJ (1989) In vitro degradation of the stereoisomers of soman in guinea-pig, mouse and human skin. *Biochem Pharmacol* **38**:2263-2268.

van Genderen J, Mol MA and Wolthuis OL (1985) On the development of skin models for toxicity testing. *Fundam Appl Toxicol* **5**:S98-111.

van Hooidonk C, Ceulen BI, Kienhuis H and Bock J (1980) Rate of skin penetration of organophosphates measured in diffusion cells. *Dev Toxicol Environ Sci* **8**:643-646.

van Smeden J, Hoppel L, van der Heijden R, Hankemeier T, Vreeken RJ and Bouwstra JA (2011) LC/MS analysis of stratum corneum lipids: ceramide profiling and discovery. *Journal of Lipid Research* **52**:1211-1221.

Vedder EB (1925) *The Medical Aspects of Chemical Warfare*. Williams and Wilkins, Baltimore.

Verstappen DR, Hulst AG, Fidder A, Vermeulen NP and Noort D (2012) Interactions of organophosphates with keratins in the cornified epithelium of human skin. *Chemico-Biological Interactions* **197**:93-102.

Walters KA and Roberts MS (2002) The structure and function of skin, in *Drugs and the Pharmaceutical Sciences. Dermatological and transdermal formulations* (Walters KA ed) pp 1-39, Marcel Dekker Inc, New York, USA.

Weinbroum AA, Rudick V, Paret G, Kluger Y and Ben Abraham R (2000) Anaesthesia and critical care considerations in nerve agent warfare trauma casualties. *Resuscitation* **47**:113-123.

Wester RC and Noonan PK (1980) Relevance of Animal-Models for Percutaneous-Absorption. *International Journal of Pharmaceutics* **7**:99-110.

Wheeler TG (1987) The behavioral effects of anticholinesterase insult following exposure to different environmental temperatures. *Aviat Space Environ Med* **58**:54-59.

Wheeler TG (1989) Soman toxicity during and after exposure to different environmental temperatures. *J Toxicol Environ Health* **26**:349-360.

Wickett RR and Visscher MO (2006) Structure and function of the epidermal barrier. *American Journal of Infection Control* **34**:S98-S110.

Wilke K, Martin A, Terstegen L and Biel S (2007) A short history of sweat gland biology. *International Journal of Cosmetic Science* **29**:169-179.

Wilkinson R, Jewell C, Wilkinson SC, Williams FM and Blain PG (2007) The effect of in vitro receptor media choice on the percutaneous absorption of methyl paraben. *Toxicology* **240**:178-179.

Wilkinson SC (2008) Biochemistry of the skin, in *Principles and Practice of Skin Toxicology* (Chilcott RP and Price S eds) pp 17-49, John Wiley & Sons Ltd., Chichester.

Wolthuis OL, Benschop HP and Berends F (1981) Persistence of the anti-cholinesterase soman in rats; antagonism with a non-toxic simulator of this organophosphate. *Eur J Pharmacol* **69**:379-383.

Worek F, Eyer P, Aurbek N, Szinicz L and Thiermann H (2007) Recent advances in evaluation of oxime efficacy in nerve agent poisoning by in vitro analysis. *Toxicology and Applied Pharmacology* **219**:226-234.

Worek F, Koller M, Thiermann H and Szinicz L (2005) Diagnostic aspects of organophosphate poisoning. *Toxicology* **214**:182-189.

Worek F, Thiermann H, Szinicz L and Eyer P (2004) Kinetic analysis of interactions between human acetylcholinesterase, structurally different organophosphorus compounds and oximes. *Biochemical Pharmacology* **68**:2237-2248.

Ya-Xian Z, Suetake T and Tagami H (1999) Number of cell layers of the stratum corneum in normal skin: Relationship to the anatomical location on the body, age, sex and physical parameters. *Archives of Dermatological Research* **291**:555-559.

Yanagisawa N, Morita H and Nakajima T (2006) Sarin experiences in Japan: Acute toxicity and long-term effects. *Journal of the Neurological Sciences* **249**:76-85.

Zilker T (2005) Medical management of incidents with chemical warfare agents. *Toxicology* **214**:221-231.